7th International Conference on Coupled THMC Processes in Geosystems

GEOPROC 2019:

Earthquake and Faulting Mechanics

Book of Abstracts

3-5 July 2019 Utrecht, Netherlands

Jianye Chen, André Niemeijer, Suzanne Hangx, Chris Spiers

Welcome note

FOREWORD

Dear Participant,
Welcome to GeoProc2019 at Utrecht University and welcome to the City of Utrecht in the heart of the Netherlands!

This 7th International Conference in the GeoProc series focuses on the role of coupled thermo-hydro-mechanical-chemical (THMC) processes in earthquake and faulting mechanics. As urban populations swell, destructive natural earthquakes pose an increasing threat in tectonically active regions. At the same time, seismicity caused by geo-resources extraction, geological storage and other subsurface activities is becoming increasingly widespread. The need to improve our understanding of faulting and seismogenesis is therefore reaching new levels of urgency. Yet these phenomena involve some of the most complex and highly coupled THMC processes imaginable. The initiation, propagation and cessation of slip instabilities on faults, for example, embody damage accumulation, frictional deformation, heat production, pore fluid pressurization, phase changes, chemical reactions, creep and reactive fluid flow - at multiple temporal and spatial scales. Advances that contribute to earthquake hazard assessment and mitigation depend on integrating different research fields and disciplines to address such processes and their coupling.

GeoProc2019 aims to bring together researchers from the full spectrum of relevant fields that may not always cross paths, from rock friction experimentalists and mechanics modellers to field geologists, seismologists, hydrogeologists, seismic hazard analysts, geo-engineers, fluid-rock interaction specialists, and Multiphysics/THMC modellers working at the frontier of computational developments. With keynote lectures, oral presentations and poster presentations from a global cast of contributors in these areas and beyond, we hope to highlight the most recent advances, the outstanding challenges and new opportunities for cutting-edge collaboration in understanding both natural and induced seismicity.

We wish you a productive and enjoyable conference with numerous interactions and inspirational discussions, whether on megathrust earthquakes at the Pacific Rim or on induced earthquakes in the giant Groningen gas field here in the Netherlands. Have a good time at GeoProc2019 and in Utrecht, professionally and socially!

Chris Spiers
On behalf of the Chairs and Organizing Committee

Committees

Chairs	Chair: Prof. Chris Spiers (High Pressure and Temperature Laboratory, Utrecht University) Co-chair: Prof. Jean Sulem (Laboratoire Navier, Ecole des Ponts Paris Tech, France) Co-chair: Prof. Klaus Regenauer-Lieb (University of Western Australia)
Local organizers	The local organizing team consists of the following members of Prof. Spiers' group at the High Pressure and Temperature Laboratory at Utrecht University Dr. André Niemeijer Dr. Suzanne Hangx Dr. Jianye Chen
Scientific committee	Dr. Jianye Chen (Utrecht University) Dr. David Dempsey (University of Auckland) Dr. Jan van Elk (Nederlandse Aardolie Maatschappij) Dr. Eiichi Fukuyama (National Research Institute for Earth Science and Disaster Resilience) Prof. Dr. Yves Guglielmi (Lawrence Berkeley National Laboratory) Dr. Suzanne Hangx (Utrecht University) Prof. Dr. Nadia Lapusta (California Institute of Technology) Dr. André Niemeijer (Utrecht University) Dr. Thomas Poulet (CSIRO, Australia) Prof. Dr. Klaus Regenauer-Lieb (University of New South Wales) Prof. Dr. François Renard (University of Oslo) Prof. Dr. Jianfu Shao (University of Lille, France)

Committees		Dr. Elena Spagnuolo (National Institute of Geophysics and Volcanology) Prof. Dr. Chris Spiers (Utrecht University) Dr. Ioannis Stefanou (Laboratorie Navier, ENPC, France) Prof. Dr. Jean Sulem (École des Ponts ParisTech) Dr. Manolis Veveakis (Duke University) Dr. Futoshi Yamashito (National Research Institute for Earth Science and Disaster Resilience)

Sponsors

GeoProc2019: Earthquake and Faulting Mechanics would not have been made possible without the sponsorship of the following companies and institutes:

NAM Nederlandse Aardolie Maatschappij B.V.

DeepNL

Universiteit Utrecht

Nouryon

ebn

Keynote speakers

- **Dr. David Dempsey (University of Auckland, New Zealand)**

Induced Earthquakes: Parameterized and Put to Use

- **Dr. Jan van Elk (NAM, The Netherlands)**

The Data Acquisition and Study program into Induced Seismicity in the Groningen Gas Field, N.E. Netherlands

- **Dr. Futoshi Yamashita (NIED, Japan)**

Two types of foreshock activities observed on a meter-scale laboratory fault: Slow-slip-driven and cascade-up

- **Prof. Yves Guglielmi (Lawrence Berkeley National Laboratory, USA)**

Probing at the source of induced seismicity: Understanding the couplings between permeability creation, stress dynamic variations and aseismic/seismic slip based on mesoscale experiments

- **Prof. Nadia Lapusta (Caltech, USA)**

Dynamic rupture of creeping fault segments due to thermal pressurization of pore fluids: insights from numerical modeling

Keynote speakers

- **Dr. Elena Spagnuolo (INGV, Italy)**

Chemical and hydro-mechanical coupling in fault zones: an experimental overview

- **Prof. Klaus Regenauer-Lieb (University of New South Wales, Australia)**

THMC instabilities and the Multiphysics of Earthquakes

- **Dr. Tom M. Mitchell (University College London, UK)**

The interplay of fault zone structure and fluid flow in controlling crustal seismicity

- **Prof. François Renard (University of Oslo, Norway)**

Dynamics of microfracture precursors during the nucleation of faulting in rocks

Table of content

al.]	in Alpine slate-belt
Li Hai-Bing [et al.]	Co-seismic graphite formation and its enrichment during faulting
Di Toro Giulio [et al.]	Frictional melting in fluid-rich faults (Bolfin Fault Zone, Chile)
14:30-16:00, 4th of July	**THMC processes in laboratory experiments: Exploring the transition from slow to fast deformation and rupture**
Yamashita Futoshi [et al.]	Two types of foreshock activities observed on a meter-scale laboratory fault: Slow-slip-driven and cascade-up
Hung Chien-cheng [et al.]	Frictional properties of fault zone gouges from the WFSD-3 drilling project (2008 Mw 7.9 Wenchuan earthquake)
Acosta Mateo [et al.]	Slip and seismicity preceding earthquakes: Insights from laboratory experiments
Yao Lu [et al.]	Thermal pressurization precedes melt lubrication in high-velocity friction experiments on dolerite under elevated pore pressure
8:30-10:30, 5th of July	**Role of THMC processes in natural faulting and seismicity: Modelling and observational studies**
Regenauer-Lieb Klaus [et al.]	THMC instabilities and the Multiphysics of Earthquakes
Gerya Taras [et al.]	Optimal formulation for visco-elasto-plastic seismo-hydro-thermomechanical-chemical geodynamic models: C-component approach
Kaneko Yoshihiko	Accelerating foreshocks of crustal earthquakes controlled by frictional heterogeneities
Stefanou Ioannis [et al.]	Apparent rate dependency of fault gouges due to thermal pressurization and grain size
10:30-12:00, 5th of July	**THMC processes in laboratory experiments: Exploring the transition from slow to fast deformation and rupture**
Spagnuolo Elena [et al.]	Chemical and hydro-mechanical coupling in fault zones: an experimental overview
Ohl Markus [et al.]	Nanoscale dissolution processes and colloid-suspension formation as possible weakening mechanism of seismogenic crustal carbonate fault
Aretusini Stefano [et al.]	Linking THMC processes to the earthquake energy budget: experimental deformation of smectite-rich gouges
Vanorio Tiziana [et al.]	Fibrous Rocks due to Chemo-Mechanical Processes
15:00-16:30, 5th of July	**Role of THMC processes in natural faulting and seismicity: Modelling and observational studies**
Guglielmi Yves	Probing at the source of induced seismicity: Understanding the couplings between permeability creation, stress dynamic variations and aseismic/seismic slip based on mesoscale experiments
Zbinden Dominik [et al.]	On the effects of multi-phase fluid flow on induced seismicity
Parisio Francesco [et al.]	Fault stability during re-injection in deep geothermal systems
van den Bogert Peter	Fault reactivation and seismic rupture along faults in depleting reservoirs with offset

Table of content

	Kanaya T. [et al.]	Fault Stabilization by Dilatant Hardening in Granular Rocks
	Kaneko Y. [et al.]	Dynamic rupture simulations of the 2016 Kaikoura (New Zealand) Earthquake
	King T. [et al.]	Time-dependent analyses of first motion derived focal mechanism solutions and machine learning algoritms in rock deformation laboratory experiments
	Kitamura M. [et al.]	Mechanical property of granite under supercritical fluid conditions
	Krietsch H. [et al.]	On the seismo-hydromechanical response of a shear zone during hydraulic stimulation
	Lecampion B. [et al.]	A-sesimic fracture growth driven by fluid injection and remote nucleation
	Liu J. [et al.]	Frictional properties of simulated fault gouges prepared from the Groningen Carboniferous: Effects of any coal present
	Liu Y. [et al.]	Slow Slip on a High-Strength Velocity-Weakening Patch in a Subduction Fault Model
	Ma K.F. [et al.]	Featuring temporal fault zone behavior and its evolution from crossing-fault vertical borehole seismic array
	MacFarlane J. [et al.]	Chemo-Mechanical Processes of Cemented Volcanic Ashes
	Marty S. [et al.]	Foreshocks occurrence and their links to nucleation during experimental earthquakes
	Masoch S. [et al.]	Seismic cycle recorded in cockade-bearing faults (Col de Teghime, Alpine Corsica)
	McGuire J.J. [et al.]	Connections between stress rotation, interseismic coupling, and fault-zone property evolution across the brittle-ductile transition of the subducted Gorda plate.
	Mollon G. [et al.]	Towards a link between local friction and interface kinematics
	Nejati M. [et al.]	Determining Mode I fracture toughness in anisotropic rocks
	Ntokos D.	Identifying active tectonic structures by Ag oxides' recording, obtained by upward migration hydrochemical fluids on their surfaces
	Ntokos D.	Dating the varnishes of active Kamena Vourla - Arkitsa fault zone (Northwestern Evoikos Gulf, Central Greece) using Portable XRF
	Nur A.	Material and Stress Rotations: The Key to Reconciling Crustal Faulting Complexity with Rock Mechanics
	Okuda H. [et al.]	Slip- and Velocity-Weakening Behaviors of Brucite Nanoparticle
	Parez S. [et al.]	Mechanics of fluid-saturated granular gauges under seismic oscillations
	Petrini C. [et al.]	Modelling earthquake cycles using a continuum based poro-visco-elasto-plastic two-phase flow formulation
	Pluymakers A. [et al.]	The effect of ion-species on limestone failure dynamics
	Pranger C. [et al.]	GARNET: A new library for modeling tightly coupled, nonlinear, transient phenomena in arbitrary spatial dimensions
	Shao J.F. [et al.]	Analysis of hydromechanical process effect on water-induced landslides
	Shigematsu N. [et al.]	Brittle-plastic fault zone architecture along the Median Tectonic Line, SW Japan
	Shreedharan S. [et al.]	Precursory changes in on- and off-fault elastic wave properties linked to accelerated fault creep during laboratory slip instabilities
	Si J.L. [et al.]	Carbonaceous Materials in the Longmenshan Fault Belt Zone: Records of Seismic Slip from the Trench and Implications for Faulting Mechanisms
	Stephenson O.[et al.]	Simplified Elastodynamic Modeling of Potential Dynamic Rupture Through Creeping Fault Sections
	Takahashi M.	Spontaneous fault slip acceleration relating to a switch of the deformation mechanism
	Tama A. [et al.]	Relationship research on anthropogenic seismicity using satellite radar interferometry and IS-EPOS data
	van den Ende M. [et al.]	Microphysical modelling of laboratory and field injection tests
	Veedu D.M. [et al.]	Panoramic View of Fault failure modes from laboratory and numerical experiments
	Verberne B.A.[et al.]	Simulated quartz-feldspar faults sheared under conditions spanning the brittle-plastic transition

	Wang H. [et al.]	Geochemistry of pseudotachylyte formed at shallow depths during large in magnitude earthquakes
	Wang L.F.	Along strike variation of fault friction constrained by GPS observations
	We X. [et al.]	The Role of Fault Slippage and Permeability Evolution of Faults in Supercritical CO2 Fracturing
	Wentinck R.	Rupture modelling of a recent substantial tremor in the Groningen field using constraints from ground motion recordings and field data
	Wu W.-J.[et al.]	Frictional properties and microstructures of the active creeping Chihshang fault from experimental slip and its implications
	Yamashita F. [et al.]	Foreshock activities controlled by slip rate on a 4-meter-long laboratory fault
	Yue Z.Q.	A gas refined theory for cause of tectonic earthquakes, illustrated with 2008 Wenchuan 8.0 Earthquake
	Ben-Zeev S. [et al.]	Compaction front in horizontally shaken granular layers: application to soil liquefaction in drained conditions
	Zhang L. [et al.]	Unstable Frictional Slip of Basalt and Slip Weakening Behavior under High Fluid Pressure
	Zhang L. [et al.]	Effects of Fault Geometrical Complexities on Rupture Process and Earthquake Sequences in Longmenshan Fault Zone
	Zhang L. [et al.]	The deep reducing seismogenic environment in Longmen Shan: evidences from the metallic iron in pseudotachylyte
	Zhou W. [et al.]	Acoustic emissions associated with slow-slip events in quartz gouge friction experiments
	Zhou W. [et al.]	P wave travel time changes in the Groningen reservoir
	Zhu S. [et al.]	Numerical simulation of rupture processes of the 2008 Wenchuan, China earthquake

GeoProc2019: Earthquake and Faulting mechanics

7th International Conference on Coupled THMC Processes in Geosystems
3-5 July 2019 Utrecht (Netherlands)

Dynamics of microfracture precursors during the nucleation of faulting in rocks

François Renard [1]

Keywords: Fault nucleation, Microfracture

During faulting initiation, microfractures nucleate, grow and coalesce until a large enough rock volume is damaged, such that a fault can propagate dynamically. These microfractures represent precursors to macroscopic failure and understanding their dynamics is crucial to predict when, where and how a fault may develop and how fluids may percolate into a high-permeability volume around the fault. Using a triaxial deformation apparatus installed on the X-ray microtomography beamline ID19 at the European Synchrotron Radiation Facility, a series of porous and non-porous rocks were imaged in situ during deformation. On each sample, the axial stress was increased by increments while the confining stress was kept constant, and time series of 3D X-ray tomograms at micrometre spatial resolution were acquired at each step increase of stress. The development of damage was imaged and quantified directly from the 3D tomograms until failure. Results show that faulting was preceded by an acceleration of damage, which developed as microfractures that nucleated either at grain boundaries or within grains. This acceleration followed either a power-law increase in non-porous rocks or was slower than a power-law in porous rocks. A micromechanical interpretation explains the difference between these two kinds of rocks. Results demonstrate the existence of precursors preceding faulting. These precursors can be imaged at the microscale and follow a predictable dynamics.

[1] The Njord Center, University of Oslo, Norway & ISTerre, University Grenoble Alpes, France, francois.renard@geo.uio.no

GeoProc2019: Earthquake and Faulting mechanics

7th International Conference on Coupled THMC Processes in Geosystems
3-5 July 2019 Utrecht (Netherlands)

Off-fault damage characterization during and after experimental slow and fast rupture in crustal rock

F.M Aben[1], *N. Brantut, T.M. Mitchell, E.C. David*

Keywords: fault damage zone, shear rupture, coseismic damage, seismic tomography, slip-weakening, microfractures

The physical properties of rock hosting a fault strongly affect the mechanics of fault rupture and slip, and influence radiation of seismic waves. During fault rupture, host rock properties predominantly change by fracturing in response to stress perturbations in the process zone of the rupture. This reduces off-fault elastic moduli, which can be the source of a substantial component of seismic radiation [1]. Further, changes in off-fault properties may also have an immediate feedback on slip-weakening mechanisms that are active in the wake of the rupture front [2]. It is thus imperative to quantify how off-fault properties evolve *during* rupture and at *in situ* loading conditions to better understand the feedback that off-fault damage has on slip and seismic radiation.

Characterizing syn-rupture off-fault physical properties remains difficult because: i) field studies on exhumed fault rock provide post-rupture data only, and these rocks have recorded a complex tectonic history, ii) geophysical measurements do not have the temporal resolution to isolate rupture-related damage from slip-related damage, and iii) data acquisition rates in rock deformation experiments are too low with respect to rupture duration for detailed characterization. Here, we monitor the syn- and post-rupture damage evolution by performing quasi-static shear rupture laboratory experiments. Additionally, we characterize post-rupture damage evolution for dynamic rupture experiments. From these data, we assess the syn-rupture damage evolution for a dynamic rupture.

Rupture experiments were performed on intact Lanhélin granite in a triaxial loading rig at 100 MPa confining pressure. Quasi-static rupture velocity was achieved by acoustic emission (AE) rate control [3], dynamic rupture by constant strain rate loading. Post-mortem microstructures were analyzed for both rupture velocities. For quasi-static rupture experiments, the syn-rupture evolution of the *in situ* P-wave structure was obtained by 3D time-resolved tomographic inversion of passive AEs and active ultrasonic data using the FaATSO algorithm [4]. Post-rupture P-wave tomography for quasi-static and dynamic ruptures were obtained from AE aftershocks and ultrasonic surveys. In addition, we performed a number of mixed rupture velocity experiments where a quasi-static propagating rupture at half the sample length was allowed to

[1] Seismolab, department of Earth Sciences, University College London, f.aben@ucl.ac.uk

accelerate to a dynamic rupture velocity. These experiments yielded syn- and post rupture P-wave structures, microstructures, and AE aftershock distributions.

For quasi-static ruptures, syn-rupture P-wave velocity drops by 25% and elastic moduli by 50% in a 2-cm wide localized zone around the fault (Fig. 1a). P-wave anisotropy increases by around 7%. P-wave velocity recovery and a decrease in anisotropy are observed near the residual frictional strength of the rock, highlighting the transient stress effect of the rupture front. We establish that off-fault energy dissipation is 10% of the fracture energy budget G_c, based on the change in elastic moduli around the fault zone.

The width of the low velocity zone is larger for dynamic ruptures, inferred from the post-rupture P-wave velocity structures of quasi-static and dynamic ruptures. Microstructural analysis shows that off-fault fracture density increases with a factor of two from quasi-static rupture to dynamic rupture (Fig 1b). Aftershock distributions reveal a seismic 'gap' for the fault section that experienced dynamic rupture in mixed-velocity rupture experiments. We suggest that this gap is due to softer host rock relative to the host rock surrounding the slow rupture section of the fault; hence this portion of the fault experienced more syn-rupture damage.

This unique dataset provides a calibration benchmark for dynamic rupture models, and provides input for assessing earthquake source properties. Also, it allows for a more thorough analysis of the feedback between syn-rupture damage and slip-weakening mechanisms such as flash heating and thermal pressurization.

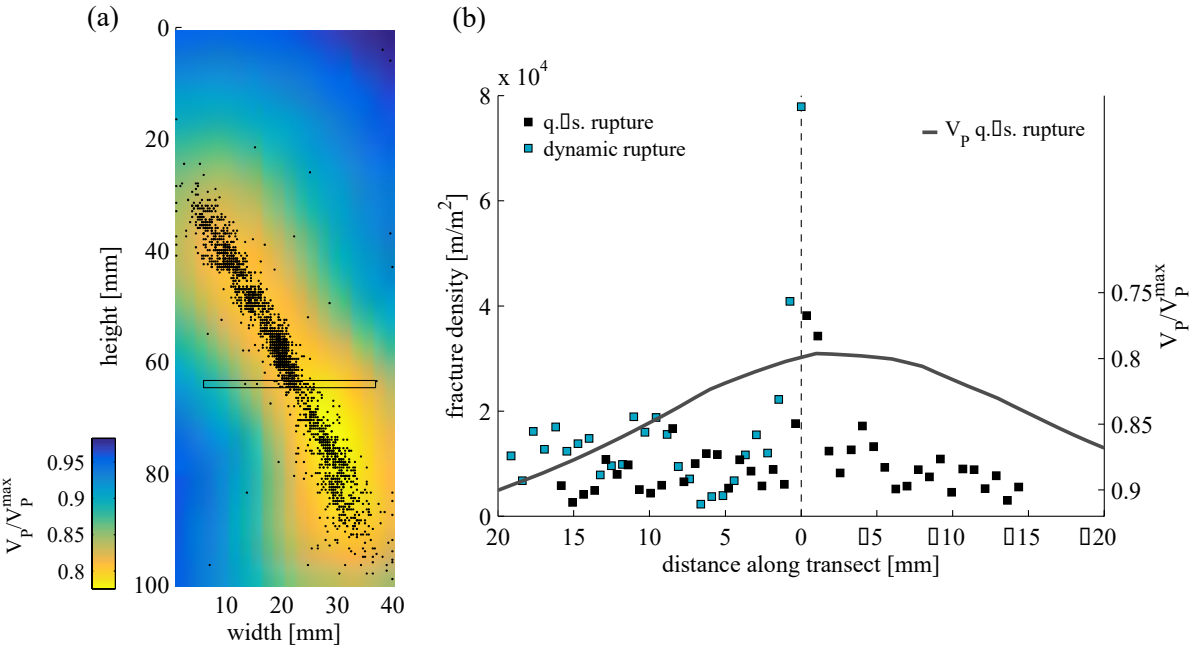

Figure 1. (a) Tomography shows P-wave velocity structure around fault formed by quasi-static rupture propagation. AE source locations are highlighted by black dots, location of microstructural analysis is highlighted by rectangular box. (b) Fracture density obtained by microstructural analysis on post-mortem samples subjected to quasi-static (black) and dynamic (blue) rupture as a function of distance to fault (at 0 mm). P-wave velocity profile (gray curve) obtained from (a).

References

[1] Ben-Zion, Y. & Ampuero, J.-P. Seismic radiation from regions sustaining material damage. *Geophys. J. Int.* **178,** 1351–1356 (2009).

[2] Rice, J. R. Heating and weakening of faults during earthquake slip. *J. Geophys. Res. Solid Earth* **111,** 1–29 (2006).

[3] Lockner, D. A., Byerlee, J. D., Kuksenko, V., Ponomarev, A. & Sidorin, A. Quasi-static fault growth and shear fracture energy in granite. *Nature* **350,** 39–42 (1991).

[4] Brantut, N. Time-resolved tomography using acoustic emissions in the laboratory, and application to sandstone compaction. *Geophys. J. Int.* (2018).

GeoProc2019: Earthquake and Faulting mechanics

7th International Conference on Coupled THMC Processes in Geosystems
3-5 July 2019 Utrecht (Netherlands)

A lubricant or a damper? The influence of pore fluids on rupture dynamics during laboratory scale earthquakes

K.S. Hayward[1], *S.F. Cox*[2], *R.P. Hawkins*[3]

Keywords: Viscous damping, thermal pressurization, dynamic fault strength, experiments

Grouping of source parameters from natural earthquakes suggests that there is a link between tectonic setting and the efficiency of large earthquakes (*Venkataraman and Kanamori*, 2004). Seismic efficiency is defined as the ratio of radiated seismic wave energy to potential energy and importantly tells us about stress drops, slip velocity and the efficiency of weakening mechanisms. Earthquakes occurring in fluid-rich tectonic settings such as subduction zone and some intraplate settings often have a lower seismic efficiency than those occurring in less fluid-rich environments. This observation is counter-intuitive given the widespread acceptance of the activation of thermal pressurisation as a dynamic weakening mechanism in fluid-saturated environments. However, due to the technical difficulty of achieving high pore fluid pressures at seismic slip rates, the activation and efficiency of thermal pressurisation remains poorly constrained in experiments.

We show results of a series of stick-slip experiments performed on Fontainebleau sandstone in a gas medium triaxial apparatus at effective confining pressures of 100MPa and pore fluid pressures between 10-100MPa. Using novel interferometry techniques (*Hayward et al*., 2016) we are able to measure displacement during rapid sliding, recording conservative estimates of slip velocities up to 1.3m/s. An unfavourably-oriented fault (50° to the loading direction (*Hayward and Cox*, 2017)) results in high normal stresses (300-675MPa) and produces frictional melting in both dry and fluid-saturated experiments.

We show that the presence and pressure of fluids within porous host rocks influences the size, style and behaviour of seismic events. Using complementary experimental, microstructural and modelling techniques I will discuss the contradiction between classic notions that fluids serve as lubricants on faults and experimental results that suggest fluids viscously damp the dynamic properties of faults during slip, leading to smaller and potentially more frequent slip events. These results have implications for understanding both seismic risk associated with injection-induced seismicity and the behaviour of high permeability fault zones.

[1] Research School of Earth Sciences, Australian National University, kathryn.hayward@anu.edu.au
[2] Research School of Earth Sciences, Australian National University, stephen.cox@anu.edu.au
[3] Laboratoire de Géologie de Lyon: Terre, Planètes et Environnement, Université Lyon 1, CNRS and Ecole Normale Supérieure de Lyon, rhys.hawkins@univ-lyon1.fr

References

Hayward, K.S., and S.F. Cox (2017), Melt Welding and its Role in the Reactivation and Localization of Fracture Damage in Seismically Active Faults, *J Geophys. Res: Solid Earth*, 122, 1-25, doi: 10.1002/2017JB014903.

Hayward, K.S., S.F. Cox, J. FitzGerald, B. Slagmolen, D. Shaddock, P. Forsyth, M. Salmon and R. Hawkins (2014), Mechanical amorphization, flash heating and frictional melting: Dramatic changes in fault surfaces during the first millisecond of earthquake slip, *Geology.*, *x*(y), 1-25, doi: 10.1130/G38242.1.

Venkataraman, A., and H. Kanamori (2004), Observational constraints on the fracture energy of subduction zone earthquakes, *J. Geophys. Res. Solid Earth*, 109, 1-26, doi:10.1029/2003JB002549.

GeoProc2019: Earthquake and Faulting mechanics

7th International Conference on Coupled THMC Processes in Geosystems
3-5 July 2019 Utrecht (Netherlands)

Pore pressure transients during sliding on laboratory faults

David A. Lockner[1], Brooks Proctor[2], Brian Kilgore[1], Tom Mitchell[3], N.M. Beeler[1,4]

Keywords: faulting, pore pressure, slow slip

Pore pressure changes affect fault stability both in natural and induced earthquakes. Proposed effects include thermal pressurization, dilatancy hardening, fluid pressure induced earthquakes and slow slip. Yet pore pressure changes are rarely measured directly in rupture nucleation zones. In laboratory experiments with external pore pressure control, restricted hydraulic communication with the fault may lead to undetected differences between fault zone pore pressure and the external control system during accelerating creep or dynamic slip. Because of additional fluid volume, control systems may have larger storativity than test faults leading to reduced change in pressure driven by dilatancy or compaction of the fault zone.

We report on triaxial deformation of model sawcut faults in Westerly granite at normal stresses to 197 MPa. Samples were 76.2 mm-diameter cylinders with a fault inclined 30° to the sample axis (Fig. 1). In most tests, the fault was hydraulically isolated from the large volume external control system and pore pressure communicated with the external pressure through the low permeability granite with a diffusion time constant > 1 hour. Thus, the fault was undrained coseismically, undrained or incompletely drained over the duration of precursors and, in some cases, over recurrence intervals. Internal pore pressure was measured with an embedded pressure transducer with a 9.5 mm diameter active face (0.8% of the fault area) adjacent to the fault.

Each test was conducted at constant confining pressure and constant axial shortening rate for both bare surface and 1 mm-thick quartz gouge layers. Precursory and coseismic pore pressure transients were observed at different stages of deformation. In some cases, premonitory dilatancy reduced pore pressure and stabilized the fault, leading to delayed instability or slow slip. In other cases (Fig. 2), shear-driven gouge compaction raised pore pressure, contributing to or controlling slip. Pore pressure transients associated with spontaneous changes in sliding rate were commonly in excess of 0.5 MPa and often exceeded strength changes predicted by rate- and state-dependent friction parameters. These experiments represent a promising first attempt at observing pore fluid/fault interactions with a passive, in situ pressure sensor.

[1]U.S. Geological Survey, Menlo Park, CA, dlockner@usgs.gov
[2]CAAA, Crane, IN, brooks_proctor@alumni.brown.edu
[3]UC London, UK, tom.mitchell@ucl.ac.uk
[4]U.S. Geological Survey, Vancouver, WA, nbeeler@usgs.gov

Figure 1. Left: Sawcut fault face with embedded pressure transducer. Right: Inverted sample assembly ready to place in pressure vessel. Coiled tubing provides pore pressure to end of granite sample (pore fluid must diffuse through granite to reach fault). Pressure transducer is embedded in lower sample half.

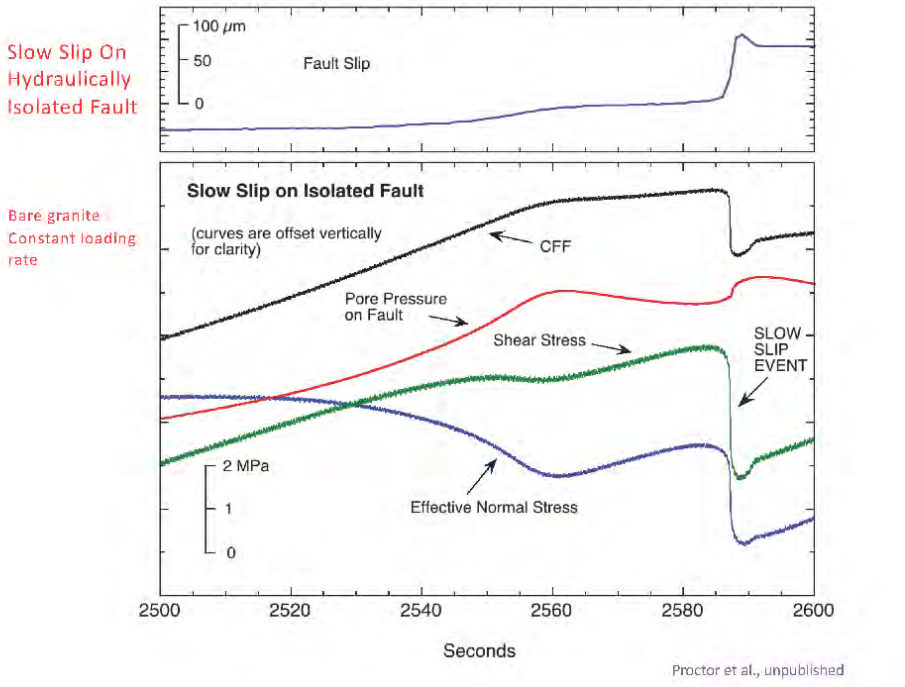

Figure 2. Constant remote loading rate leads to a slow slip event at 2587 s preceded by a smaller slip event between 2545 and 2560 s. Both slip events include ~0.4 MPa pore pressure rise driven by transient compaction of the fault zone. The rise in pore pressure destabilizes the fault.

GeoProc2019: Earthquake and Faulting mechanics

7th International Conference on Coupled THMC Processes in Geosystems
3-5 July 2019 Utrecht (Netherlands)

The Data Acquisition and Study program into Induced Seismicity in the Groningen Gas Field, N.E. Netherlands

Jan van Elk [1]

Keywords: Induced Seismicity, Groningen Gas Field

The Mw 3.6 earthquake near the village of Huizinge on the 16th August 2012, prompted field operator, NAM, to expand its research program into the induced seismicity in the Groningen field. I will introduce the programme and the issue of induced seismicity in Groningen to the GeoProc community in this 2019 meeting on earthquake and faulting mechanics here in The Netherlands.

The program consists of two parts. The main research effort focuses on the assessment of hazard and risk the community living above the field is exposed to. This is a very targeted program consisting of monitoring of the seismicity in the field area and studies supporting the modelling of the link between the cause, the production of gas from the Groningen field, to the effect, building damage and potential risk to people in and around these buildings. This part of the research was executed under tight deadlines set by the regulator and Minister of Economic Affairs and Climate Policy.

Additionally, a program was set up with the aim to better understand the physical processes leading to the destabilisation of the faults in the field and the induced seismicity. The components of this research are (1) geophysical data acquisition, analysis and modelling (2) geomechanical modelling on a single fault and at the field scale and (3) laboratory experiments on the complex coupled processes controlling rupture of faults and friction during the fault movement. Synthesis of these field and laboratory observations with the geomechanical models of faults has much improved understanding of the coupling between gas production, reservoir deformation, fault rupture and seismic wave generation. Moreover, huge amounts of data have been produced and are available for advancing this understanding further, in the context of Groningen and of induced seismicity in general.

[1] NAM BV, Schepersmaat 2, 9405 TA Assen, The Netherlands Jan.Van-Elk@shell.com

GeoProc2019: Earthquake and Faulting mechanics

7th International Conference on Coupled THMC Processes in Geosystems
3-5 July 2019 Utrecht (Netherlands)

Evaluating the potential of induced seismicity during reservoir operations – case study of Groß Schönebeck (Germany)

M. Cacace[1], G. Blöcher[1], A.B Jacquey[1], A. Zang[1],O. Heidbach[1], H. Hofmann[1],K. Kluge[1], G. Zimmermann[1]

Keywords: Fault Reactivation, Enhanced Geothermal Systems (EGS), induced seismicity, Thermal-Hydraulic-Mechanical (THM) process simulations

Stimulation treatments and/or reservoir operations can significantly alter the in-situ stress state and can induce variations in the mechanical state of existing fault zones. These changes can lead to (a)seismic fault reactivation.

In this study, we carry out an evaluation of the potential for induced seismicity arising from hydraulic stimulation of low to intermediate enthalpy porous reservoirs, by taking the geothermal reservoir of Groß Schönebeck (northern Germany) as our natural study case. The aim of the study is to evaluate the spatial and temporal distribution of 26 micro-seismic events which were triggered by a performed hydraulic stimulation in the volcanic section of the reservoir. In doing so, the results from coupled Thermal-Hydraulic-Mechanical (THM) simulations are compared to available field observations (Cacace and Jacquey, 2017; Blöcher et al., 2018). Two fault stability analysis are carried out assuming (a) Terzaghi's effective stress concept, and (b) the more complete Biot's effective stress concept. Particular attention is given towards quantifying the reactivation potential of existing fault planes under: (i) the in-situ stress state, (ii) a waterfrac stimulation treatment, and, (iii) a projected 30 years production and injection at the in-situ geothermal test-site Groß Schönebeck (see Figure 1).

The analysis of field data indicates that the stress state in the sandstone and volcanic sections of the reservoir differs with a minimum horizontal stress gradient up to 0.17 MPa/m. Such variations in the minimum horizontal stress could not be explained by relative variations of rock properties with depth, thus leading to the conclusion that the stress state in the reservoir is most likely to be uncertain. By comparing the recorded micro-seismicity (both in terms of the locations and temporal variability of the events) with the model scenarios we were able to ascertain that the stress state in the sandstone section is more representative of the whole reservoir. Given such in situ conditions, we found no potential for fault reactivation.

[1] Helmholtz Centre Potsdam, GFZ German Research Centre for Geosciences, cacace@gfz-potsdam.de

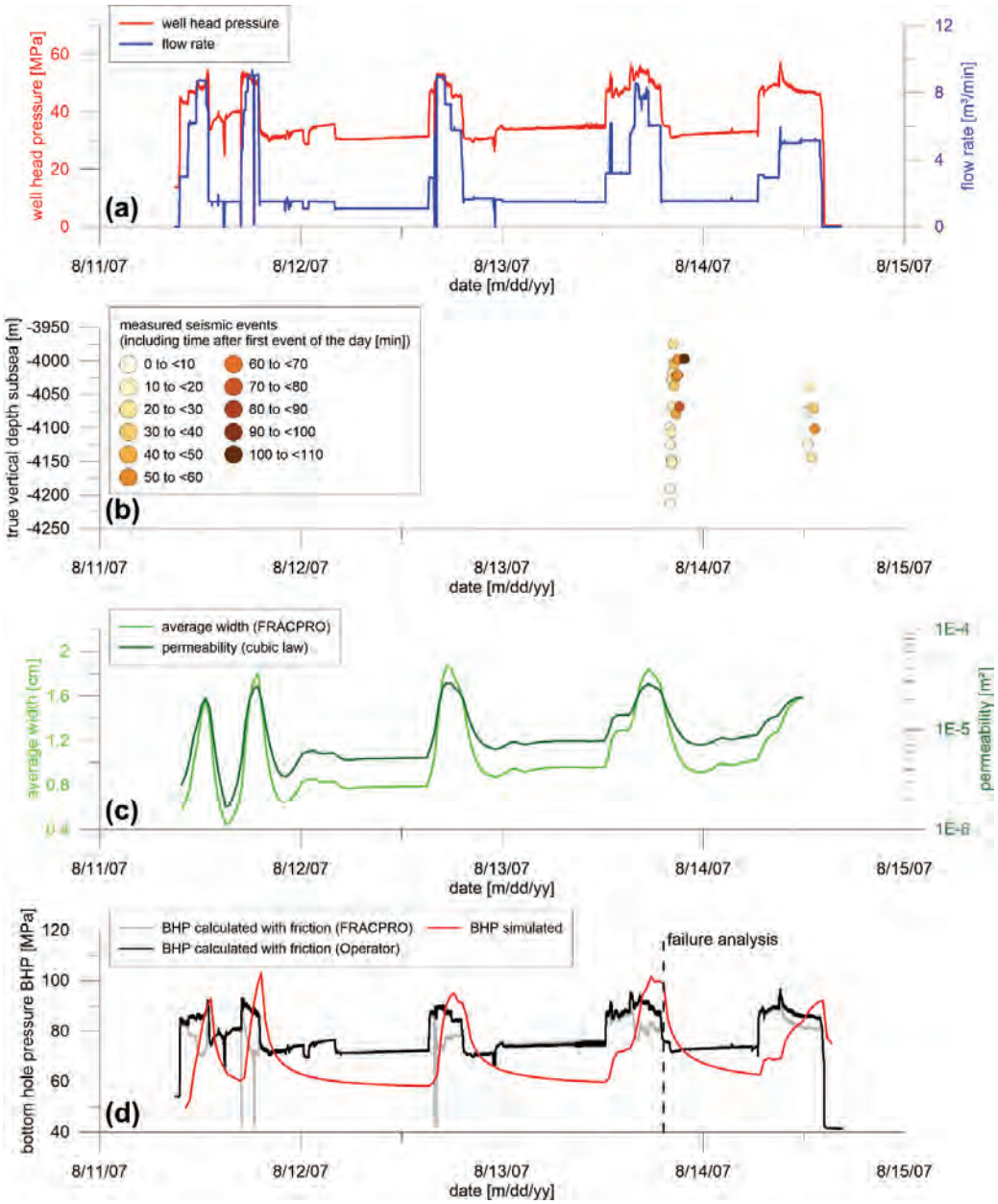

Figure 1 Schedule of the waterfrac stimulation treatment carried out at the geothermal research well GtGrSK4/05 in Groß Schönebeck in 2007 (Zimmermann et al., 2010). (a) Applied slurry rate at the well head and corresponding surface pressure; (b) depth correlation of measured seismic events (Kwiatek et al., 2010) during the stimulation; (c) calculated average fracture width and corresponding permeability; (d) calculated and simulated bottom hole pressures.

A 5 day waterfrac simulation treatment was carried out in the low permeable volcanic section in 2007 with alternating flow rates (up to 9 cubic meter per minute) with low concentration of quartz sand added during the high flow rates to support the opening of the induced fracture (Figure 1a and c). During the waterfrac stimulation treatment, micro-seismic events were recorded in the field mainly occurring during the 4th and 5th pressure cycle (Figure 1b). The recorded events first clustered in the volcanic section of the reservoir and then propagated upwards into the sandstone layer. The analysis of these micro seismic events indicates that slip during the hydraulic stimulation occurred probably along a fault with a NNE014° strike and 52° dip. The orientation of such a plane is consistent with the results of the slip tendency analysis

which identified NNE-SSW striking faults with dip varying between 50°-60° as prone to reactivation under a normal faulting mode (Figure 2).

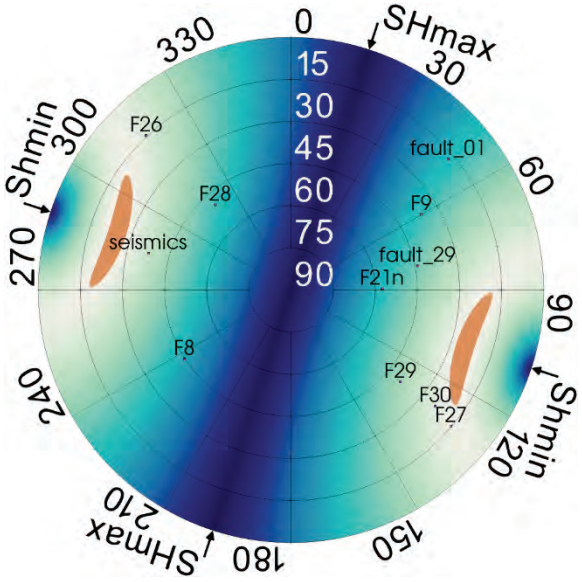

Figure 2 : Slip tendency calibrated for the stress state representative of the sandstone section.

The results from the THM simulations of the waterfrac treatment are in agreement with the calculated overpressure (Figure 1d) and indicate that the increase in the reservoir fluid pressure is most likely responsible for the recorded micro-seismicity. Our current evaluation shows an increase of slip and dilation tendency during the treatment, of magnitudes close to the failure level as based on the Mohr-Coulomb friction concept which would have led to a reactivation of the fault plane and related seismic activity.

During the projected production and injection period (30 years), despite increased in thermal stress, the values for slip and dilation tendency are constrained below the threshold for fault reactivation. This is again consistent with available observations indicating that micro seismic events only occurred during the extensive waterfrac treatment at the production well GrSK4/05 in 2007.

References

Blöcher, G., Cacace, M., Jacquey, A.B., Zang, A., Heidbach, O., Hofmann, H., Kluge, C., Zimmermann, G. (2018) Evaluating micro-seismic events triggered by reservoir operations at the geothermal site of Groß Schönebeck (Germany), Rock Mechanics and Rock Engineering, 51 :3265-3279, doi: 10.1007/s00603-018-1521-2.

Cacace, M., and A.B. Jacquey (2017), Flexible parallel implicit modelling of coupled termal-hydraulic-mechanical processes in fractured rocks, Solid Earth, 8(5), 921-941, doi: 10.5194/se-8-921-2017.

Kwiatek, G., Bohnhoff, M., Dresen, G., Schulze, A., Schulte T, Zimmermann, G., Huenges E. (2010) Microseismicity induced during fluid-injection: a case study from the geothermal site at Groß Schönebeck and North German Basin. Acta Geophys 58:995–1020, doi:10.2478/s1160 0-010-0032-7.

Zimmermann G., Moeck I., Blöcher G. (2010) Cyclic waterfrac stimulation to develop an enhanced geothermal system (EGS) —conceptual design and experimental results. Geothermics 39(1):59–69,doi:10.1016/j.geoth ermic s.2009.10.003.

GeoProc2019: Earthquake and Faulting mechanics

7th International Conference on Coupled THMC Processes in Geosystems
3-5 July 2019 Utrecht (Netherlands)

Impact of Induced Seismicity on Earthquake Risk – with examples of the Central and Eastern USA

M. Nyst[1], *J.L. Maurer*[2], *D. Kane*[3], *J. Velasquez*[4]

Induced, seismicity, earthquake, USA, risk

Induced and triggered seismicity (ITS) has been a growing problem around the world, including the Central and Eastern US (CEUS). This provides both challenges and opportunities to learn more about earthquake hazard and risk in areas with historically low rates of earthquakes, and many studies have considered seismic hazard from ITS in the CEUS and elsewhere. Few scientific studies, though, have directly considered the financial risk implications of damage caused by ITS. In this study, we directly address this issue, using the one-year hazard model for the CEUS released by the United States Geological Survey (USGS) to determine earthquake hazard in the CEUS and the RiskLink™ software developed by Risk Management Solutions, Inc. (RMS), to model expected losses. We explore the sensitivity of certain risk metrics to choices in catalog declustering algorithm, and how earthquake rates are subsequently modeled.

The multi-billion-dollar insurance industry uses hazard models to estimate earthquake insurance premiums, to manage capital for pay-out at certain loss levels, as well as to transfer some of its risk to the reinsurance industry and capital markets. We will explain how catastrophe modeling companies like RMS develop risk metrics for insured risk management. Commonly used risk metrics are average annual loss (AAL) and exceedance probability (EP) curves. AAL is the product of location loss and annual rate for all events, and is used to set annual premiums, while keeping the long-term risk in mind. The EP curve is also derived from the full set of events that impact an exposure. It plots the probability of exceeding a particular loss level and provides quantification to solvency assessment and portfolio management.

In this presentation we will discuss the following highlights in more detail:

1. Seismicity inside regions of ITS has a change in the frequency-magnitude distribution around MW 4.5. The declustered catalog used in the USGS calculations matches the distribution above MW 4.5, but a distribution based on the full catalog and single b-value does not. The result is a factor of ten difference in the predicted rate of MW 6 events.

[1] Risk Management Solutions, Inc., USA, mnyst@rms.com
[2] NASA Jet Propulsion Laboratory, USA
[3] Risk Management Solutions, Inc., USA
[4] Risk Management Solutions, Inc., USA

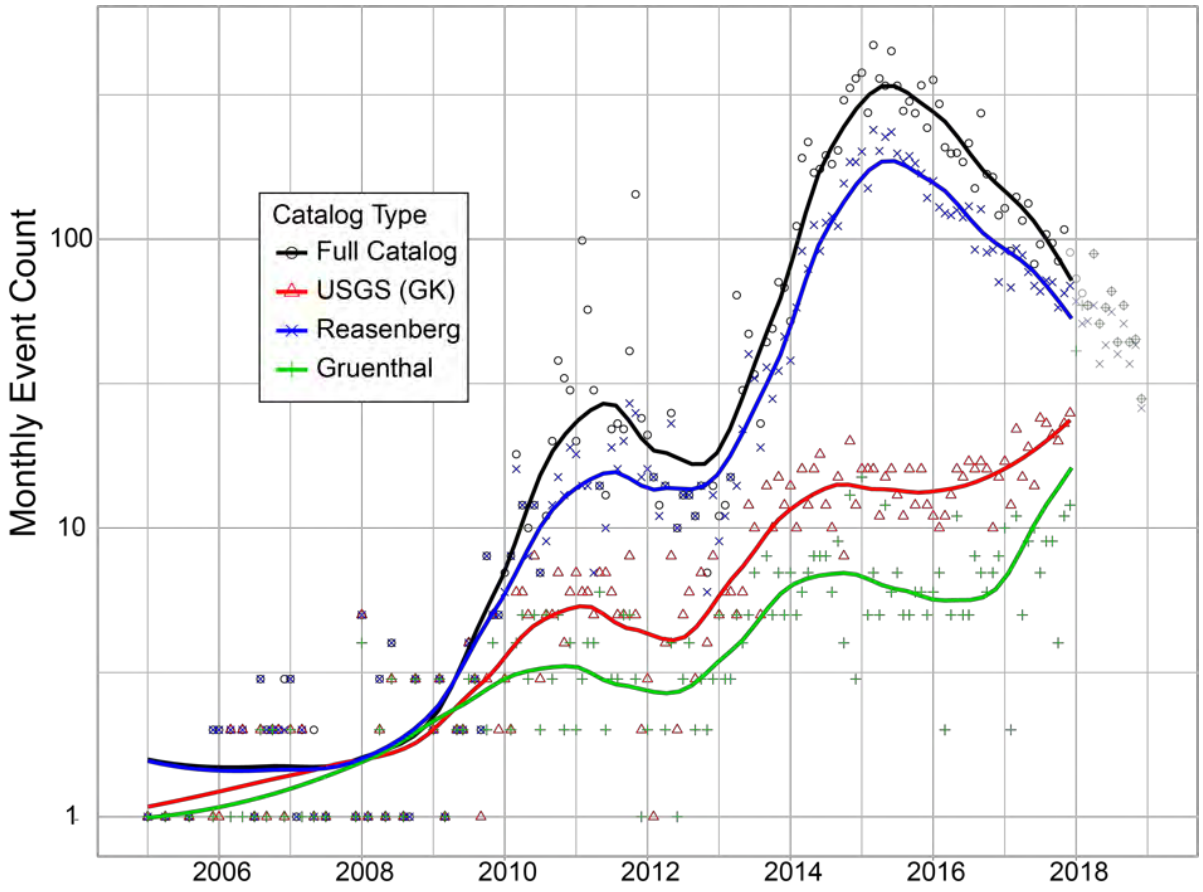

Figure 1. Monthly earthquake counts (MW2.7+) inside the USGS polygons from 2005-2017. Symbols are the actual counts, lines are a smoothed loess fit. The lines end at the end of 2017, the grayed-out symbols represent the approximate rates for 2018 based on the COMCAT catalog.

2. Due to the large difference in estimated earthquake rates at high magnitudes, estimated losses for using the USGS catalog are much higher than those estimated using the full catalog (or the Reasenberg-declustered), despite the lower total number of events.

3. Estimated losses using the USGS catalog are relatively constant for 2016-2018, compared to estimated losses using the full catalog that sharply decrease over the same time period.

4. Traditional declustering methods and a single b-value may not be appropriate for ITS. New methods should be developed that account for the physics of triggering and allow for time-varying rates.

GeoProc2019: Earthquake and Faulting mechanics

7th International Conference on Coupled THMC Processes in Geosystems
3-5 July 2019 Utrecht (Netherlands)

Modeling of Fault Reactivation and CO_2 migration with the HISS Elasto-Plastic Model and Compositional Fluid Transport

J. Ryu [1], S. Tavassoli [2], Z. Sun [2], M.T. Balhoff [3], D.N. Espinoza [4]

Keywords: elasto-plasticity, relative permeability, dynamic sealing capacity

The geomechanical stability and storage efficiency in carbon geological storage projects are contingent upon the dynamic sealing capacity of the caprock and neighboring faults. Fault seals are critical for determining suitable injection rates and volumes and determining the carbon dioxide (CO_2) sealing capacity of the formation. Fault reactivation is a complex thermo-hydro-mechanical coupled process, and impacts directly on the migration of fluids along the fault.

We approach this problem by utilizing a solution that couples elasto-plasticity and compositional reservoir simulation. The numerical solution uses the elasto-plastic geomechanical model (Hierarchical Single Surface – HISS, Desai 2000) that captures accurately strain softening, strain hardening, and therefore post-yield plastic deformations involved in fault reactivation. CO_2 mass transfer is simulated with a compositional fluid flow model that incorporates advective and diffusive mass transfer. The model also captures the change of brine density with CO_2 dissolution. The geomechanical and fluid flow models are coupled through poro-elasticity and a volumetric strain-permeability law. The numerical simulation is conducted with the simulator CMG GEM.

The results show that the model is capable of capturing fault reactivation and the resulting change of permeability and migration of brine and CO_2 (Figure 1). We simulate the reactivation of a fault with a strain-softening behavior. Fault reactivation results in dilation of the fault gouge. Permeability changes the most near the injection compartment. The evolution of fault gouge properties is critical for determining the extent of fault reactivation, the pressure relief during injection, and the migration of CO_2 through the fault. For example, fault reactivation can result in pressure relief as pushed brine enters adjacent formations. A sensitivity study with injection rate, stress anisotropy, reservoir volume, initial pore pressure, and flow boundary conditions shows that (1) only total stress anisotropy changes the critical pressure required for reactivation, (2) the variation of all other sensitivity parameters (other than boundary conditions) only accelerates or postpones reactivation, and (3) flow boundary conditions only change the length of the reactivated area.

[1] The University of Texas at Austin, jenny_ryu@utexas.edu
[2] The University of Texas at Austin, s.tavassoli@utexas.edu
[3] The University of Texas at Austin, balhoff@mail.utexas.edu
[4] The University of Texas at Austin, espinoza@austin.utexas.edu

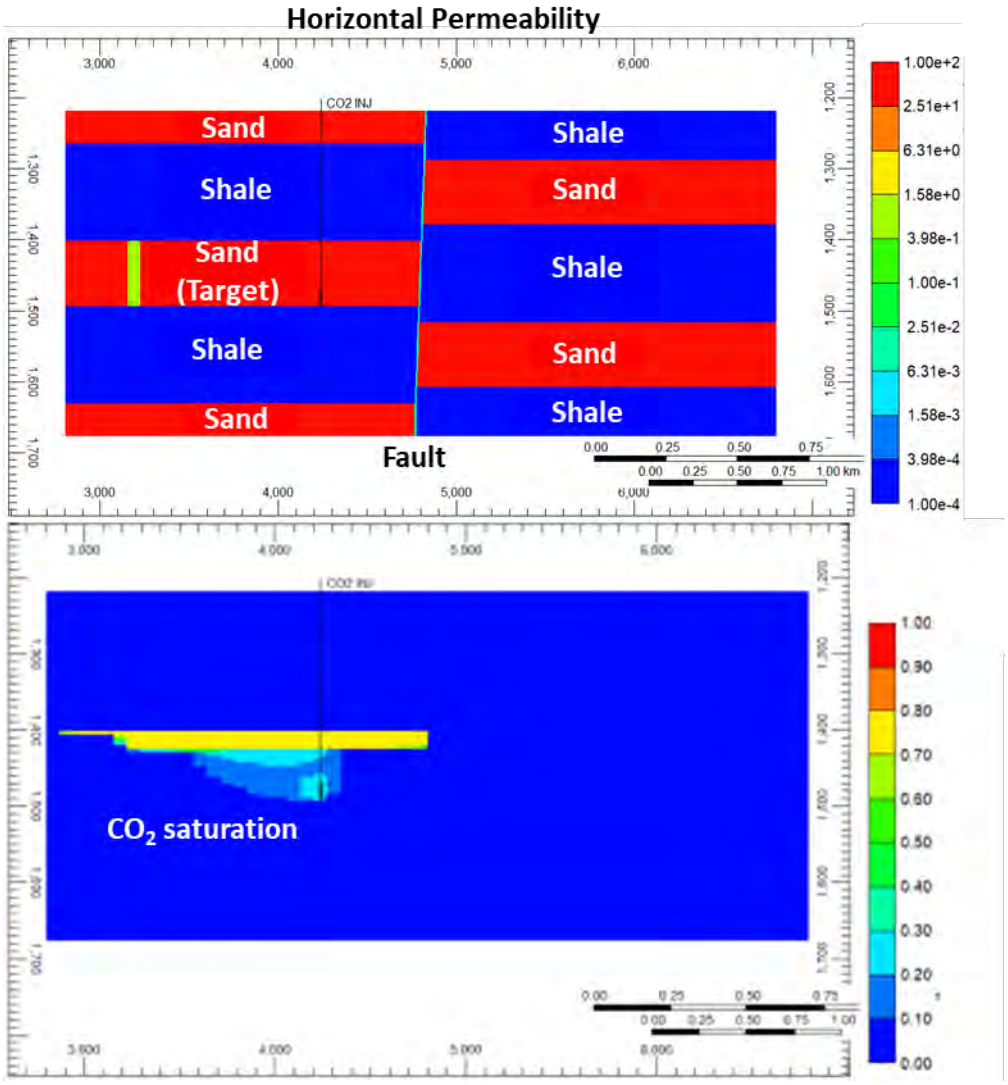

Figure 1. Transport of CO_2 resulting from injection and fault reactivation after 50 years.

References

Desai, C.S., (2000), Mechanics of materials and interfaces: The disturbed state concept. CRC press.

GeoProc2019: Earthquake and Faulting mechanics

7th International Conference on Coupled THMC Processes in Geosystems
3-5 July 2019 Utrecht (Netherlands)

Dynamic rupture of creeping fault segments due to thermal pressurization of pore fluids: insights from numerical modeling

N. Lapusta[1]

Keywords: earthquake rupture, dynamic modeling, enhanced dynamic weakening

Faults accommodate slow relative motion between tectonic plates through a combination of slow slip and dynamic rupture events perceived as earthquakes. The slow and fast slip is often assumed to occur on fault segments with different friction properties. Rate-and-state fault models associate creeping regions with velocity-strengthening (VS) friction, suggesting that they act as barriers to earthquakes since their strength increases with their slip velocity (also called slip rate). Indeed, earthquakes often arrest at the boundaries of creeping regions. However, experimental and theoretical studies reveal that several weakening mechanisms, such as thermal pressurization of pore fluids, can be activated at high seismic slip rates. As earthquake rupture penetrates into the VS fault areas, it significantly increases slip rates there, potentially activating the additional co-seismic weakening and turning the stable fault areas into seismogenic ones.

We have explored such behavior in numerical models with fault properties measured using rock samples obtained from the Chelungpu fault, the site of the 1999 Chi-Chi earthquake (Noda and Lapusta, 2013). The model reproduces a number of both long-term and coseismic observations about faults that hosted the 2011 Tohoku-Oki and 1999 Chi-Chi earthquakes. Moreover, only models in which the largest earthquake events rupture a shallow creeping region can reproduce the 1000-year recurrence interval proposed for the Tohoku-Oki-like events (Cubas et al, 2015).

In short, it is physically plausible for a creeping fault region to sustain dramatic seismic slip, and this may have occurred in the 2011 Tohoku-Oki and 1999 Chi-Chi earthquakes. After seismic slip, such regions would stay locked for a while, but eventually accumulate enough stress to start creeping again, obscuring the evidence of their violent past.

The possibility that seismic rupture can be sustained in a creep-prone, VS region due to coseismic weakening implies that earthquake ruptures can potentially penetrate below the locked seismogenic zone, into the deeper creeping fault extensions (Jiang and Lapusta, 2016, 2017). Our strike-slip fault models mimicking segments of the San Andreas Fault (SAF) in California show that the depth extent of the largest events is determined by the boundary where enhanced coseismic weakening stops being efficient. The depth extent of coseismic rupture influences the microseismicity pattern throughout the post-seismic and inter-seismic period. When large events are confined in the traditionally defined seismogenic region, with velocity-weakening (VW) rate-and-state

[1] California Institute of Technology, lapusta@caltech.edu

friction properties, streaks of microseismicity are seen at and above the VS/VW transition, due to stress concentration between the locked and creeping regions being in the VW area, similar to the Parkfield segment of the SAF. In the cases with deeper penetration due to the enhanced dynamic weakening, the microseismicity streaks disappear, with seismic quiescence, similar to the Carrizo and some other segments of the SAF.

The much larger occasional extent of earthquake ruptures in our numerical models than what would be inferred based on currently locked fault areas highlights the potential for extreme, unexpected earthquake events. Our recent modeling results suggest that a sufficiently large earthquake can propagate through the creeping segment of the SAF due to thermal pressurization of pore fluids, for a range of plausible fault properties (Stephenson and Lapusta, 2018). To improve our understanding of earthquake hazard, we need to study the structure, properties, and past behavior of creeping regions to evaluate their propensity for coseismic weakening, and hence their ability to sustain large seismic slip.

References

Noda H., and N. Lapusta (2013), Stable creeping fault segments can become destructive as a result of dynamic weakening, *Nature*, doi:10.1038/nature11703.

Cubas, N., N. Lapusta, J.-P. Avouac, H. Perfettini (2015), Numerical modeling of long-term earthquake sequences on the NE Japan megathrust: Comparison with observations and implications for fault friction, *Earth Planet. Sci. Lett.*.

Jiang, J., and N. Lapusta (2016), Deeper penetration of large earthquakes on seismically quiescent faults, *Science*, 352.

Stephenson, O., and N. Lapusta (2018), Exploring the possibility of dynamic rupture through the creeping section of the San Andreas Fault in a simplified 2D model, AGU Fall Meeting Abstract.

GeoProc2019: Earthquake and Faulting mechanics

7th International Conference on Coupled THMC Processes in Geosystems
3-5 July 2019 Utrecht (Netherlands)

Thermal pressurized gouges record stress states of faults after earthquakes

L.-W. Kuo[1], *V. Luzin*[2], *P. C. Chen*[3], *E.-C. Yeh*[4], *Y.-J. Hsu*[5], *K.-F. Ma*[6]

Keywords: TCDP, thermal pressurization, active Chelungpu fault, Neutron analysis

Earthquakes, as the result of fast slip on faults due to various dynamic weakening mechanisms (e.g., flash heating and thermal pressurization)[1-3], could result in a reduced stress state in the region[4]. Determining *in situ* stress states on faults right after earthquakes and the associated released tectonic stress, commonly obtained from borehole breakouts[5-6], remain challenging because severely limited stress information can be unraveled in slipping-zone materials. Here we present data on the continuous Neutron scan across the active fault zone of the Chelungpu fault corresponding to the 1999 Mw7.6 Chi-Chi earthquake. Results indicate the orientation of clay within the Chi-Chi slipping-zone materials, different from most of samples predominantly parallel to bedding planes, were preferentially rearranged after thermal pressurization[7]. On the basis of the orientation of clay as a result of compaction by regional maximum principal stress, stress inversion shows incompletely released principal stress after earthquakes and the stress state of strike-slip fault regime that was changed from the one of reverse fault regime before earthquakes: it may explain the occurrence of changed focal mechanisms after main shocks. In addition, thermal pressurization is proposed as a widespread process for earthquake generation and propagation[8], the investigation of gouge orientation of a fault offers the opportunity to study the stress drop and recovery during the seismic cycle.

[1] National Central University, Taiwan, liweikuo@ncu.edu.tw
[2] Australian Nuclear Science & Technology Organisation, Bragg Institute, Lucas Heights, Austrlia, vll@ansto.gov.au
[3] National Taiwan University, Taiwan, s300621213@gmail.com
[4] National Taiwan Normal University, Taiwan, ecyeh@ntnu.edu.tw
[5] National Central University, Taiwan, kuofongm@gmail.com
[6] Academia Sinica, Taiwan, yaru@earth.sinica.edu.tw

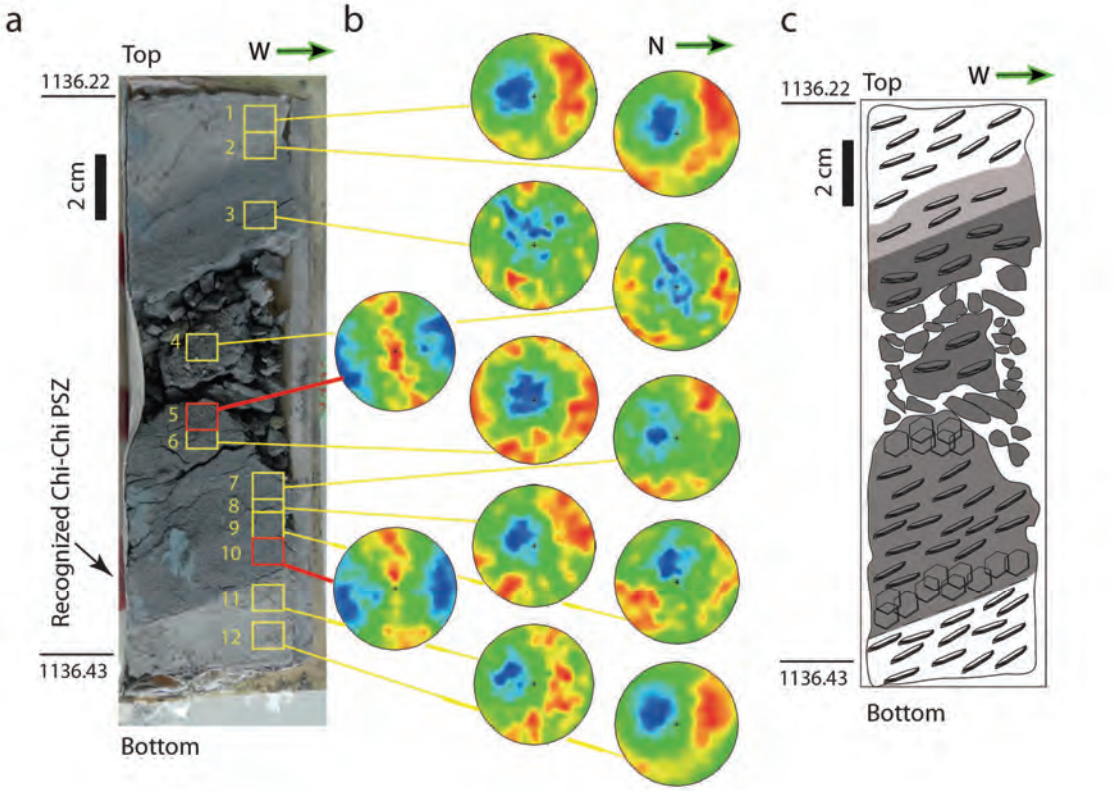

Figure 1. The continuous Neutron scan across the active fault zone of the Chelungpu fault corresponding to the 1999 Mw7.6 Chi-Chi earthquake

References

[1] Han, R., Shimamoto, T., Hirose, T., Ree, J. H. & Ando, J. I. Ultralow friction of carbonate faults caused by thermal decomposition. Science 316, 878-881 (2007).

[2] Goldsby, D. L. & Tullis, T. E. Flash heating leads to low frictional strength of crustal rocks at earthquake slip rates. Science 334, 216-218 (2011).

[3] Di Toro, G. et al. Fault lubrication during earthquakes. Nature 471, 494-498 (2011).

[4] Stein, R.S. The role of stress transfer in earthquake occurrence. Nature 402, 605-609 (1999).

[5] Lin, W. et al. Current stress state and principal stress rotations in the vicinity of the Chelungpu fault induced by the 1999 Chi-Chi, Taiwan, earthquake. Geophys. Res. Lett. 34, L16307 (2007).

[6] Lin, W. et al. Stress state in the largest displacement area of the 2011 Tohoku-Oki earthquake. Science 339, 687-690 (2013).

[7] Boullier, A.-M., Yeh, E.-C., Boutareaud, S., Song, S.-R. & Tsai, C.-H. Microscale anatomy of the 1999 Chi-Chi earthquake fault zone. G cubed 10(3), Q03016 (2009).

[8] Viesca, R. & Garagash, D. Ubiquitous weakening of faults due to thermal pressurization. Nature Geoscience 8, 875-879 (2015).

GeoProc2019: Earthquake and Faulting mechanics

7th International Conference on Coupled THMC Processes in Geosystems
3-5 July 2019 Utrecht (Netherlands)

Dilatancy strengthening stabilizes earthquake rupture and promotes aseismic slip on East Pacific Rise ridge transform fault

Y. Liu[1], *J. J. McGuire*[2], *M. D. Behn*[3]

Keywords: oceanic transform faults, rupture barriers, dilatancy strengthening

By contrast to continental transform faults, oceanic ridge transform faults (RTFs) release a small percentage (~ 15% global average) of accumulated moment seismically, and the largest earthquakes observed are small (Mw 6-7) despite the large thermally defined potential rupture area[1]. However, due to their remote locations and lack of near-source instrumentation, studies on the rupture processes of RTF earthquakes and slip budget have primarily relied on statistical analysis of global earthquake catalogs and source inversions of large events using teleseismic recordings[2,3]. Recent ocean bottom seismometer deployment experiment along the Gofar, Discovery, Quebreda transforms of East Pacific Rise has started to provide near-field seismic data that sheds lights on the source mechanism of RTF earthquake rupture patterns[4-7]. On the Gofar transform, magnitude M~6 earthquakes repeat quasi-periodically every 5-6 years on ~ 15-20 km long western and eastern segments, separated by a ~ 10 km long barrier zone that appears to fail primarily aseismically (e.g., not in M6 ruptures). The rupture pattern is recently confirmed by the 2007-2008 earthquake sequence, of which the 2008 Mw6.0 event on the western segment was captured by the 2008 QDG OBS experiment including its numerous foreshocks and aftershocks[4].

The persistent rupture barrier is imaged to coincide with a several km wide damage zone of a 10-20% reduction in P-wave velocities[6], and have experienced a large (5-10%) velocity reduction at the time of the 2008 Mw6.0 mainshock, indicating strong spatial and temporal variations of fault mechanical properties. Observations from continental transform faults indicate that a <1 km offset is insufficient to stop a M6 dynamic rupture[8], while the Gofar fault trace is offset laterally by at most ~600 m at the boundary between the rupture and barrier zones[5]. The offset may produce transtensional (e.g., pull-apart) conditions, favorable for seawater to permeate to greater depths. Persistent supply of excess fluids can result in large fluid-filled porosity and high pore pressure, both of which promote the effects of dilatancy[9]. When strong dilatancy is imposed in a numerical earthquake cycle model representing western Gofar, with three segments straddling two M6 rupture areas, coseismic ruptures are limited to two ~20-km zones separated by a “barrier” of ~15 km (Fig. 1). This suggests dilatancy is an effective mechanism for stabilizing seismic

[1] McGill University, yajing.liu@mcgill.ca
[2] Woods Hole Oceanographic Institution, jmcguire@whoi.edu
[3] Boston College, mark.behn@bc.edu

slip on RTFs, even under velocity-weakening conditions. In addition to steady interseismic slip accumulation, the barrier zone episodically accelerates to a creep event (Fig. 1b-e), where the majority of the creep is released in ~10 days, resulting in an average along-strike migration speed of ~1 km/day, matching that of seismic swarm migration on EPR RTFs. Thus, aseismic transient slip may be the driving mechanism for seismicity swarms on Gofar, such as inferred for continental strike-slip faults and possibly a manifestation of porosity wave migration within the rupture barrier. Although no transient slip events have been observed geodetically along RTFs, their appearance in our numerical model that reproduces the rupture segmentation and foreshock migration along Gofar suggests they may be a common mode of slip release along oceanic ridge transform faults, and prevalent slip mechanism within rupture barriers.

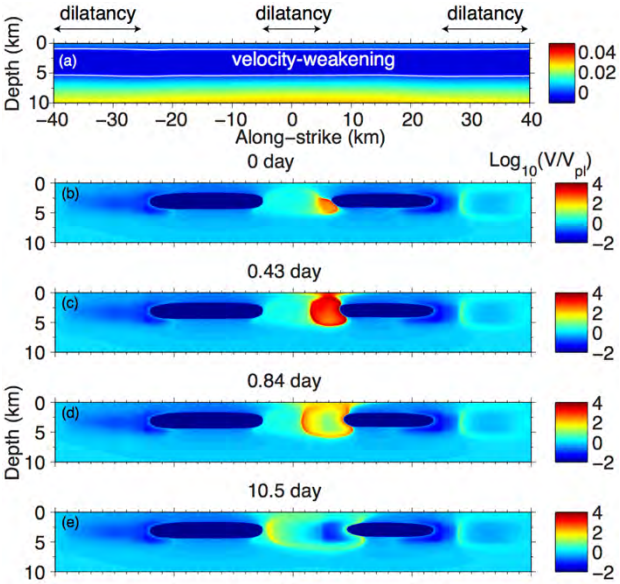

Figure 1. (a) Distribution of rate-state friction parameter (a–b) on a transform fault modeled after Gofar west. Area within the white lines is velocity-weakening (a–b<0, seismogenic); velocity-strengthening (a–b>0, stable sliding) is assigned above and beneath the seismogenic zone. Three along-strike segments, [-40, -25] km, [-5, 5] km and [25, 40] km, are under strong dilatancy-strengthening effect. (b)-(e) Snapshots of fault slip velocity, represented as $\log_{10}(V/V_{pl})$ (V_{pl} is the full spreading rate, 140 mm/yr), during one modeled creep event within the central [-5, 5] km segment. Peak along-strike migration speed is 10-15 km/day. Porosity ϕ =0.05, dilatancy coefficient $\varepsilon = 10^{-4}$.

References

1. Boettcher, M. S., and T. Jordan (2004), Earthquake scaling relations for mid-ocean ridge transform faults. *Journal of Geophysical Research* **109**, doi:10.1029/2004jb003110.
2. Abercrombie, R. E. & Ekstrom, G. (2001), Earthquake slip on oceanic transform faults. *Nature* **410**, 74-77, doi:10.1038/35065064.
3. McGuire, J. J. (2008), Seismic Cycles and Earthquake Predictability on East Pacific Rise Transform Faults. *Bulletin of the Seismological Society of America* **98**, 1067-1084, doi:10.1785/0120070154.
4. McGuire, J. J. *et al.* (2012), Variations in earthquake rupture properties along the Gofar transform fault, East Pacific Rise. *Nature Geoscience* **5**, 336-341, doi:10.1038/ngeo1454.
5. Froment, B. *et al.* (2014), Imaging along-strike variations in mechanical properties of the Gofar transform fault, East Pacific Rise. *Journal of Geophysical Research: Solid Earth* **119**, 7175-7194, doi:10.1002/2014jb011270.
6. Roland, E., Lizarralde, D., McGuire, J. J. & Collins, J. A. (2012), Seismic velocity constraints on the material properties that control earthquake behavior at the Quebrada-Discovery-Gofar transform faults, East Pacific Rise. *Journal of Geophysical Research* **117**, doi:10.1029/2012jb009422 .
7. Wolfson-Schwehr, M., Boettcher, M. S., McGuire, J. J. & Collins, J. A. (2014), The relationship between seismicity and fault structure on the Discovery transform fault, East Pacific Rise. *Geochemistry, Geophysics, Geosystems* **15**, 3698-3712, doi:10.1002/2014gc005445.
8. Harris, R.A., and S. M. Day (1999), Dynamic 3D simulations of earthquakes on En Echelon faults, *Geophys. Res. Lett.*, doi:10.1029/1999GL900377.
9. Segall, P. & Rice, J. R. (1995), Dilatancy, compaction, and slip instability of a fluid-infiltrated fault. *Journal of Geophysical Research* **100**, 22,155-122,171.

GeoProc2019: Earthquake and Faulting mechanics

7th International Conference on Coupled THMC Processes in Geosystems
3-5 July 2019 Utrecht (Netherlands)

A thermo-chemo-mechanical model to explain the velocity dependence of friction in fault gouges

H. Rattez[1], M. Veveakis[2]

Keywords: Fault mechanics, THCM couplings, viscoplasticity, pseudo-arclength continuation methods.

A dramatic decrease of friction has been observed in many experiments performed on synthetic or recovered fault core samples at seismic slip rates for different materials (Di Toro et al. 2011). This phenomenon has major implications to understand the creation of earthquakes in the brittle part of the lithosphere as it plays a role on the stress drop and thus the energy budget (Scholz 2002), but also on the stability of a fault (Spagnuolo et al. 2016). These observations have become possible thank to the development of new experimental apparatus that allows to shear the material at high velocities under high normal stresses (Di Toro et al. 2010; Tsutsumi and Shimamoto 1997).

In this study, we show that this behavior of the friction coefficient can be explained as a coupled multi-physical effect. We consider the fault core an infinite sheared layer and deploy thermo-chemo-mechanical couplings to account for the most important mechanisms involved in a fault zone (Rattez 2017). In particular, the increasing velocity during a seismic slip induces a temperature rise, which in turn can trigger chemical reactions that affect the shear stress of the system (Veveakis et al. 2010). The steady state of the system of equations obtained can be studied using pseudo-spectral methods together with a pseudo-arclength continuation algorithm (Alevizos, Poulet, and Veveakis 2014).

The evolution of friction at steady state for a given imposed velocity is general and can account for a wide variety of chemical processes. The model fits adequately results of experiments performed on various materials encountered in fault zones (Figure 1) such as clay (Ferri et al. 2011), halite (Buijze et al. 2017), carbonate (Boneh and Reches 2018) and granite (Spagnuolo et al. 2016). This study also allows to obtain the activation energy for the temperature weakening and chemical strengthening processes and highlight the importance of thermo-chemo-mechanical couplings in the nucleation and propagation of seismic slips.

[1] Duke University, hadrien.rattez@duke.edu
[2] Duke University, manolis.veveakis@duke.edu

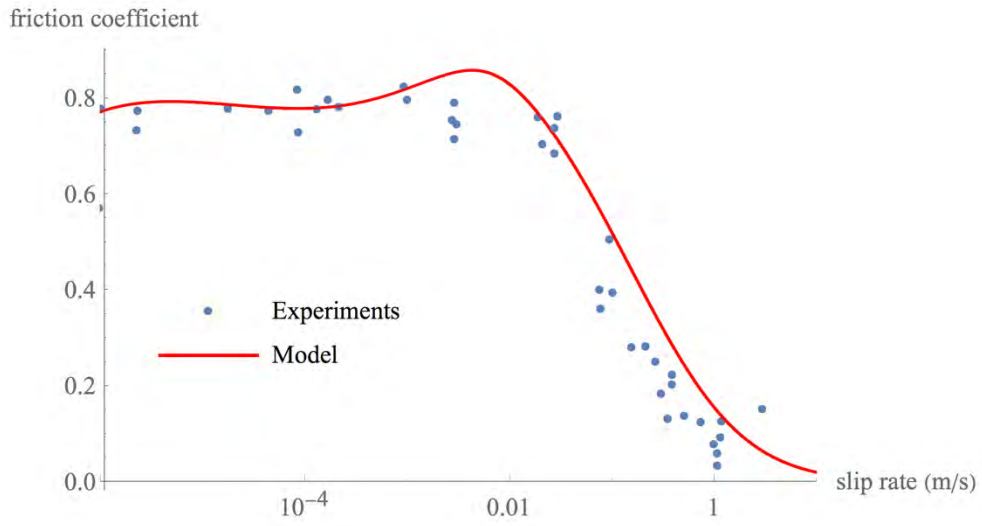

Figure 1. Comparison of the model with experimental data for carbonate rocks gathered in (Boneh and Reches 2018) and in (Spagnuolo et al. 2016)

References

Alevizos, S., Thomas Poulet, and Manolis Veveakis. 2014. "Thermo-Poro-Mechanics of Chemically Active Creeping Faults. 1: Theory and Steady State Considerations." *Journal of Geophysical Research: Solid Earth*.

Boneh, Yuval, and Ze'ev Reches. 2018. "Geotribology - Friction, Wear, and Lubrication of Faults." *Tectonophysics* 733(July 2017): 171–81.

Buijze, Loes et al. 2017. "Friction Properties and Deformation Mechanisms of Halite(-Mica) Gouges from Low to High Sliding Velocities." *Earth and Planetary Science Letters* 458: 107–19.

Ferri, Fabio et al. 2011. "Low- to High-Velocity Frictional Properties of the Clay-Rich Gouges from the Slipping Zone of the 1963 Vaiont Slide, Northern Italy." *Journal of Geophysical Research: Solid Earth* 116(9): 1–17.

Rattez, Hadrien. 2017. "Thermo-Hydro-Mechanical Couplings and Strain Localization in Cosserat Continuum: Application to Stability Analysis of Rapid Shear in Faults." Université Paris-Est.

Scholz, Christopher H. 2002. *The Mechanics of Earthquakes and Faulting*. Second Edi. Cambridge.

Spagnuolo, E., S. Nielsen, M. Violay, and G. Di Toro. 2016. "An Empirically Based Steady State Friction Law and Implications for Fault Stability." *Geophysical Research Letters* 43(7): 3263–71.

Di Toro, Giulio et al. 2010. "From Field Geology to Earthquake Simulation: A New State-of-The-Art Tool to Investigate Rock Friction during the Seismic Cycle (SHIVA)." *Rendiconti Lincei* 21(Suppl. 1): 95–114.

Di Toro, Giulio et al. 2011. "Fault Lubrication during Earthquakes." *Nature* 471(7339): 494–98.

Tsutsumi, Akito, and Toshihiko Shimamoto. 1997. "High-Velocity Frictional Properties of Gabbro." *Geophysical Research Letters* 24(6): 699–702.

Veveakis, E et al. 2010. "Chemical Reaction Capping of Thermal Instabilities during Shear of Frictional Faults." *Journal of the Mechanics and Physics of Solids* 58(9): 1175–94.

GeoProc2019: Earthquake and Faulting mechanics

7th International Conference on Coupled THMC Processes in Geosystems
3-5 July 2019 Utrecht (Netherlands)

Induced Earthquakes: Parameterized and Put to Use

David Dempsey [1]

Keywords: Induced seismicity

Every observation of an induced earthquake is a small window into the crustal conditions where that event was triggered. Collating a large catalog of these windows leads us to establish a kind-of “best consensus” about the properties and state of the crust. This inference alone can be valuable, for instance, in revealing where and by how much permeability has been increased around a stimulated well. However, characterising the crust is also a helpful precursor to generating induced seismicity forecasts. Knowing (in a probabilistic sense) where, how many, and what magnitude earthquakes to expect in the next several years can help communities prepare for the future, or governments and operators to change their behaviour.

In this talk, I will introduce the earthquake hypocentre density and its uncertainty, and how this links to fluid pressure, rock permeability, and crustal stress. Then, I will show how computer models can be trained to replicate the hypocentre density, thereby imaging the stimulation at Enhanced Geothermal System wells. I will also show how such models can make predictions of future seismicity in Groningen and Oklahoma under different modes of operation.

[1] University of Auckland, New Zealand, d.dempsey@auckland.ac.nz

GeoProc2019: Earthquake and Faulting mechanics

7th International Conference on Coupled THMC Processes in Geosystems
3-5 July 2019 Utrecht (Netherlands)

Numerical Modeling of Fluid-Induced Slip on a Rate-and-State Fault Motivated by a Field Experiment

S. Larochelle[1], *N. Lapusta*[2], *J.-P. Ampuero*[3], *F. Cappa*[4]

Keywords: induced seismicity, numerical modeling, fluid injections, aseismic slip, hydro-mechanical coupling

Numerous activities in the geo-energy industry (e.g., hydraulic fracking, wastewater disposal, CO_2 sequestration and enhanced geothermal systems) involve fluid injections into the shallow crust (~1 to 5 km depth). That these fluid injections can induce fault slip (either seismic or aseismic) is now well recognized from surface and borehole observations. When injected directly into a fault system, fluids decrease fault strength by increasing pore pressure. This strength drop may in turn result in seismic or aseismic slip. However, what conditions promote stable versus unstable failure, and the exact physical mechanisms at play are still poorly understood. For example, the fluid-injection field experiment described by Guglielmi et al. (2015) resulted in aseismic slip first, followed by a sequence of 80 seismic events (i.e. microearthquakes), with the initial aseismic slip attributed to velocity-strengthening rate-and-state properties based on a spring-slider model.

In this study, we seek to determine the range of frictional regimes consistent with these experimental observations through numerical simulations of slip on a fault in a continuum medium. Specifically, we simulate slip on a rate-and-state fault embedded in a homogeneous elastic medium and subjected to increasing pore pressure at the injection site, with the fault and pore pressure parameters informed by the Guglielmi et al.'s study. We use an elastodynamic boundary-integral code (Lapusta et al., 2000; Noda and Lapusta, 2013) supplemented with fluid pressure diffusion along the fault. We find that fault models with velocity-weakening friction can better explain the initial aseismic slip than velocity-strengthening ones. Indeed, attempted but arrested nucleation events generated in the velocity-weakening simulations might be the cause of the episodes of (aseismic) slip acceleration observed during the experiment. Constraining the frictional parameters further, however, would require more experimental studies with simultaneous measurements of fluid pressure, fault-normal

[1] California Institute of Technology, Pasadena, CA, USA, stacy.larochelle@caltech.edu
[2] California Institute of Technology, Pasadena, CA, USA, lapusta@caltech.edu
[3] Université Côte d'Azur, France, ampuero@geoazur.unice.fr
[4] Université Côte d'Azur, France, cappa@geoazur.unice.fr

and fault-parallel displacements and seismicity, both at the injection site and its surroundings.

By extending the simulations to a longer injection schedule, we can also investigate whether injecting fluids in this particular setting could eventually induce significant seismicity. Holding the injection pressure constant at its maximum value for an additional hour after the initial half-hour injection, we find that the model can produce continued aseismic slip (Figure 1), contained seismic event(s) (Figure 1) and/or a runaway rupture (Galis et al., 2017) depending on the frictional parameters prescribed (as reported by Gischig, 2015). These fully-dynamic simulations could be a helpful tool to assist in the design and planning of future injection experiments (e.g., SEISMS, Savage et al., 2017) which could provide invaluable insight into the physics of both induced and natural earthquakes.

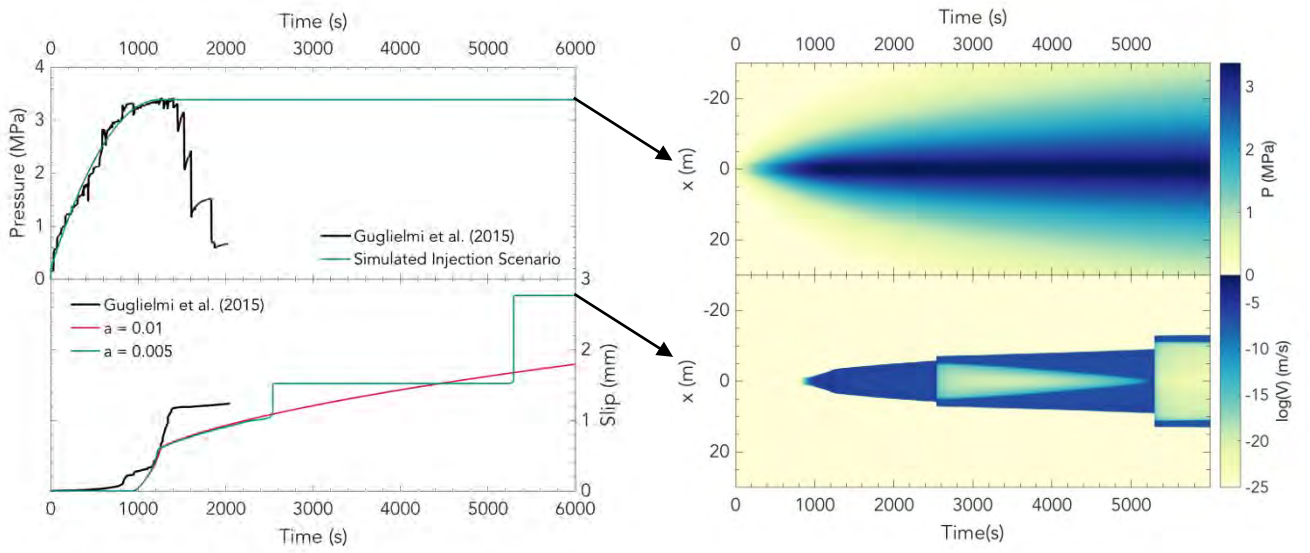

Figure 1. Sample modeled and measured pressure and fault slip at a point at the center of the fault (left) and for the central portion of the fault (right). The left bottom panel shows that extending the injection can result in stable aseismic slip or in substantial seismic events, depending on the frictional parameters prescribed.

References

Galis, M., J.-P. Ampuero, P. M. Mai and F. Cappa (2017), Induced seismicity provides insight into why earthquake ruptures stop, *Science Adv.* 3(12), eaap7528, doi: 10.1126/sciadv.aap7528.

Gischig, V. S. (2015), Rupture propagation behavior and the largest possible earthquake induced by fluid injection into deep reservoirs, *Geophys. Res. Lett*, *42*(18), 7420–7428, doi: 10.1002/2015GL065072.

Guglielmi, Y., F. Cappa, J.-P. Avouac, P. Henry and D. Elsworth (2015), Seismicity triggered by fluid injection-induced aseismic slip, *Science*, *348*(6420), 1224–1226, doi: 10.1126/science.aab0476.

Lapusta, N., J. R. Rice, Y. Ben-Zion and G. Zheng (2000), Elastodynamic analysis for slow tectonic loading with spontaneous rupture episodes on faults with rate- and state- dependent friction, *J. Geophys. Res. Solid Earth, 105*(B10), 23765-23789, doi: 10.1029/2000JB900250.

Noda, H. and N. Lapusta (2013) Stable creeping fault segments can become destructive as a result of dynamic weakening, *Nature, 493*, 518-521, doi: 10.1038/nature11703.

Savage, H. M., J. D. Kirkpatrick, J. J. Mori, E. E. Brodsky, W. L. Ellsworth, B. M. Carpenter, X. Chen, F. Cappa and Y. Kano (2017), *Sci. Dril., 23*, 57-63, doi: 10.5194/sd-23-57-2017.

GeoProc2019: Earthquake and Faulting mechanics

7th International Conference on Coupled THMC Processes in Geosystems
3-5 July 2019 Utrecht (Netherlands)

Injection-Induced Seismicity and Aseismic Fault Slip in Laboratory and In-Situ Experiments and Hydromechanical Models

Marco Maria Scuderi[1], Frédéric Cappa[2,3], Cristiano Collettini[1,4], Yves Guglielmi[5] and Jean-Philippe Avouac[6]

Keywords: induced seismicity, multiscale study, fluid injection experiments

Injection of fluids into the deep subsurface can at times generate measurable or even damaging earthquakes, but often they only produce aseismic deformations along faults and fractures. Understanding the relationship between variations in the state of stress associated with injected pressure and aseismic vs. seismic deformation is a fundamental problem in the estimation of how the crust responds to fluid injection and the associated induced seismic hazard.

In this study, we couple laboratory and in-situ measurements of fault-parallel ('slip') and fault-perpendicular ('opening') displacement during controlled fluid injection experiments. We compare the in-situ fluid injection experiment with laboratory unconventional creep tests and find that in both cases increasing fluid pressure causes accelerated aseismic creep that is accompanied by fault dilation.

To unravel the origin of the observed fault behavior, we characterized fault frictional stability at different levels of fluid pressure by performing velocity step experiments and retrieve the rate- and state- frictional properties. We show that as fluid pressure is increased the fault evolves from velocity strengthening to weakening at slow slip rate. However, as the slip rate is increased we document a transition to velocity strengthening independently of the fluid pressure level.

We use the results from laboratory experiments to inform a three-dimensional hydromechanical model to test if these properties are consistent with the in-situ observations and shed light on the origin of aseismic deformation and seismicity. We find that aseismic slip initiates within the pressurized region, however, earthquakes nucleation is inhibited because the size of the critical nucleation length remains bigger than the pressurized radius. Nonetheless, sustained aseismic creep can accumulate shear stress beyond the pressure front favoring seismicity in nearby prone areas.

Through our multiscale investigation, we demonstrate that fault slip induced by fluid injection in a natural fault at the decametric scale is quantitatively consistent with fault slip and frictional properties measured in the laboratory. The increase in fluid pressure first induces accelerating aseismic creep and fault opening. As the fluid pressure increases further, friction becomes significantly rate-strengthening favoring aseismic slip. Our study reveals how coupling between fault slip and fluid flow promotes stable fault creep during fluid injection. Seismicity is most probably triggered indirectly by the fluid injection due to loading of non-pressurized fault patches by aseismic creep.

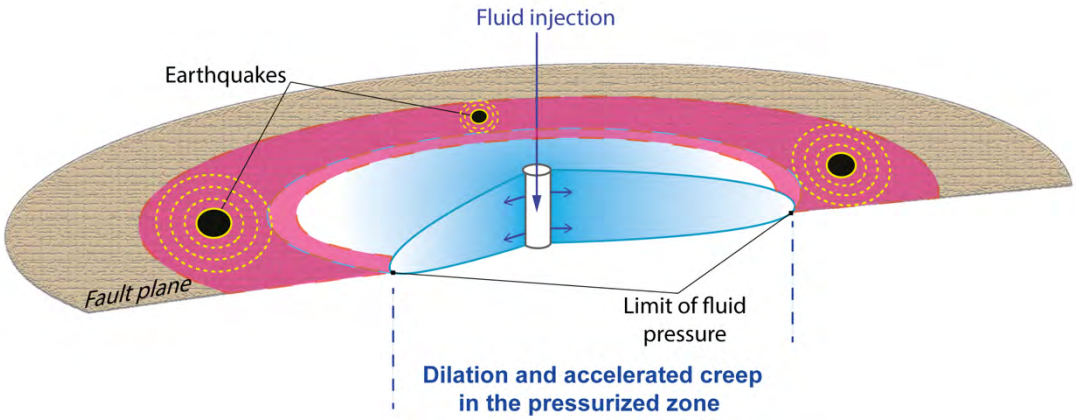

Figure: Conceptual illustration of evolution of fault stability during fluid injection derived from experimental evidence and numerical modeling. Fault opening and accelerating creep occur in the pressurized area, whereas, at its limit and beyond, the fault accumulates shear stress caused by propagating creep, which, at least, helps to trigger seismic slip.

Affiliations

[1] Dipartimento di Scienze della Terra, La Sapienza Università di Roma, Piaz. Aldo Moro 5, 00185 Rome, Italy

[2] Université Côte d'Azur, CNRS, Observatoire de la Côte d'Azur, IRD, Géoazur, 06560 Sophia Antipolis, France

[3] Institut Universitaire de France, Paris, France

[4] Istituto Nazionale di Geofisica e Vulcanologia, via di Vigna Murata 605, 00143 Rome, Italy

[5] Lawrence Berkeley National Laboratory, Earth and Environmental Sciences, Berkeley, CA 94720, USA

[6] California Institute of Technology, Seismological Laboratory, Pasadena, CA 91125, USA

GeoProc2019: Earthquake and Faulting mechanics

7th International Conference on Coupled THMC Processes in Geosystems
3-5 July 2019 Utrecht (Netherlands)

Subsurface Sensing of Fault and Fracture Networks with Nonlinear Chemical Wave Tracing

T. Dewers[1], *J. Heath*[2], *R. Jensen*[3], *K. Kuhlman*[4]

Keywords: chemical waves, fracture networks, nonlinear tracers, unconventional computing

Detection and characterization of fault and fracture networks is a prerequisite toward understanding and control of subsurface engineering endeavors. Here we discuss use of chemical waves in a novel nonlinear tracing method to detect aspects of fracture networks at subseismic resolution. Chemical waves are self-sustaining disturbances in chemical or other variables that propagate over distance with minimal attenuation (Ortoleva, 1992). Such spatio-temporal waves stem from nonlinear coupling of transport and chemical reaction, phase transition, or electrical excitation under far-from-equilibrium conditions. Much of fundamental understanding on chemical waves owes to the famous Belousov-Zhabotinsky (BZ) reaction (Field et al., 1972) involving a metal-catalyzed oxidation of an organic substrate by bromate. Under certain chemical conditions, the autocatalytic production of $HBrO_2$ is a positive feedback which underlies a range of processes including temporal oscillations between oxidized and reduced states, spatial propagation of chemical wave fronts of various morphologies, excitability, and bi-stability. From this richness in behavior have sprung concepts associated with “liquid chemical computing”: chemical waves interacting with a geometrical medium can be used as chemical switches (Rossler, 1974); logic gates (Hjelmfelt and Ross, 1995); chemical neural networks and Turing machines (Hjelmfelt et al., 1991); and coherent chemical clocks (Winfree, 2002). Generally, chemical kinetics systems with multiple stationary states coupled to transport can support chemical waves with the ability to provide information on spatial networks through which they propagate (Hjelmfelt et al., 1993; Steinbeck et al., 1996).

We apply these concepts to fracture/fault networks in the geologic subsurface. Microfluidic experiments and accompanying simulation of a modified BZ system (Figures 1 and 2) demonstrate chemical waves interacting with porous and fractured media, which can serve as subsurface computational tools and a mechanism for subsurface sensing. Propagation of excitable chemical waves is dependent on morphology of the microfluidic cells, and thus advancement or hindrance of wave

[1] Nuclear Waste Disposal Research and Analysis, Sandia National Laboratories, Albuquerque, New Mexico, USA, tdewers@sandia.gov
[2] Geomechanics, Sandia National Laboratories, Albuquerque, New Mexico, USA, jeheath@sandia.gov
[3] Geomechanics, Sandia National Laboratories, Albuquerque, New Mexico, USA, rpjense@sandia.gov
[4] Applied Systems Analysis and Research, Sandia National Laboratories, Albuquerque, New Mexico, USA, klkuhlm@sandia.gov

propagation by pore or fracture of critical size form simple chemical switches and/or logic gates. We show how operation of rock texture on the chemical dynamics provides information unique to the porous medium. Contrasting with typical linear tracers, chemical waves can propagate faster than conservative tracers, and even propagate against an advective gradient. With a generalized “oregonator” (Field and Noyes, 1974) type dynamics (employed in simplified 2D push-pull numerical experiments), we suggest that chemical waves act as nonlinear tracers reporting on form, connectivity, and aperture distributions of connected fault and/or fracture networks.

Funding for this research was graciously provided by the Sandia National Laboratories Laboratory Directed Research and Development program. Sandia National Laboratories is a multimission laboratory managed and operated by National Technology & Engineering Solutions of Sandia, LLC, a wholly owned subsidiary of Honeywell International Inc., for the U.S. Department of Energy’s National Nuclear Security Administration under contract DE-NA0003525. SAND2018-12720A.

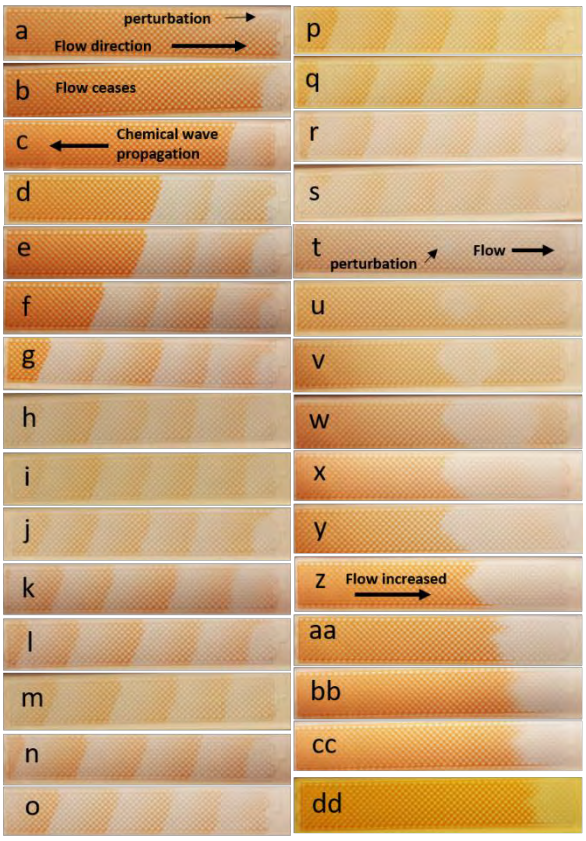

Figure 1 (Left). Bromate-Ferroin-CHD BZ reaction system in regular microfluidic cell. Orange indicates presence of Fe^{3+}; white indicates presence of Fe^{2+}. Under zero flow condition, a series of traveling chemical waves initiates (b) and propagates (d-s) from right to left with periodic spacing. When flow at a rate of 3 μL/min initiates from left to right, the waves are wiped out, but an initial perturbation of Fe^{2+} reduced region (t) grows (u), and the right boundary propagates (v-y) with flow. With higher flow (z), the reduced region propagates with the flow replaced by oxidized region. (aa-dd). **Figure 2** (below). Results for time-dependent chemical oscillations showing sensitivity and excitability to porous domains and fracture-matrix interaction.

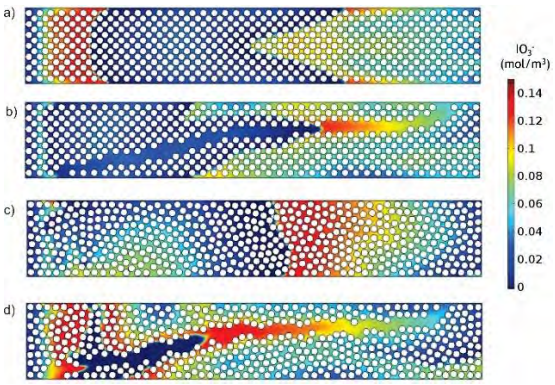

References

Field, R.J., Koros, E., and Noyes, R.M., 1972, Oscillations in chemical systems. II. Thorough analysis of temporal oscillation in the bromate-cerium-malonic acid system. J. Am. Chem. Soc. 94, 8649-8664.

Field, R.J., and Noyes, R.M. (1974) Oscillations in chemical systems. IV. Limit cycle behavior in a model of a real chemical reaction. J. Chem. Phys. 60, 1877-1884.

Hjelmfelt, A., Weinberger, E., and Ross, J., 1991, Chemical implementation of neural networks and Turing machines. Proc. Natl. Acad. Sci. 88, 10983-10987.

Hjelmfelt, A., Schneider, F.W., and Ross, J., 1993, Pattern recognition in coupled chemical kinetic systems. Science 260 (5106), 335-337.

Steinbeck, O., Kettunen, P., and Showalter, K. (1996) Chemical wave logic gates. J. Phys. Chem. 100, 18970-18975.

Ortoleva, P. (1992) Nonlinear Chemical Waves. John Wiley and Sons, New York, 302p.

Winfree, A. (2002) On emerging coherence. Science 298, 2336-2337.

GeoProc2019: Earthquake and Faulting mechanics

7th International Conference on Coupled THMC Processes in Geosystems
3-5 July 2019 Utrecht (Netherlands)

The interplay of fault zone structure and fluid flow in controlling crustal seismicity

T.M. Mitchell[1]

Keywords: Faults, fluid flow, seismicity, fluid injection, Andean tectonics, Iceland

Faults zones are not only the loci for both coseismic and aseismic displacement, but they also accommodate significant fluid flow. Fault damage provides heterogenous permeability structures that allow fluids (*e.g. magma, water, CO_2*) to migrate in time and space. This heterogenous structure and subsequent flow also generates heterogenous pore pressure distributions, and therefore spatial variations in effective pressure and fault strength can be directly rated to fault hydraulic structure. The rate these variations in effective pressures build up are dependent on the rate the fluids are generated at source, and the dynamic permeability structure in fault zones controlling the subsequent distribution. Fault structure therefore plays a key role on the migration of fluid-driven seismicity. In this study, I will show two examples of fault systems where heterogenous fault structures and fluid pressures control the generation and migration of seismicity, where fluid sources are from 1) natural deep magmatic sources in the central Chilean Andes and 2) induced anthropogenic sources in an Icelandic geothermal system. Fault structure is mapped using high resolution multiscale datasets of fault zone damage patterns from the micro- to km-scale, on active and inactive fault zones. This damage has been quantified using state of the art damage analysis techniques, from CT scanning at the microscopic scale, to using drones and photogrammetry/structure-from-motion to produce high resolution macroscopic structure, damage and alteration maps both along strike and perpendicular to, major active and inactive fault structures.

In Chile, results will be shown from data collected from a seismic network deployed for 2 years in the south-central Chilean Andes. The study focuses around the volcanically and seismically active Tinguiririca and Planchon-Peteroa volcanoes that are considered to be tectonically related to the major Miocene-Pliocene El Fierro thrust fault system, providing high-resolution earthquake locations and seismic tomography that can be directly related to detailed fault structure at the surface, in addition to inversions with gravimetric and magnetotelluric surveys. In Iceland, results will be shown from the Hengill geothermal system in south-west Iceland, where significant seismicity is induced and recorded during fluid injection into reservoirs used for geothermal energy extraction and carbon dioxide capture, and is strongly controlled by pre-existing highly-permeable fault structures. The Hengill geothermal system is located in a divergent plate boundary between the North America and Eurasia plates, where new oceanic crust is constantly created forming the current basaltic platform that constitutes Iceland.

[1] UCL Rock deformation laboratory & Seismolab, University College London, tom.mitchell@ucl.ac.uk

GeoProc2019: Earthquake and Faulting mechanics

7th International Conference on Coupled THMC Processes in Geosystems
3-5 July 2019 Utrecht (Netherlands)

Strain induced chemico-mechanical feedbacks suggest cyclic seismic behaviour in Alpine slate-belt

Ismay Vénice Akker[1], Christoph E. Schrank[2], Michael W. M. Jones[3], Cameron M. Kewish[4,5,6], Alfons Berger[1] and Marco Herwegh[1]

Keywords: Accelerating foreshocks, Frictional heterogeneities, Earthquake cycle simulations, Rate and state friction, Earthquake Dynamics, Slow slip

The strength of the upper crust is defined by frictional processes (brittle behaviour) and viscous processes dominate in the middle and lower crust. The transition between brittle and viscous behaviour represents the base of the seismogenic zone (e.g. Wintsch and Yeh, 2013). Here, we show for slates with peak metamorphic temperatures around 300°C, evidence for both mechanisms by a strong coupling between mechanical and chemical feedback processes.

The studied slates are part of the sedimentary sequence of Flysch, making up the Alpine paleo-accretionary wedge in eastern Switzerland (Dielforder et al., 2015). In the slates, zones of strain localisation are characterised by densely foliated tectonites with a reduced grainsize relatively to the surrounding host rock. In addition, such zones are dominated by many layer parallel shear veins, forming vein arrays. The shear veins indicate a multitude of stages of brittle incremental slip (few 10th of microns) resulting in the opening of fractures. Such fractures are subsequently filled with calcite.

We show along an increase of strain the evolution from a carbonate-rich and sheet-silicate-poor rock to a carbonate-poor and sheet-silicate-rich rock (Figure 1). We suggest that strain weakening by pressurized intergranular fluids leads to slip events along the shear planes of the shear veins, where during these slip events the fluids move into the dilatant parts. This process precipitates calcite inside the newly formed gaps. Such combined slip and precipitation processes are fast, maybe even at seismic rates. In contrast, slow dissolution of calcite in the slate domains under viscous granular flow conditions leads to (a) a depletion in calcite and (b) a related relative enrichment of sheet silicates. In addition, the sheet silicates (mainly white mica and chlorite) are recrystallizing, which generates a densely spaced foliation as well as an overall grain size reduction. The resulting strain softening helps to localize strain further and indicates where the renewed mobilization of fluids will take place. Solution/precipitation, recrystallization (sheet silicates), grain boundary sliding and pressure solution (calcite) are interacting processes. Our data

[1] Institute of Geological Sciences, University of Bern, Bern, Switzerland ; [2] School of Earth, Environmental, and Biological Sciences, Queensland University of Technology, QLD 4000, Australia ; [3] Central Analytical Research Facility, Institute of Future Environments, Queensland University of Technology, QLD 4000, Australia; [4] Department of Chemistry and Physics, La Trobe Institute for Molecular Science, La Trobe University, Victoria 3086, Australia ; [5] Australian Nuclear Science and Technology Organisation, Australian Synchrotron, Victoria 3168,Australia; [6] ARC Centre of Excellence in Advanced Molecular Imaging, La Trobe Institute for Molecular Sciences, La Trobe University, Victoria 3086, Australia

on the quantification of the microstructures (fabric intensity, grain size) in combination with mineral chemistry support these different slow processes. This is also the case for the loci of repeating vein formation as described above.

Hence, the chemico-mechanical feedback in this system suggests a cyclical behaviour of slow (pressure solution, viscous flow) and fast (fractures and related veins) processes as typical for seismic cycles. Given the fact that such high strain zones are spatially rather regularly distributed (50-100 m intervals) at the kilometre-scale, this may indicate that a link exists between grain-scale and wedge-scale processes, which contributes to an overall dehydration of the originally water-rich slate rocks. It is this link which could be in charge for the background seismic activity in slate-belts.

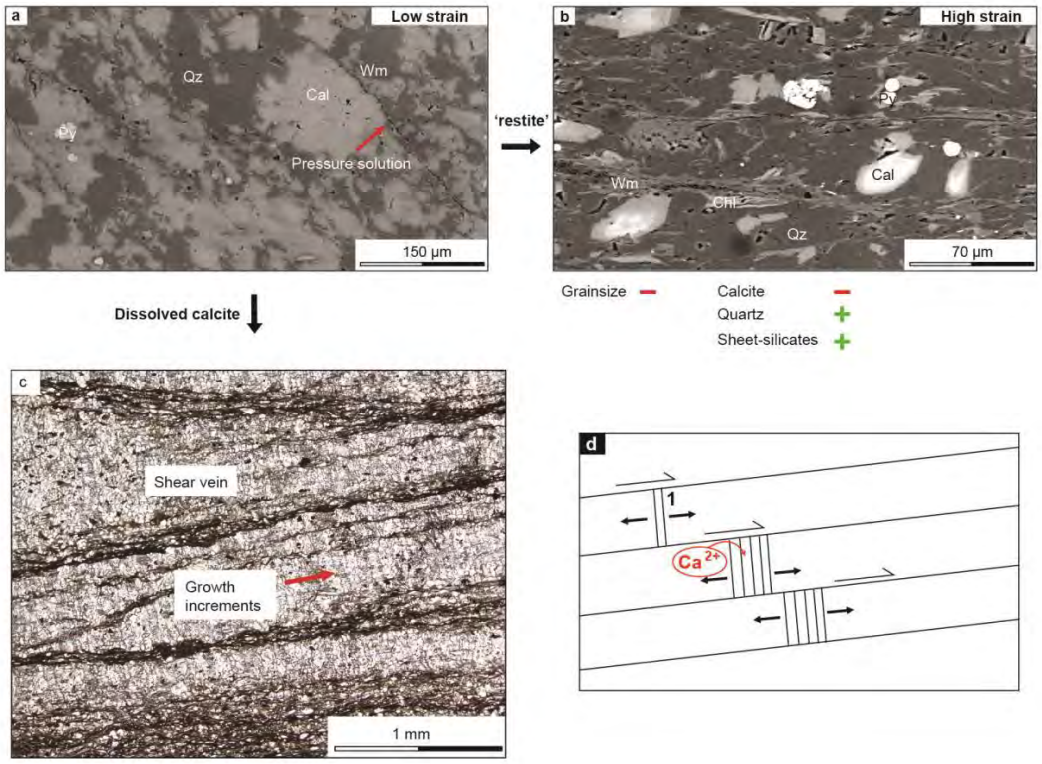

Figure 1. The mechanical and chemical alteration of a slate with increasing strain. a) At the low strain site calcite dissolves seen by pressure solution seams. b) The host rock (‘restite’) at the high strain site is a calcite poor rock, rich in recrystallized sheet-silicates. c) The dissolved calcite precipitates in shear veins. d) incremental dilatancy vein growth of calcite after Fagereng et al., 2010. Qz: quartz, Cal: calcite, Wm: white mica, Chl: chlorite, Py: pyrite.

References

Dielforder, A., Vollstedt, H., Vennemann.T., Berger, A., Herwegh, M., (2015). Linking megathrust earthquakes to brittle deformation in a fossil accretionary complex. Nature Communications, 6, 7504. doi: 10.1038/ncomms8504

Fagereng, Å., Remitti, F., & Sibson, R. H. (2010). Shear veins observed within anisotropic fabric at high angles to the maximum compressive stress. *Nature Geoscience*, *3*(7), 482, doi: 10.1038/ngeo898

Wintsch, R. P., & Yeh, M. W. (2013). Oscillating brittle and viscous behavior through the earthquake cycle in the Red River Shear Zone: Monitoring flips between reaction and textural softening and hardening. *Tectonophysics*, *587*, 46-62, doi: 10.1016/j.tecto.2012.09.019

GeoProc2019: Earthquake and Faulting mechanics

7th International Conference on Coupled THMC Processes in Geosystems
3-5 July 2019 Utrecht (Netherlands)

Co-seismic graphite formation and its enrichment during faulting

H.B. Li[1], J.L. Si[2], C. Janssen[3], L.-W. Kuo[4], H. Wang[5], R. Wirth[6], S.-R. Song[7], Y.-F. Song[8]

Keywords: WFSD, graphite, principal slip zone, Wenchuan earthquake, Longmen Shan

Graphite, a well-known lubricant for the strength reduction, was documented to be produced from the graphitization of carbonaceous materials (CM) during seismic faulting. CM graphitization was extensively investigated by rock deformation experiments under restricted conditions, however, due to the difficulty in determining the cause of seismic faulting, how it processes in natural geological setting remains unclear. Here we report results from the Wenchuan earthquake Fault Scientific Drilling project-1 (WFSD-1) drilled along the Longmen Shan fault belt, which hosted the 2008 Wenchuan earthquake. Borehole logging and drilling core research show that the principal slip zone (PSZ) of the Wenchuan earthquake was located at ~589.2 m (Li et al., 2013), where CM graphitization occurred during fast fault motion. TEM and in situ synchrotron radiation X-ray analyses reveal that graphite was present in a very thin zone (<1 mm) in the PSZ where stress aggregated. Strain is very efficient for triggering CM graphitization (Kuo et al., 2014, 2017), but strain distribution within the PSZ is differential. Our natural observation show CM graphitization occurred only along Y- and P-planes by localized strain, instead of the whole PSZ. CM grains transformed to graphite along Y- and P-planes. Numerical modeling corroborates that P-plane formed in the early stage is transformed into Y-plane during the shear process (Bose et al., 2018). Therefore, once graphite was formed, it might be transported to the Y-plane during the following deformation and enriched in a layer, where the slip strength is very low during the large earthquake.

[1] Key Laboratory of Deep-Earth Dynamics of Ministry of Natural Resources, Institute of Geology, Chinese Academy of Geological Sciences, China, lihaibing06@163.com
[2] Key Laboratory of Deep-Earth Dynamics of Ministry of Natural Resources, Institute of Geology, Chinese Academy of Geological Sciences, China, gongrenbaqin@126.com
[3] GeoForschungsZentrum Potsdam, Germany, jans@gfz-potsdam.de
[4] National Central University, Taiwan, liweikuo@ncu.edu.tw
[5] Key Laboratory of Deep-Earth Dynamics of Ministry of Natural Resources, Institute of Geology, Chinese Academy of Geological Sciences, China, wanghuan4585@126.com
[6] GeoForschungsZentrum Potsdam, Germany, wirth@gfz-potsdam.de
[7] National Taiwan University, Taiwan, srsong@ntu.edu.tw
[8] National Synchrotron Radiation Research Center, Taiwan, song@nsrrc.org.tw

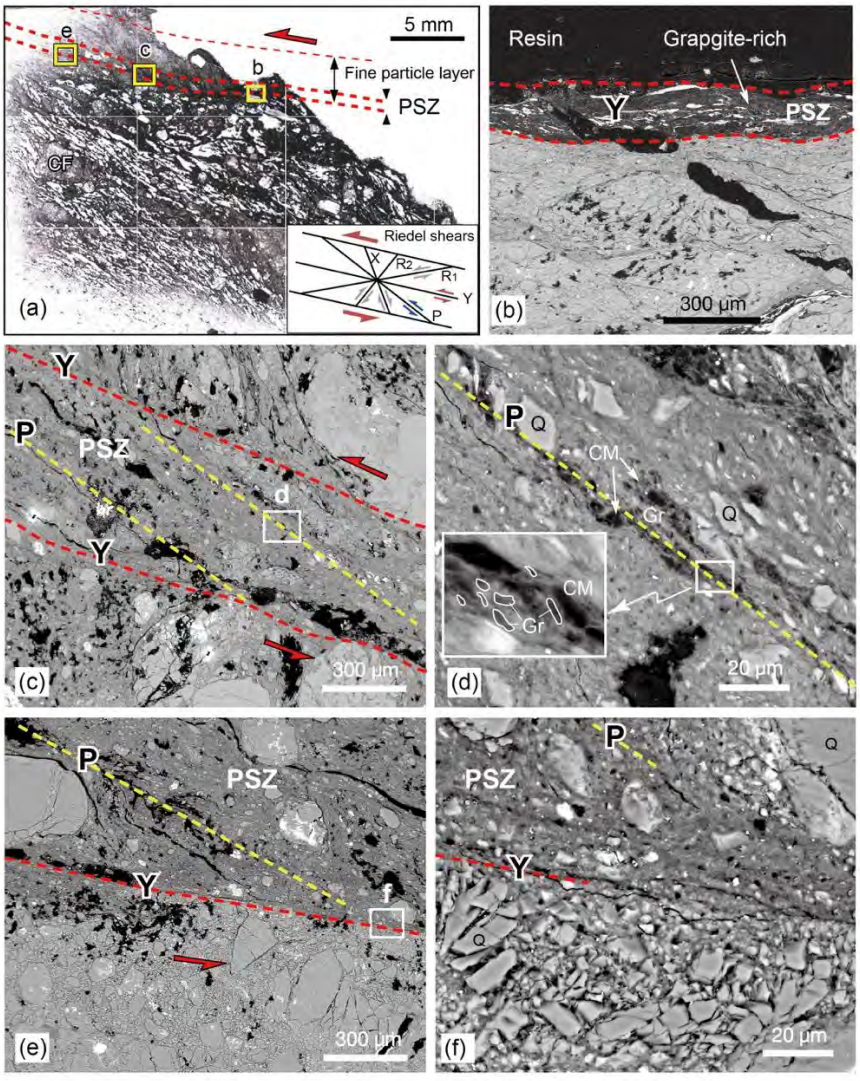

Figure 1. Microstructure of the PSZ of the 2008 Wenchuan earthquake in WFSD-1 drilling cores. Faulting and reworking of shear banding foliation by new Y- and P-planes (red and yellow dotted lines). (a) Microscopic photograph of the PSZ (bold red dotted line range in the fine particle layer). (b-f) Scanning electron microscope (SEM) images. The graphite is enriched along the Y-plane in the PSZ (b). P- and Y-planes developed in the PSZ (c-e). Earlier P-shears are crosscut by Y-shear zones that extend throughout the PSZ(c). The CM and graphite are distributed along the P-plane (f).

References

Li, H.B., H. Wang, Z.Q. Xu, J.L. Si, J.L. Pei, and T.F. Li, et al. Characteristics of the fault-related rocks, fault zones and the principal slip zone in the wenchuan earthquake fault scientific drilling project hole-1 (wfsd-1). *Tectonophysics,* 2013, 584, 23-42.

Kuo L.-W., H.B. Li, S.A.F Smith, G. Di Toro, J. Suppe, S.-R. Song, S. Nielsen, H.-S. Sheu, and J.L Si. Gouge graphitization and dynamic fault weakening during the 2008 Mw 7.9 Wenchuanearthquake. *Geology*, 2014, 42(1): 47-50.

Kuo, L.-W., F. Di Felice, E. Spagnuolo, G. Di Toro, S.-R. Song, S. Aretusini, H.B. Li, J. Suppe, and, et al. Fault gouge graphitization as evidence of past seismic slip. *Geology*, 2017, 45(11): 979-982.

Bose N., D. Dutta, S. Mukherjee. Role of grain-size in phyllonitisation: Insights from mineralogy, microstructures, strain analyses and numerical modeling. *Journal of Structural Geology*, 2018, 112, 39-52.

GeoProc2019: Earthquake and Faulting mechanics

7th International Conference on Coupled THMC Processes in Geosystems
3-5 July 2019 Utrecht (Netherlands)

Frictional melting in fluid-rich faults (Bolfin Fault Zone, Chile)

G. Di Toro[1], M. Fondriest[1], T. Mitchell[2], R. Gomila[1], E. Jensen[3], C. Sommacampagna[1], S. Masoch[1], A. Bistacchi[4], G. Magnarini[2], D. Faulkner[5], J. Cembrano[6], [4]S. Mittempergher

Keywords: pseudotachylyte, foliated cataclasites, fluid-rock interaction, Atacama Fault System, earthquakes

Pseudotachylytes (solidified friction melts produced during seismic slip) are currently considered one of the very few geological markers of seismic faulting in exhumed faults (Rowe and Griffith, 2015). Pseudotachylytes are considered to be rare in the geological record because they are typical of particular seismogenic environments characterized by water-deficient cohesive rocks (Sibson and Toy, 2006) and possibly associated with particular earthquakes with exceptionally large static stress drops (Smith et al., 2013; Beeler et al., 2016). However, experimental evidence suggests that frictional melting may easily occur in the presence of pressurized liquid water (Violay et al., 2014). This possibility is supported by (though rare) occurrence of vesiculated and amygdules-rich pseudotachylytes (Magloughlin, 1989). But even if produced during seismic slip, the delicate pseudotachylyte matrix may alter when permeated by post-seismic fluids and the pseudotachylyte lost from the geological record (Kirkpatrick and Rowe, 2013).

Here we discuss the occurrence of poorly to strongly altered pseudotachylytes hosted in a fluid-rich exhumed fault strand of the Atacama Fault System (Chile, Fig. 1a). The Bolfin Fault Zone (BFZ) is > 30 km long and cuts amphibolites and diorites of the Coastal Cordillera (Cembrano et al., 2005). The BFZ records a series of deformation and veining events lasting from the Jurassic (under granulitic facies) to the Pliocene (T < 150°C). The pseudotachylytes are associated with a dark green in color, foliated, ultracataclastic to mylonitic fault core ~1 m thick which accommodated > 5 km of strike-slip displacement at 6-8 km depth and 280-350°C ambient temperature (Arancibia et al., 2014). The fault core is bounded by an up to 50 m thick damage zone characterized by intense hydrothermal sub-greenschist to greenschist facies alteration. The pseudotachylytes include black to brownish in color cm-thick fault and injection veins, with spectacular flow structures (Fig. 1b-c). The pseudotachylyte consists of suspended clasts of saussiritized feldspar, albite and minor quartz immersed (locally) in a poorly altered and homogenous (glassy-like) feldspathic in composition matrix with tabular microlites of feldspar (Fig. 1d) and (more often) in a strongly altered matrix made of tens of micrometer in size albite, chlorite, and epidote crystals (Fig. 1e). The matrix hosts rounded to ellipsoidal concentric features up to ~1 mm in size with an inner core of

[1] Università degli Studi di Padova, giulio.ditoro@unipd.it (I), [2]University College of London (UK), [3]CIGIDEN (CL), [4]Università di Milano Bicocca (I), [5]University of Liverpool (UK), [6]Pontificia Universidad Catolica de Chile (CL)

chlorite, epidote or calcite and an external rim of quartz (Fig. 1e). These latter features are interpreted as vesicles filled by post-seismic sub-greenschist facies minerals precipitated from the percolating hydrothermal fluids (i.e., amygdules, Fig. 1e).

The identification of pseudotachylytes, the first so far to our knowledge in South America, and its association with intense pre- and post-seismic alteration challenges the common belief that these fault rocks are rare. Consistent with the experimental evidence, pseudotachylytes (1) could be a common coseismic fault product at intermediate crustal depths, (2) may easily be produced in fluid-rich hydrothermal environments as well as fluid absent conditions but, (3) are easily lost from the geological record because they are prone to alteration.

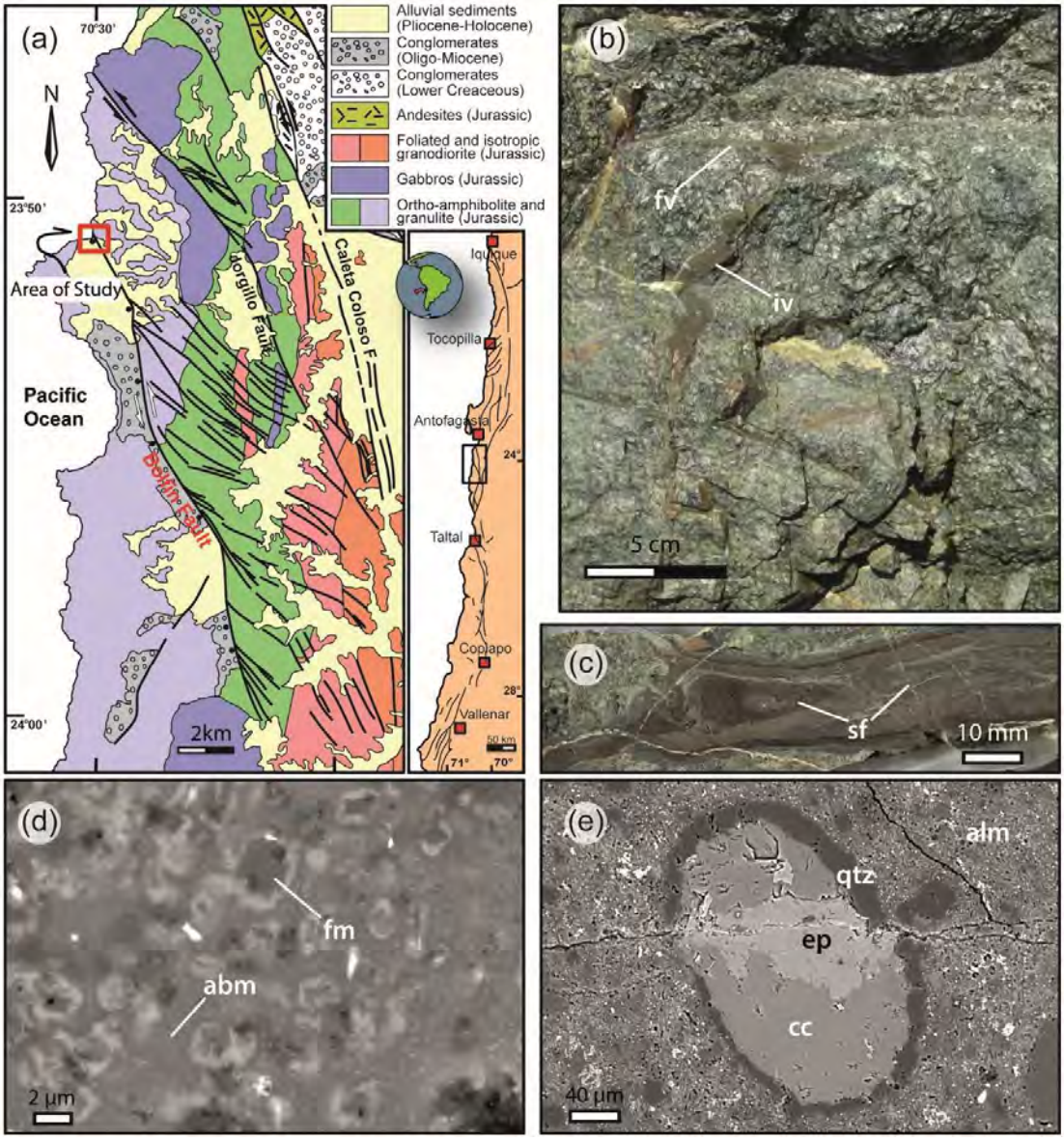

Figure 1. The pseudotachylytes of the Bolfin Fault Zone. **(a)** Geological setting (modified from Cembrano et al. 2005 and Mitchell and Faulkner, 2010). **(b)** Pseudotachylyte fault (fv) and injection (iv) vein (Playa Escondida locality). **(c)** Flow structures with sheath fold-like (sf) structures in the pseudotachylyte (polished sample). **(d)** Tabular feldspar microlites (fm) in the glassy-like altered albitic in composition matrix (abm). **(e)** Ellipsoidal amygdule with external rim of quartz (qtz) and core of calcite (cc) cut by an epidote-bearing vein (ep). The amygdule is hosted in the strongly hydrothermally altered pseudotachylyte matrix (alm) with a typical sub-greenschist facies assemblage (chlorite, epidote and albite). (d) and (e) are Back Scattered Scanning Electron Microscope images.

GeoProc2019: Earthquake and Faulting mechanics

7th International Conference on Coupled THMC Processes in Geosystems
3-5 July 2019 Utrecht (Netherlands)

Two types of foreshock activities observed on a meter-scale laboratory fault: Slow-slip-driven and cascade-up

F. Yamashita[1], *E. Fukuyama*[2], *S. Xu*[3]

Keywords: laboratory experiment, foreshock, slow slip, cascade up

Foreshocks presumably triggered by slow slips were often observed preceding large earthquakes (e.g. Bouchon *et al*., 2011; Kato *et al*., 2012). However, what kind of mechanisms causes foreshocks is still in debate (Ellsworth and Bulut, 2018). To reproduce and investigate foreshock activities in the laboratory, we have conducted stick-slip experiments using large-scale friction apparatus at NIED (Figure 1; Yamashita *et al*., 2015). This apparatus uses a large-scale shaking table as a driving force to apply shear load to the simulated fault. We used two rectangular metagabbro blocks from India as experimental specimens. A longer block (2 m long and 0.1 m wide) was fixed on the shaking table by the frame and a shorter block (1.5 m long and 0.5 m wide) was stacked on the longer one. Therefore, the nominal contacting area was 1.5 m long and 0.1 m wide. Normal load was applied with three jacks via a steel plate on the top block. Side face of the top block was supported with a reaction force bar, the opposite end of which was fixed on the outside floor, so that the top block stayed against the frictional force on the simulated fault. To monitor stress changes and seismic activities on the fault, we installed dense arrays of 32 triaxial rosette strain gauges and 64 PZT seismic sensors along the fault. We repeatedly conducted experiments with the same pair of rock specimens, causing the evolution of damage on the fault. We focus on two experiments successively conducted under the same loading condition (normal stress of 6.7 MPa and loading rate of 10 μm/s) but different initial fault surface conditions; the first experiment preserved the gouge generated from the previous experiment while the second experiment started with all gouge removed. Note that the distribution of gouge was heterogeneous, because we did not make the gouge layer uniform. We observed many foreshocks in both experiments, but found that the *b*-value of foreshocks was smaller in the first experiment with pre-existing gouge (PEG). In the second experiment without PEG, we observed premonitory slow slips during the nucleation process preceding most of the main events. We also found that foreshocks were triggered by the slow slips at the end of the nucleation process. In the experiment with PEG, on the contrary, no clear premonitory slow slips were found. Instead, foreshock activities accelerated towards the main event, as confirmed by a decreasing *b*-value. Spatiotemporal distribution of foreshock hypocenters suggests that foreshocks migrated and cascaded up to the main event. We infer that the heterogeneously distributed gouge caused stress-concentrated and

[1] National Research Institute for Earth Science and Disaster Resilience, Japan, yamafuto@bosai.go.jp
[2] National Research Institute for Earth Science and Disaster Resilience, Japan, fuku@bosai.go.jp
[3] National Research Institute for Earth Science and Disaster Resilience, Japan, shiqing@bosai.go.jp

unstable patches, which impeded stable slow slips but promoted foreshocks on the fault. Further, our results suggest that *b*-value is a useful parameter for characterizing these observations.

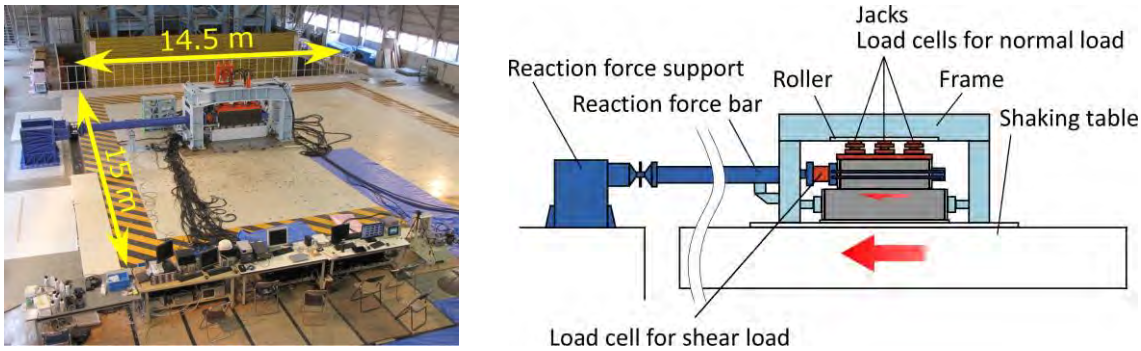

Figure 1. Large-scale friction apparatus at NIED

Acknowledgements: This study was supported by the NIED research project "Large Earthquake Generation Process" and JSPS Kakenhi Grant Numbers JP17H02954, JP16H06477.

References

Bouchon, M., H. Karabulut, M. Aktar, S. Ozalaybey, J. Schmittbuhl, and M.-P. Bouin (2011), Extended nucleation of the 1999 M_w 7.6 Izmit earthquake. *Science*, *331*(6019), 877–880. doi:10.1126/science.1197341.

Ellsworth, W. and F. Bulut (2018), Nucleation of the 1999 Izmit earthquake by a triggered cascade of foreshocks, *Nature Geosci.*, *11*, 531–535, doi: 10.1038/s41561-018-0145-1.

Kato, A., K. Obara, T. Igarashi, H. Tsuruoka, S. Nakagawa, and N. Hirata (2012), Propagation of Slow Slip Leading Up to the 2011 M_w 9.0 Tohoku-Oki Earthquake. *Science*, *335*(6069), 705–708. doi: 10.1126/science.1215141.

Yamashita, F., E. Fukuyama, K. Mizoguchi, S. Takizawa, S. Xu, and H. Kawakata (2015), Scale dependence of rock friction at high work rate, *Nature*, *254*, 257-528, doi:10.1038/nature16138.

GeoProc2019: Earthquake and Faulting mechanics

7th International Conference on Coupled THMC Processes in Geosystems
3-5 July 2019 Utrecht (Netherlands)

Frictional properties of fault zone gouges from the WFSD-3 drilling project (2008 *Mw* 7.9 Wenchuan earthquake)

C.-C. Hung [1], *L.-W. Kuo** [2], *F. Di Felice* [3], *H. Li* [4], *E. Spagnuolo* [5], *G. Di Toro* [6], *J. Si* [7], *H. Wang* [8]

Keywords: WFSD, SHIVA, Longmenshan fault belt, frictional property

The 2008 *Mw* 7.9 Wenchuan earthquake produced two surface ruptures: the Yingxiu-Beichuan fault zone (YBF; ~270 km in length) and the Guanxian-Anxian fault zone (GAF; ~80km in length)[1], the latter proposed both seismic sliding and long-term creeping behavior as the possible deformation mechanism operated during the seismic cycle[2]. However, it remains unknown the frictional strength of the GAF deformed either at seismic slip rates or during creep. Here we first report laboratory strength measurement on the fault gouges recovered from the Wenchuan earthquake Fault Scientific Drilling project-3 (WFSD-3) corresponding to the GAF. The fault gouge (composed of quartz, plagioclase, illite, kaolinite and clinozosite) were deformed at slip velocities of 10 μm s^{-1} to 2 m s^{-1} and normal stresses from 3 to 15 MPa under both room-humidity and water-dampened conditions. Mechanical data of water-dampened gouges at all slip velocities show (1) weaker (apparent friction coefficient ($\mu < 0.1$) than the one under room-humidity conditions ($0.15 < \mu < 0.6$) and, (2) the presence of negligible peak friction. To date, the mineralogical and microstructural characterization of the experimental products were not completed, but our preliminary results indicate that frictional properties of wet WFSD-3 fault gouge could facilitate the transition from aseismic creep to seismic slip in the GAF at shallow crustal depths.

[1] National Central University, Taiwan, cchung08a@gmail.com
[2] National Central University, Taiwan, liweikuo@ncu.edu.tw
[3] Istituto Nazionale di Geofisica e Vulcanologia, Italy, fabio.difelice@ingv.it
[4] Chinese Academy of Geological Sciences, China, lihaibing06@163.com
[5] Istituto Nazionale di Geofisica e Vulcanologia, Italy, elena.spagnuolo@ingv.it
[6] Istituto Nazionale di Geofisica e Vulcanologia, Italy, and University of Padova, Italy, giulio.ditoro@unipd.it
[7] Chinese Academy of Geological Sciences, China, gongrenbaqin@126.com
[8] Chinese Academy of Geological Sciences, China, wanghuan4585@126.com

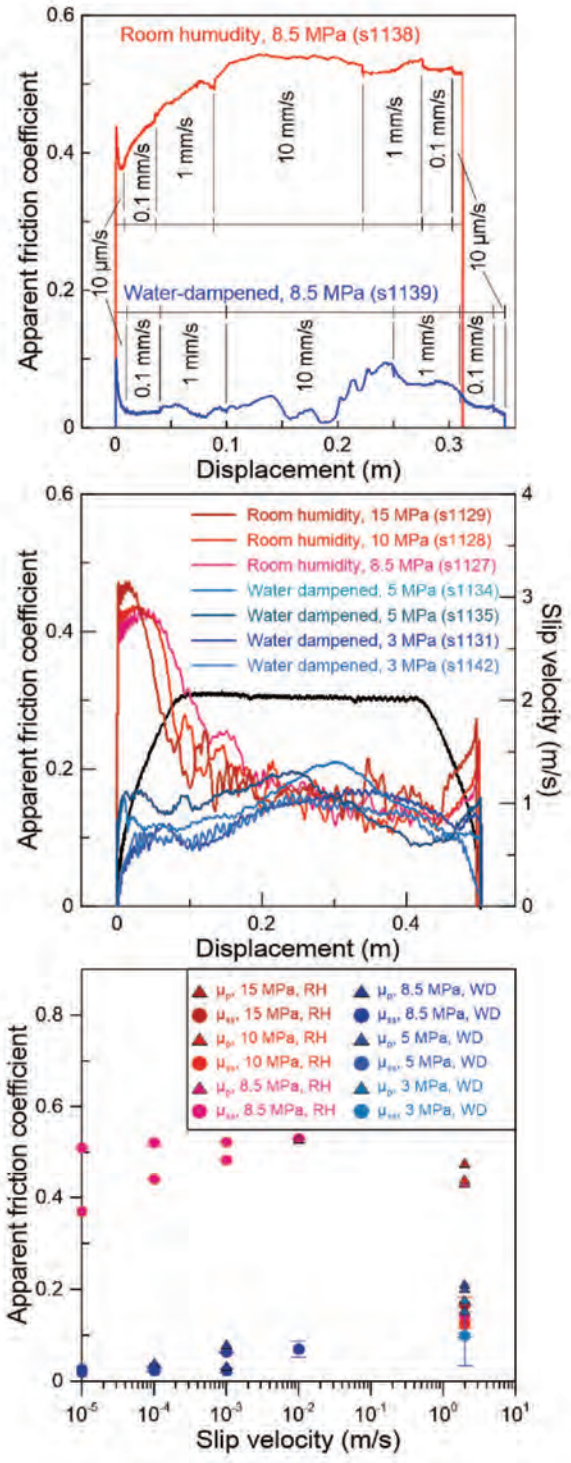

Figure 1. Representative friction experiments performed at low (a) and high (b) velocities under room-humidity and water-dampened conditions. Peak and steady-state apparent friction coefficients derived from (a) and (b) were shown in (c).

References

1. Xu, X., Wen, X., Yu, G., Chen, G., Klinger, Y., Hubbard, J., and Shaw, J. Coseismic reverse- and oblique-slip surface faulting generated by the 2008 Mw7.9 Wenchuan earthquake, China: Geology 37, 515–518 (2009).
2. He, X. L., Li, H. B., Wang, H., Zhang, L., Xu, Z. Q., and Si., J. L. Creeping along the Guanxian-Anxian fault of the 2008 Mw7.9 Wenchuan earthquake in the Longmen Shan, China. Tectonics 37(7), 2124-2141 (2018).

GeoProc2019: Earthquake and Faulting mechanics

7th International Conference on Coupled THMC Processes in Geosystems
3-5 July 2019 Utrecht (Netherlands)

Slip and seismicity preceding earthquakes: Insights from laboratory experiments

M. Acosta[1], F.X. Passelègue[1], A. Schubnel[2], R.Madariaga[2] M. Violay[1]

Keywords: Earthquake Nucleation, Interseismic Coupling, Laboratory Earthquakes

Recent seismological observations highlighted that both aseismic silent slip and/or foreshock sequences can precede large earthquake ruptures (Tohoku-Oki, 2011, Mw 9.0 *(Kato et al., 2012)*; Iquique, 2014, Mw 8.1 *(Ruiz et al, 2014; Socquet et al., 2017)*; Illapel, 2015, Mw 8.3 *(Huang and Meng, 2018);* Nicoya, 2012, Mw 7.6 *(Voss et al., 2018)*). However, the evolution of such precursory markers during earthquake nucleation remains poorly understood. Here, we report for the first time, experimental results regarding the nucleation of laboratory earthquakes (stick slip events) conducted on Westerly Granite saw-cut samples under both dry and fluid pressure conditions. Experiments were conducted under stress conditions representative of the upper continental crust, i.e confining pressures from 50 to 95 MPa; fluid pressures (water) ranging from 0 to 45 MPa.

At given effective confining pressure, different precursory slip behaviors are observed. In dry conditions, we observe that slip evolves exponentially up to the main instability and is escorted by an exponential increase of acoustic emissions. With pressurized fluids, precursory slip evolves first exponentially then switches to a power law of time. There, precursory slip remains silent, independently of the fluid pressure level. The temporal evolution of precursory fault slip and seismicity are controlled by the fault's environment, limiting its prognostic value. Nevertheless, we show that, independently of the fault conditions, the total precursory moment release scales with the co-seismic moment of the main instability. The relation follows a semi- empirical scaling relationship between precursory and co-seismic moment release (*EQ 1*) by combining nucleation theory (*Ida, 1972; Campillo and Ionescu, 1992*) with the scaling between fracture energy and co-seismic slip which has been demonstrated experimentally (*Nielsen et al., 2016; Passelègue et al., 2016*), theoretically (*Viesca and Garagash; 2015*) and by natural observations (*Abercrombie and Rice; 2005*). We then compile data from natural earthquakes, and show that, over a range of Mw6.0 to Mw9.0 the proposed scaling law holds for natural observations. In summary, the amount of moment released prior to an earthquake is directly related to its magnitude, increasing therefore the detectability of large earthquakes. The scaling relationship between precursory and co-seismic moment should motivate detailed studies of precursory deformation of moderate to large earthquakes.

[1] EPFL, LEMR, Lausanne, CH mateo.acosta@epfl.ch
[2] Laboratoire de Géologie, CNRS, UMR, ENS, Paris, FR,

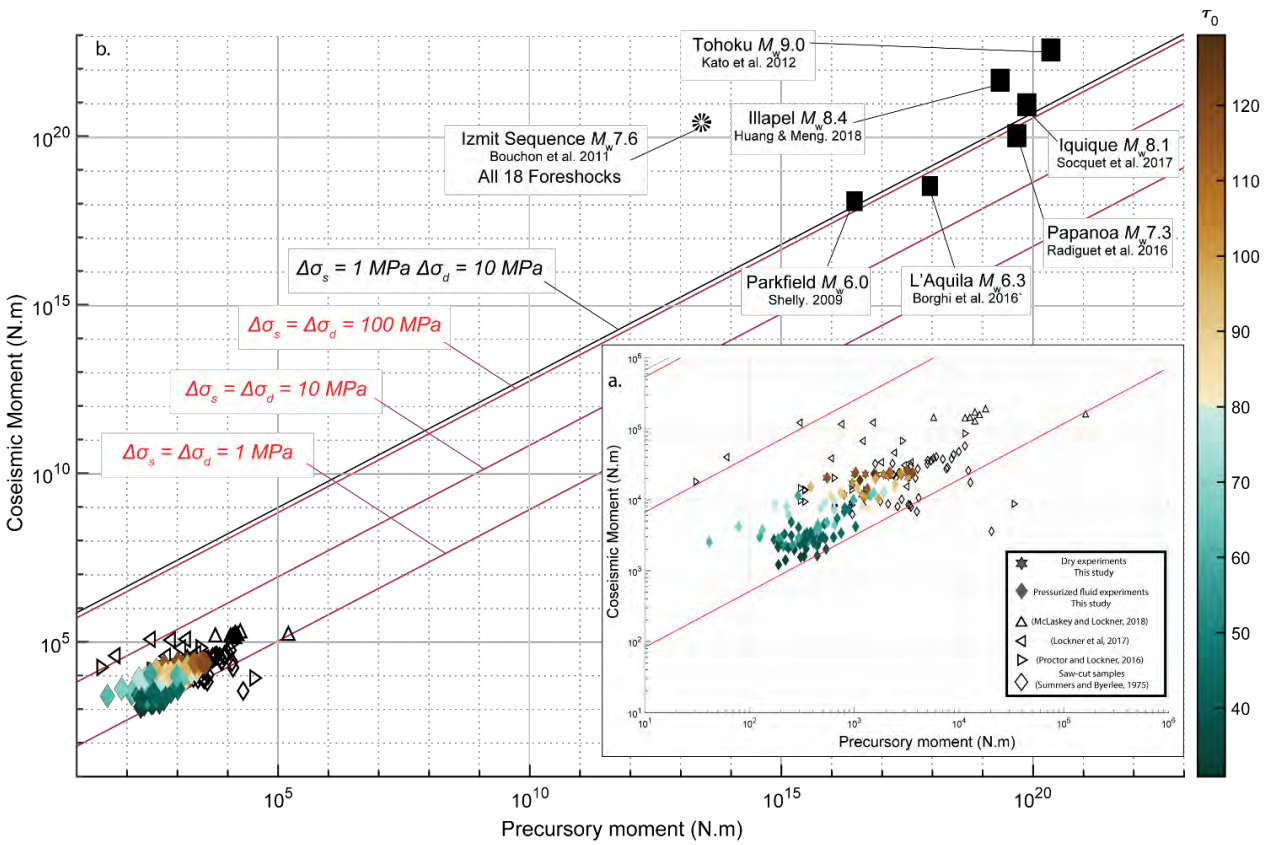

Figure 1. Earthquake moment release in natural and laboratory earthquakes.

a. Precursory vs Co-seismic moment release for all stick-slip cycles analyzed from the laboratory. Color bar accounts for maximum shear strength. b. Precursory vs Co-seismic moment release for laboratory and natural earthquakes. Full squares account for Mprec inferred from integrated analysis of a combination of geodetic, and seismic precursory moment release in natural earthquakes. Black star corresponds to the Izmit sequence and accounts for all 18 foreshock moment release. Red lines correspond to Mcos vs. Mprec from equation (4) taking Δσ_s=Δσ_d shown in the plot. Black line Corresponds to (Δσ_s)/(Δσ_d)=0.1 (Twardzik et al. 2012).

Equation :

$$M_{prec} = \frac{(2a.\mu^{1-\alpha})^3}{C^{2\alpha}} . \frac{\Delta\sigma_s^{2\alpha}}{\Delta\sigma_{s/d}^{5}} . M_{cos}^{\alpha} \qquad (1)$$

References

Kato, A., et al., Propagation of Slow Slip Leading Up to the 2011 Mw 9.0 Tohoku-Oki Earthquake. Science, 335(6069), 705–708. (2012) https://doi.org/10.1126/science.1215141

Socquet, A., et al., An 8-month slow slip event triggers progressive nucleation of the 2014 Chile megathrust. Geophys. Res. Lett., 44(9), 4046–4053. (2017) https://doi.org/10.1002/2017GL073023

Huang, H. and Meng, L., Slow Unlocking Processes Preceding the 2015 Mw 8.4 Illapel, Chile, Earthquake. Geophys. Res. Lett, 45(9), 3914-3922. (2018)

Voss, N., et al., Do slow slip events trigger large and great megathrust earthquakes? Science advances, 4(10), (2018)

Passelègue, F., et al., Dynamic rupture processes inferred from laboratory microearthquakes. J. Geophys. Res., 121(6), pp.4343-4365. (2016).

Nielsen, S., et al., G: Fracture energy, friction and dissipation in earthquakes. J. seism., 20(4), pp.1187-1205. (2016)

Abercrombie, R.E., Rice, J.R., Can observations of earthquake scaling constrain slip weakening?. Geophys. J. Int, 162(2), 406-424. (2005)

Viesca, R.C., Garagash, D.I., Ubiquitous weakening of faults due to thermal pressurization. Nat. Geosc., 8(11), p.875. (2015)

GeoProc2019: Earthquake and Faulting mechanics

7th International Conference on Coupled THMC Processes in Geosystems
3-5 July 2019 Utrecht (Netherlands)

Thermal pressurization precedes melt lubrication in high-velocity friction experiments on dolerite under elevated pore pressure

L. Yao[1], S. Ma[2], T. Shimamoto[3]

Keywords: Frictional melting, thermal pressurization, dynamic weakening, pore pressure, supercritical pore water.

Frictional melting on seismic faults has gained widespread attention in the studies on the genesis of pseudotachylite, the mechanics of seismic faulting and the earthquake rupture dynamics. Despite the fruitful theoretical and experimental results that support frictional melting as an effective dynamic fault weakening mechanisms, the scarcity of pseudotachylite on natural faults may suggest that melting and melt lubrication could be inhibited by thermal pressurization of pore water (e.g. Sibson, 1973; 2006). However, recent experimental work by Violay et al. (2015) shows that frictional melting could occur in the presence of water and thermal pressurization weakening of cohesive rocks can be negligible during earthquakes, leaving the sparse record of melting on natural fault zones more enigmatic.

In this study, high-velocity (V_{eq} = 2.0 m/s) friction experiments were performed on dolerite under pore water pressure (P_p) up to 25 MPa, with effective normal stresses (σ_{n_eff}) ranging from 3 to 10 MPa (see pressure vessel and dolerite samples in Figure 1a and 1b). Unlike the frictional behavior observed in a control test under room humidity, a drastic weakening contemporaneous with a sharp pore pressure rise was observed following the peak friction under P_p = 10 and 25 MPa (see pink-colored region in Figure 1c and 1d), with minimum μ of 0.01 in the closely followed stage. At larger displacement (> 8 m), slip strengthening is followed by modest weakening, with a final μ of 0.3–0.4 (comparable to that in the room-humidity test). Experimental data integrated with microstructures suggest that the rapid weakening in incipient stage and the closely followed frictionless state result from thermal pressurization, while frictional melting control the friction evolution in latter stage after the pressurized water escapes from the slip surface.

At higher σ_{n_eff} of 6 and 10 MPa, both the rapid weakening and sharp pore pressure rise disappears in incipient stage and the overall slip weakening resembles that in the room-humidity test (Figure 1e and 1f). The absence of thermal pressurization in these cases is consistent with what Violay et al. (2015) observed. However, with pitted (SS-2 in Figure 1b) rather than flat (SS-1) slip surface (he amount of immersed water is slightly larger for

State Key Laboratory of Earthquake Dynamics, Institute of Geology, China Earthquake Administration.
[1] luyao@ies.ac.cn; yaolu_cug@163.com
[2] masl@ies.ac.cn;
[3] shima_kyoto@yahoo.co.jp

the former), we could observe thermal pressurization preceding melt lubrication in all the experiments (see Figure 1g and 1h; σ_{n_eff} = 6–10 MPa). Natural faults have larger roughness and more irregular geometry than experimental faults, thus there may exist enough pore water on fault plane required to activate thermal pressurization even for faults in low-porosity crystalline rocks. Thermal pressurization could be activated much quicker and thus postpones or even inhibits (depending on displacement) bulk frictional melting as we observed in the experiments, which is more or less consistent with Sibson's interpretation on the scarcity of pseudotachylite in nature.

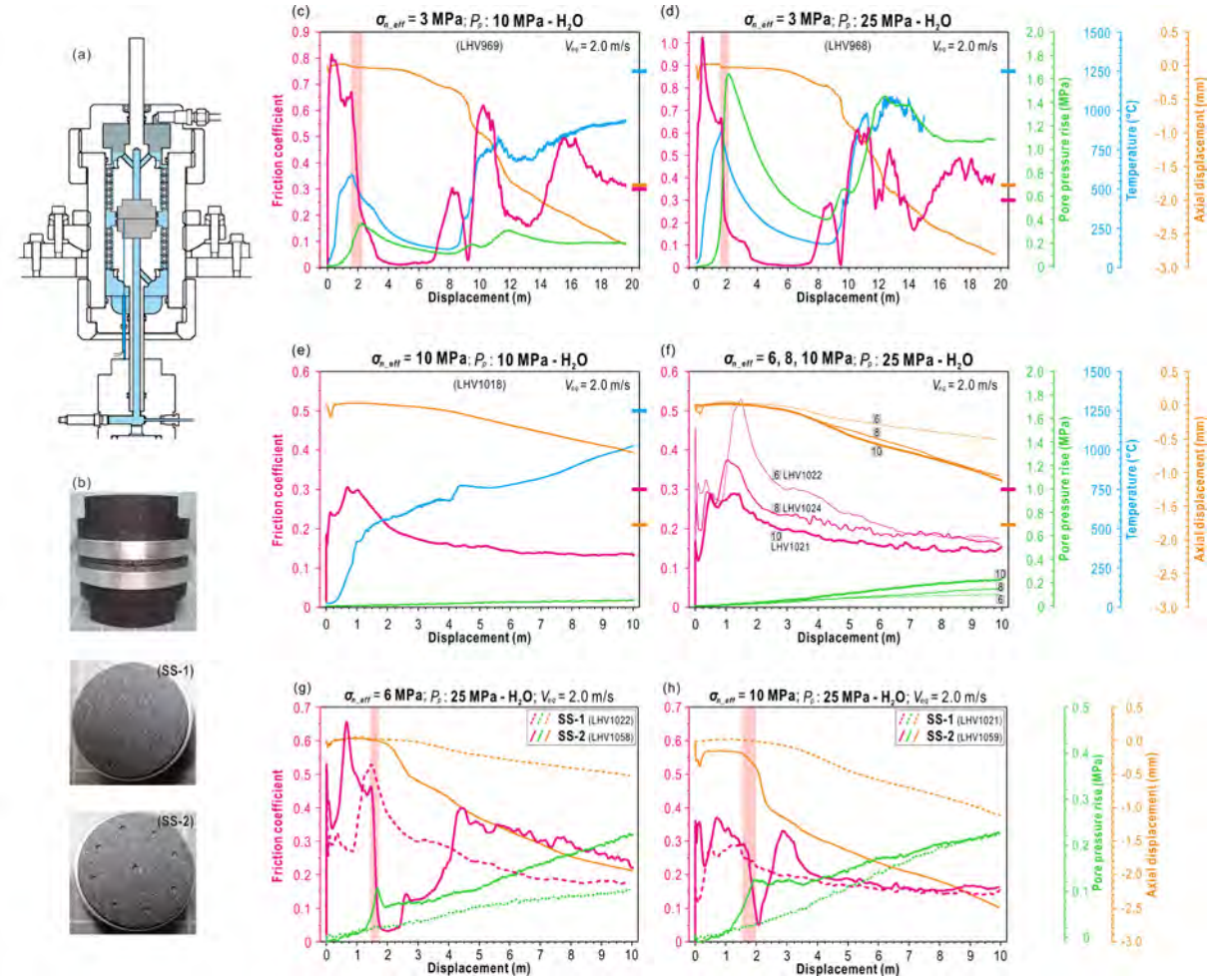

Figure 1. (a) Schematic diagram of pressure vessel for the rotary-shear high-velocity friction apparatus. (b) Close-up photos of dolerite samples and slip surfaces. (c)–(h) Evolution of friction, temperature, pore pressure and axial shortening with shear displacement in the friction experiments.

References

Sibson, R. H. (1973), Interactions between temperature and pore-fluid pressure during earthquake faulting and a mechanism for partial or total stress relief, Nature, 243(126), 66-68.

Sibson, R., and V. Toy (2006), The habitat of fault-generated pseudotachylyte: presence vs. absence of friction-melt, in *Earthquakes: Radiated Energy and the Physics of Faulting*, edited by R. Abercrombie, A. McGarr, G. Di Toro and H. Kanamori, pp. 153–166, American Geophysical Union, Washington, D. C.

Violay, M., G. Di Toro, S. Nielsen, E. Spagnuolo, and J. P. Burg (2015), Thermo-mechanical pressurization of experimental faults in cohesive rocks during seismic slip, *Earth Planet. Sci. Lett.*, *429*, 1–10, doi:http://dx.doi.org/10.1016/j.epsl.2015.07.054.

GeoProc2019: Earthquake and Faulting mechanics

7th International Conference on Coupled THMC Processes in Geosystems
3-5 July 2019 Utrecht (Netherlands)

THMC instabilities and the Multiphysics of Earthquakes

Klaus Regenauer-Lieb[1], Thomas Blach[2], Christoph Schrank[3], Manman Hu[4], Xiao Chen[5] and Hamid Roshan[6]

Keywords: Solitary Waves, Multiphysics Coupling, Multiscale System Dynamics

We present the hypothesis that material instabilities based on multiscale, multiphysics dissipative waves hold the key for understanding the universality of physical phenomena that can be observed over many orders of scale [1]. We propose a new mathematical approach for coupling the rates of chemical reactions, failure and fluid flow instabilities and thermo-mechanical instabilities of materials. The approach gives physics-based insights into the processes that are commonly described by empirical relationships.

The approach is inspired and can be derived from an upscaled wave mechanics approach of the quantum-scale. We skip, however, here the quantum scale and start with molecular-scale processes, which are defined by the chemical reactions and mass exchange processes under thermodynamic driving forces triggering thermodynamic fluxes. In the following, without loss of generality, we discuss a specific example.

Thermodynamic forces and fluxes in a THMC-system are defined in Table 1. Thermodynamic forces are the gradients of a THMC-system. They drive thermodynamic fluxes. At the molecular scale, the thermodynamic force is, for instance, the gradient of a chemical species C, which drives a chemical flux (C) parameterized by Fick's law, where ξ is the chemical diffusivity. The capital $D../Dt$ denotes the material derivative. Such chemical reactions can in turn become a driver for the next scale up in the multiscale system. For example, a dissolution-precipitation reaction in an HMC-coupled system can create mechanical pressure gradients due to the associated volume change and fluid release/precipitation, which in turn induces mechanical (M) stress diffusion based the Beltrami-Michell-type compatibility condition [2] and Darcy-type fluid diffusion (H). In the mechanical sense, the dissolution-reaction process creates an overpressure $\bar{p}_s$ in the matrix. Its momentum conservation law leads to a slow diffusion wave equation (no inertia) traveling at a wave velocity $\boldsymbol{v} = Dx/Dt$ (see companion abstract by Hu and Regenauer-Lieb, this volume). The Darcy flux (H) is defined by κ the rock permeability and μ_f is the fluid viscosity. The dissolution-precipitation reaction is an endo-/exo-thermal reaction and also induces a gradient in temperature which in turn drives a thermal Fourier

[1] UNSW Sydney, klaus@unsw.edu.au
[2] UNSW Sydney, t.blach@unsw.edu.au
[3] Queensland University of Technology QUT, christoph.schrank@qut.edu.au
[4] UNSW Sydney, manman.hu@unsw.edu.au
[5] UNSW Sydney, xiao.chen@student.unsw.edu.au
[6] UNSW Sydney, h.roshan@unsw.edu.au

flux (T), where the thermal diffusivity is defined by the thermal conductivity k divided by ρc_p . The afore mentioned cross-scale coupling introduces source/sink terms in the individual conservation laws identified by r^C, r^M, r^H and r^T respectively.

Table 1 Generalised Thermodynamic Fluxes and Forces (1-D)

	Thermodynamic Force (1-D)	Thermodynamic Flux (1-D)	Reaction-Diffusion Equations (1-D)
C	$F_C = \frac{\P C}{\P x}$	$q_C = - x \frac{DC}{Dt}$	$\frac{DC}{Dt} = - \frac{\P F_C}{\P x} + r^C$
M	$F_M = \frac{\P \bar{p}_s}{\P x}$	$q_M = - \frac{D\bar{p}_s}{Dt}$	$\frac{1}{K}\frac{Dx}{Dt} F_M = - D_M \frac{\P^2 \bar{p}_s}{\P x^2} + r^M$
H	$F_H = \frac{\P p_f}{\P x}$	$q_H = - \frac{k}{m_f} \frac{Dp_f}{Dt}$	$\frac{1}{M}\frac{Dp_f}{Dt} = - \frac{\P F_H}{\P x} + r^f$
T	$F_T = \frac{\P T}{\P x}$	$q_T = - k \frac{DT}{Dt}$	$rC_p \frac{DT}{Dt} = - \frac{\P F_T}{\P x} + r^T$

The conservation laws must also be extended to allow a multitude of THMC processes to occur simultaneously, which can introduce cross-diffusion fluxes. In a chemical system with two species, for instance, cross-diffusion is the phenomenon in which a flux of species A is induced by a gradient of species B [3]. In more general THMC terms, cross-diffusion is the phenomenon that a gradient of one generalised thermodynamic force drives another generalised thermodynamic flux. Staying with the chemical example of species A and B:

$$\begin{aligned} \frac{\partial A}{\partial t} &= D_A \frac{\partial^2 A}{\partial z^2} + h_1 \frac{\partial^2 B}{\partial z^2} + r^{C1} \\ \frac{\partial B}{\partial t} &= D_B \frac{\partial^2 B}{\partial z^2} - h_2 \frac{\partial^2 A}{\partial z^2} + r^{C2} \end{aligned} \qquad (1)$$

where $h_1 \geq 0, h_2 \geq 0, h_1 + h_2 > 0$ are the cross-diffusion coefficients triggering wave instabilities from solid-fluid interaction at the chemical microscale (see [3] for examples of different chemical wave forms). The self-diffusion D_A, D_B and cross-diffusion coefficients h_1, h_2 and the chemical source rate terms r^{C1} and r^{C2} generate in total six competing reaction-diffusion time scale processes. We propose that this phenomenon is at the heart of macro-scale failure. The importance of cross-diffusion is to link one thermodynamic force with a thermodynamic flux at a different scale thus synchronising the dynamics of vastly different diffusional time and length scales; an important element for an earthquake instability that was previously overlooked. The approach raises the possibility that dissipative waves can be detected prior to earthquake instabilities.

In this presentation, we will show first laboratory tests illustrating the theoretically postulated dissipative waves at larger than chemical scale. Please refer also to the presentation on "*Cross-Diffusion Triggered Hydro-Mechanical Wave Instabilities*" by Manman Hu for a discussion of HM coupled dissipative waves.

References

1. Sethna, J.P., K.A. Dahmen, and C.R. Myers, *Crackling noise.* Nature, 2001. **410**(6825): p. 242-250.
2. Rice, J.R. and M.P. Cleary, *Some basic stress diffusion solutions for fluid-saturated elastic porous media with compressible constituents.* Reviews of Geophysics, 1976. **14**(2): p. 227-241.
3. Vanag, V.K. and I.R. Epstein, *Cross-diffusion and pattern formation in reaction–diffusion systems.* Physical Chemistry Chemical Physics, 2009. **11**(6): p. 897-912.

GeoProc2019: Earthquake and Faulting mechanics

7th International Conference on Coupled THMC Processes in Geosystems
3-5 July 2019 Utrecht (Netherlands)

Optimal formulation for visco-elasto-plastic seismo-hydro-thermomechanical-chemical geodynamic models: C-component approach

T. Gerya[1], *C. Petrini*[2], *V. Yarushina*[3]

Keywords: fluid-solid coupling, seismicity, numerical modeling, geodynamic processes

Seismo-hydro-thermomechanical-chemical (SHTMC) modelling is an important nascent branch of geodynamic modelling, which investigates evolution of coupled fluid/melt-solid systems under conditions of both slow geodynamic and fast seismic deformation rates. One important point to discuss is how fluid-solid coupling could be implemented self-consistently into existing visco-elasto-plastic thermomechanical (TM) and seismo-thermomechanical (STM) geodynamic codes thereby making them capable to model SHTMC processes. From this point of view, an optimal self-consistent visco-elasto-plastic formulation has recently been developed by Yarushina and Podladchikov [1], who derived their system of mass and momentum conservation equations based on principles of irreversible thermodynamics formulated for a two-phase fluid-solid system. This formulation is also consistent with Biot's poroelasticity theory (Biot, 1941) thereby allowing to model visco-elasto-plastic deformation on all ranges of time scales. Based on this formulation, we develop a simple generic treatment of complex solid-fluid mass transfer processes (i.e., resulting from several simultaneously operating multi-component chemical reactions) based on considering a single chemically complex pseudo-component C. We characterize the reactive mass transfer simply by considering a net mass transfer (ΔM) from the solid to the fluid during a time increment Δt: positive ΔM values corresponds to the mass transfer from the solid to the fluid (dehydration, melting, dissolution, etc.), whereas negative ΔM values imply the mass transfer from the fluid to the solid (hydration, solidification, precipitation, etc.). The transferred mass is formally described as a single chemically complex pseudo-component of the solid and fluid (we call it C-component, [2]) that has different density in its solid and fluid state, which can also differ from the bulk density of the solid and fluid. The advantage of this approach is that the form of the discretized conservation equations becomes independent of the actual chemistry, thermodynamics and kinetics of mass transfer, which can be computed separately during SHTMC-iteration. In this case, all mass transfer terms can be formulated locally as a function of six independent quantities: porosity and density of the solid and fluid before (i.e., for the beginning of the

[1] Institute of Geophysics, ETH Zurich, Switzerland, taras.gerya@erdw.ethz.ch
[2] Institute of Geophysics, ETH Zurich, Switzerland, claudio.petrini@erdw.ethz.ch
[3] Institute for Energy Technology, Kjeller, Norway, Viktoriya.Yarushina@ife.no

time step Δt) and after (for the end of the time step Δt) multi-component chemical reactions at given pressure, temperature and composition of the system. We present examples of using the geodynamical approach for subduction zones evolution and seismicity.

References

[1] Yarushina, V. M., Podladchikov, Y. Y. (2015) (De)compaction of porous viscoelastoplastic media: model formulation, Journal of Geophysical Research, 120, 4146–4170.

[2] Gerya T. V. (2019) Introduction to Numerical Geodynamic Modelling. Second Edition. Cambridge University Press. https://www.cambridge.org/us/academic/subjects/earth-and-environmental-science/structural-geology-tectonics-and-geodynamics/introduction-numerical-geodynamic-modelling-2nd-edition?format=HB&isbn=9781107143142

GeoProc2019: Earthquake and Faulting mechanics

7th International Conference on Coupled THMC Processes in Geosystems
3-5 July 2019 Utrecht (Netherlands)

Accelerating foreshocks of crustal earthquakes controlled by frictional heterogeneities

Y. Kaneko[1]

Keywords: Accelerating foreshocks, Frictional heterogeneities, Earthquake cycle simulations, Rate and state friction, Earthquake Dynamics, Slow slip

While most earthquakes start abruptly, with no evidence for a nucleation process, accelerating foreshocks within or in the vicinity of the eventual mainshock rupture zone for some moderate to large crustal earthquakes have been documented recently. For example, Tape et al. (2018) reported nucleation signals of crustal earthquakes in the Minto Flats fault zone in central Alaska, manifested by ~20 seconds of simultaneous high-frequency foreshocks and a very low-frequency earthquake (VLFE). One potential explanation for such observations is a slow slip front propagating over the fault and triggering foreshocks as it transitions into the mainshock rupture. Another explanation may be that accelerating foreshocks represent cascading sequences of fault ruptures due to static and/or dynamic stress changes, without underlying slow slip. Here we show that a numerical fault model incorporating full inertial dynamics and rate-and-state friction laws with frictional heterogeneities can reproduce the accelerating foreshocks of crustal earthquakes in the Minto Flats fault zone. Our results suggest that a slow physical process, such as slow slip or fluid diffusion, in between small-scale, velocity-weakening asperities is needed to generate accelerating foreshocks. Our model further shows that the time scale of accelerating foreshock sequences depends on the degree and size of frictional heterogeneities. Our model may also explain why the occurrence of accelerating foreshocks is relatively uncommon.

[1] GNS Science, y.kaneko@gns.cri.nz

GeoProc2019: Earthquake and Faulting mechanics

7th International Conference on Coupled THMC Processes in Geosystems
3-5 July 2019 Utrecht (Netherlands)

Apparent rate dependency of fault gouges due to thermal pressurization and grain size

I. Stefanou[1], *H. Rattez*[2], *J. Sulem*[3]

Keywords: Rate dependence, Grain size, THM couplings, Cosserat continuum, Fault mechanics

Rapid shear tests of granulated fault gouges show pronounced rate-dependency. For this reason rate-dependent constitutive laws are frequently used for describing fault friction (see Dieterich, 1979; Platt, Rudnicki, & Rice, 2014; Scholz, 2002).

Here we propose a micromechanical, physics-based continuum approach by considering the characteristic size of the microstructure and the thermal- and pore-pressure-diffusion mechanisms that take place in fault gouges during rapid shearing. It is shown that even for rate-independent materials, the apparent, macroscopic behavior of the system is rate-dependent. This is due to the competition of the various length and time scales originating from the characteristic grain size and the thermal and hydraulic diffusivities of the fault gouge material.

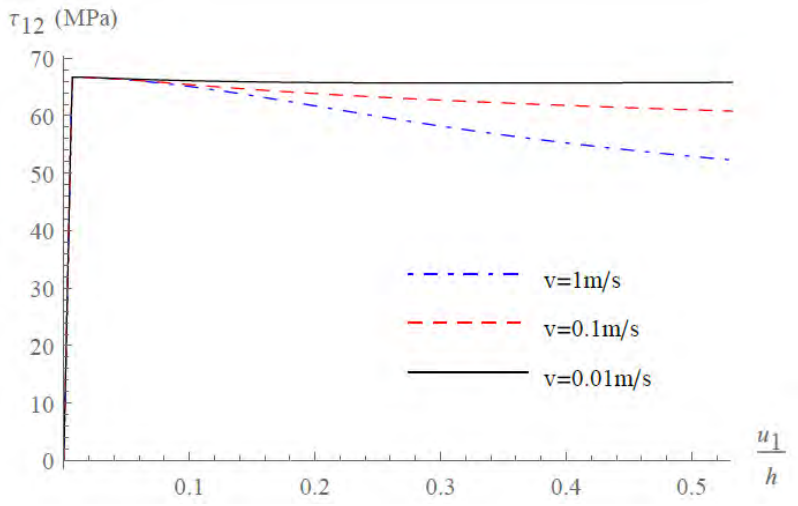

Figure 1. Dependency of the apparent shear stress, τ_{12}, , in function of the slip, u_1, for a fault gouge of total height, h, modeled with a Cosserat continuum for different orders of magnitude of the applied shearing velocity, v (see Rattez, Stefanou, & Sulem, 2018; Rattez, Stefanou, Sulem, Veveakis, & Poulet, 2018a, 2018b).

[1] NAVIER, UMR 8205, Ecole des Ponts, IFFSTAR, CNRS, UPE, ioannis.stefanou@enpc.fr
[2] Duke University, hadrien.rattez@duke.edu
[3] NAVIER, UMR 8205, Ecole des Ponts, IFFSTAR, CNRS, UPE, jean.sulem@enpc.fr

Both weakening and shear band thickness depend on the applied velocity, despite the fact that the constitutive description of the material was considered rate-independent. Moreover the size of the microstructure, which here is identified with the grain size of the fault gouge (D_{50}), plays an important role in the slope of the softening branch of the shear stress-strain response curve and consequently in the transition from aseismic to seismic slip.

References

Dieterich, J. H. (1979). Modeling of rock friction 2. Simulation of preseismic slip. *Journal of Geophysical Research: Solid Earth*, *84*(B5), 2169–2175. http://doi.org/10.1029/JB084iB05p02169

Platt, J. D., Rudnicki, J. W., & Rice, J. R. (2014). Stability and localization of rapid shear in fluid-saturated fault gouge: 2. Localized zone width and strength evolution. *Journal of Geophysical Research: Solid Earth*, *119*(5), 4334–4359. http://doi.org/10.1002/2013JB010711

Rattez, H., Stefanou, I., & Sulem, J. (2018). The importance of Thermo-Hydro-Mechanical couplings and microstructure to strain localization in 3D continua with application to seismic faults. Part I: Theory and linear stability analysis. *Journal of the Mechanics and Physics of Solids*, *115*, 54–76. http://doi.org/10.1016/j.jmps.2018.03.004

Rattez, H., Stefanou, I., Sulem, J., Veveakis, M., & Poulet, T. (2018a). Numerical Analysis of Strain Localization in Rocks with Thermo-hydro-mechanical Couplings Using Cosserat Continuum. *Rock Mechanics and Rock Engineering*. http://doi.org/10.1007/s00603-018-1529-7

Rattez, H., Stefanou, I., Sulem, J., Veveakis, M., & Poulet, T. (2018b). The importance of Thermo-Hydro-Mechanical couplings and microstructure to strain localization in 3D continua with application to seismic faults. Part II: Numerical implementation and post-bifurcation analysis. *Journal of the Mechanics and Physics of Solids*, *115*, 1–29. http://doi.org/10.1016/j.jmps.2018.03.003

Scholz, C. H. (2002). *The mechanics of earthquakes and faulting*. Cambridge.

GeoProc2019: Earthquake and Faulting mechanics

7th International Conference on Coupled THMC Processes in Geosystems
3-5 July 2019 Utrecht (Netherlands)

Chemical and hydro-mechanical coupling in fault zones: an experimental overview

E. Spagnuolo[1], M. Violay[2], C. Cornelio[2], S. Nielsen[3], P. Giacomel[4] , S. Aretusini[1], G. Di Toro[5]

[1] Istituto Nazionale di Geofisica e Vulcanologia, IT, elena.spagnuolo@ingv.it, stefano.aretusini@ingv.it
[2] EPFL, LEMR, CH, marie.violay@epfl.ch, chiara.cornelio@epfl.ch
[3] Durham University, UK, stefan.nielsen@durham.ac.uk
[4] La Sapienza Università di Roma, IT, piercarlo.giacomel@uniroma1.it
[5] Università di Padova, IT, giulio.ditoro@unipd.it

Keywords: Fluids, faults, friction, earthquakes, seismic slip, aseismic slip

The interaction between the mechanical deformation and fluid flow in fault zones results in chemical and coupled hydro-mechanical processes controlling fault stability, increasing the potential for fault reactivation and the transition from aseismic to seismic slip. During the seismic cycle, the circulation, injection or production of pressurized fluids reduce the effective normal stress acting on a fault, but also affect the strength of fault zone rocks, for example:

(1) via chemical reactions (e.g., hydrothermal reactions and fluid-rock interactions) and formation of new “weak” (e.g., clays, micas) or “strong” (e.g., epidote, K-feldspar, quartz) mineral assemblages affecting fault strength during the interseismic period (Giulio Di Toro & Pennacchioni, 2005; Wintsch & Dunning, 1985).

(2) via mechanical and thermal pressurization of trapped fluids in the slipping zone during slip initiation, slip transients and seismic slip (Faulkner, Sanchez-Roa, Boulton, & den Hartog, 2018; Rice, 2006; Segall & Rice, 2006; S. R. H. Sibson, 1973; Violay, Di Toro, Nielsen, Spagnuolo, & Burg, 2015)

(3) via thermally activated mechano-chemical reactions resulting in the breakdown of fault zone minerals (calcite, dolomite, gypsum, smectites, etc.), release of fluids pressurizing the slipping zone and buffering the temperature rise during seismic slip(Brantut, Sulem, & Schubnel, 2011; Ferri et al., 2011; Mitchell et al., 2015; Sulem & Famin, 2009; Violay et al., 2013);

(4) via elastohydrodynamic and melt lubrication governed by fluid viscosity during seismic slip (Brodsky & Kanamori, 2001; G Di Toro, Hirose, Nielsen, Pennacchioni, & Shimamoto, 2006; R. H. Sibson, 1975;Cornelio et al. 2018);

To investigate the individual contribution of the above fluid-related processes and establish their relevance respective to their characteristic temporal and spatial scale, we

discuss a large experimental data set obtained under vacuum, water damped, room humidity and pressurized fluids conditions with the rotary shear apparatus SHIVA (INGV, Rome, (Giulio Di Toro et al., 2010). Samples consisted in non-cohesive smectite-rich gouge layers and cohesive rocks representative of the Earth's crust (Carrara marble, gabbro, westerly granite and basalts). Cohesive rocks were inserted in a vessel for fluid confinement and put in frictional contact under a variety of loading conditions. In the experiments, we investigated fault stability by: (1) changing the frictional power dissipated (product of slip rate per shear stress) on the experimental fault under either water damped, drained or undrained conditions, (2) varying fluid viscosity over three orders of magnitude (mixtures of glycerol and H2O) and (3) injecting fluids with different composition (CO2, H2O, Ar).

As a starting point, we exploited the observation that under room humidity conditions, given the stiffness of SHIVA, all the studied experimental faults evolved towards frictional instability (Spagnuolo, Nielsen, Violay, & Di Toro, 2016). Our experimental observations, supported by numerical modelling, suggest that the presence of fluids either inhibits or facilitate this evolution depending on the time of interaction between fluids and the sliding surface asperities (or fault roughness) and the gouge layer, fluid viscosity and frictional power density.

Finally, chemical and hydromecanical effects operating in the laboratory are discussed in terms of breakdown energy to scale the experimental observations to natural and man-induced earthquakes.

References

Brantut, N., Sulem, J., & Schubnel, A. (2011). Effect of dehydration reactions on earthquake nucleation: Stable sliding, slow transients, and unstable slip. Journal of Geophysical Research: Solid Earth, 116(5), 1–16. https://doi.org/10.1029/2010JB007876

Brodsky, E. E., & Kanamori, H. (2001). Elastohydrodynamic lubrication of faults. Journal of Geophysical Research, 106, 16,316-357,374.

Cornelio C., Spagnuolo E., Di toro G., Nielsen S., Violay M (2018) Mechanical behaviour of fluid-lubricated faults. Under revision.

Di Toro, G., Hirose, T., Nielsen, S., Pennacchioni, G., & Shimamoto, T. (2006). Natural and experimental evidence of melt lubrication of faults during earthquakes. Science, 311, 647–649.

Di Toro, G., Niemeijer, A. R., Tripoli, A., Nielsen, S., DiFelice, F., Scarlato, P., … Mariano, S. (2010). From field geology to earthquake simulation: a new state-of-the-art tool to investigate rock friction during the seismic cycle (SHIVA. Rend. Fis. Acc. Lincei, 21, S95–S114.

Di Toro, G., & Pennacchioni, G. (2005). Fault plane processes and mesoscopic structure of a strong-type seismogenic fault in tonalites (Adamello batholith, Southern Alps). Tectonophysics. https://doi.org/10.1016/j.tecto.2004.12.036

Faulkner, D. R., Sanchez-Roa, C., Boulton, C., & den Hartog, S. A. M. (2018). Pore Fluid Pressure Development in Compacting Fault Gouge in Theory, Experiments, and Nature. Journal of Geophysical Research: Solid Earth. https://doi.org/10.1002/2017JB015130

Ferri, F., DiToro, G., Hirose, T., Noda, R. H. H., Quaresimin, T. S. S., & DeRossi, N. (2011). Low- to high- velocity frcitional properties of the clay-rich gouges from the slipping zone of the 1963 Vajont slide, northern Italy. Journal of Geophysical Research, 116, B09208.

Mitchell, T. M., Smith, S. A. F., Anders, M. H., Di Toro, G., Nielsen, S., Cavallo, A., & Beard, A. D. (2015). Catastrophic emplacement of giant landslides aided by thermal decomposition: Heart Mountain, Wyoming. Earth and Planetary Science Letters. https://doi.org/10.1016/j.epsl.2014.10.051

Rice, J. R. (2006). Heating and weakening of faults during earthquake slip. JOURNAL OF GEOPHYSICAL RESEARCH, 111, B05311. https://doi.org/10.1029/2005JB004006

Segall, P., & Rice, J. R. (2006). Does shear heating of pore fluid contribute to earthquake nucleation? JOURNAL OF GEOPHYSICAL RESEARCH, 111, B09316. https://doi.org/10.1029/2005JB004129

Sibson, R. H. (1975). Generation of Pseudotachylyte by Ancient Seismic Faulting. Geophysical Journal of the Royal Astronomical Society. https://doi.org/10.1111/j.1365-246X.1975.tb06195.x

Sibson, S. R. H. (1973). Interactions between temperature and pore-fluid pressure during earthquake faulting and a mechanism for partial or total stress relief. Nature, 243(126), 66–68.

Spagnuolo, E., Nielsen, S., Violay, M., & Di Toro, G. (2016). An empirically based steady state friction law and implications for fault stability. Geophysical Research Letters, 43(7), 3263–3271. https://doi.org/10.1002/2016GL067881

Sulem, J., & Famin, V. (2009). Thermal decomposition of carbonates in fault zones: slip-weakening and temperature-limiting effects. Journal of Geophysical Research, 114, B03309. https://doi.org/10.1029/2008JB006004

Violay, M., Di Toro, G., Nielsen, S., Spagnuolo, E., & Burg, J. P. (2015). Thermo-mechanical pressurization of experimental faults in ochesive rocks during seismic slip. Earth and Planetary Sceince Letters, 429. https://doi.org/http://www.sciencedirect.com/science/article/pii/S0012821X15004975

Violay, M., Nielsen, S., Spagnuolo, E., Cinti, D., Di Toro, G., & Di Stefano, G. (2013). Pore fluid in experimental calcite-bearing faults: Abrupt weakening and geochemical signature of co-seismic processes. EPSL, 361, 74–84. https://doi.org/doi.org/10.1016/j.epsl.2012.11.021

Wintsch, R. P., & Dunning, J. (1985). The effect of dislocation density on the aqueous solubility of quartz ans some geological implications: a theoretical approach. Journal of Geophysical Research. https://doi.org/10.1029/JB090iB05p03649

GeoProc2019: Earthquake and Faulting mechanics

7th International Conference on Coupled THMC Processes in Geosystems
3-5 July 2019 Utrecht (Netherlands)

Nanoscale dissolution processes and colloid-suspension formation as possible weakening mechanism of seismogenic crustal carbonate fault

M. Ohl[1], J. Chen[1], A. Niemeijer[1], H.E. King[1], L. Polerecky[1], J.N. Audinot[2], T. Wirtz[2], O. Pluemper[1]

Keywords: stable isotopes, dissolution, seismic slip, deformation mechanisms

Deformation in natural carbonate faults is apparent in grain size reduction and dissolution processes. Because crustal fault zones are major fluid pathways it is important to understand how fluid-rock interaction controls the rheology during seismic slip in the presence of fluid phases. Therefore, the rheological behavior of crustal carbonate faults is governed by the physico-chemical properties of the resulting, small-grained deformation products in interaction with fluids. It is assumed that a combination of granular flow, nanoscale diffusion and dissolution-precipitation processes dictate the stability of faults situated in the seismogenic zone (De Paola et al., 2015).

To quantify and track possible nanoscale dissolution-precipitation processes we conducted deformation experiments on monomineralic carbonate fault gouges (Fig. 1 A). We used water enriched in ^{18}O (97 at%) as pore fluid for deformation under seismic conditions (v = 1 m/s) with a normal load of σ_n = 2 and 4 MPa. With a total displacement of the deformed fault gouge of 20 m we noted a drop in friction coefficient from μ = 0.8 at the onset of the experiment to μ = 0.2 after 1 m of displacement. Variation of the normal load did not change the reached minimum value of μ = 0.1 steady slip throughout the experiment. Raman spectroscopy confirms the presence of ^{18}O-bearing carbonate isotopologues (Fig. 1 B) within newly nucleated grains associated with the occurrence of an amorphous phase. Nano – Secondary Ion Mass Spectrometry (Nano-SIMS) and Helium Ion Microscope – Secondary Ion Mass Spectrometry (HIM-SIMS) (Wirtz et al., 2016) (Fig. 1 C-E)) isotope mapping show an ^{18}O isotope enrichment only inside the fault gouge matrix. Focused Ion Beam – Scanning Electron Microscopy (FIB-SEM) and Transmission Electron Microscopy (TEM) are employed for the investigation of the deformation nanostructure associated with the ^{18}O isotope enrichment.

Here, for the first time we are able to present evidence for a phase transformation of the carbonate fault gouge under wet conditions into a colloid-suspension deformation product. Our observations demonstrate the importance of the occurring decarbonation

[1] Utrecht University, m.ohl@uu.nl, j.chen3@uu.nl, A.R.Niemeijer@uu.nl, H.E.King@uu.nl, O.Plumper@uu.nl, L.Polerecky@uu.nl
[2] Luxembourg Institute of Science and Technology, jean-nicolas.audinot@list.lu, tom.wirtz@list.lu

reaction during seismic fault slip. Consequently, our results show that deformation-induced decarbonation and colloid formation can result in major weakening of crustal carbonate fault gouges affecting the overall rheological behavior of the fault gouge.

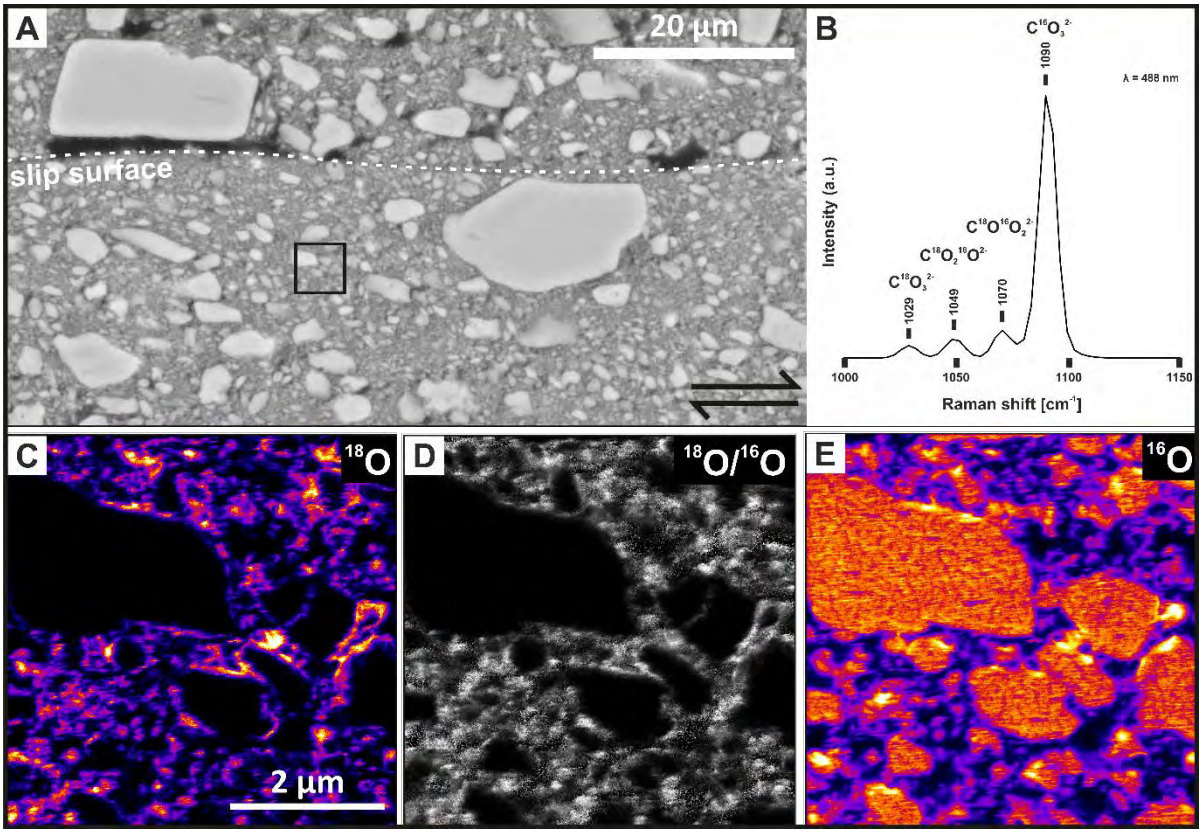

Figure 1: A: Fault gouge microstructure showing small-grained matrix and survivor clasts. B: Representative Raman spectrum containing ^{18}O carbonate isotopologues. C – E: HIM-SIMS maps for ^{16}O, ^{18}O and $^{18}O/^{16}O$ distribution from black rectangle in A.

References

De Paola, N., Holdsworth, R.E., Viti, C., Collettini, C. Bullock, R. (2015), Can grain sensitive flow lubricate faults during the initial stages of earthquake propagation?, *Earth and Planetary Science Letters, V. 431, 48-58*
doi.org/10.1016/j.epsl.2015.09.002

Wirtz, T., Dowsett, D., Philipp, P. (2016), SIMS on the Helium Ion Microscope: a powerful tool for high-resolution high-sensitivity nano-analytics*, Helium Ion Microscopy. NanoScience and Technology, Springer, 297-323*
doi.org/10.1007/978-3-319-41990-9_13

GeoProc2019: Earthquake and Faulting mechanics

7th International Conference on Coupled THMC Processes in Geosystems
3-5 July 2019 Utrecht (Netherlands)

Linking THMC processes to the earthquake energy budget: experimental deformation of smectite-rich gouges

S. Aretusini[1], E. Spagnuolo[2], G. Di Toro[3]

Keywords: smectite, megathrust earthquake, fracture energy, thermal pressurization

Ca-montmorillonite is a common clay mineral (smectite) composing fault cores of shallow megathrusts faults (e.g., Japan Trench) and plate boundary mature faults (e.g., San Andreas). The shear strength evolution of smectites at seismic slip rates controls the propagation of seismic slip, the total coseismic displacement and therefore the magnitude of the earthquake.

To investigate the deformation processes controlling fault shear strength, we performed experiments with a rotary machine on 2-mm-thick smectite-rich gouge layers (70/30 wt. % Ca-montmorillonite/opal), at 5 MPa normal stress and slip rates of 0.001, 0.01, 0.1, and 1.3 m/s for a total displacement of 3 m. The role of water content was assessed by testing: (1) oven-dried gouges at 150 and 100 °C under vacuum conditions (<10^{-3} mbar) and (2) room-dry gouges under room humidity or water dampened conditions. Permeability (2 - 4.3·10^{-16} m^2) of the room-dry gouge layer was measured with the pore pressure oscillation method before the experiments.

Shear strength and transport properties were included in finite elements numerical models including Thermo-Hydro-Mechano-Chemical processes (Chen et al., 2013): thermal pressurization of pore water and thermochemical pressurization from dehydration and dehydroxylation of smectite and opal-CT to quartz reaction.

Modelling results show that the combined effects of the frictional heating, the compressibility of pore water and the transport properties of the gouge layer promote a nearly adiabatic pressure-temperature-time path (i.e., without pressurization) in the water-depleted cases and pressure increase by thermal pressurization in the water-rich case (Figure 1a). In the water-depleted case, extensive dehydration, thermal decomposition and melting are predicted; instead, under water-rich conditions, no breakdown reaction is predicted, in accordance with the microstructural observations (Aretusini et al., 2017, 2018).

In the experiments performed under water-rich conditions and at seismic slip rates, the scaling of frictional shear fracture energy G_f with total slip resembles the scaling of seismologic breakdown work G' with average slip for large megathrust earthquakes (Viesca & Garagash, 2015). This similarity suggests that dynamic weakening is

[1] Istituto Nazionale di Geofisica e Vulcanologia, stefano.aretusini@ingv.it
[2] Istituto Nazionale di Geofisica e Vulcanologia, elena.spagnuolo@ingv.it
[3] Università degli Studi di Padova, giulio.ditoro@unipd.it

controlled by thermal pressurization in both our experiments and natural large megathrust earthquakes, but with diverse characteristic distances ratio $R=L^*/\delta_c$ (Figure 1b).

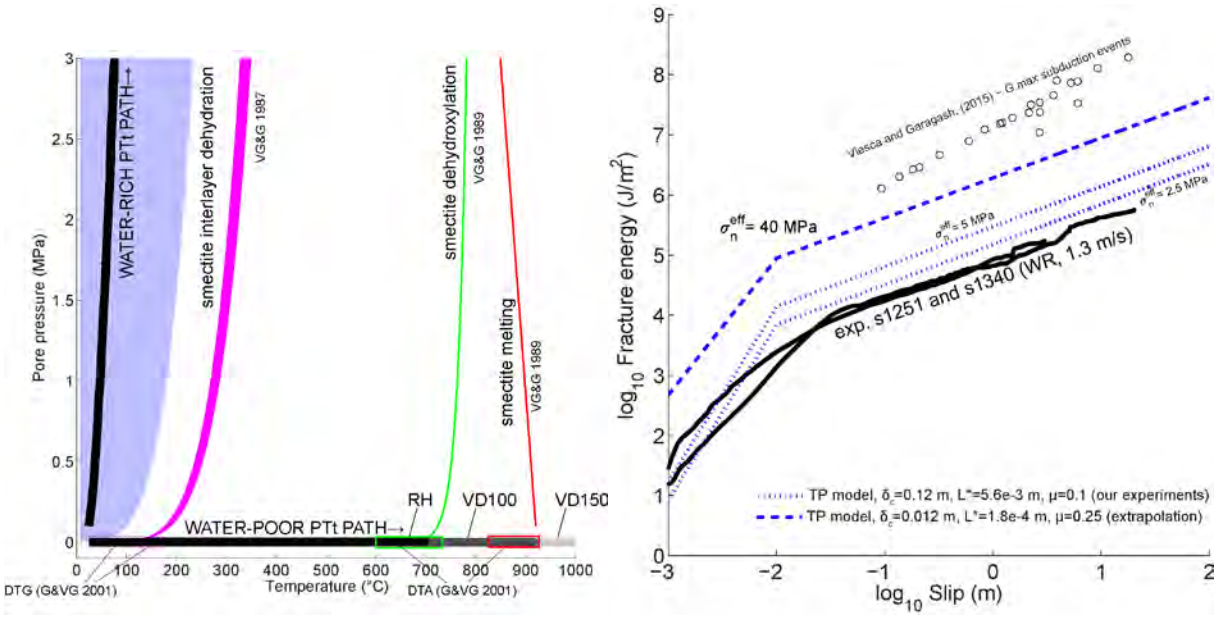

Figure 1. a) Numerical model results. Water-rich conditions promote thermal pressurization whereas water-poor conditions promote an adiabatic temperature increase intercepting dehydration, dehydroxylation, and melting reactions. (Guggenheim & Van Groos, 2001; Van Groos & Guggenheim, 1989, 1987). b) Scaling of experimental shear fracture energy G_f vs. slip (Nielsen et al., 2016) and of seismologic breakdown work G' vs. average seismic slip (R=10, Viesca & Garagash, (2015)), with overlaid G_f predicted by thermal pressurization in experiments (R=0.047, dotted line) and extrapolated to 10 km depth (R=0.0093 dashed line).

References

Aretusini, S., Mittempergher, S., Plümper, O., Spagnuolo, E., Gualtieri, A. F., & Di Toro, G. (2017). Production of nanoparticles during experimental deformation of smectite and implications for seismic slip. *Earth and Planetary Science Letters*, *463*, 221–231. https://doi.org/10.1016/j.epsl.2017.01.048

Aretusini, S., Plumper, O., Spagnuolo, E., & Di Toro, G. (2018). Seismic slip on clay nano-foliation. Under review in *Geology*.

Chen, J., Yang, X., Yao, L., Ma, S., & Shimamoto, T. (2013). Frictional and transport properties of the 2008 Wenchuan Earthquake fault zone: Implications for coseismic slip-weakening mechanisms. *Tectonophysics*, *603*, 237–256. https://doi.org/10.1016/j.tecto.2013.05.035

Guggenheim, S., & Van Groos, A. K. (2001). Baseline Studies of the Clay Minerals Society Source Clays: Thermal Analysis. *Clays and Clay Minerals*, *49*(5), 433–443. https://doi.org/10.1346/CCMN.2001.0490509

Nielsen, S., Spagnuolo, E., Violay, M., Smith, S., Di Toro, G., & Bistacchi, A. (2016). G: Fracture energy, friction and dissipation in earthquakes. *Journal of Seismology*, *20*(4), 1187–1205. https://doi.org/10.1007/s10950-016-9560-1

Van Groos, A. K., & Guggenheim, S. (1989). Dehydroxylation of Ca-and Mg-exchanged montmorillonite. *American Mineralogist*, *74*(5–6), 627–636.

Van Groos, A. K., & Guggenheim, S. (1987). Dehydration of a Ca- and a Mg-exchanged montmorillonite (SWy-1) at elevated pressures. *American Mineralogist; (USA)*, *72:3–4*.

Viesca, R. C., & Garagash, D. I. (2015). Ubiquitous weakening of faults due to thermal pressurization. *Nature Geoscience*, *8*(11), 875–879. https://doi.org/10.1038/ngeo2554

GeoProc2019: Earthquake and Faulting mechanics

7th International Conference on Coupled THMC Processes in Geosystems
3-5 July 2019 Utrecht (Netherlands)

Fibrous Rocks due to Chemo-Mechanical Processes

T. Vanorio[1], *J. MacFarlane*[1], *A. C. Clark*[1]

Keywords: Volcanic Ash, Cementation, Calderas, Fibers, and Polymers

The presence of fibrous minerals in rocks is becoming increasingly more common in the Geosciences, thanks to the technological advance in the spatial resolution of imaging techniques. Fibrous minerals are identified across a wide range of observational scales (from nano- to micro-scales) and geological environments, which include fibrous *'beef'* and ash beds in oil and gas reservoirs (Rodrigues et al., 2009), fibrous *'nanoparticles'* in fault mirror surfaces (Verberne et al., 2014; Siman-Tov et al., 2013), and fibrous calcium silicate minerals in volcanic areas (Ahmad and Yaseen, 2014; Vanorio & Kanitpanyacharoen, 2015). The resistance of a material to fracture and crack propagation relates to its microstructure, in particular the cementation and fabric. Fibrous minerals reflect fluid-mediated, chemo-mechanical processes and are key features of the rock fabrics. When fibers are dispersed in a matrix, they impart yield strength and serve as a crack arrestor, thus retarding the propagation of cracks that lead to catastrophic failure (Figure 1). As such, fibers transform the mode of mechanical failure from brittle-to-ductile, thus offering additional energy absorbing capability with respect to the matrix

The focus of this study is on the rock physics properties deriving from the cementation of volcanic ash from calc-alkaline volcanism above subduction zones. Within engineering, lime and sulfur are long recognized as important binders improving the cementation and performance of ash-based (i.e., pozzolanic) concrete. Since both lime and sulfur are naturally found in calc-alkaline calderas and hydrothermal solfataras, it becomes fundamental to understand their control on the mechanical behavior of sealing caprocks in subcaldera environments. *How do lime and sulfur influence the damage (or rupture) style of ash-bonded fabrics? What fabrics enable the dissipation of strain energy through slow-slip events (or creep) and which ones favor its sudden release through catastrophic brittle failure?* The reaction of lime with volcanic ash produces fibrous microstructures made of calcium-alumino-silicate hydrates (CASH). Strength of the fibrous microstructure is specifically controlled by the bonding mechanisms that take place across the interfacial area between the matrix and the fiber. These mechanisms include fiber macromolecules (i.e., polymers) entangled with the matrix molecules, electrostatic attraction between the fiber and matrix, and functional groups within organic molecules participating in chemical reactions at the matrix-fiber interface (Campilho, 2015; Pickering et al.,

[1] Stanford Rock Physics Laboratory, Stanford University, tvanorio@stanford.edu

2016). Potassium-sodium alkalis, specifically, are important coupling agents bridging the fiber to the matrix through polymerization of the lime-ash reaction. Long polymeric chains are critical because they control strength and favor a ductile failure behavior. Therefore, any physical and chemical process that favors fiber's growth and entanglement contributes to the reinforcement of the cementation process, leading to strain hardening (Figure 1b). As with lime, crystalline sulfur is also reported as cementing agent of both high-strength but brittle ash-based concrete and hydrothermal seals. We show polymeric sulfur-rich compounds being found in calderas, suggesting the existence of processes that prevent the reversion of heat-induced polymer sulfur to its crystalline brittle form.

The effects of these reactions are currently ignored at volcanoes. This intertwine between the cementation of ash-based mortars and ash-beds in volcanoes is an opportunity for cross-fertilizing knowledge across the Geosciences and Engineering.

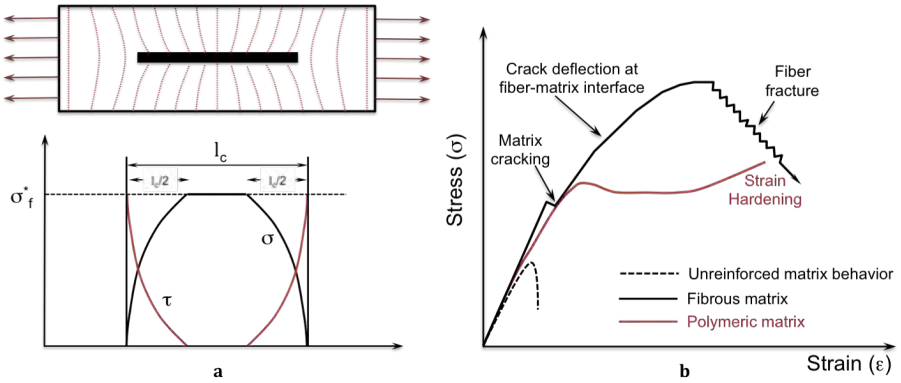

Figure 1. Stress transfer from the matrix to the fiber at the interfacial bond. At each fiber extremity, shear stress has its maximum value where the axial stress is zero. As we move along the fiber length, shear stress decreases up to reaching its minimum at the central region of the fiber (l/2) while the axial stress reaches its maximum (*left*, *bottom*). Schematic of stress-strain damage styles of unreinforced, fibrous, and polymeric matrices (*right*).

References

Ahmad I., A. B. Yaseen, 2014 Petrography and Mineral Chemistry of the Almanden Garnet, and Implication for Kelyphite Texture in the Miocene Alkaline Basaltic Rocks North East Jordan, International Journal of Geosciences**,** 5, 2, DOI:10.4236/ijg.2014.52024

Campilho R.D.S.G., 2015, Natural Fiber Composites, Edited by *R. D. S. G. Campilho*. CRC Press 2015. Pages 319–340. Print ISBN: 978-1-4822-3900-3

Pickering K.L., M.G. Aruan Efendy, T.M. Le, 2016, A review of recent developments in natural fibre composites and their mechanical performance, Composites Part A: Applied Science and Manufacturing, 83, 98-112, doi:10.1016/j.compositesa.2015.08.038

Rodrigues, N., Cobbold, P. R., Loseth, H., & Ruffet, G. (2009). Widespread bedding-parallel veins of fibrous calcite ('beef') in a mature source rock (Vaca Muerta Fm, Neuquen Basin, Argentina): evidence for overpressure and horizontal compression. *Journal of the Geological Society*, *166*(4), 695–709. doi: 10.1144/0016-76492008-111.

Siman-Tov, S., Aharonov, E., Sagy, A., & Emmanuel, S. (2013). Nanograins form carbonate fault mirrors. *Geology*, *41*(6), 703–706. doi: 10.1130/G34087.1.

Vanorio, T., & Kanitpanyacharoen, W. (2015). Rock physics of fibrous rocks akin to Roman concrete explains uplifts at Campi Flegrei Caldera. *SCIENCE*, *349*(6248), 617–621. doi: 10.1126/science.aab1292

Verberne B. A., O. Plümper, D.A. M. de Winter, C. J. Spiers, 2014, Superplastic nanofibrous slip zones control seismogenic fault friction, *SCIENCE*, 346, 6215, pp. 1342-1344 doi: 10.1126/science.1259003.

GeoProc2019: Earthquake and Faulting mechanics

7th International Conference on Coupled THMC Processes in Geosystems
3-5 July 2019 Utrecht (Netherlands)

Probing at the source of induced seismicity: Understanding the couplings between permeability creation, stress dynamic variations and aseismic / seismic slip based on mesoscale experiments

Yves Guglielmi [1]

Keywords: induced seismicity, mesoscale experiments

Scientists have known since the late 1960s that injecting fluids underground can cause earthquakes if those fluids find their way into slip-prone fault zones. Evidence of fluid-induced quakes has continued mounting in recent years with observations of abnormally high levels of seismicity in the central U.S. and in many other countries, coincident with increased injection of wastewater — mostly related to oil- and gas-mining operations — into the ground. But understanding the inner workings of fluid-filled faults is challenging because researchers have largely been limited by how close they can get to study them. This talk is offering a glimpse into some mechanisms of induced-seismicity by monitoring fault motions at field scale and in real time. Through the overview of various fault activation experiments we discuss the following key concepts. How sufficient is it to apply a simple effective stress law that considers a uniform pore pressure variation in a planar fault to accurately predict fault activation and leakage? Are Laboratory Experiments a Good Enough Indicator of Field-Scale Behavior?

[1] Lawrence Berkeley National Laboratory, USA, yguglielmi@lbl.gov

GeoProc2019: Earthquake and Faulting mechanics

7th International Conference on Coupled THMC Processes in Geosystems
3-5 July 2019 Utrecht (Netherlands)

On the effects of multi-phase fluid flow on induced seismicity

D. Zbinden[1], A. P. Rinaldi[2], S. Wiemer[3]

Keywords: multi-phase fluid flow, hydro-mechanical modeling, induced seismicity

Operations that involve fluid injection into the deep subsurface (e.g. geothermal energy, wastewater disposal, CO_2 sequestration) may induce earthquakes. If such seismicity is felt by people, it may jeopardize the acceptance of projects and, in the worst case, damage infrastructure and pose a threat to the population. It is generally understood that injection leads to pressure and stress changes in the subsurface, having the potential to reactivate pre-existing faults. Despite the many studies that have been performed during the last decades, induced seismicity remains difficult to be controlled and mitigated, since the relevant processes are largely hidden in the subsurface. Numerical modeling is one possible approach to better understand the rock-fluid interaction at depth. In the context of injection-induced seismicity, numerical models have so far mainly focused on undisturbed reservoirs (i.e. hydrostatic pressure conditions, single phase flow). However, *in-situ* conditions may also be disturbed, especially if a gas phase is present, strongly affecting pressure and flow conditions. Seismicity associated with multi-phase fluid flow has been observed both in the natural and induced context, and may play a major role at volcanic sites (e.g., Fischer et al., 1994). The gas may have an effect on the timing, distribution and size of induced earthquakes.

In this study, we thus focus on the modeling and analysis of fluid injection into a disturbed reservoir taking into account multi-phase fluid conditions. We use TOUGH2-based simulators (Pruess et al., 2011) to accurately model the multi-phase and multi-component fluid interaction accounting for relative permeability and capillary pressure. We study the hydro-mechanical processes during fluid injection into a reservoir, incorporating effective pressure of the gas-water mixture. We then simulate the reactivation of a nearby fault under disturbed conditions (Figure 1). We test multiple scenarios with different *in-situ* conditions and evaluate the relative influence of the gas on the timing and size of the induced events.

The results show that a gas phase may influence the induced seismicity in various ways: (i) the gas may pre-stress the fault, leading to earlier reactivation compared to single-phase hydro-static conditions, (ii) fault slip and magnitude are generally larger if a gas phase is present (Figure 2), and (iii) the influence of the gas decreases with increasing reservoir depth. These findings provide a first step toward a more detailed understanding of the coupling between multi-phase fluid flow and induced seismicity.

[1] Swiss Seismological Service (ETH Zürich), dominik.zbinden@sed.ethz.ch
[2] Swiss Seismological Service (ETH Zürich), antoniopio.rinaldi@sed.ethz.ch
[3] Swiss Seismological Service (ETH Zürich), stefan.wiemer@sed.ethz.ch

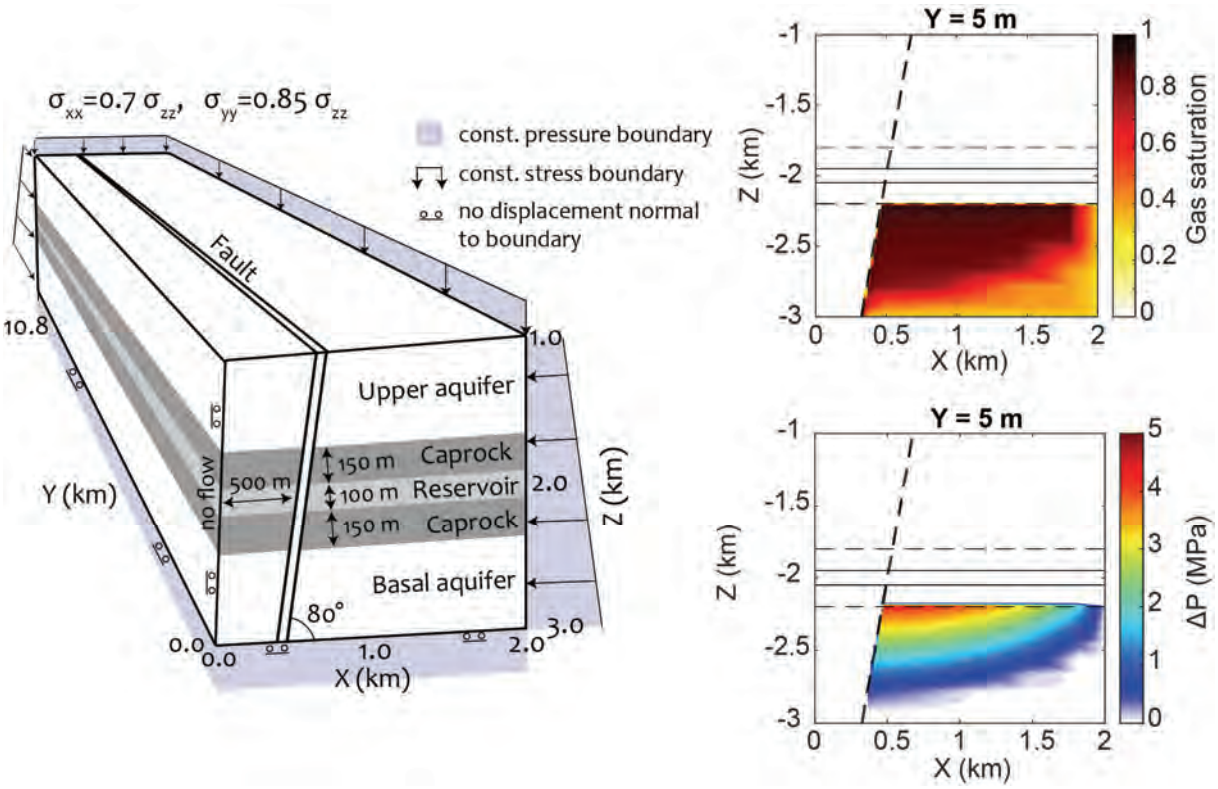

Figure 1. TOUGH-FLAC model (Rutqvist, 2011) with an overpressurized gas phase below a 2 km deep injection reservoir.

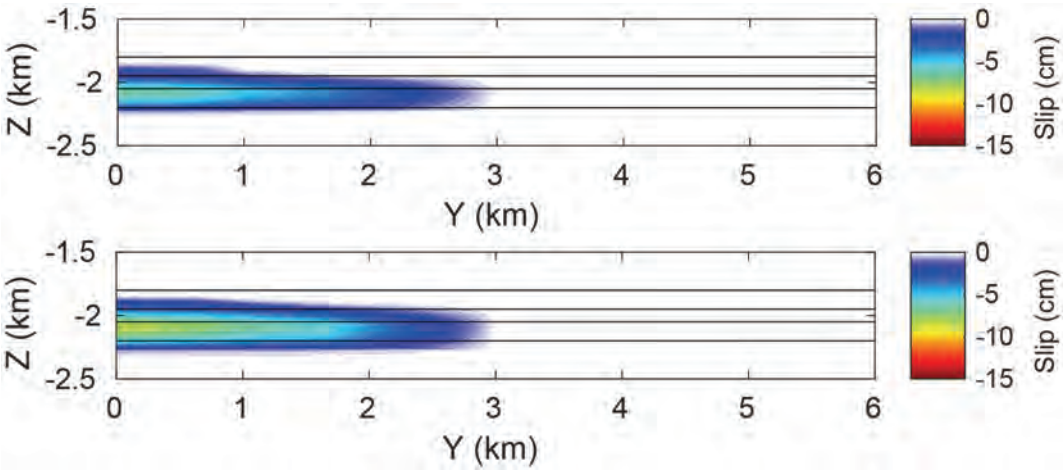

Figure 2. Comparison of fault slip for a single-phase reference case and a scenario with an overpressurized gas phase in place.

References

Fischer, T. P., M. M. Morrissey, V. M. L. Calvache, M. D. Gomez, C. R. Torres, J. Stix, and S. N. Williams (1994), Correlations between SO2 flux and long-period seismicity at Galeras volcano, *Nature, 368*(6467), 135, https://doi.org/10.1038/368135a0.

Pruess, K., C. M. Oldenburg, and G. Moridis (2011), TOUGH2 User's Guide, Version 2.1. Paper LBNL-43134 (revised), Lawrence Berkeley National Laboratory, Berkeley, CA, USA.

Rutqvist, J. (2011), Status of the TOUGH-FLAC simulator and recent applications related to coupled fluid flow and crustal deformations. *Computers & Geosciences, 37*(6), 739–750, https://doi.org/10.1016/j.cageo.2010.08.006.

GeoProc2019: Earthquake and Faulting mechanics

7th International Conference on Coupled THMC Processes in Geosystems
3-5 July 2019 Utrecht (Netherlands)

Fault stability during re-injection in deep geothermal systems

F. Parisio[1], V. Vilarrasa[2], W. Wang[3], O. Kolditz[4], T. Nagel[5]

Keywords: Induced Seismicity, Geothermal Reservoirs, OpenGeoSys

During operation, geothermal reservoirs experience strong deformation connected to pore pressure variations and cooling during cold water re-injection performed to balance fluid depletion. The induced thermal stress is proportional to thermal deformation and to effective stress change connected to pore pressure variation. For deep reservoirs, the risk of strong cooling is even more pronounced. The reduction of effective stress can reactivate large fault, which are ultimately responsible for earthquakes that can reach magnitudes M>3. We have investigated here the potential of cold fluid injection in the induced seismicity of deep geothermal reservoirs.

We have performed THM finite element analyses with the object-oriented, C++ based and open source finite element solver OpenGeoSys. We have modeled a deep geothermal reservoir with a large fault between a doublet system. To assess seismic risks, we have computed rate of seismic production (Dietrich, 1994; Chang and Segall, 2016).

The flow of cold water outgoing from the re-injection well crosses the fault toward the production well (Figure 1). Deformation follows mostly the cooling front and it is less affected by pressure changes. Fluid velocity is highest in the fault, while major mechanical effect happens because of thermal deformation, highlighting the importance of controlling injection conditions not only in terms of pore pressure, but temperature as well. Possible risk mitigation strategies could include limiting cold-water injection by either increasing inflow temperature or by decreasing its flow rate.

---

1 Department of Environmental Informatics, Helmholtz Centre for Environmental Research – UFZ, Leipzig, Germany, francesco.parisio@protonmail.com

2 Institute of Environmental Assessment and Water Research (IDAEA), Spanish National Research Council (CSIC), Barcelona, Spain, victor.vilarrasa@idaea.csic.es

3 Department of Environmental Informatics, Helmholtz Centre for Environmental Research – UFZ, Leipzig, Germany, wenqing.wang@ufz.de

4 Applied Environmental Systems Analysis, Technische Universität Dresden, Dresden, Germany, olaf.kolditz@ufz.de

5 Chair of Soil Mechanics and Foundation Engineering, Institute of Geotechnics, Technische Universität Bergakademie Freiberg, Freiberg, Germany, thomas.nagel@ifgt.tu-freiberg.de

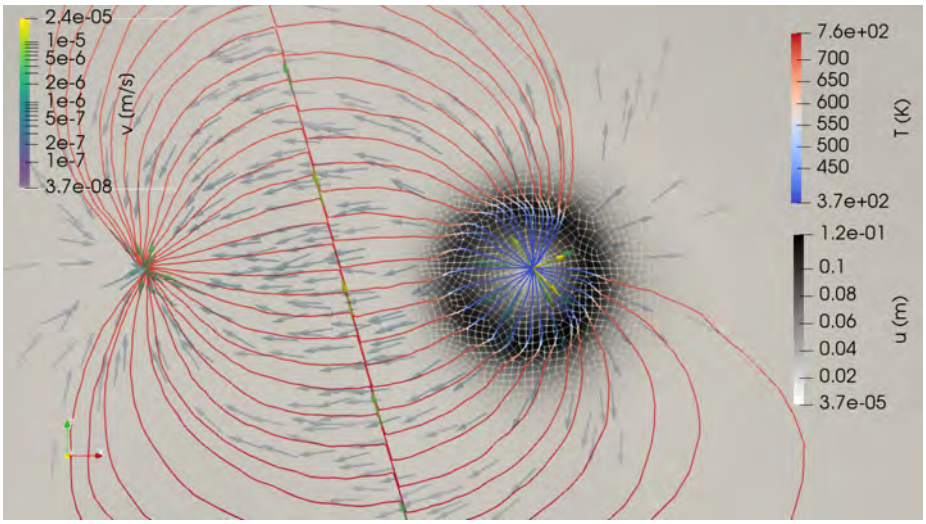

Figure 1. Flow tracers with temperature and deformation.

References

Dieterich, J. (1994). A constitutive law for rate of earthquake production and its application to earthquake clustering. *Journal of Geophysical Research: Solid Earth*, *99*(B2), 2601-2618.

Chang, K. W., & Segall, P. (2016). Injection-induced seismicity on basement faults including poroelastic stressing. *Journal of Geophysical Research: Solid Earth*, *121*(4), 2708-2726.

GeoProc2019: Earthquake and Faulting mechanics

7th International Conference on Coupled THMC Processes in Geosystems
3-5 July 2019 Utrecht (Netherlands)

Fault reactivation and seismic rupture along faults in depleting reservoirs with offset

P.A.J. van den Bogert[1]

Keywords: Induced-seismicity, reservoir depletion, dynamic rupture simulation, reservoir offset, linear slip-weakening

The seismic events recorded in the depleting Groningen gas field in The Netherlands are mapped on known, natural faults with increasing confidence (Willacy et al., 2018). The Groningen field is in a normally stressed environment where the reservoir offset (Figure 1a) is less than half the reservoir thickness over more than 80% of the length of known faults. Fault reactivation and the development of aseismic slip patches is expected to start at the top of the hanging wall and at the bottom of the foot wall reservoir (Figure 1a). Aseismic slip patches become seismic if their length exceeds the critical slip length L_c as defined by Uenishi and Rice (2003) when using a linear fault slip-weakening relationship (Figure 1b, Buijze et al., 2017).

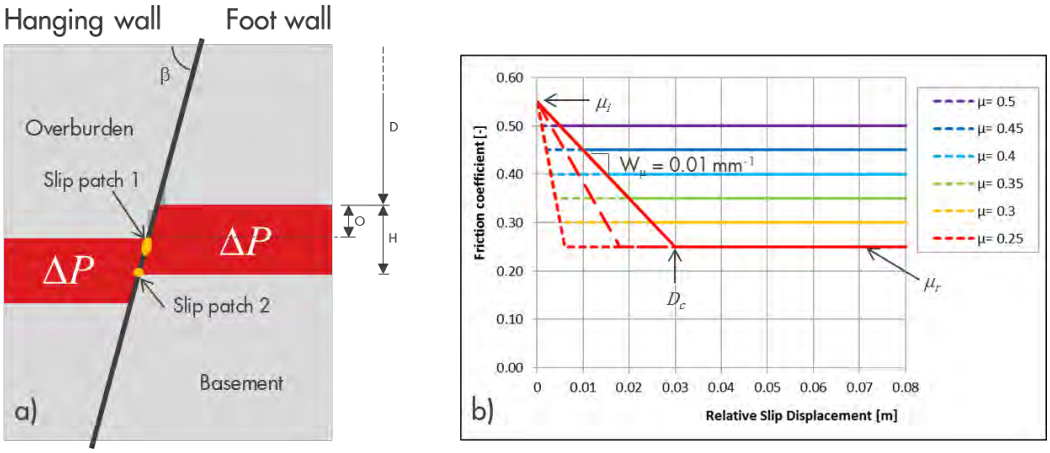

Figure 1. a) Typical reservoir-fault configuration in the Groningen field and the locations where fault start, and b) the parameters of the linear slip-weakening relationships varied in this paper.

Based on a large number of 2D dynamic rupture simulations, this paper demonstrates that reservoir offset not only influences the onset of fault slip, but also the onset of seismic rupture. Reservoirs with a normalised offset of about 1 are most prone to fault slip and seismic rupture, while reservoirs with a small normalised offset ($\bar{O} < 0.2$) sustain a significantly larger reservoir depletion before onset of seismic rupture occurs. Also, the slope of the descending branch of the linear slip-weakening diagram W_μ strongly influences the onset of seismic rupture. A steeply descending branch causes

[1] Shell Global Solutions, Rijswijk, The Netherlands, peter.vandenbogert@shell.com

individual slip patches to become unstable at a relatively small size, which means that seismic rupture follows onset of fault slip after a small incremental reservoir depletion (Figure 2a). Furthermore, this paper shows that three different rupture mechanisms may occur depending on the reservoir offset and the slope W_μ and the residual friction coefficient μ_r, namely:

1. *Merging of the two slip patches*
2. *Instability of a single slip patch*
3. *Instability of a single slip patch followed by merging with an adjacent slip patch* during seismic rupture.

The source-time function has distinctively different characteristics for each rupture mechanism, which may provide the opportunity to identify the rupture mechanism for observed seismic events in the Groningen field. The rupture mechanism and the residual friction coefficient strongly influence the moment magnitude of the simulated seismic event (Figure 2b). It is demonstrated that any of the three rupture mechanisms can occur on any fault configuration by selecting appropriate fault slip parameters. However, fault slip parameters can be significantly constrained if actual seismic events can be located on known natural faults and if the associated rupture mechanism can be identified.

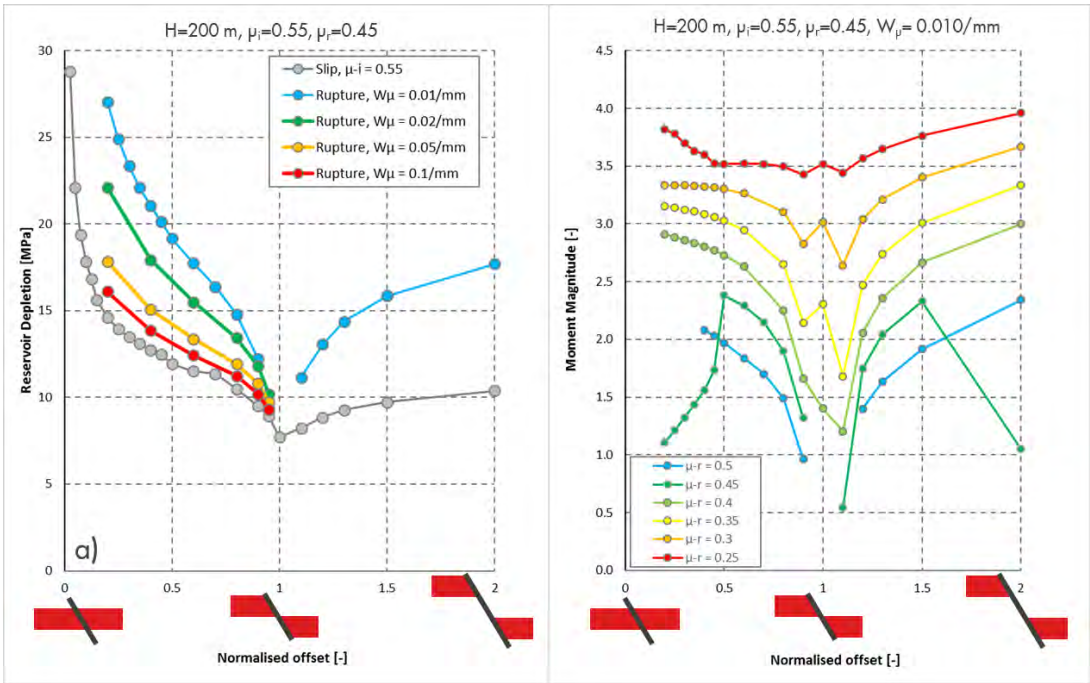

Figure 2. a) Reservoir depletion pressure causing fault reactivation (gey line) and seismic rupture for different values for the slope W_μ, and b) moment magnitude M_w for different values of the residual friction coefficient μ_r both as a function of the reservoir offset normalised for reservoir thickness.

References

Buijze, L., P.A.J. van den Bogert, B.B.T. Wassing, B. Orlic, and J. ten Veen (2017), Fault reactivation mechanisms and dynamic rupture modelling of depletion-induced seismic events in a Rotliegend gas reservoir. Netherlands Journal of Geosciences, 96 (5), s131-s148.

Uenishi, K. and J.R. Rice (2003), Universal nucleation length for slip-weakening rupture instability under nonuniform fault loading, J. Geophys. Res., 108(B1), 2042, doi:10.1029/2001JB00168.

Willacy, C., E. van Dedem, S. Minisini, J. Li, J.W. Blokland, I. Das, and A. Droujinine (2018), Application of Full Waveform Event Location and Moment Tensor Inversion for Groningen Induced Seismicity, The Leading Edge, 37(2), 92–99.

GeoProc2019: Earthquake and Faulting mechanics

7th International Conference on Coupled THMC Processes in Geosystems
3-5 July 2019 Utrecht (Netherlands)

Compaction bands formation in a high porosity limestone: Experimental observations and modelling

Y. Abdallah[1], *J. Sulem*[2], *M. Bornert*[3], *I. Stefanou*[4], *S. Ghabezloo*[5]

Keywords: Compaction bands, Carbonate rocks, Microstructure, Digital volume correlation.

Compaction bands in porous sedimentary rocks have been observed in field and in laboratory (Cilona *et al.* 2012). These bands can have a huge impact on a geosystem performance. Pore collapse can generate a pore-fluid pressurization and enhance pressure solution phenomenon in wet conditions. In addition, compaction bands can lead to a dramatic permeability reduction of several orders of magnitude as they act as barriers to fluid transport. Although identified in the field, compaction bands in carbonate rocks are still difficult to identify in laboratory experiments (Baud *et al.* 2009).

Our study aims at exploring the mechanisms which control the formation of compaction bands in a porous carbonate rock and develop the appropriate modelling tools for describing their evolution.

The chosen rock is a high porosity limestone (ϕ=37%) from the Paris Basin, Saint-Maximin limestone. Cylindrical samples, 40 mm in diameter, are tested in a high pressure triaxial cell in combination with X-ray tomography observations. Digital volume correlation (DVC) analyses are performed on the images taken before and after loading, using the in-house software CMV3D (Lenoir *et al.* 2007). This procedure permits to build 3D incremental deformation maps at a spatial resolution of 1 mm and to detect when strain localization is triggered and how it evolves. Porosity maps can be calculated from calibrated grey values of X-ray images of samples in the intact state and then are compared to deformation maps in order to assess the role of porosity heterogeneities in localization.

An example of the strain field evaluated in a sample tested in axisymmetric triaxial conditions at a confining pressure of 10.5 MPa is shown in Figure 1. One can observe

[1] Université Paris-Est, Laboratoire Navier (ENPC-IFSTTAR-CNRS), Ecole des Ponts ParisTech, Marne-la-vallée, France, youssouf.abdallah@enpc.fr
[2] Université Paris-Est, Laboratoire Navier (ENPC-IFSTTAR-CNRS), Ecole des Ponts ParisTech, Marne-la-vallée, France, jean.sulem@enpc.fr
[3] Université Paris-Est, Laboratoire Navier (ENPC-IFSTTAR-CNRS), Ecole des Ponts ParisTech, Marne-la-vallée, France, michel.bornert@enpc.fr
[4] Université Paris-Est, Laboratoire Navier (ENPC-IFSTTAR-CNRS), Ecole des Ponts ParisTech, Marne-la-vallée, France, ioannis.stefanou@enpc.fr
[5] Université Paris-Est, Laboratoire Navier (ENPC-IFSTTAR-CNRS), Ecole des Ponts ParisTech, Marne-la-vallée, France, siavash.ghabezloo@enpc.fr

several deformation bands that have been formed just after the onset of plastic deformation. From the kinematic characteristics of these bands, they are identified as compaction bands. These bands take place in porous zones, while denser zones appear to remain intact. Porosity heterogeneities are thus controlling the localization pattern and evolution. While increasing the loading, new bands form and coalesce to form a thicker zone of compaction, whereas the stress-strain curve exhibits an overall hardening of the material.

Standard constitutive laws in a Cauchy continuum are unable to predict deformation bands with finite thickness. This deficiency can be overcome by resorting to constitutive models that account for the microstructure of the material. This is the case for the so-called micromorphic continuum models which contain additional degrees of freedom and/or higher order strain gradients in their formulation and consequently internal lengths in the constitutive relations. However, a major difficulty with these models is to give a physical significance to the introduced internal lengths in relation with the material microstructure, and a reliable method to measure it in experiments. In this study, we develop a second-gradient plasticity model by considering a yield function which depends upon the porosity and its spatial gradient. Considering the sample as a heterogeneous structure, it is possible to evaluate from density maps averaged over some mesoscopic scale, both the porosity field and its second-gradient and to calibrate the considered gradient plasticity model relevant for this scale of analysis. Predictions of the compaction bands thickness and its evolution are compared to the experimental evaluation performed using DVC analysis.

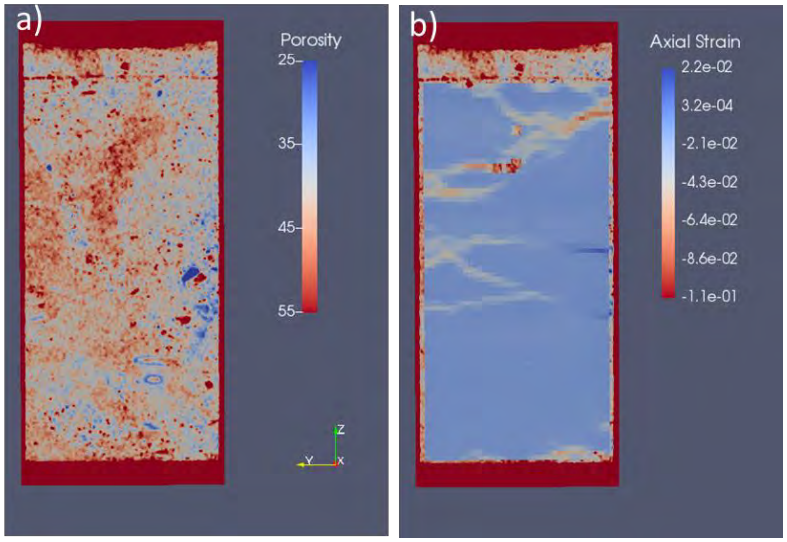

Figure 1. Vertical section of Saint-Maximin limestone sample: a) Porosity map before loading; b) Axial strain field after the onset of plasticity.

References

Baud, P., Vinciguerra, S., David, C., Cavallo, A., Walker, E., & Reuschlé, T. (2009). Compaction and failure in high porosity carbonates: Mechanical data and microstructural observations. Pure and Applied Geophysics, 166(5-7), 869-898, doi:10.1007/s00024-009-0493-2.

Cilona, A., Baud, P., Tondi, E., Agosta, F., Vinciguerra, S., Rustichelli, A., & Spiers, C. J. (2012). Deformation bands in porous carbonate grainstones: Field and laboratory observations. *Journal of Structural Geology*, *45*, 137-157, doi:10.1016/j.jsg.2012.04.012.

Lenoir, N., Bornert, M., Desrues, J., Bésuelle, P., & Viggiani, G. (2007). Volumetric digital image correlation applied to X-ray microtomography images from triaxial compression tests on argillaceous rock. Strain, 43(3), 193-205, doi:10.1111/j.1475-1305.2007.00348.

GeoProc2019: Earthquake and Faulting mechanics

7th International Conference on Coupled THMC Processes in Geosystems
3-5 July 2019 Utrecht (Netherlands)

Modeling of Japanese fault (The Japan Trench) instability by cohesive zone elements

Kyeung hye. AHN[1], Amade POUYA[2]

Keywords: The Japan Trench, Subduction zone, The Disroc finite element, Elastoplastic with softening damage

The Japanese trench subduction zone is one of the most active seismic zones where the Pacific plate is subducted below the North American plate at an annual rate of 8 to 9 cm due to an inverse fault mechanism.

In 2011, the largest earthquake (M 9) occurred at a distance of 24km from Japan's Trench to Japan (Tohoku Earthquake). Numerous observations indicate that the slip of faults in or near the trench exceeded 50 m. The M9 was a very large magnitude but it showed a relatively too great displacement.(Chester, F.M., et al 2013)

The objective of this study is to take advantage of models existing in rock mechanics for rock joints damage and fracture propagation, in particular cohesive zone models, to approach the tectonic behavior of a fault system, including its recurrent slip instabilities and the genesis of fractures in the inner zone of the fault system.

In order to model the structural characteristics of the subduction zone, the ocean bottom seismographs (OBS, 2D velocity structure in the forearc region off Miyagi) data were used as the basis for the geometry before the Tohoku earthquake (Miura, S., et al 2005). Also, the characteristics of the Japanese fault were modeled in the present work based on the data of the Japan Fast Trench Drilling Project (JFAST) conducted after the Tohoku earthquake (Ikari, M. J et al 2015)

To model the fault slip, it is necessary to well represent the stress-strain behavior of the interface determined by the gouge material and decollement roughness properties of the fault. It is also necessary to define the rheology of the surrounding crust environment by means of appropriate constitutive laws. We defined the geometry and the Finite Element mesh of the Japan's Trench as presented in the following figure. We applied first the weigh action in order to create the initial state of stresses. Then boundary displacements representing the tectonic movement were applied on the right side of the model when the left side was kept fixed.

The DISROC Finite Element code (Fracsima 2016) used for this modeling has damaging interface elements based on cohesive zone models.

1 Laboratoire Navier (IFSTTAR, CNRS, ENPC), Ecole des Ponts ParisTech,, Champs-sur-Marne, France. kyeung-hye.ahn@eleves.enpc.fr

2 Laboratoire Navier (IFSTTAR, CNRS, ENPC), Ecole des Ponts ParisTech,, Champs-sur-Marne, France amade.pouya@enpc.fr

In the subduction zone, there are two bending points where the subduction angle changes (5° to 13° around 143.2°E and 13° to 23° around 142.3°E). These points also coincide with the edges of rupture zone and their presence affects the process of plate boundary seismicity in this area (Ito.A. et al 2005) because the elastic energy of deformation is accumulated around these points.

After the shear stress exceeds the damage limit on the fault surface, it decreases and the energy is dissipated instantaneously because of instability effects. The stress concentration is then gradually transferred to the lower parts of the fault.

In our model, we focused on the two points considered to be epicenters of Tohoku seismic events on 1978 and 2011. These events occurred when the damage criterion was exceeded at the corresponding points. The movement measured at the sea bottom corresponding the second event (2011) was an uplift of 5m with a horizontal displacement of more than 60m (Ito, Y. et al 2011). The values obtained in our model for the displacement of the hanging wall were 25m in horizontal and 5m in vertical direction, so very similar to measured values. We think that including the plasticity of the fault zone in the model can improve this result.

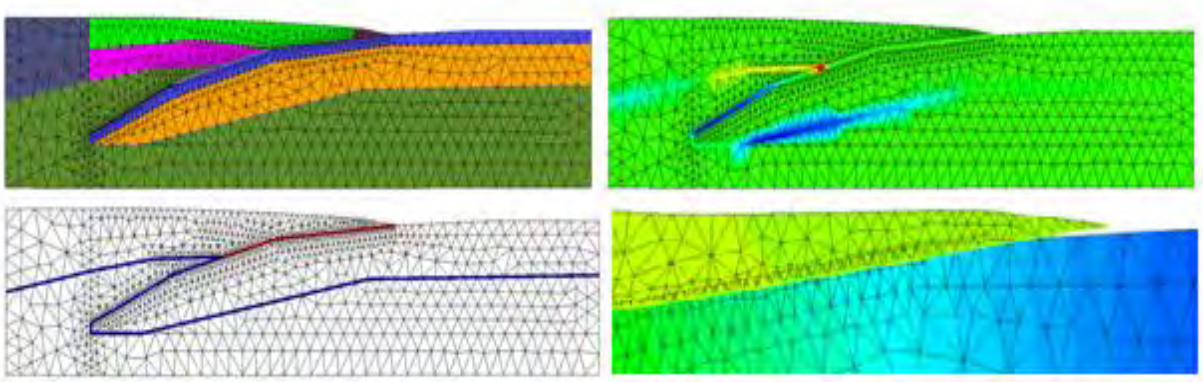

Figure 1. Modele of Japan Trench by GID

References

Chester, F. M., Rowe, C., Ujiie, K., Kirkpatrick, J., Regalla, C., Remitti, F., ... & Kameda, J. (2013). Structure and composition of the plate-boundary slip zone for the 2011 Tohoku-Oki earthquake. Science, 342(6163), 1208-1211.

Fracsima 2016 : Disroc, a Finite Element Code for modelling Thermo-Hydro-Mechanical processes in fractures porous media (http://www.fracsima.com/DISROC/Disroc.html)

Ikari, M. J., Kameda, J., Saffer, D. M., & Kopf, A. J. (2015). Strength characteristics of Japan Trench borehole samples in the high-slip region of the 2011 Tohoku-Oki earthquake. Earth and Planetary Science Letters, 412, 35-41.

Ito, A., Fujie, G., Miura, S., Kodaira, S., Kaneda, Y., & Hino, R. (2005). Bending of the subducting oceanic plate and its implication for rupture propagation of large interplate earthquakes off Miyagi, Japan, in the Japan Trench subduction zone. Geophysical Research Letters, 32(5).

Ito, Y., Tsuji, T., Osada, Y., Kido, M., Inazu, D., Hayashi, Y., ... & Fujimoto, H. (2011). Frontal wedge deformation near the source region of the 2011 Tohoku-Oki earthquake. *Geophysical Research Letters*, *38*(7).

Miura, S., Takahashi, N., Nakanishi, A., Tsuru, T., Kodaira, S., & Kaneda, Y. (2005). Structural characteristics off Miyagi forearc region, the Japan Trench seismogenic zone, deduced from a wide-angle reflection and refraction study. Tectonophysics, 407(3-4), 165-188.

GeoProc2019: Earthquake and Faulting mechanics

7th International Conference on Coupled THMC Processes in Geosystems
3-5 July 2019 Utrecht (Netherlands)

The Physics of Wormhole Formation in Carbonate Rocks

A. Alazman[1], H. Alarji[2], F. Hussain[3], K. Regenauer-Lieb[4]

Keywords: Carbonate Acidizing, Coreflooding, Wormhole Formation, Microstructure

Hydrochloric acid is frequently used during carbonate acidizing to reduce formation damage and improve near-wellbore productivity by creating deep conductive flow channels to the formation, called" wormholes". Several studies have revealed that the formation of wormholes primarily depends on the acid concentration, injection rate, rock property, rock mineralogy, and temperature. Rock dissolution and wormhole structures formed during hydrochloric acid stimulation process may differ from face dissolution at a lower injection rate to uniform dissolution resulting in ramified wormholes structure at a higher injection rate, whereas single dominant wormhole channel and most efficient stimulation are attained at intermediate injection rate. Damköhler and Péclet numbers are primary parameters that control stimulation fluid flow during carbonate acidizing. Consequently, Damköhler and Péclet numbers control the required pore volumes of acid for channel breakthrough. This paper studies wormhole formations and investigates the effects of acid concentration and injection rate parameters on wormhole configuration and growth using different rock minerology.

In this paper, core flooding experiments were carried out on two source rocks namely; Mount Gambier and Indiana limestone cores (1 in. diameter × 2 in. long) at room temperature. The injected fluid was diluted hydrochloric acid (HCI) solution at a wide range of pH values and prepared through the dilution of 32 wt% HCL with fresh water. Carbonate acidizing experiments were performed at diverse scenarios of hydrochloric acid concentration (0.00001–0.1 M) and injection rate. Microscopic imaging was taken on core samples prior and post coreflooding experiments allowing the assessment of the wormhole evolution throughout the experiments. The coreflooding effluent samples were chemically analyzed for cations using Inductively Coupled Plasma (ICP) spectroscopy to assess the dissolution reaction phenomena. Optimum acid concentration and injection rate were attained through coreflooding experiments and the effects of varying Damköhler & Péclet numbers were analyzed.

The experimental results shown in figure -1.c revealed an observed single dominant wormhole on Indiana limestone core sample at an acid concentration of 0.1 M HCI and injection rate of 10 cm^3/min. Face dissolution patterns shown in figure-1.a &b were noted on Mount Gambier core samples at an acid concentration of 0.001 M HCI and injection rate of 1 & 3 cm^3/min. Damköhler and Péclet numbers defined in table -1.

[1] UNSW Sydney, a.alazman@student.unsw.edu.au
[2] UNSW Sydney, h.alarji@student.unsw.edu.au
[3] UNSW Sydney, furqan.hussain@unsw.edu.au
[4] UNSW Sydney, klaus@unsw.edu.au

Damköhler and Péclet numbers have been implemented to design and predict the optimum wormhole structure for different rock mineralogy. As the acidic level and injection rate of the injected solutions increased, face dissolution or wormhole developments were observed. The wide range of the used acid concertation and injection rate helped in achieving a comprehensive understanding of the wormhole creation and structure throughout the core sample. Experiment results showed different outcomes from face dissolution to single dominant wormhole.

a. Face dissolution on Mount Gambier core sample at an acid concentration of 0.001 M HCI and injection rate of 1 cm^3/min.

b. Face dissolution on Mount Gambier core sample at an acid concentration of 0.001 M HCI and injection rate of 3 cm^3/min.

c. Single dominant wormhole on Indiana limestone core sample at an acid concentration of 0.1 M HCI and injection rate of 10 cm^3/min.

Figure -1 Microscopic imaging taken on core samples prior and post coreflooding experiments

Table -1 Damköhler and Péclet numbers

Péclet number (N_{Pe})	Damköhler number (N_{Da})
$N_{Pe} = \frac{Q\sqrt{k}}{AD_e}$	$N_{Da} = \frac{\pi dL\kappa}{Q}$
Q = the flow rate	d = the core diameter
k = the matrix permeability	L = the core length
A = the flow area	κ = the overall dissolution rate constant
D_e = the effective diffusion coefficient	Q = the flow rate

Several analyses have been carried out to examines carbonate response with diverse acids at distinct acid concentrations, injection rates and temperatures. Nevertheless, limited investigations have stated the pore and micro-structure effects on carbonate acidizing. Wang et al. (1993) confirmed the major effect of rock mineralogy on carbonate stimulation treatment. Several researchers have applied Nuclear Magnetic Resonance (NMR), Scanning Electrode Microscopy (SEM), High Pressure Mercury Injection (HPMI) and tracer experiment to identify flowing fraction for pore structure characterization. Additional rock properties such as porosity and permeability and structure analysis are recommended to complement and fully characterize wormhole formation and growth.

Damköhler and Péclet numbers describe the major factors that affect wormhole formation namely acid concentration, injection rate, rock mineralogy and temperature. Micro-structure analysis through X-Ray Computed Tomography (CT) before and after acid injection will enhance pore structure description and complement the characterization of wormhole formation in addition to Damköhler and Péclet numbers analysis. Further studies and analysis of the rock microstructure are needed to complement the current work to seek in-depth understanding of the rock reaction with different acidic flooding conditions.

References

1. Mahmoud, M., Barri, A. & Elkatatny, S., 2017. Mixing chelating agents with seawater for acid stimulation treatments in carbonate reservoirs. *Journal of Petroleum Science and Engineering*, 152, pp.9–20. Available at: https://www.sciencedirect.com/science/article/pii/S0920410517303248 [Accessed August 18, 2018].
2. Theresa Sibarani, T. et al., 2018. The Impact of Pore Structure on Carbonate Stimulation Treatment Using VES-Based HCl. Available at: https://www.onepetro.org/download/conference-paper/SPE-192066-MS?id=conference-paper%2FSPE-192066-MS [Accessed January 19, 2019].
3. Yoo, H. et al., 2018. An experimental study on acid-rock reaction kinetics using dolomite in carbonate acidizing. *Journal of Petroleum Science and Engineering*, 168, pp.478–494. Available at: https://ac.els-cdn.com/S0920410518304340/1-s2.0-S0920410518304340-main.pdf?_tid=7dea453c-e71e-4b2e-9a6e-a85ba968b334&acdnat=1531449211_20d811abb1ee8d0af37985d903a57745 [Accessed July 13, 2018].

GeoProc2019: Earthquake and Faulting mechanics

7th International Conference on Coupled THMC Processes in Geosystems
3-5 July 2019 Utrecht (Netherlands)

Laboratory earthquakes across the brittle-plastic transition

J. Aubry[1], A. Schubnel[1], F.X. Passelègue[2], J. Gasc[1], M. Page[3], S. Marty[1], D. Deldicque[1] and J. Escartin[4]

Keywords: Brittle-plastic transition, surface evolution, fault weakening, stick-slip.

The transition from brittle to plastic deformation corresponds to the regime where brittle fracturing and plastic flow coexist. This transition is fundamental to understand how natural faults behave at varying crustal depth and why large earthquakes generally nucleate at the bottom of the seismogenic zone, at PT conditions where deformation is not fully brittle anymore.

Frictional sliding experiments were performed on Carrara marble saw-cut faults, at confining pressures ranging between 45 and 235MPa, i.e. across the brittle-ductile transition of this well studied lithology (Fredrich et al., 1989). Two different axial loading rates (1.3 µm/s and 0.02 µm/s) and initial surface roughness were investigated. A carbon layer was deposited on the top surface to image heat heterogeneities at the micro-scale (Aubry et al. 2018). White light interferometry was used to measure fault surface topography, before and after the experiments. Depending on the range of pressures and strain rates tested and the roughness of the fault interface, different slip modes and deformation processes were observed.

For all the experiments on smooth faults, static fault friction coefficients ranged between ~0.2-0.45. Regardless of confining pressure, lower loading rates promoted stick-slips. At high loading rates, we observed a transition from quasi-stable sliding (a unique slip event followed by stable sliding) resulting in mirror-like surfaces at low confining pressures (from 45 to 135 MPa) to a stick-slip regime resulting in matte surfaces at high confining pressure (from 180 MPa). Above 90 MPa, laboratory earthquakes were observed in a regime where most of the axial strain (up to 70% at the highest confining pressure) was accommodated by bulk plastic deformation of the rock specimen while the fault interface remained locked. Temperature mapping showed that the temperatures reached 1100°C and sometimes over 1500°C along

[1] Laboratoire de Géologie, École Normale Supérieure/CNRS UMR 8538, PSL Research University, 24 rue Lhomond, F-75005 Paris, France, jerome.aubry@ens.fr, alexandre.schubnel@ens.fr, julien.gasc@ens.fr, samson.marty@ens.fr, damien.deldicque@ens.fr
[2] Ecole Polytechnique Fédérale, CH-1015 Lausanne, Switzerland, francois.passelegue@epfl.ch
[3] Centre de Recherche et de Restauration des Musées de France, Palais du Louvre - Porte des Lions 14 quai François Mitterrand, F-75001 Paris, France, marine.page@culture.gouv.fr
[4] Institut de Physique du Globe de Paris, Sorbonne Paris Cité, Université Paris Diderot, CNRS UMR 7154, 1 rue Jussieu, F-75005 Paris, France, escartin@ipgp.fr

these fault interfaces. Evidence of melting and decarbonation were observed SEM while EBSD revealed that intra-crystalline plastic deformation occurred near the fault interface. The static friction was always higher for all initially rough interfaces, ranging between ~0.3-0.6. On these rough interfaces, only stable sliding was observed at high loading rates. At 45 and 90 MPa, we observed slow slips and stick-slips, while at 180 MPa, only creep was observed.

We conclude that: (i) laboratory earthquakes may nucleate on inherited fault interfaces at brittle-plastic transition conditions; (ii) in this regime where plastic deformation of the bulk and dynamic fault slip may coexist, laboratory earthquakes are promoted when the interface is smooth, or when the loading rate is slow; (iii) stable sliding tends to produce mirror-like surfaces, while stick-slips are associated with matte surfaces, on which the size of the asperities grows with increasing confining pressure, (iv) in a rather counterintuitive manner, when compared to purely brittle rheologies, slower loading rates and higher confining pressures promote the occurrence of laboratory earthquakes associated with increasing plastic deformation, while increasing initial roughness promotes stable sliding.

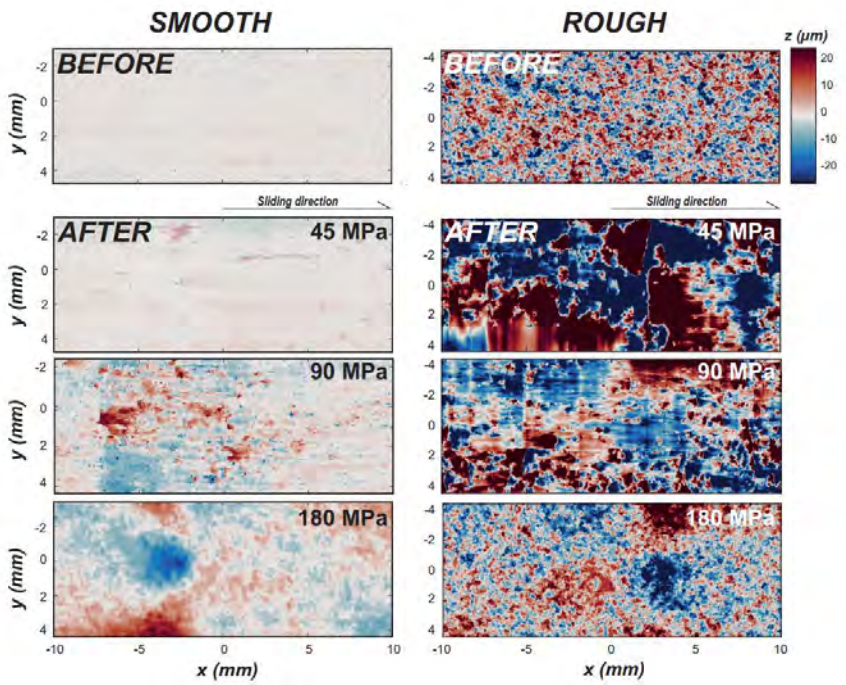

Figure 1. Microtopographies before and after laboratory earthquakes, using smooth and rough initial fault surfaces, between 45 and 180 MPa (loading rate of 1.3 µm/s). Damage on post-mortem surfaces and asperity size increase with increasing confining pressure.

References

Aubry, J., Passelègue, F.X., Deldicque, D., Girault, F., Marty, S., Lahfid, A., et al. (2018), Frictional heating processes and energy budget during laboratory earthquakes, *Geophysical Research Letters*, *45*, 12,274-12,282, doi:10.1029/2018GL079263.

Fredrich, J. T., Evans, B., & Wong, T. F. (1989), Micromechanics of the brittle to plastic transition in Carrara marble, *Journal of Geophysical Research: Solid Earth*, *94(B4)*, 4129-4145, doi:10.1029/JB094iB04p04129.

GeoProc2019: Earthquake and Faulting mechanics

7th International Conference on Coupled THMC Processes in Geosystems
3-5 July 2019 Utrecht (Netherlands)

The impact of CO_2-brine-rock interactions on the frictional behaviour of clay-rich fault gouges

E. Bakker[1], J. Kaszuba[2], S.A.M. den Hartog[3], S.J.T. Hangx[4]

Keywords: CO_2 storage, fault stability, chemo-mechanical coupling

The impact of long-term fluid-rock interactions on the frictional properties of faults is one of the main concerns when ensuring safe geological storage of CO_2. Mineralogical changes may affect the frictional strength and seismogenic potential of pre-existing faults within or bounding a storage complex. However, most of these reactions are too slow to be reproduced on laboratory timescales and can only be assessed using geochemical modelling.

As an analogue for clay-rich caprocks overlying potential CO_2 storage sites in Europe, we used the Opalinus Claystone (Mont Terri laboratory, Switzerland). We combined geochemical modelling of CO_2-charged formation water and clay-rich fault gouges (1–1000 years residence time, i.e. 10–10^6 pore volume flushes) with friction experiments on simulated fault gouges (T = 22–150°C; σ_n^{eff} = 50 MPa; P_f = 25 MPa; v = 0.2-100 µm/s). The simulated gouges were prepared from finely powdered Opalinus Claystone or mineral mixtures, having mineralogical compositions as predicted by the models.

Our experiments showed that, although significant mineralogical changes occurred, they did not significantly change the frictional behaviour of faults. Instead, initial fault-gouge mineralogy imposed a stronger control on clay-rich fault behaviour than the extent of the predicted CO_2-brine-rock interactions, even under chemical conditions allowing for significant reaction. We demonstrated that the impact of mineralogical changes due to fluid-rock interactions on the frictional behaviour and seismogenic potential of faults could be assessed using our combination of geochemical modelling and friction experiments. Note that a complete understanding requires evaluation of additional effects, such as that of shear velocity, effective normal stress, and other fault characteristics (maturity, shear strain).

[1] Department of Earth Sciences, Utrecht University, Utrecht, Netherlands and Royal Haskoning DHV, Amersfoort, Netherlands ; elisenda.bakker@RHDHV.com
[2] Department of Geology and Geophysics and School of Energy Resources, University of Wyoming, Laramie, WY, USA
[3] The Lyell Centre, Heriot-Watt University, Edinburgh, UK
[4] Department of Earth Sciences, Utrecht University, Utrecht, Netherlands

GeoProc2019: Earthquake and Faulting mechanics

7th International Conference on Coupled THMC Processes in Geosystems
3-5 July 2019 Utrecht (Netherlands)

Frequency content of lab earthquakes for the spectrum of failure modes from slow slip to elastodyanamic rupture

D. Bolton[1], S. Shreedharan[1], J. Rivière[2], P. Shokouhi[2], and C. Marone[1]

Keywords: slow-fast slip, friction, frequency content, ultrasonics

Tectonic faults slip in a range of failure modes from slow-slip to fast, elastodynamic events. In general, slow slip represents a group of failure modes, including aseismic creep, low-frequency earthquakes, very-low-frequency, and episodic-tremor and slip. Previous studies have noted that slow earthquakes generate lower frequency energy and are deficient in high frequency radiation compared to dynamic rupture events (Ide et al. 2007). However, the connection between elastic radiation frequency and the mode of faulting is difficult to establish and there are few systematic data sets for the full seismic cycle. Moreover, scaling relations between radiated seismic energy, stress drop and slip duration for the spectrum of failure modes (McLaskey et al. 2012) have not been systematically documented. Laboratory friction experiments coupled with acoustic emission (AE) measurements provide the perfect opportunity to address this question. In this work, we attempt to expand our knowledge of slow and fast slip in the laboratory by analyzing the frequency content of AEs for a range of failure modes. We conduct a suite of friction experiments in a bi-axial loading frame using a double-direct shearing configuration. We shear layers of quartz powder (avg. particle diameter 10.5 µm and initial layer thickness of 3 mm) over a range of normal stresses from 7-11 MPa and shearing velocities from 3-40 µm/s. We vary the elastic loading stiffness, k, and impose the condition $k/k_c \sim 1$, where k_c is the critical frictional weakening rate. By systematically varying the ratio k/k_c we produce the complete spectrum of failure events from slow to fast slip, with peak slip velocities ranging from (< 100 to > 1000 µm/s) (Leeman et al. 2016; Scuderi et al. 2016). We record acoustic emission data continuously throughout the experiments at 4 MHz using broad-band piezoceramic sensors (~.02-2 MHz). The sensors are placed inside a steel loading block and positioned adjacent to the fault zone. We document the frequency content of the full range of slip events and illuminate differences using a combination of bandpass and notch filters. The frequency content of major failure events scales systematically with peak slip velocity. Slow slip events lack high frequency energy and fast slip events

[1]Department of Geosciences, The Pennsylvania State University, University Park, PA, dcb31@psu.eud; srisharan.nitk@gmail.com; chrisjmarone@gmail.com

[2]Department of Engineering Science and Mechanics, Pennsylvania State University, University Park, Pennsylvania, pxx990@psu.edu; jvr5626@psu.edu

have both low and high frequency energy. However, large slow slip events are preceded and accompanied by smaller events with high frequency radiation. We observe that acoustic energy scales directly with stress drop and peak slip velocity during large events. Our work has the potential to improve understanding of the elastic radiation emanating from slow and fast ruptures, while at the same shedding light on how seismic energy scales with earthquake source properties.

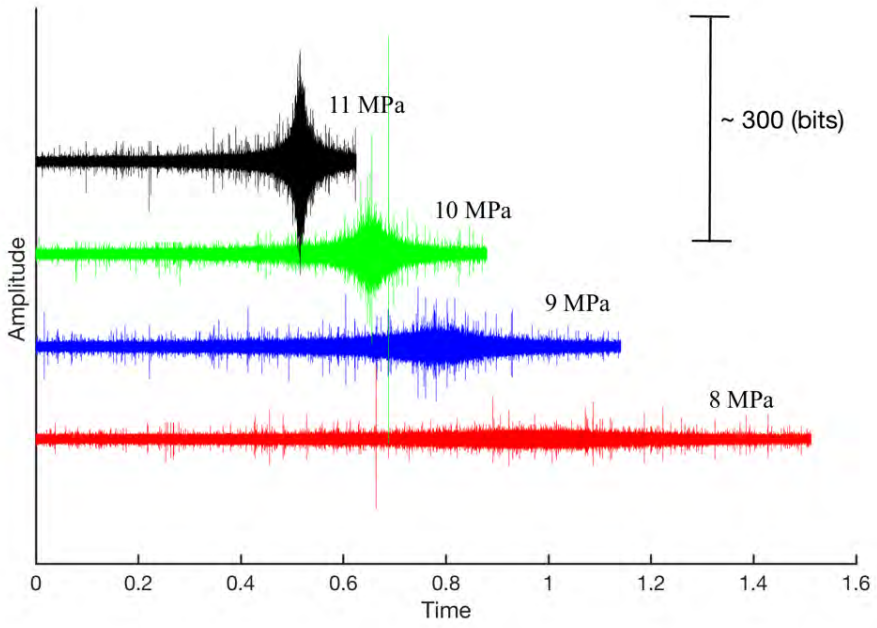

Figure 1 Plotted above are four acoustic time series signals that occur during the co-seismic slip phase of four slow slip events at different normal stresses. The trace length of each time series signal corresponds to the duration of the co-seismic slip phase. With increasing normal stress, the acoustic emissions become larger in amplitude and more impulsive.

References:

1. Ide, S., Beroza, G. C., Shelly, D. R., & Uchide, T. (2007). A scaling law for slow earthquakes. *Nature*, *447*(7140), 76.
2. Leeman, J. R., Saffer, D. M., Scuderi, M. M., & Marone, C. (2016). Laboratory observations of slow earthquakes and the spectrum of tectonic fault slip modes. *Nature communications*, *7*, 11104.
3. McLaskey, G. C., Thomas, A. M., Glaser, S. D., & Nadeau, R. M. (2012). Fault healing promotes high-frequency earthquakes in laboratory experiments and on natural faults. *Nature*, *491*(7422), 101.
4. Scuderi, M. M., Marone, C., Tinti, E., Di Stefano, G., & Collettini, C. (2016). Precursory changes in seismic velocity for the spectrum of earthquake failure modes. *Nature geoscience*, *9*(9), 695.

GeoProc2019: Earthquake and Faulting mechanics

7th International Conference on Coupled THMC Processes in Geosystems
3-5 July 2019 Utrecht (Netherlands)

FRICTIONAL STRENGTH AND STABILITY OF CALCITE-MONTMORILLONITE GOUGE MIXTURES AT 40 °C, 80 °C, and 120 °C

Carolyn Boulton[1] and André R. Niemeijer[2]

Keywords: friction, stability, mixtures, subduction zones

Subduction margins are responsible for ~85% of global moment release. Subduction zone seismic activity is primarily controlled by the hydrological and frictional properties of fluids and sediments within subduction margin fault(s). Worldwide, carbonates and clays occur in twenty of the twenty-six trenches drilled by the Ocean Drilling Program and Deep Sea Drilling Project (Plank, 2014). To explore the frictional behaviour of carbonates, clays, and carbonate-clay mixtures, we performed hydrothermal friction experiments on calcite, montmorillonite, and calcite-montmorillonite gouges.

Experiments were performed in a hydrothermal ring shear apparatus under conditions of a constant 60 MPa effective normal stress and temperatures of 40 °C, 80 °C, and 120 °C. To avoid pore fluid overpressure development and to establish a steady state microstructure, all gouges were sheared at 0.3 μm/s for 20 mm, after which velocity was stepped to 1 μm/s and back five times. From these velocity steps, we determined the velocity dependence of friction (a–b) and its reproducibility or strain dependence. Montmorillonite (Clay Minerals Society standard Swy-2) gouges exhibit temperature-independent friction coefficients (μ) between 0.10 and 0.15. The friction coefficient of calcite (crushed Iceland spar) gouges decreases with increasing temperature, from 0.49 at 40 °C to 0.42 at 120 °C. We observe a nonlinear relationship between the friction coefficient and amount of calcite in the gouge mixtures; frictional strength increases markedly in gouges with ≥60 wt.% calcite.

Under the conditions tested, calcite and calcite-montmorillonite (≥60 wt.% calcite) mixtures display positive values of (a–b); velocity-neutral behaviour was observed in montmorillonite and montmorillonite-calcite gouge mixtures with <60% calcite. Our results indicate that the presence of smectite-rich gouges along the subduction interface promotes potentially unstable slip behaviour at shallow depths. As the proportion of calcite increases, gouge mixtures become frictionally stronger and velocity strengthening, properties conducive to creep given sufficient driving stress. Intriguingly, the transition in strength and stability occurs at ≥60 wt.% calcite. General mixture rules for mélanges, numerical models of mélange behaviour, and fibre-loading theory (Bealle et al., 2019 and references therein) similarly predict a change in two-phase mixture behavior when competent “clasts” comprise ≥~50% of a two-phase mixture. The consistency between laboratory results, numerical models, and rheological theory suggests that our results are scalable to natural fault zones.

References

Bealle, A., Å. Fagereng, and S. Ellis (2019). Strength of strained two-phase mixtures: Application to rapid creep and stress amplification in subduction zone mélange. Geophys. Res. Lett., 46, https://doi.org/10.1029/2018GL081252.

Plank, T. (2014), The chemical composition of subducting sediments. *Treatise on Geochemistry (Second Edition)*, 4, 607-629.

[1] Victoria University of Wellington, PO Box 600, Wellington 6140, New Zealand

[2] Utrecht University, PO Box 80021, Utrecht 3508 TA, The Netherlands

GeoProc2019: Earthquake and Faulting mechanics

7th International Conference on Coupled THMC Processes in Geosystems
3-5 July 2019 Utrecht (Netherlands)

Fluid pressure drop and vaporisation during dynamic rupture

N. Brantut[1]

Keywords: Dilatancy, Fluid pressure, Earthquakes

Dilatancy during rock failure is a key process promoting fluid flow in the crust. Since rock failure is linked to spatio-temporal localisation of deformation, dilatancy is expected to be strongly localised around the fault plane, and to lead to dramatic local reductions in fluid pressure during rupture, severely impacting dynamic weakening processes such as thermal pressurisation. The existence of co- seismic fluid pressure drops have been inferred from field studies, notably in gold deposits which are thought to be formed by this process, but reliable quantitative predictions are still lacking.

Here, experimental results are presented where local on- and off-fault fluid pressure variations were measured in situ during dynamic rock fracture and frictional slip under upper crustal stress conditions. During the main rupture, the on-fault fluid pressure dropped rapidly to zero, indicating vaporisation (Figure 1). Strong differences in wave speed drop between ray paths propagating along (e.g., path A, Figure 1) and across the fault (path C, Figure 1) localisation of the fault zone damage and dilation; the wave speed measured along the fault dropped in two stages, consistenly with (1) damage generation and fluid pressure drop during rupture, and (2) resaturation and pore pressure recharge after rupture.

Further deformation produced stick-slip events systematically associated with near-instantaneous drops in fluid pressure, providing direct experimental evidence of seismic pumping.

Extrapolation of the laboratory results indicate that dilatancy-induced fluid

[1] Department of Earth Sciences, University College London, London, UK, n.brantut@ucl.ac.uk

pressure drop and vaporisation might be a widespread phenomenon in the upper 5 km of the crust.

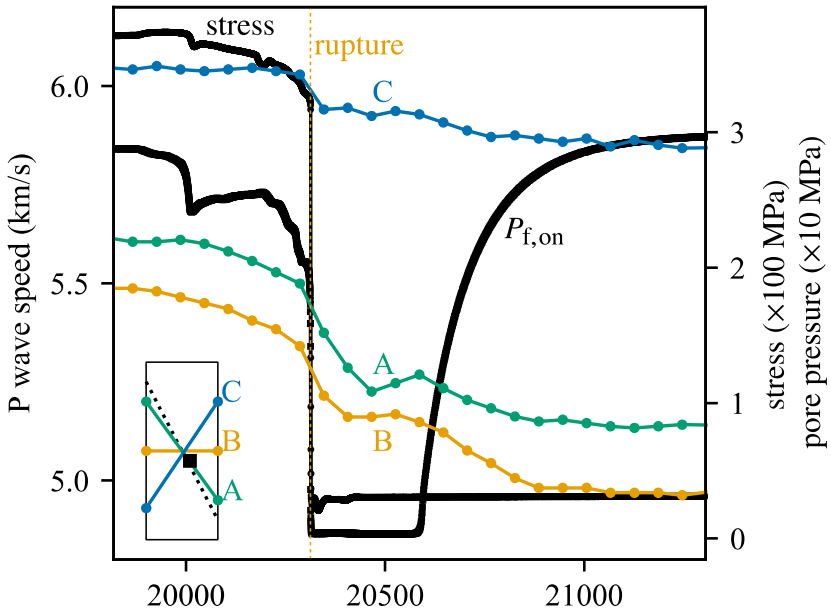

Figure 1. Evolution of differential stress, on-fault fluid pressure and P wave speed during rupture in initially intact Westerly granite at a confining pressure of 70 MPa and a nominal pore pressure of 30 MPa.

GeoProc2019: Earthquake and Faulting mechanics

7th International Conference on Coupled THMC Processes in Geosystems
3-5 July 2019 Utrecht (Netherlands)

Characterization of thermo-hydro-mechanical couplings of claystone using a novel transient experiment

P. Braun[1,2], S. Ghabezloo[2], P. Delage[2], J. Sulem[2], N. Conil[3]

Keywords: Claystone, Thermo-poro-elasticity, Transient method, Permeability

In laboratory thermo-hydro-mechanical (THM) experiments on geomaterials, the homogeneity of the pore pressure field within a specimen plays an important role whether drained or undrained conditions predominate. Especially for low permeability materials, such as shales, time intensive tests are required for achieving fully drained conditions. In undrained tests, which can be generally carried out more rapidly, one has to correct measurements with respect to the deformability of the drainage system (Wissa 1969; Bishop 1976; Ghabezloo and Sulem 2010), which might induce additional experimental uncertainties.

To improve basic rock mechanics tests under isotropic THM loads, a new loading protocol consisting of three THM loading stages is proposed in this study. Due to the low permeability the specimen remains first in true undrained conditions, when the loading is fast enough with respect to the time necessary for pore pressure dissipation. Afterwards the generated pore pressures are allowed to drain, which causes a transient deformation measured on the specimen (Figure 1). The applied loading can be a change of isotropic stress, similar to the protocol presented by Hart and Wang (2001). In this work we demonstrate that the same principle can be used analogously for thermal tests. The presented procedure allows to determine three material parameters (drained and undrained bulk moduli or thermal expansion coefficients, Skempton's coefficient or thermal pressurization coefficient), the Biots' modulus H and to back-calculate the permeability (Braun et al. 2018) in one single experiment. We show an application example of the transient testing protocol on the Callovo-Oxfordian claystone (COx), a candidate host rock for the geological radioactive waste disposal in France which has a permeability of 10^{-20} m² or smaller. Four material parameters are obtained in a thermal test, optimized to a duration of 20 h. These values compose an overdetermined set of parameters, which can be evaluated for their compatibility within the thermo-poroelasticity framework and are able to characterize the THM coupling of the COx claystone.

[1] Andra, Paris, France, philipp.braun@enpc.fr
[2] Ecole des Ponts ParisTech, Paris, France
[3] Andra, Bure, France

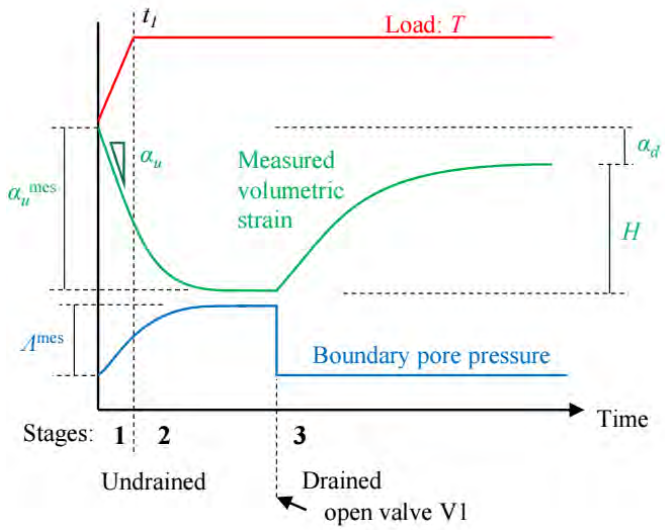

Figure 1. Schematic boundary conditions applied on a specimen during the transient test.

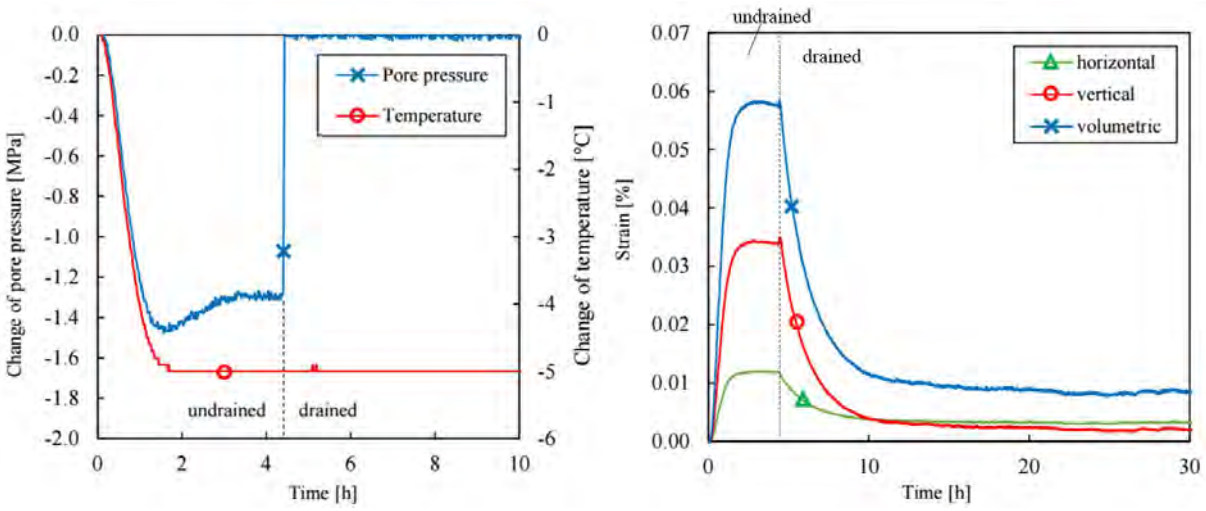

Figure 1. Thermal test on COx claystone showing thermally induced pore pressure, undrained and drained strains and transient pore pressure dissipation in the drained phase.

References

Bishop, A.W. (1976), The influence of system compressibility on the observed pore-pressure response to an undrained change in stress in saturated rock, *Géotechnique, 26*, 371–375.

Braun, P., Ghabezloo, S., Delage, P., Sulem, J. and N. Conil (2018), Theoretical Analysis of Pore Pressure Diffusion in Some Basic Rock Mechanics Experiments, *Rock Mech. Rock Eng., 51*(5), 1361-1378, doi: 10.1007/s00603-018-1410-8.

Ghabezloo, S. and J. Sulem (2010), Effect of the volume of the drainage system on the measurement of undrained thermo-poro-elastic parameters, *Int. J. Rock Mech. Min. Sci., 47*, 60–68, doi: 10.1016/j.ijrmms.2009.03.001

Hart, D.J. and H.F. Wang (2001), A single test method for determination of poroelastic constants and flow parameters in rocks with low hydraulic conductivities, *Int. J. Rock Mech. Min. Sci., 38*, 577–583, doi: 10.1016/S1365-1609(01)00023-5

Wissa, A.E.Z. (1969), Pore pressure measurement in saturated stiff soils, *J. Soil Mech. Found. Div. 95*, 1063–1073.

GeoProc2019: Earthquake and Faulting mechanics

7th International Conference on Coupled THMC Processes in Geosystems
3-5 July 2019 Utrecht (Netherlands)

Fault zone heterogeneity can promote rupture nucleation: Insights from large-scale experiments

L. Buijze[1,2], Y.-S. Guo[3], A.R. Niemeijer[1], S.-L. Ma[3], and C.J. Spiers[1]

Keywords: seismic instability, large-scale experiments, frictional heterogeneity

Fault zones are frictionally heterogeneous at many length-scales. This is important, as frictional properties affect the potential to nucleate seismic instability, with regions that are prone to rupture nucleation (asperities) or that deform by stable processes such as creep. In addition, friction also affect seismic rupture propagation and afterslip. Frictional heterogeneity and its effects on rupture are relevant for large, crustal-scale faults, as well as for smaller scale upper crustal faults. In particular, frictional properties may also play a large role in the nucleation and propagation of induced seismic events. One example is Groningen field, where faults cross-cut through anhydrites, clay-rich sections, and reservoir sandstones sections. The spatially varying fault zone properties, in conjunction with the depletion-induced stresses, will likely exert a dominant control on the nucleation and propagation of induced events. Thus far most experiments investigating frictional behavior have been conducted using a single fault gouge material. Here we aim to understand the behavior of spatially heterogeneous faults zones and the effect of heterogeneity on the average fault stability.

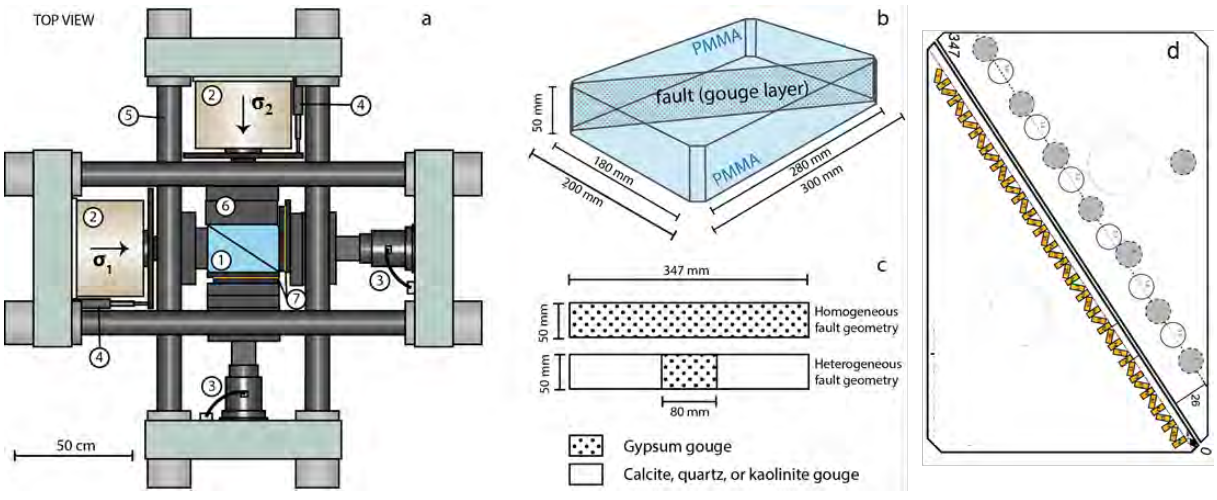

Figure 1. Experimental setup. a) Biaxial deformation rig, b) Sample assembly, c) Fault zone geometry, d) Instrumentation with strain gauges (yellow rectangles) and AE sensors (white : top, gray : bottom).

[1] High Pressure Temperature Laboratory, Department of Earth Sciences, Utrecht University, The Netherlands, loes.buijze@tno.nl
[2] Applied Geosciences, TNO, Utrecht, The Netherlands.
[3] State Key Laboratory of Earthquake Dynamics, China Earthquake Administration, Beijing, China

Large-scale friction experiments allow for inclusion of spatially varying fault properties and detailed instrumentation. Here a 350 mm x 50 mm fault zone was created along the diagonal of a rectangular block of 300 x 200 mm, which was inserted in a biaxial loading frame (Figure 1). A load of 0.3 - 5 MPa was applied to both sides of the block, and the fault zone was sheared at ~1 µm/s by increasing the stress along the length axis of the sample assembly. A 2 mm thick gouge layer was inserted along the fault zone. Four different gouges were used to control the fault properties: gypsum gouge (strong, unstable), quartz (strong, near-neutral), calcite (strong, stable), and kaolinite (weak stable). One homogeneous gypsum fault was sheared, and three faults with an 80 mm long gypsum segment in the center, flanked by one of the other three gouges. The forcing blocks were made of PMMA to down-scale the nucleation process. Strain gauges (46 single-component) and 16 AE sensors were placed along the fault to record deformation.

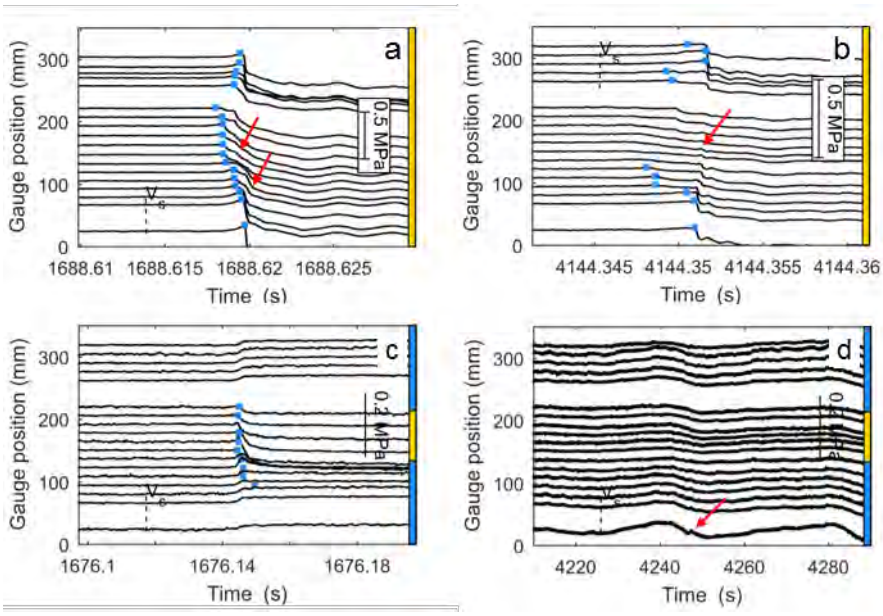

Figure 2. Shear stress recorded along the fault as a function of time. Color bar to the side indicate the position of gypsum (yellow), and calcite (blue). Homogeneous gypsum fault at a) σ_2 = 5 MPa and b) σ_2 = 1 MPa confining pressure. Calcite-gypsum fault at c) σ_2 = 5 MPa, and d) σ_2 = 1 MPa.

The results show that

- spontaneous nucleation occurred on the unstable gypsum faults (Figure 1a). Events on this homogeneous fault were the largest. The nucleation zone size increased with decreasing normal stress, in agreement with theory (Figure 2b).
- rupture nucleated at the gypsum segment for the heterogeneous faults, and was arrested in the flanking segments (partial rupture, Figure 2c). With lower normal stress either slow-slip events over the whole fault started to occur (calcite-gypsum, Figure 2d), stick-slips disappeared (quartz-gypsum), or stick-slip kept occurring as partial rupture, starting at the gypsum segment.
- a high compaction difference between gypsum gouge and the flanking segment concentrated the normal load on the gypsum segment, making it more unstable. This is supported by FE modeling of the experimental setup.

These findings show that fault zone heterogeneity can promote rupture nucleation through differences in friction strength, as well as differences in compaction behavior.

GeoProc2019: Earthquake and Faulting mechanics

7th International Conference on Coupled THMC Processes in Geosystems
3-5 July 2019 Utrecht (Netherlands)

Microphysical modeling of fault friction: extension from nucleation to seismic velocity

Jianye Chen[1], *A.R. Niemeijer*[1], *C.J. Spiers*[1]

Keywords: rock friction, seismic slip, dynamic weakening, microphysical model

Recent experimental studies show that laboratory fault friction values vary over a wide range of sliding velocities. Slow sliding exhibits high friction and rate-and-state behavior, yet remarkable weakening occurs as the sliding velocity approaches seismic speeds. A microphysically-based model has been proposed to explain frictional and healing behavior for granular fault gouges at low slip rates (Chen and Spiers, 2016; Niemeijer and Spiers, 2007; hereafter referred to as the CNS model). In this model, frictional behavior is controlled by dilatant granular flow operating in parallel with contact creep. Using this model, typical low-speed friction behavior can be simulated. Various mechanisms and models have been proposed to explain the dynamic weakening at seismic slip rates, such as thermal pressurization, flash heating and superplasticity, but consensus on the link with microphysical processes is lacking.

In this study, we extend the CNS model to the high-velocity regime, by introducing additional creep mechanism(s) activated by frictional heating. Considering a carbonate fault gouge and following previous laboratory studies (e.g. De Paola et al., 2015), diffusion-accommodated grain boundary sliding (GBS) is incorporated as an additional thermally activated mechanism, besides pressure solution. As slip rate and temperature increase, this leads to a continuous transition of GBS with accommodation by frictional slip to diffusional creep.

We assume a spring-slider fault system and employ an across-fault structure as observed in laboratorically-simulated faults. The governing (ordinary) equations are solved in combination with a finite element model for calculating the temperature evolution and grain size growth over the fault zone thickness. Localization and grain size of the "principal slip zone" (PSZ) is prescribed based on the laboratory observations. The numerical implementation is done using the finite element package Comsol.

The modeling results capture all of the main features and trends seen in experiments, including both steady state and transient aspects, with reasonable quantitative agreement. Notably, the extended model

(1) predicts a steady-state frictional strength profile over a wide velocity range (cf. Figures A1 and A2).

[1] HPT Laboratory, Department of Earth Science, Utrecht University. Email : j.chen3@uu.nl, A.R.Niemeijer@uu.nl, C.J.Spiers@uu.nl

(2) reproduces typical laboratory high-velocity friction experiments, including both the friction and compaction/dilatation data (Figures B1 and A2)
(3) predicts dynamic weakening after a "prolonged strengthening phase" (Figure B1, e.g. De Paola et al., 2015), which shortens with increasing normal stress and slip rate.
(4) predicts a "Sintering Gradient" (SG, Pozzi et al., 2018) ,extending beyond the PSZ, and characterized by low-porosity and nearly-uniform grain size (Figure B2-B4).

Finally, we discuss the mechanical and microstructural implications of the extended CNS model for natural seismogenic faults and suggest future work such as including the implementation of the microphysical model into numerical earthquake cycle simulators.

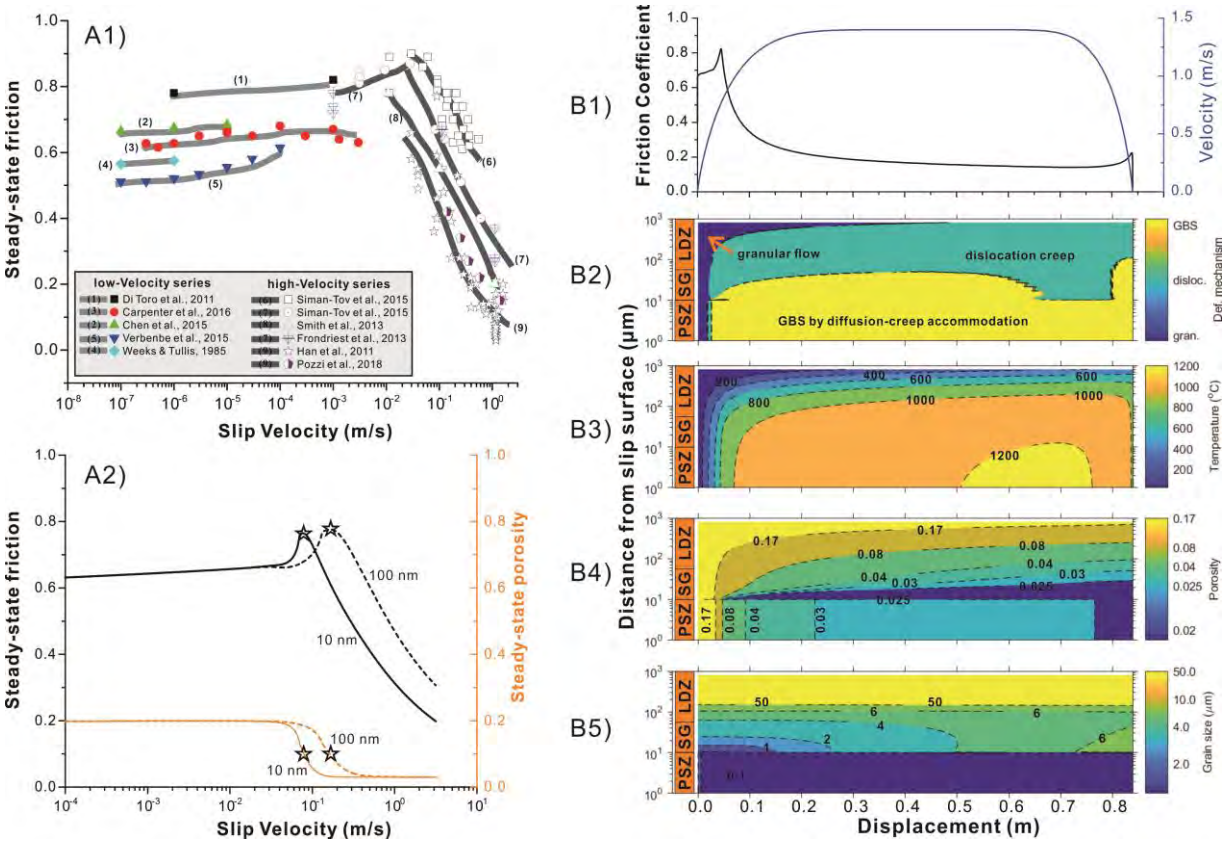

Figure 1: A1: Compiled data on steady-state friction of carbonate materials at slow-to-fast slip rates. A2: Steady-state friction and porosity predicted by the extended CNS model. B1-B4: Simulations of typical friction experiments on a carbonate fault gouge, including the evolution of (B2) deformation mechanism, (B3) temperature, (B4) porosity, and (B5) grain size over the gouge thickness with displacement.

References

Niemeijer, A. R., & Spiers, C. J. (2007). A microphysical model for strong velocity weakening in phyllosilicate-bearing fault gouges. Journal of Geophysical Research, 112, B10405.

Chen, J., & Spiers, C. J. (2016). Rate and state frictional and healing behavior of carbonate fault gouge explained using microphysical model. Journal of Geophysical Research, 121, 8642–8665.

De Paola, N., Holdsworth, R.E., Viti, C., Collettini, C., and Bullock, R. (2015). Can grain size sensitive flow lubricate faults during the initial stages of earthquake propagation?: Earth and Planetary Science Letters, 431, 48–58.

Pozzi, G., De Paola N., Nielsen, S. B., Holdsworth R. E., Bowen L. (2018). A new interpretation for the nature and significance of mirror-like surfaces in experimental carbonate-hosted seismic faults. Geology, 46(7), 583–586.

GeoProc2019: Earthquake and Faulting mechanics

7th International Conference on Coupled THMC Processes in Geosystems
3-5 July 2019 Utrecht (Netherlands)

Role of fluid viscosity in earthquake nucleation

C. Cornelio[1], *F. Passelegue*[1], *E.Spagnuolo*[2],*G. Di Toro*[3], *M.Violay*[1]

Keywords: Earthquake cycle, fluid viscosity, elastohydrodynamic lubrication

Fluids are pervasive in most fault zones and contribute to the nucleation and the propagation of upper-crustal earthquakes (Terakawa et al., 2010). Fluid pressure reduces the normal effective stress, lowering the frictional strength of the fault and potentially triggering earthquake ruptures. Fluid injection induced earthquakes, such as those nucleating in geothermal reservoirs, evidence the effect of fluid pressure on the fault strength (Ellsworth, 2013). While numerous studies estimated the frictional strength of faults based on fluid pressure and flow rate, the influence of the chemical and the physical properties of the fluid on fault reactivation has been often ignored. Here, we investigate the role of fluid viscosity during earthquake nucleation.

We reproduced the earthquake cycle in experimental granitic faults under both room-humidity and drained pore fluid conditions (i.e., P_f=2 MPa, with fluids having viscosities of 1, 10, 108 and 1226 mPa·s at 20 °C, respectively), using a rotary shear apparatus SHIVA (Di Toro et al., 2010). The experimental procedure consisted in increasing step-wise the shear stress ($\Delta\tau$=0.5 MPa every t=1000 s) acting on the faults loaded at a constant effective normal stress σ_n=10 MPa and allowing the slip rate and slip to adjust spontaneously. In all the investigated environmental conditions, once a shear stress τ > 6 MPa (i.e. friction coefficient > 0.6) was overcome, the samples underwent to successive slip episodes with a maximum (regulated by the operator) slip rate of 0.1 m/s. This phase was accompanied by a loss in shear stress regulation and multiple and rapid shear stress drops. It is possible to divide this phase in a sequence of short-lived events ending with a long-lived slip event. Short-lived events had slip distances smaller than 0.25 m during which the shear stress, after dropping from the imposed shear stress τ_{imp} to a minimum value τ_{min}, recovered spontaneously up to a peak shear stress τ_{peak} (Fig1a). On the contrary, the final long-lived events had long slip distances (>1 m) at the maximum allowed slip rate of 0.1 m/s. The shear stress drops and slip distances of both the short-lived and long-lived events were governed by elasto-hydro-dynamic lubrication with high viscous fluids (Cornelio et al., under review). Moreover, the measured breakdown (Wb) and re-strengthening work (Wr, see definitions in Fig1.a) scale with slip (Figs 1.b-c). In conclusion, independently from the fluids viscosity, Wb follows the same scaling law with slip distance than the one for natural earthquakes and the presence of viscous fluid does not influence the nucleation phase of earthquakes in terms of energy budget.

[1] LEMR, EPFL chiara.cornelio@epfl.ch, francois.passelegue@epfl.ch, marie.violay@epfl.ch
[2] INGV, elena.spagnuolo@ingv.it
[3] Università degli Studi di Padova, giulio.ditoro@unipd.it

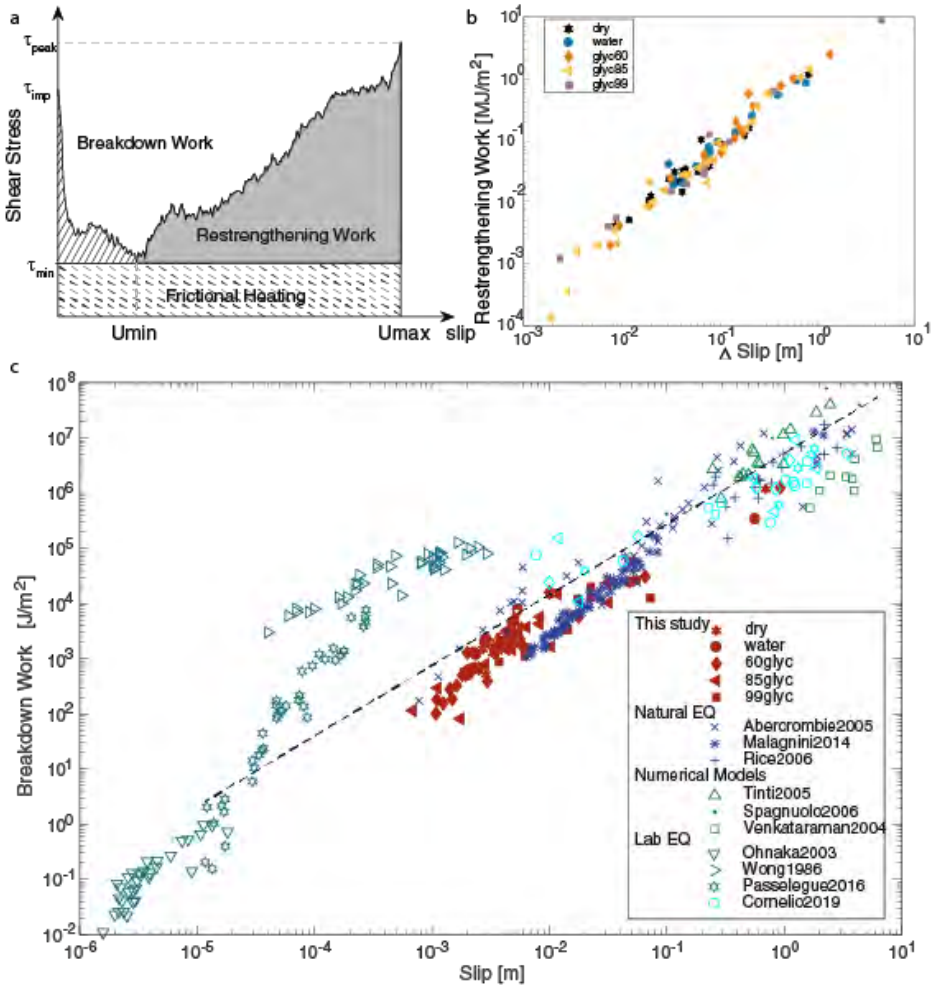

Figure 1. Earthquake energy budget. **a)** Schematic partitioning of the earthquake energy budget for the first short-lived event of the experiment s1488 performed in presence of a mixture 60%glycerol/40%water. The area with long inclined lines is the breakdown work Wb. The area in light grey color is the restrengthening work Wr. The rectangular area with short inclined lines is the minimum frictional heat dissipated during sliding. **b)** Restrengthening work versus slip for short-lived and long-lived slip events under room humidity conditions (black in color stars), in presence of pore water (blue dots) and of a mixture 60%glyc/40%water (orange diamonds), 85%glyc/15%water (yellow triangles), and glycerol (purple squares). **c)** Laboratory and seismological estimates of breakdown work. The red in color symbols are the Wb measured in the short-lived and long-lived slip events presented in this study (rotary shear configuration). Blue symbols are seismological Wb estimates for natural earthquakes (Abercrombie & Rice, 2005; Malagnini et al., 2014; Rice, 2006) Green symbols are seismological estimation of Wb in numerical model of earthquakes (Spagnuolo, 2006; Tinti et al., 2005; Venkataraman & Kanamori, 2004); teal-blue symbols are laboratory measurements of Wb in biaxial or triaxial experimental configurations (Ohnaka 2003; Wong 1982; Passelègue et al., 2016).

References

Cornelio, C., Spagnuolo, E., Di Toro, G., Nielsen, S., & Violay, M. (under review). Mechanical behaviour of fluid-lubricated faults.

Ellsworth, W. L. (2013). Injection-Induced Earthquakes. *Science*, *341*(6142), 1225942–1225942. https://doi.org/10.1126/science.1225942

Terakawa, T., Zoporowski, A., Galvan, B., & Miller, S. A. (2010). High-pressure fluid at hypocentral depths in the L'Aquila region inferred from earthquake focal mechanisms. *Geology*, *38*(11), 995–998. https://doi.org/10.1130/G31457.1

Di Toro, G., Niemeijer, A., Tripoli, A., Nielsen, S., Di Felice, F., Scarlato, P., et al. (2010). From field geology to earthquake simulation: A new state-of-The-art tool to investigate rock friction during the seismic cycle (SHIVA). *Rendiconti Lincei*, *21*, 95–114. https://doi.org/10.1007/s12210-010-0097-x

GeoProc2019: Earthquake and Faulting mechanics

7th International Conference on Coupled THMC Processes in Geosystems
3-5 July 2019 Utrecht (Netherlands)

Magnetic properties of fault rocks

M.J. Dekkers[1], L.V. de Groot[2], T. Yang[3]

Keywords: magnetic properties, slip zone, preliminary geothermometer

Magnetic minerals, essentially iron-titanium oxides and some iron sulfides, can retain information from the (distant) geological past. This information is used to make paleogeographic reconstructions. Here, we briefly outline the merit of mineral magnetic methodology to identify seismic slip along with its peak temperature through examination of magnetic mineral assemblages. Examples include IODP Expedition 343, the Japan Trench Fast Drilling Project, where pyrrhotite was identified in three mm-thick slip zones of splay faults in the Asia-Pacific Plate subduction channel.

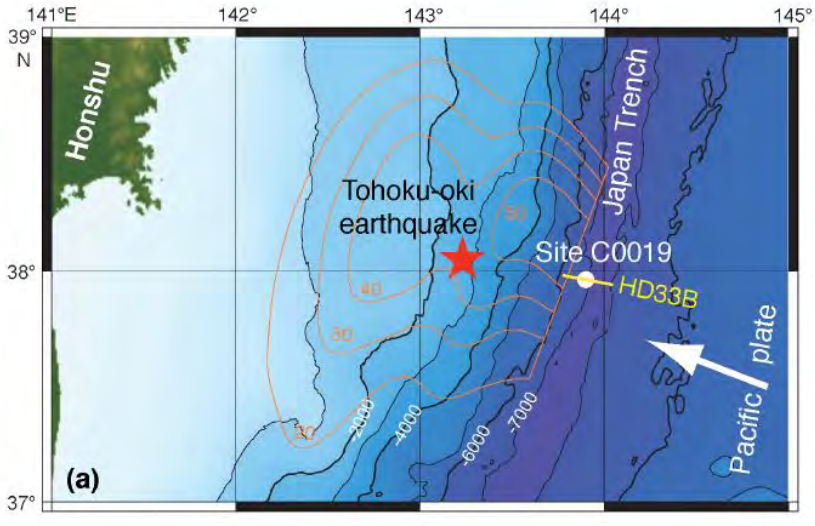

Figure 1. IODP 343 drill site studied (Yang et al., 2016).

[1] UU Utrecht (The Netherlands), m.j.dekkers@uu.nl
[2] UU, Utrecht (The Netherlands), l.v.degroot@uu.nl
[3] CUG Wuhan (China), yangtao@cug.edu.cn

Trace amounts of pyrrhotite were established rock magnetically; they are restricted to the slip zones in the frontal prism sediments and absent in the host rock. The maximum temperature experienced as a consequence of frictional heating was estimated between 640 and 800℃ with the help of pyrite-to-pyrrhotite kinetic reaction modeling (Yang et al., 2018). What is thought to be the main decollement of the underthrusting Pacific Plate drilled during the same IODP cruise shows particular magnetic properties distinct from neighboring host rocks, when plotted on a plot of the hysteresis ratios, Mr/Ms (saturation remanence Mr over saturation magnetization Ms) versus Bcr/Bc (remanent coercive force Bcr over coercive force Bc), cf. figure 2 (Yang et al., 2016). This makes magnetic property analysis attractive to diagnose slip zones. By testing for reversibility of magnetic susceptibility during sequential heating to increasingly elevated temperature it is in principle possible to check for the maximum temperature a slip zone has experienced in its geologic past. This geothermometer senses temperatures between 300 and 600℃ but has at present a preliminary character. In future research we plan to visualize individual magnetic particles with a Quantum Diamond Magnetometer. In this manner we intend to map a temperature distribution function straddling slip zones which would enable reconstruction of the energy dissipated during earthquakes.

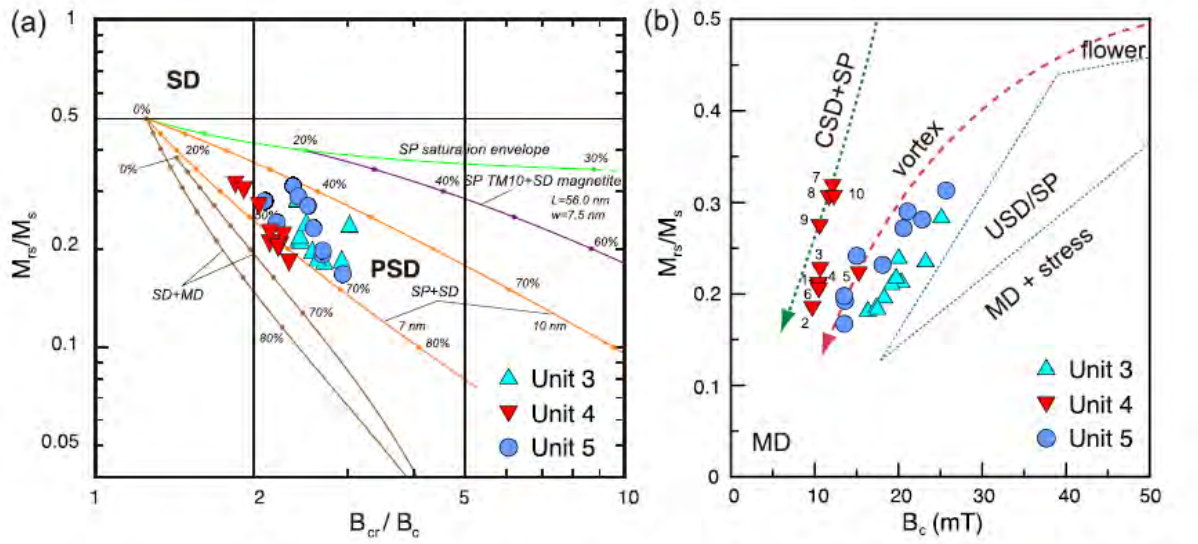

Figure 2. Hysteresis parameters plotted in two ways (Yang et al., 2016). Magnetic grain states : SD = single domain, PSD = pseudo-single-domain, SP = superparamagnetic, CSD = cubic single domain, USD = uniaxial single domain, MD = multidomain. Unit 4 is the principal decollement, the slip zone between Asia and the underthrusting Pacific Plate.

References

Yang T., Dekkers M.J., and Chen J. (2018), Thermal alteration of pyrite to pyrrhotite during earthquakes: New evidence of seismic slip in the rock record. J. Geophys. Res.: Solid Earth, 123, 1116–1131. doi: 10.1002/2017JB014973

Yang T., Dekkers M.J., and Zhang B (2016), Seismic heating signatures in the Japan Trench subduction plate-boundary fault zone: evidence from a preliminary rock magnetic 'geothermometer', *Geophys. J. Int.*, *205*, 332–344, doi: 10.1093/gji/ggw013.

GeoProc2019: Earthquake and Faulting mechanics

7th International Conference on Coupled THMC Processes in Geosystems
3-5 July 2019 Utrecht (Netherlands)

Slip surfaces associated with seismic faults and gravitational slope deformations in carbonate-built rocks

L. Del Rio[1], M. Fondriest[1], M. Moro[2], M. Saroli[3], S. Gori[2], E. Falcucci[2], E. Spagnuolo[2], G. Di Toro[1,2]

Keywords: faults, landslides, earthquakes, cataclasites, carbonates, slip surfaces

Carbonate-built rocks of the Central Italian Apennines are systematically cut by active sharp slip surfaces bounding less than few cm-thick slipping zones surrounded by cm to hundreds meter-thick damage zones. Recent paleo-seismological, geological and geomorphological observations pointed out that the principal slipping zones (PSZs) may accommodate either large landslides (Deep-Seated Gravitational Slope Deformation. DGSD, Galadini, 2006; Moro et al., 2007, 2012; Gori et al., 2014) and seismic or aseismic crustal scale fault deformation (normal tectonic faults, NF). Clearly, the distinction between DGSD and NF structures based on field and microstructural observations and the individuation of the processes forming the PSZs is of outstanding relevance in geological hazard studies. Currently, most of the sharp slip surfaces exposed in the Italian Central Apennines are mapped as active normal faults, even if the different geomorphological and secondary fault/fracture networks, associated to the main slip surfaces, would suggest a different behavior of such structures.

Depending on the associated geological process (i.e., DGSD vs. NF), the slip surfaces and associated slipping zones reach different depths along dip (100-1000 meters for DGSD, 10-12 km for NF), and are formed and active over a different range of temperatures (0-30 °C for DGSD vs. 0-100°C for NF), pressures (< 20 MPa for DGSD, 0 to 200 MPa for NF) and slip rates (usually < 10^{-3} m/s for DGSD, up to ~1 m/s for NF). Such large differences in loading conditions should result in the formation of distinctive secondary fault/fracture networks in the damage zones recognizable at the outcrop scale and in peculiar microstructures in the slipping zones. For this reason, this study aims at identifying the geological structures and deformation mechanisms associated to both DSGD and NF by (1) conducting extensive field surveys (Fig. 1a), (2) investigating in the laboratory the origin of the different slipping zones under controlled deformation conditions and, (3) performing microstructural studies on natural and experimental PSZs (Fig 1b).

The microstructures of the PSZs will be investigated by optical and scanning electron microscopy, X-ray diffraction, micro-Raman spectroscopy, Electron Microprobe analyses, and cathodoluminescence. The microstructures of the natural PSZs and wall rocks will be compared with those produced under controlled deformation conditions (normal stress, presence of fluids, slip rate) on carbonate rocks with the rotary shear (SHIVA - Slow to HIgh Velocity Apparatus) installed at the Istituto Nazionale di Geofisica e Vulcanologia in Rome.

1. Università degli Studi di Padova (Padua, Italy)
2. Istituto Nazionale di Geofisica e Vulcanologia (INGV, Rome, Italy)
3. Università degli Studi di Cassino

Preliminary microstructural analyses of end-member cases (i.e., shallow and small DSGD cutting Quaternary deposits vs. large NF producing > Mw 6.5 earthquakes) and intermediate cases (i.e., NF reactivated as DGSD) have shown neat differences in the deformation style and microstructural maturity of the PSZs (Fig 1b). These results show how the characterization of the microstructures in PSZs from scarps hosted in carbonate rocks could represent a powerful tool to discriminate seismic faulting from DGSDs and provide new grounds for the mapping of active faults in Italy and in other seismically active worldwide.

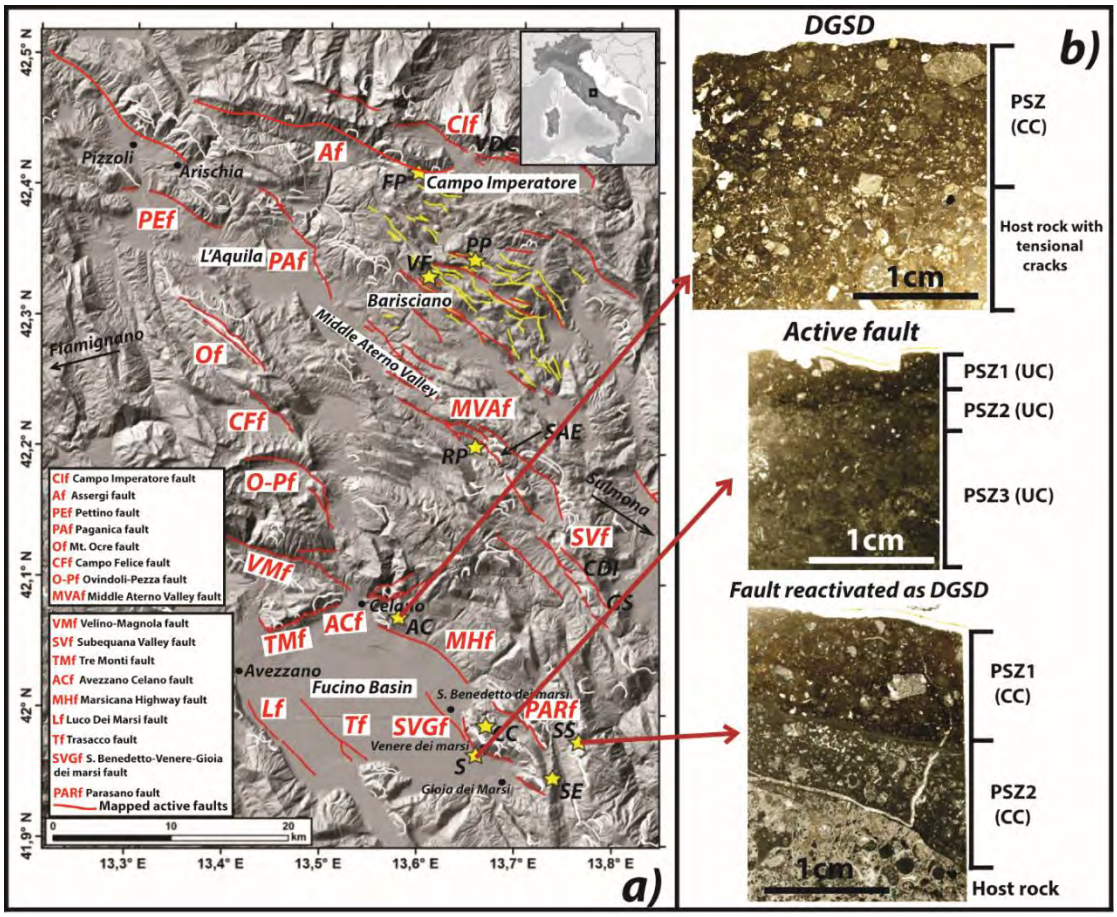

Fig.1: Deep-Seated Gravitational Slope Deformations (DGSD) and normal faults of the study area (Italian Central Apennines). (a) Map of active faults (red in color segments), DGSDs (white segments) and minor faults bordering intra-mountain basins (yellow segments). Yellow stars are the sampling sites of the studied fault rocks. **(b)** Principal slipping zones (PSZs) of the Alto di Cacchia DGSD (top), Santilli normal fault (middle) and San Sebastiano normal fault reactivated by DGSD (bottom). The slip surface is located to the top of each thin section. Though these PSZs are all associated to sharp slip surfaces, the PSZ of the Alto di Cacchia DGSD, formed at very shallow crustal conditions (< 400 m depth), is less evolved (i.e., larger average grain size and thinner PSZ) than the PSZs of seismic faults (Santilli and San Sebastiano faults).

References

Galadini, F., 2006. Quaternary tectonics and large-scale gravitational deformations with evidence of rock-slide displacements in the Central Apennines (central Italy). *Geomorphology* 82, 201–228.

Gori, S., Falcucci E., Dramis F., Galadini F., Galli P., Giaccio B., Messina P., Pizzi A., Sposato A., Cosentino D., 2014. Deep-seated gravitational slope deformation, large-scale rock failure, and active normal faulting along Mt. Morrone (Sulmona basin, Central Italy): Geomorphological and paleoseismological analyses. *Geomorphology* 208, 88–101.

Moro, M., Saroli, M., Salvi, S., Stramondo, S., Doumaz, F., 2007. The relationship between seismic deformation and deep-seated gravitational movements during the 1997 Umbria–Marche (Central Italy) earthquakes. *Geomorphology* 89, 297–307.

Moro, M., Saroli, M., Gori, S., Falcucci, E., Galadini, F., Messina, P., 2012. The interaction between active normal faulting and large scale gravitational mass movements revealed by paleoseismological techniques: a case study from central Italy. Geomorphology 151 (152), 164–174.

GeoProc2019: Earthquake and Faulting mechanics

7th International Conference on Coupled THMC Processes in Geosystems
3-5 July 2019 Utrecht (Netherlands)

Quantifying surface roughness development on experimentally sheared fault gouges.

A. Eijsink[1], *M. Ikari*[2]

Keywords: surface roughness, friction experiments, fault anisotropy

The surface roughness of fault planes determines the effective contact area across the fault and is therefore an important parameter for the frictional behavior of faults. The notion that the rate- and state-dependent friction parameters might depend on asperity size and distribution suggests that surface roughness might be an important controlling mechanism for these friction laws. We performed direct shear experiments on Rochester Shale powder, which produced fault surfaces of which the topography was measured using a Confocal Laser Scanning Microscope (CLSM). Microstructural analyses confirm that the measurements, where possible, were performed on the principal slip surface. Using different sets of experiments, we show the effect of varying displacement, normal stress and sliding velocity on the roughness of the fault surface. This approach also allows for direct comparison between friction parameters and surface roughness.

Surface roughness is analyzed in terms of Power Spectrum Density (PSD), a measure of how strong sinusoidal waves of each wavelength are present in the fault surface. The linear relationship between the logarithm of the PSD and the logarithm of the wavelength having the slope β allows extrapolation of the µm-mm scale experimental surfaces to large-scale natural fault conditions. We converted β to the more commonly used Hurst exponent (H), which for these experiments varies between 0.4 and 0.9.

Preliminary results show that with increasing displacement, faults become smoother in the shear parallel direction and rougher in the shear perpendicular direction. Fault anisotropy increases from a displacement of 4 mm onwards, a value similar to the wavelength where PSD values in the shear parallel and shear perpendicular directions are equal, the isotropy point. The effect of normal stress is smaller; an increase from 1 to 10 MPa lowers the Hurst exponent in both directions by 0.1, making the overall surface smoother but not affecting anisotropy. Water content has a similar effect, where air-drying the surface before the measurement lowers the Hurst exponent by 0.10 to 0.15 in both directions compared to a surface of a water-saturated sample measured directly after shearing. The effect of increasing velocity seems more complex and more work is needed to resolve this. Together, this shows that fault surface roughness varies systematically as a function of experimental conditions. Quantification of these relationships and their meaning for effective contact area and friction parameters is ongoing work, as well as

[1] MARUM – Centre for Marine Environmental Sciences, University of Bremen, aeijsink@marum.com
[2] MARUM – Centre for Marine Environmental Sciences, University of Bremen, mikari@marum.com

their application for natural rock samples sheared in lab experiments and how these compare to in-situ faults.

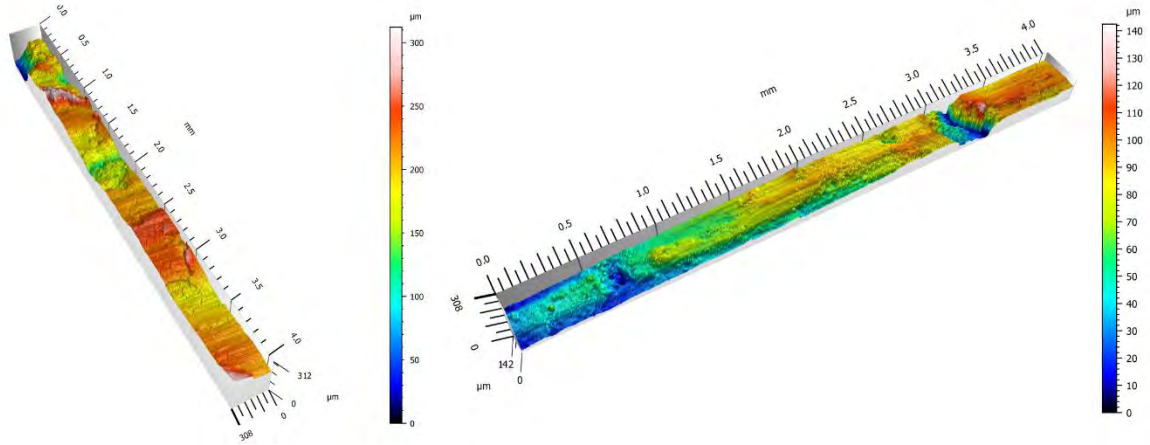

Figure 1. Example of measured surface after 16 mm of displacement in the shear perpendicular direction (left) and shear parallel direction (right).

GeoProc2019: Earthquake and Faulting mechanics

7th International Conference on Coupled THMC Processes in Geosystems
3-5 July 2019 Utrecht (Netherlands)

Near-well analysis of stresses utilizing a fast coupled thermo-hydro-poro-elasto-plastic model

Peter A. Fokker[1], *Thibault G. Candela*[2]

Keywords: coupled modelling, wellbore stability; semi-analytic approach

Induced seismicity and failure in the near-wellbore area around injection wells is critically dependent on the state of effective stress. A fast analysis of proximity to failure is thus helped much by a fast tool that evaluates these stresses. This requires, however, the incorporation of temperature, fluid flow, poro-elasticity and plastic behavior. We report the development of a semi-analytical model incorporating these ingredients, targeted at geothermal operations and injection of cold water.

We formulate our treatment for radial symmetry and in plane-strain conditions. We treat the rock as a single-porosity medium with effective properties characterizing its behavior.

Far away from an injection or production well, the pressure, temperature and stress changes with respect to the virgin ones are limited. As a result, the behavior can be captured with linear poro-thermo-elasticity [Palciauskas & Domenico, 1982]. We formulate the full transient diffusivity equation for this region – it deploys a diffusivity constant different from the traditional one in which flow only is considered: the effect of the poromechanical and thermomechanical response is incorporated. The diffusivity equation can be solved under the assumption that the boundary conditions are known, and the solution can be approximated by a logarithmic function with a moving radius of the pressure disturbance, to allow time-dependent changes of the permeability. This approximation implies that the flow is fully developed – i.e. that storage effects may be discarded.

Moving the viewpoint from infinity towards the well, two major effects must be incorporated: the progressive reservoir cooling due to the injection of cold water and the mechanical failure because of the decreased effective stresses and the presence of the well. If the cooled zone is larger than the failed zone, the linear relations still hold for the not-failed cooled zone; otherwise part of the failed zone is not cooled (Fig. 1).

The effect of cooling on the flow can be addressed using a temperature-dependent fluid viscosity [Boughrara et al, 2007]. The extent of the cooled zone is calculated using the assumption that the transport of thermal energy is by convection only, and

[1] TNO Applied Geoscience and Utrecht University, peter.fokker@tno.nl
[2] TNO Applied Geosciences, thibault.candela@tno.nl

that conduction and radiation can be neglected. This is presumably warranted in a zone with extended thickness (so not much thermal energy can be lost to the over- and underburden) and with considerable flow rates (so the temperature front will be dominated by convection). The result is a cooled cylinder at injection fluid temperature in a subsurface of which the remainder is at initial temperature; with dimensions controlled by the height of the reservoir in which the injection is taking place and a balance of thermal energy.

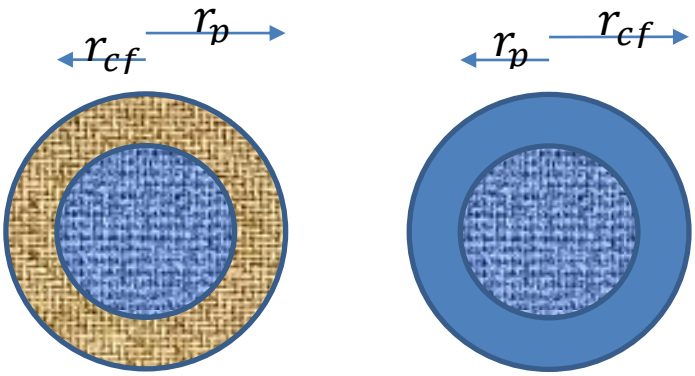

Figure 1. Radii of cooled zone and plastic zone

A common approach to failure is to use the Mohr-Coulomb criterion. It indicates that failure occurs once the shear stress exceeds a maximum that is linearly dependent on the effective normal stress. The region where failure occurs is inside a radius of plasticity, determined by the radius at which, moving from infinity towards the well, the failure line is reached. We assume that within this radius plastic behavior causes the shear stress to be limited to the value at the failure line [Han & Dusseault, 2003]. An important deficient assumption is that the plastic zone is cylindrical, even in a subsurface with anisotropic horizontal stress.

Two constants still need to be determined in the process of formulating the solutions in the various zones: an integration constant for the stress solution in the linearly elastic zone and the radius of plasticity. These are determined by imposing continuity of radial stress at the plasticity radius and a stress at the failure envelope for the elastic solution at this radius.

Finally, the loop must be closed with the effect of failure on injectivity. Ideally one would employ a flow rule in which the plastic strain is calculated and the resulting total strain is used as input for porosity and permeability. The resulting permeability field can then be used as input for the pressure distribution at the subsequent timestep. In the current first approach, however, we use a direct relationship between effective stress and permeability. The aperture of fractures in a fracture network is related to the permeability and changed when the porosity is changed due to changes in the mean effective stress.

References

Boughrara, A. A., et al. (2007). Approximate analytical solutions for the pressure response at a water-injection well. *SPE Journal*, *12*(01), 19-34.

Han, G. & m.B. Dusseault, (2003). Description of fluid flow around a wellbore with stress-dependent porosity and permeability. *Journal of Petroleum science and engineering*, *40*(1-2), 1-16.

Palciauskas, V. V., & P.A. Domenico (1982). Characterization of drained and undrained response of thermally loaded repository rocks. *Water Resources Research*, *18*(2), 281-290.

GeoProc2019: Earthquake and Faulting mechanics

7th International Conference on Coupled THMC Processes in Geosystems
3-5 July 2019 Utrecht (Netherlands)

Pseudotachylytes alteration and their loss from the geological record

M. Fondriest[1], J. Mecklenburgh[2], F.X. Passelegue[3], G. Artioli[1], F. Nestola[1], E. Spagnuolo[4], G. Di Toro[1]

Keywords: pseudotachylytes, hydrothermal alteration, glass argillification

Tectonic pseudotachylytes are solidified friction-induced melts produced along faults by seismic slip associated to the propagation of earthquake ruptures (Sibson, 1975) (Fig.1a). Though pseudotachylytes remain the most convincing marker of seismic ruptures among fault rocks, the report of pseudotachylytes within fault zones is rare if compared with the frequency and distribution of earthquakes in crustal rocks (Kirkpatrick and Rowe, 2013). This observation reinforces the idea that pseudotachylytes are produced only in very dry tectonic settings or at fault asperities sustaining very high shear stresses (Sibson and Toy, 2006). However, the ubiquitous production of pseudotachylytes both in dry and wet conditions during laboratory earthquakes indicates frictional melting as a diffuse and efficient fault weakening mechanism (Tsustumi et al, 1999; Violay et al., 2014). Reconciling such a dispute implies to address a long-lasting question in the earthquake mechanics community: are pseudotachylytes rarely generated or are they only rarely preserved?

We addressed this question by performing hydrothermal alteration tests on fresh pseudotachylyte samples. Pseudotachylytes hosted in different lithologies (tonalite, microgabbro, ultramafic gabbro) were produced under vacuum by sliding at seismic slip rates (> 1 m/s) solid rock cylinders using the rotary shear apparatus SHIVA at INGV-Rome (Di Toro et al., 2010). The melt-welded rock samples were then cored along the fault interface to obtain smaller rock cylinders with the experimental pseudotachylyte oriented parallel to the long axis (Fig.1b). These samples were finally cooked with water as pore fluid at confining (Pc) and pore pressure (Pp) of 150-200 MPa and temperatures (T) of 300-600°C for 18-35 days using two Nimonic triaxial apparatuses at the Rock Deformation Laboratory of the University of Manchester (Rutter et al., 1984) (Fig.1c). The experimental conditions were chosen to be representative of the pressures and temperatures at which natural pseudotachylytes occurred in their host rocks.

Detailed microstructural and mineralogical investigations (FE-SEM, EDX, X-ray micro-diffraction, micro-Raman) documented that post alteration pseudotachylytes were very different from the original ones. In particular, altered pseudotachylytes were characterized by a peculiar clastic micro-texture deriving from the intense dissolution of the original glassy to cryptocrystalline matrix. This process determined the formation of a significant amount of porosity and the growth within the matrix of few micrometres in size

[1] University of Padova – **michelefondriest@yahoo.it**, [2] SEES – University of Manchester, [3] EPFL Lausanne, [4] INGV Rome

acicular mineral aggregates with random orientation (Fig.1c). In the case of the tonalite-derived pseudotachylyte, the original glassy matrix was K-rich in composition, had no porosity and quartz clasts displayed cuspate-lobate boundaries (Fig.1b,d). After hydro-thermal alteration, the sample contained only few relics of the original micro-texture embedded within a highly porous matrix depleted in alkali. Preliminary micro-analyses suggest that the acicular aggregates likely were Ca-Mg smectitic clays (Fig.1e).

This study first demonstrates that the preservation potential of pseudotachylytes is very short (days to months) and is likely to increase only within very dry tectonic settings. The presence of pore fluids instead determines the alteration of the pseudotachylyte matrix and the development of a clastic micro-texture which resembles well the one of other much more common fault rocks such as ultracataclasites.

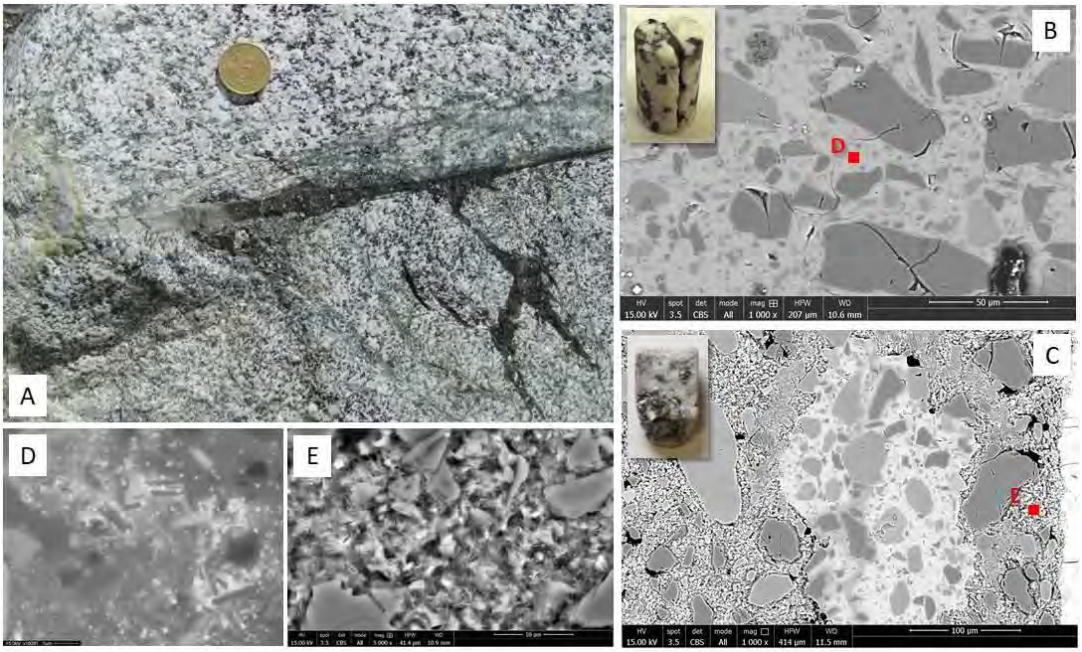

Figure 1. (A) Natural pseudotachylyte (PT) with incipient alteration (the left termination of the PT vein is fading into a greenish fault rock). (B) BSE-SEM image of fresh experimental PT produced with SHIVA; clasts are Plag, Qtz with cuspate lobate boudaries and are embedded in a glassy withish matrix (inset : macroscopic sample 10 mm diameter). (C) BSE-SEM image of altered experimental PT produced with Nimonic (Pc=Pp=150 MPa, T=300°C, tme =35 days). Note the clastic microtexture and a remnant of more fresh (still glassy) PT preserved (inset : macroscopic sample 10 mm diameter). (D) Detail of fresh PT glass (BSE-SEM image). Note the low porosity texture of the glass and the Plag microlites. (E) Detail of altered PT glass (BSE-SEM image). Note the clastic microtexture and the acicular mineral aggregates which likely are Ca-Mg smectitic clays.

References

Sibson, R.H. (1975), Generation of Pseudotachylyte by Ancient Seismic Faulting, *Geophys. J. Int.*, *43*(3), 775–794, https://doi.org/10.1111/j.1365-246X.1975.tb06195.x.

Kirkpatrick, J.D, and C.D Rowe (2013), Disappearing ink: How pseudotachylytes are lost from the rock record, *J. Struct. Geol.*, *52*, 183-198, https://doi.org/10.1016/j.jsg.2013.03.003.

Sibson, R.H., and V.G. Toy (2006), The Habitat of Fault-Generated Pseudotachylyte: Presence vs. Absence of Friction-Melt, *Geoph. Monograph Series*, 170, 153–166, doi:10.1029/170GM16.

Tsutsumi, A., and T. Shimamoto (1997), High-velocity frictional properties of gabbro, *Geophys. Res. Lett.*,24(6), 699–702, https://doi.org/10.1029/97GL00503.

Violay, M. et al. (2014), Effect of water on the frictional behavior of cohesive rocks during earthquakes, *Geology*, *42*(1), 27–30, https://doi.org/10.1130/G34916.1.

Di Toro, G. et al. (2010), From field geology to earthquake simulation: a new state-of-the-art tool to investigate rock friction during the seismic cycle (SHIVA), *Rendiconti Lincei.*, *21*, 95–114.

Rutter, E.H. et al. (1984), Experimental 'syntectonic' hydration of basalt, *J. Struct. Geol.*, *7*(2), 251–266.

GeoProc2019: Earthquake and Faulting mechanics

7th International Conference on Coupled THMC Processes in Geosystems
3-5 July 2019 Utrecht (Netherlands)

Depletion-induced permeability loss' influence on induced seismicity

B. Fryer[1], G. Siddiqi[2], L. Laloui[3]

Keywords: Fluid production, induced seismicity, compaction, permeability

Introduction: Fluid production from subsurface reservoirs can induce stress changes that lead to seismicity (Segall 1989). These stress changes arise due to the presence of the gradient of pore pressure as an internal force in the balance of momentum equation. The implication here is that, the larger the pore pressure gradient induced to produce fluid, the larger the stress changes in the reservoir and surrounding rock masses that will result. This has direct implications for induced seismicity.

Darcy's Law shows that the gradient of pore pressure used to produce an amount of fluid is inversely proportional to the permeability. This implies that the permeability reductions that result due to compaction during fluid production (e.g., Schutjens et al., 2004) may have an influence on induced seismicity. In this work, this possibility is investigated and it is shown that this is indeed the case: permeability loss due to fluid production can lead to larger stress changes and therefore higher induced seismicity rates. This is especially true for inelastic compaction, which results in especially large permeability losses.

Methodology: Pore pressure and stress changes are modelled with a sequentially coupled 2-D plane strain Finite Volume flow and Finite Element mechanical model. The permeability loss due to compaction is included through the use of a linear relationship between permeability and mean effective stress, a relationship valid for the near-elastic range of sandstones as defined by Schutjens et al., 2004. The pore pressure and stress changes are then input into an existing seismicity model developed by Dieterich 1994 to calculate the seismicity rate. This setup allows for the comparison of the seismicity rate for the cases where production induced permeability loss is and is not included.

Results & Discussion: In the case where permeability loss was not included, it was clearly seen how fluid production can lead to induced seismicity. Focusing on a reverse faulting stress regime, in Figure 1a, it is clear that production causes a significant increase in Coulomb stressing rate (up to 0.03 MPa/yr). This stress rate is on the order of that seen on the San Andreas Fault and results in an increased seismicity rate (Figure 1b). When permeability loss (approximately 10% total at maximum) is included, the stressing rate increases by up to 0.004 MPa/yr (Figure 1c); over a 10% increase. This results in a 7 %

[1] Laboratory of Soil Mechanics – Chair "Gaz Naturel" Petrosvibri, EPFL, Switzerland, barnaby.fryer@epfl.ch
[2] Swiss Federal Office of Energy, Switzerland, gunter.siddiqi@bfe.admin.ch
[3] Laboratory of Soil Mechanics – Chair "Gaz Naturel" Petrosvibri, EPFL, Switzerland, lyesse.laloui@epfl.ch

predicted increase in seismicity rate for this case (Figure 1d), although these results should be treated qualitatively as opposed to quantitatively. This analysis is repeated for the other two stress regimes with similar results. It is important to note that these results are for elastic permeability loss, which is generally small. Inelastic permeability loss can be up to an order of magnitude larger. It is found that these types of permeability losses can have a very large effect on induced seismicity rate.

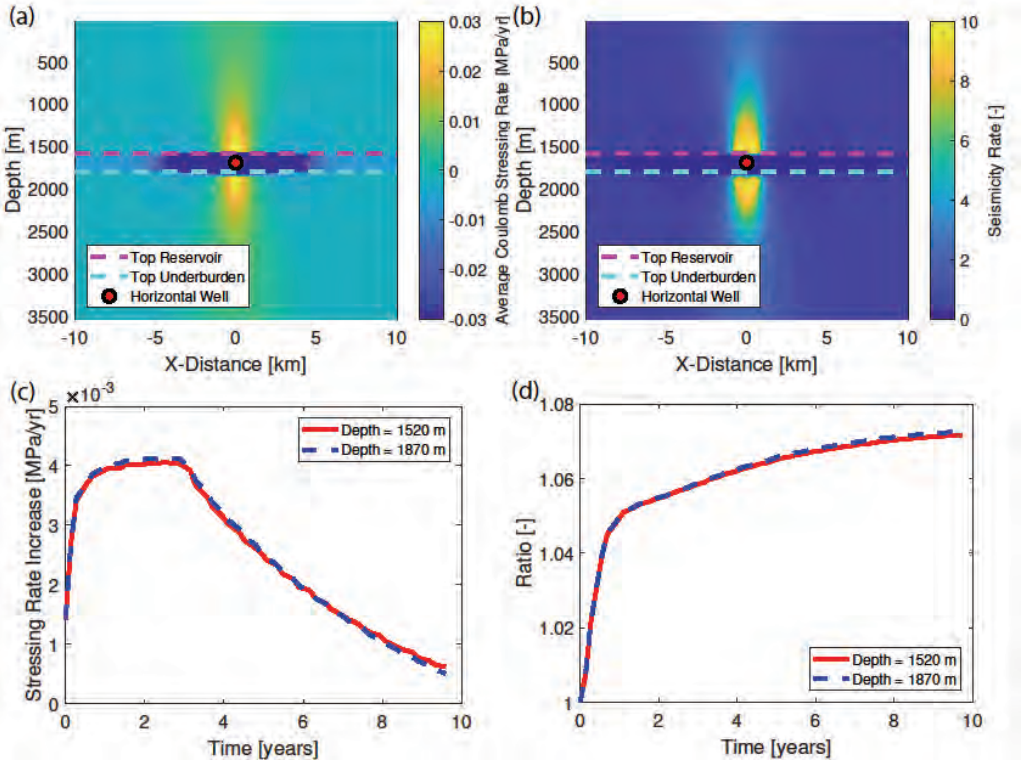

Figure 1. Reverse faulting stress regime a) average Coulomb stressing rate over 10 years due to fluid production without considering the permeability loss due to compaction. b) the predicted seismicity rate after 10 years without considering the permeability loss due to compaction. c) the difference in Coulomb stressing rate when elastic permeability loss is considered at two locations vertically in-line with the well. d) the ratio of seismicity rate at two locations vertically in-line with the well. A ratio higher than one means that the seismicity rate has increased.

Acknowledgements: This work has been supported by a research grant (SI/500963-01) of the Swiss Federal Office of Energy.

References

Dieterich, J. (1994), A constitutive law for rate of earthquake production and its application to earthquake clustering, *Journal of Geophysical Research*, 99, 2601-2618, doi: 10.1029/93JB02581.

Schutjens, P., T. Hanssen, M. Hettema, J. Merour, P. de Bree, J. Coremans, G. Helliesen (2004), Compaction-induced porosity/permeability reduction in sandstone reservoirs: data and model for elasticity-dominated deformation, *SPE Reservoir Evaluation & Engineering*, 7, 202-216. doi : 10.2118/88441-PA.

Segall, P. (1989), Earthquakes triggered by fluid extraction, *Geology*, 17, 942–946, doi: 10.1130/0091-7613(1989)017<0942:ETBFE>2.3.CO;2.

GeoProc2019: Earthquake and Faulting mechanics

7th International Conference on Coupled THMC Processes in Geosystems
3-5 July 2019 Utrecht (Netherlands)

Earthquakes nucleation influenced by fluid pore-pressure rate; a laboratory investigation

M. Gori[1], V. Rubino, A. J. Rosakis, N. Lapusta

Keywords: friction, earthquake nucleation

It is well known that fluids play a central role in earthquake source processes and can induce a variety of earthquake source behaviors ranging from quasi-static to dynamic motions, as a number of field studies suggest. However, elevated pore-pressure has the dual role of reducing the frictional strength of the fault, promoting slip motion, and of increasing the nucleation size, promoting stable motion. Due to the complex frictional problem arising at the fault interface, understanding which rupture mode - stable vs. unstable - prevails is still an open research question. Motivated by this, we developed a new setup capable of reproducing a broad range of rupture behaviors, from slow-slip to fully dynamic events, via the precise control of the pressure time history delivered to the fault plane, and experimentally explored the influence the pore-pressure rate has on the rupture nucleation by modulating the rate of injection. We discovered that slow vs. rapid pore-pressure rates have strong influence over the nucleation phase in term of storable amount of fluid in the fault, sustainable pressure level prior to the initiation of a dynamic rupture, and extension of the slow-slipping area around the injection location. The results of this investigation have important implications for hazard mitigation in relation to practices of fluid-injection into the subsurface, as well as promoting a better understanding of naturally occurring fluid-induced seismicity.

[1] NASA Jet Propulsion Laboratory (JPL) , California Institute of Technology, marcello.gori00@gmail.com

GeoProc2019: Earthquake and Faulting mechanics

7th International Conference on Coupled THMC Processes in Geosystems
3-5 July 2019 Utrecht (Netherlands)

Hydro-Mechanical Stability of RJD Multilaterals

M.R Hajiabadi[1], *H.M. Nick*[2]

Keywords: Hydro-Mechanical Stability, RJD Laterals, numerical modelling

Radial Jet Drilling is an emerging enhanced oil recovery technology that uses high pressurized water to drill a radial pattern of small-diameter laterals into a producing or injecting formation, from an existing vertical or horizontal main well. By successfully applying Radial Drilling, it is feasible to bypass formation (skin) damage zones and establish significant radial contact with the reservoir. Depending on in situ stress, utilized fluid velocity and geo-mechanical material property, RJD laterals can reach up to 100 m long with a hole of 2~5 cm diameter. In addition to these factors, the cross-section size and the shape of the laterals can be affected by the nozzle type. While rotating nozzle cut bigger round circular shape, static nozzle can excavate star shape with wings of the length up to 5 cm under specific condition (Medetbekova et al., 2017 & 2018).

Due to the lack of casing in RJD laterals, it's important to minimize the risk of mechanical failure. This paper investigates the numerical modeling of a single open lateral to evaluate their mechanical stability under various condition of cross section shape, in-situ stress and rock strength during drilling and production operation based on a damage-plasticity finite element model in ABAQUS. In addition, the risk of multilateral junction failure is studied under several conditions due to pressure depletion in a 3D model. Results from drilling with static nozzle show that the material within wing zone can break off the formation during production and increase the risk of blockage in laterals (Figure 1). The simulation results provide guidelines for an improved design of RJD laterals in geothermal and hydrocarbon reservoirs.

[1] Danish Hydrocarbon Research and Technology Centre (DHRTC), mreza@dtu.dk
[2]Danish Hydrocarbon Research and Technology Centre (DHRTC), hamid@dtu.dk

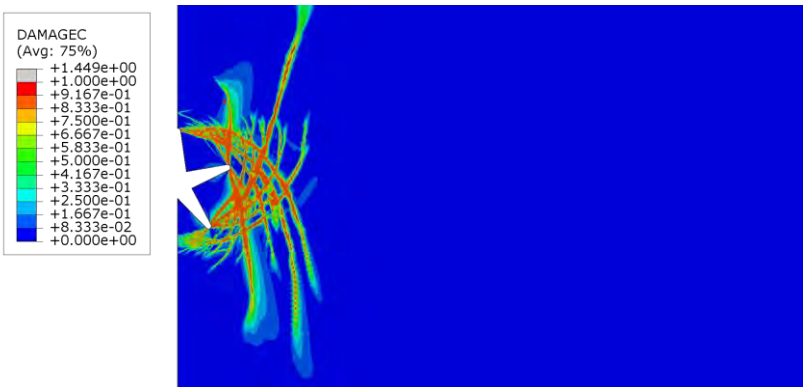

Figure 1. Compression damage zone after 10 MPa pore pressure depletion.

References

Medetbekova, M.K., S. Salimzadeh, H.F. Christensen, H.M. Nick (2017), Stability Analysis of Radial Jet Drilling in Chalk Reservoirs, In Poromechanics VI, 1842-1849.

Medetbekova, M. K., S. Salimzadeh, H.F. Christensen, H.M. Nick (2018), Experimental and Numerical Study of the Stability of Radially Jet Drilled Laterals in Chalk Reservoirs, In 80th EAGE Conference and Exhibition 2018.

GeoProc2019: Earthquake and Faulting mechanics

7th International Conference on Coupled THMC Processes in Geosystems
3-5 July 2019 Utrecht (Netherlands)

Sensitivity of compaction and stability analysis to rate dependent constitutive model of chalk and porous rocks

M.R Hajiabadi[1], *H.M. Nick*[2]

Keywords: Rate-dependent chalk material, Sensitivity analysis

This paper discusses the implementation of a rate-dependent chalk material in COMSOL multi-physics. For the chalk, a modified stress strain model [1] is used, which reproduces pore collapse, the rate dependent behavior resulting in creep and the water sensitivity of pore collapse strength and shear strength. While pore collapse is the dominant failure mechanism within a full field compaction analysis, shear failure plays main the role in stability analysis. In this implementation an elliptical rate-dependent yield surface is used for the pore collapse failure and modified Mohr-Coulomb criterion is defined for shear failure. Pore collapse yield surface is rate-dependently defined as a function of volumetric plastic strain. The implementation is qualified by the back analysis of laboratory triaxial tests performed on chalk from an oilfield. The application show that the model can reproduce the observed stress strain behavior of chalk. Within several analysis for field-scale compaction and well bore stability, the sensitivity of these analysis to rate-dependency is evaluated.

Reference

De Waal J.A., R.M.M. Smits (1988), Prediction of Reservoir Compaction and Surface Subsidence: Field Application of a New Model, SPE 14214.

[1] Danish Hydrocarbon Research and Technology Centre (DHRTC), mreza@dtu.dk
[2]Danish Hydrocarbon Research and Technology Centre (DHRTC), hamid@dtu.dk

GeoProc2019: Earthquake and Faulting mechanics

7th International Conference on Coupled THMC Processes in Geosystems
3-5 July 2019 Utrecht (Netherlands)

A microphysical model explaining effects of water on phyllosilicate friction

S.A.M. den Hartog[1], *D.R. Faulkner*[2], *C.J. Spiers*[3]

Keywords: phyllosilicates, friction, microphysical model

Fault slip often is localized in phyllosilicate-rich fault gouges, consistent with the relatively low friction coefficient measured for phyllosilicates in laboratory experiments. However, no quantitative, physical model exists to explain this low friction coefficient. Here, we predict the absolute value of the friction coefficient of pure phyllosilicates by means of a microphysical model inspired by microstructural observations. Experimentally produced phyllosilicate gouges suggest that shearing is controlled by sliding along (001) grain/platelet interfaces operating in series with removal of overlapping grain edge barriers by basal cleavage.

We derive a model incorporating a subcritical crack propagation equation for the latter, constrained by subcritical crack growth data for muscovite. Model predictions for muscovite agree well with experimental data for wet versus dry muscovite, chlorite and biotite (Figure 1). While experimentally observed effects of normal stress on friction coefficient at these stresses is captured, the model values predicted at low normal stresses at too high. This and the slip hardening behaviour generally seen in the initial stages of phyllosilicate gouge shearing experiments can potentially be explained by the effects of grain size and porosity on the friction coefficient. While numerous qualitative explanations have been proposed previously for the low friction coefficient exhibited by phyllosilicates, especially in the presence of water, our study provides a quantitative, physically based model that can aid extrapolation of laboratory data to natural conditions.

[1] The Lyell Centre, Heriot-Watt University, Edinburgh, UK, s.den_hartog@hw.ac.uk
[2] Rock Deformation Laboratory, University of Liverpool, Liverpool, UK, faulkner@liverpool.ac.uk
[3] HPT Laboratory, Utrecht University, Utrecht, The Netherlands, C.J.Spiers@uu.nl

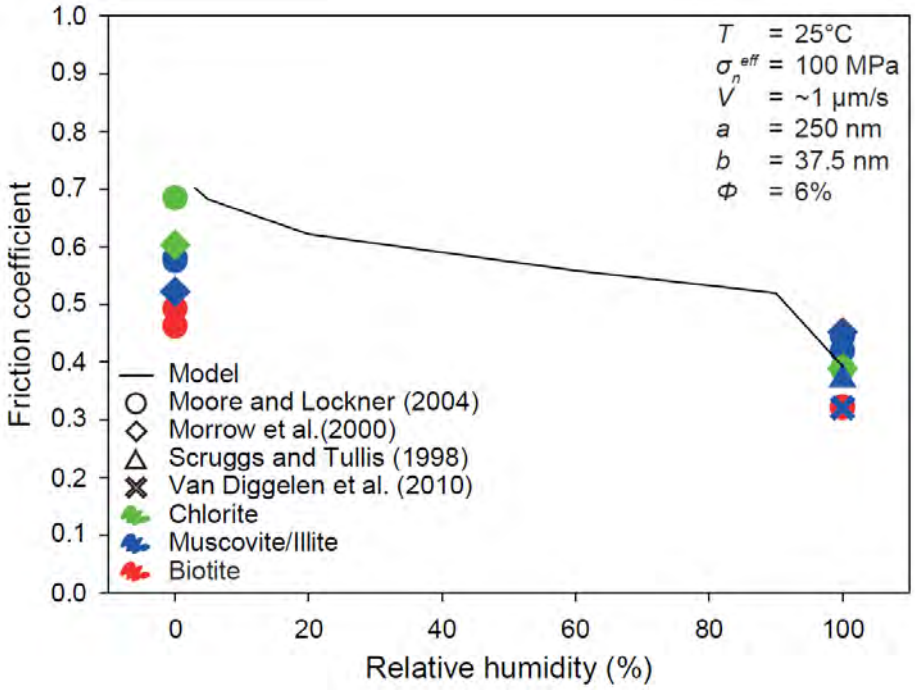

Figure 1. Friction coefficient versus relative humidity, showing model predictions (line) and experimental data (symbols). The data of Moore and Lockner (2004) and Morrow et al. (2000) are obtained at a slip velocity of 0.58 µm/s, at displacements of ~4.5 mm (dry) and ~10.3 mm (wet). The data of Scruggs and Tullis (1998) are obtained at a slip velocity of 1-10 µm/s, at steady state displacements of >10 mm. The data of Van Diggelen et al. (2010) are obtained at a slip velocity of 1 µm/s, at steady state displacements of >10 mm.

References

Moore, D. E. and D. A. Lockner (2004). Crystallographic controls on the frictional behavior of dry and water-saturated sheet structure minerals. *J. Geophys. Res. 109*, *B03401*, doi:10.1029/2003JB002582.

Morrow, C. A., et al. (2000). The effect of mineral bond strength and adsorbed water on fault gouge frictional strength. *Geophys. Res. Lett. 27(6),* 815-818, doi:10.1029/1999GL008401.

Scruggs, V. J. and T. E. Tullis (1998). Correlation between velocity dependence of friction and strain localization in large displacement experiments on feldspar, muscovite and biotite gouge. *Tectonophysics* 295(1–2): 15-40, doi:10.1016/S0040-1951(98)00113-9.

Van Diggelen, E. W. E., et al. (2010). High shear strain behaviour of synthetic muscovite fault gouges under hydrothermal conditions. *J. Struct. Geol.* 32: 1685-1700, doi:10.1016/j.jsg.2009.08.020.

GeoProc2019: Earthquake and Faulting mechanics

7th International Conference on Coupled THMC Processes in Geosystems
3-5 July 2019 Utrecht (Netherlands)

Yield-strength focusing of fracture networks in weak viscoplastic materials

Nicholas W. Hayman[1], *Mohammadreza Shafiei*[2], *Thomas A. Dewers,*[3], *Matthew Balhoff*[4]

Keywords: viscoplasticitiy, cabopol, slow-fracture, creep, localization

Viscous flow following plastic failure of weak, elastic media is a reasonable rheologic description of many earth processes, notably transient creep of tectonic faults in the crust (Hayman and Lavier, 2014; Reber et al., 2015). Such a rheological model may also describe the formation of gas-escape fluid conduits (also known as “chimneys”) through sedimentary systems. Here, we explore chimney formation in viscoplastic materials with physical experiments and numerical simulations. The experiments were done with a pressure-input valve into a Hele-Shaw cell containing a layer of the polyacrylic acid, cross-linked polymer known as Carbopol. The numerical simulations were conducted with COMSOL using the Phase-Field method (e.g., Lee et al., 2015) and laminar flow Multiphysics toolboxes. With the two methods we have documented the possible morphology of fractures, the range of fracture-branching patterns, and general controls on localization that might occur within chimney systems.

The yield strength of Carbopol was determined through rheometer experiments and is a function of the concentration of the hydrogels that comprise the polymer and the pH of the mixing solution, both microstructurally expressed as a jammed granular material (Shafiei et al., 2018). The viscosity of Carbopol is defined by the yield-stress value, and does not dynamically evolve further in rheometer experiments.

In our latest experiments, wherein a lower-viscosity dyed gelatin is injected into Carbopol for a range of yield stresses, we find in all cases that the post-failure viscous behavior leads to fracture propagation wherein the branching fractures have parabolic tips and trajectories reminiscent of viscous fingering. The macroscopic behavior in the physical experiments allowed a comparison with propagation patterns in the numerical simulations of Saffman-Taylor instabilities that propagate along a trajectory defined by

[1] University of Texas, Institute for Geophysics, Jackson School of Geosciences, 10100 Burnet Rd, Austin, TX, 78758, United States, hayman@ig.utexas.edu; also at the US National Science Foundation.
[2] McKetta Department of Chemical Engineering, University of Texas at Austin, 200 E. Dean Keeton St, Stop C0400, Austin, TX, 78712-1589, United States, shafieimo@gmail.com
[3] Geomechanics Department, Sandia National Laboratories, Albuquerque, New Mexico, 87185, United States, tdewers@sandia.gov
[4] Hildebrand Department of Petroleum and Geosystems Engineering, University of Texas at Austin, 200 E. Dean Keeton St, Stop C0300, Austin, TX, 78712-1585, United States, balhoff@mail.utexas.edu

the pressure gradient. Most of our results to date result in a relatively delocalized branching pattern wherein fractures continue to branch and evolve behind the frontal crack tip. However, we have found a narrow range of yield strength that localizes the fracture propagation, and future work can explore the underlying mechanisms that lead to such focusing.

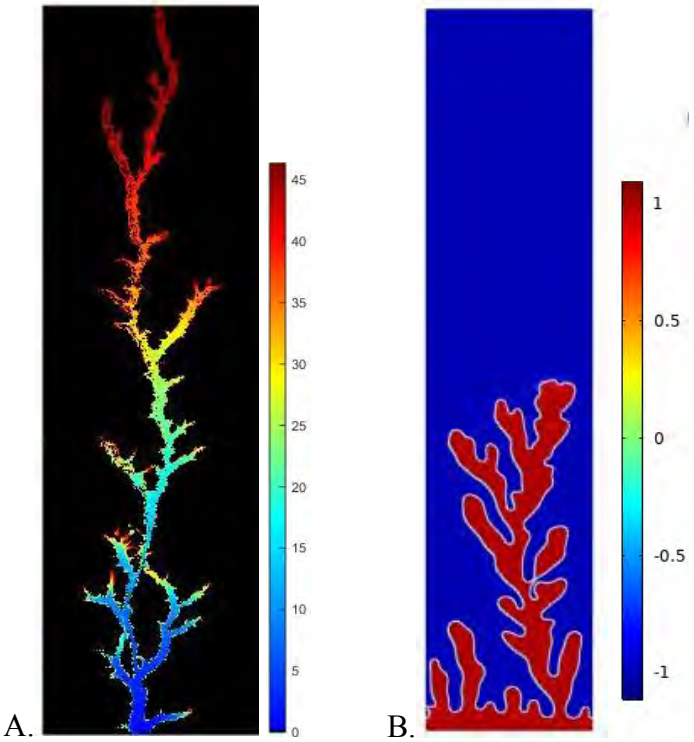

A. Fracture propagation as dyed glycerin is injected at the base of a hele-shaw cell and moves toward the release valve at the top. The colors track the time in seconds of fracture-tip propagation. Note that some small amount of crack growth continues behind the crack front.

B: Results of a COMSOL simulation wherein the color bar represents the two different mechanical phases: a weak viscoplastic host (blue) and a fluid injectant with lower viscosity (red).

References

Hayman, N. W., & L. L. Lavier, (2014), The geologic record of deep episodic tremor and slip. *Geology*, *42*(3), 195-198. DOI: 10.1130/G34990.1.

Lee, S., J. E. Reber, N. W.Hayman, N. W., and M. F. Wheeler (2016), Investigation of wing crack formation with a combined phase-field and experimental approach. *Geophysical Research Letters*, *43*(15), 7946-7952. DOI: doi.org/10.1002/2016GL069979

Reber, J. E., L. L. Lavier, L. L. , & N.W. Hayman (2015), Experimental demonstration of a semi-brittle origin for crustal strain transients, *Nature Geoscience*, *8*(9), 712. doi : 10.1038/ngeo2496.

Shafiei, M., M. Balhoff, & N. W. Hayman (2018), Chemical and microstructural controls on viscoplasticity in Carbopol hydrogel. *Polymer*, *139*, 44-51, DOI: 10.1016/j.polymer.2018.01.080

GeoProc2019: Earthquake and Faulting mechanics

7th International Conference on Coupled THMC Processes in Geosystems
3-5 July 2019 Utrecht (Netherlands)

An Experimental Exploration of Elastic Softening of Limestone due to Decarbonation with Episodic CO2 Release

D. Head[1], *T. Vanorio*[2], *A. Clark*[3]

Keywords: Decarbonation, carbonates, velocity-sensitivity, THMC experiments, DEM

Reactive fluid flow through porous media under stress leads to complex thermo-hydro-mechanical-chemical (THMC) alterations. Thermal decomposition of carbonates in crustal settings can cause failure due to carbon dioxide (CO_2) release, solid volume or strength reduction, and/or nanograins/fiber production (Brantut et al., 2012; Collettini et al., 2013; Green II et al., 2015; Verberne et al., 2014). We exposed three tight limestone cores to hydrothermal conditions conducive to the wollastonite-producing decarbonation reaction. We injected the samples with an aqueous suspension of colloidal silica and heated them in the presence of water at confining pressure up to 15 MPa, pore pressure up to 13 MPa, and temperature up to 425 C. The experiments mimic pulsing flow in crustal systems and mitigate the accumulation of CO_2 through episodic release of pore fluid pressure.

The reacted samples showed the development of a new calc-silicate phase (confirmed by EDS) with a non-uniform needly to bladed morphology, which contained soft (highly compliant) porosity. The new phase was found on the surface of all three reacted samples and throughout the interior of the pore space of one sample, which was cut vertically.

The physical changes to the carbonate frame are due to complex THMC alteration with several components – reduction in solid volume due to the decarbonation reaction, water expansion due to heating, and sudden water flashing to steam during some episodic pore pressure release events. All three decarbonated samples showed a large increase in velocity sensitivity to confining pressure as well as a large decrease in velocity magnitude. To explore the contributions from the water expansion and flashing, two additional carbonate samples were heated in the same manner in the presence of water in the reactor vessel but without silica. One had the pulsing flow and thus the water flashing to steam events, and the other did not. In both cases, water was found to cause a decrease in velocity, but allowing flashing events appears to enhance velocity sensitivity to confining pressure, and decarbonation appears to enhance it even further.

A crustal THMC process such as decarbonation that is accompanied by a large change in velocity and elastic properties violates the general assumption of constant rock

[1] Stanford University, dulcieh@stanford.edu
[2] Stanford University, tvanorio@stanford.edu
[3] Stanford University, clarkac@stanford.edu

microstructure, as in non-interacting fluid-substitution models. Therefore, rocks that have experienced THMC frame alteration cannot be modeled as though their elastic properties are independent of time. We explore DEM modeling to estimate changes in the rock frame by quantifying the rock-frame drained moduli before and after decarbonation (i.e., frame substitution), which result from the soft porosity developed due to this type of reaction. Having the P- and S-wave velocity time-lapse data is key to improve saturation and pore pressure estimates, which has implications for remote monitoring of subsurface fluid in seismogenic areas.

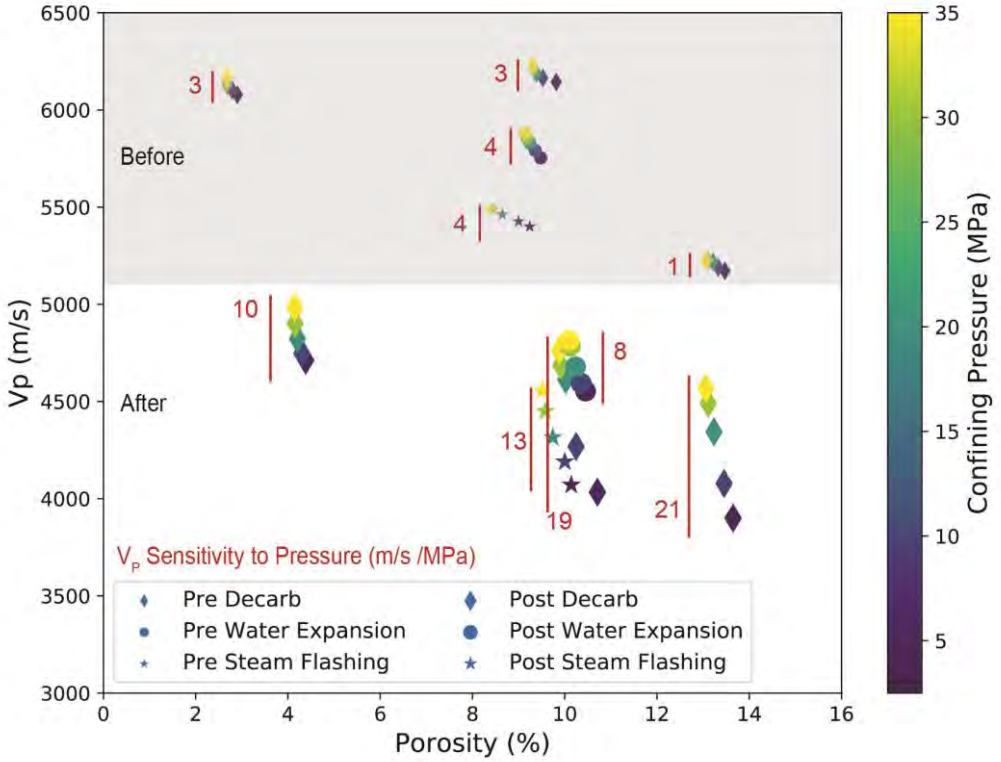

Figure 1. P wave velocity as a function of porosity colored by confining pressure. Smaller symbols on a grey background are pre-reaction, while larger symbols on a white background are post- reaction. Red bars show the velocity sensitivity to confining pressure. The three samples with diamond symbols were injected with silica before heating in the presence of water, resulting in a decarbonation reaction that produced a new calc-silicate phase. The samples heated in the present of water without silica are marked by the circular symbols (no water flashing) and the star symbols (water flashing).

References

Brantut, N., Schubnel, A., David, E. C., Héripré, E., Guéguen, Y., & Dimanov, A. (2012). Dehydration-induced damage and deformation in gypsum and implications for subduction zone processes. J. Geophys. Res. Solid Earth, 117(B3), 1–17, doi:10.1029/2011JB008730.

Collettini, C., Carpenter, B. M., Viti, C., Cruciani, F., Mollo, S., Tesei, T., Trippetta, F., Valoroso, L., & Chiaraluce, L. (2014). Fault structure and slip localization in carbonate-bearing normal faults: An example from the Northern Apennines of Italy. J. Struct. Geology, 67(PA), 154–166, doi:10.1016/j.jsg.2014.07.017.

Green II, H. W., Shi, F., Bozhilov, K., Xia, G., & Reches, Z. (2015). Phase transformation and nanometric flow cause extreme weakening during fault slip. *Nat. Geoscience*, 8(6), 484–489. doi:10.1038/ngeo2436.

Verberne, B. A., Plumper, O., de Winter, D. A. M., & Spiers, C. J. (2014). Superplastic nanofibrous slip zones control seismogenic fault friction. *Science*, 346(6215), 1342–1344. Doi:10.1126/science.1259003.

GeoProc2019: Earthquake and Faulting mechanics

7th International Conference on Coupled THMC Processes in Geosystems
3-5 July 2019 Utrecht (Netherlands)

The influence of differential compaction on fault re-activation in depleting reservoirs

Dr. Marc Hettema[1]

Key words: Mechanical fault re-activation, Coulomb stability function, Poro-elastic stressing, Differential compaction, Earthquakes

As a result of pore pressure depletion the reservoir rock starts to compact, causing changes in the stresses and strains inside and surrounding the reservoir. One of the consequences can be mechanical re-activation along fault planes of weakness posing a hazard for seismicity. The developed methodology starts by defining various fault categories present in the Dutch subsurface, based on reservoir setting and fault properties, such as throw, dip, strike and transmissibility. A new general Coulomb stability relationship has been developed that allows determination of the stability of all fault types in depleting reservoirs in a normal-faulting stress regime. The critical reservoir pressure depletion under which mechanical re-activation along fault planes of weakness can occur has been developed analytically. Resolving the normal and shear stresses on the fault plane allows determination of the contributions from poro-elastic stressing and the differential displacement-induced shear stresses separately.

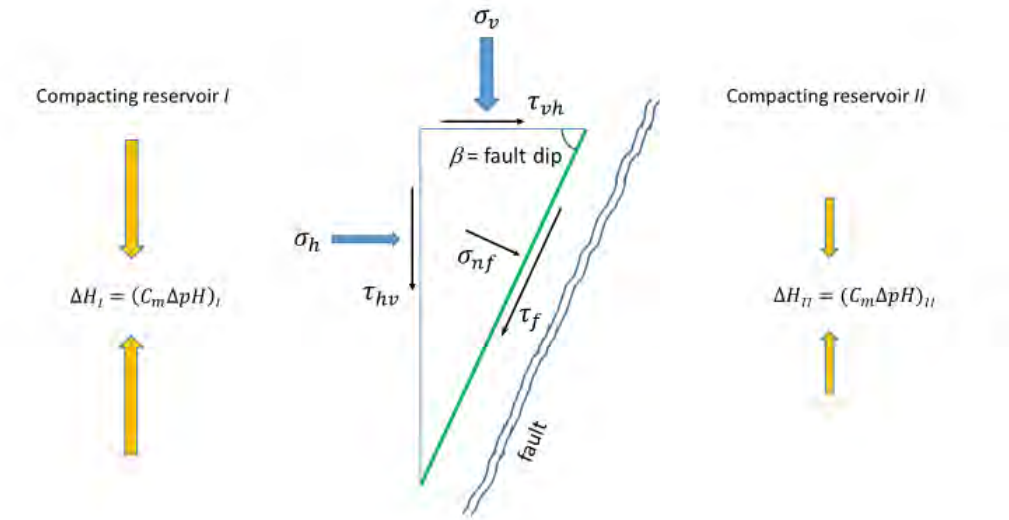

The analysis shows how the fault dip controls these two contributions for both normal dipping and reverse fault dipping faults. Three fault categories are analysed: open

[1] Geo-mechanical Engineering Expert, EBN, the Netherlands, marc.hettema@ebn.nl

intra-reservoir, (partly) sealing intra-reservoir and boundary. Important input parameters are the reservoir stress paths, which are analytically estimated for simple geometries. The poro-elastic stressing depends on the reservoir stress paths and the ratio of pore pressure depletion from either side of the fault plane caused by (partly) sealing faults. The induced shear stress profiles are developed using analytical vertical displacement profiles from either side of the fault plane applying the theory of Geertsma (1973).

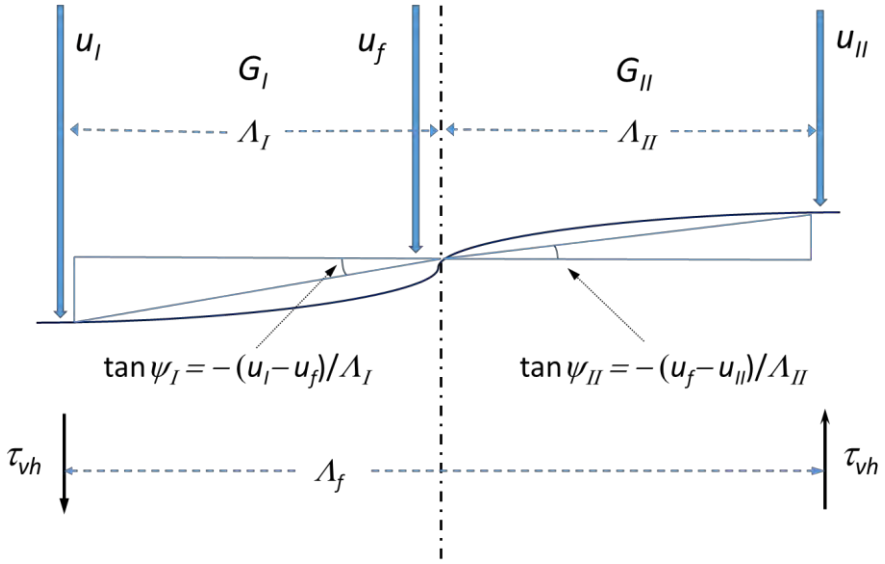

The induced shear stress is either caused by the fault throw or by the pressure difference caused by the (partly) sealing fault or by boundary faults. They are written in terms of the driving stress (related to reservoir compaction or pressure depletion) and two dimensionless geometrical functions. The induced shear stress also causes a rotation of the near-fault stresses. The contributions from both poro-elastic stressing and differential compaction are combined in a Coulomb stability function. The critical reservoir pressure depletion for fault re-activation to occur has been determined for all three fault categories. Satisfying this Coulomb criterion is a necessary mechanical condition for seismicity to occur. Of the three differential compaction mechanisms investigated, only the fault throw leads to a reduction of the critical depletion pressure. The cases of (partly) sealing faults and boundary faults lead unexpectedly to an increase of the critical depletion pressure. This seems to contradict the conclusion of van Wees et al. (2014), who stated that at the edge of the reservoir the strongest destabilization occurs.

These results can be used to determine the initiation pressures at which seismicity occurs in depleting gas reservoirs in the Netherlands and can in addition explain why the observed seismicity at the Groningen gas field can be attributed to very steep dipping fault planes. Kortekaas and Jaarsma (2017) have shown that the majority of dips range between 74 and 81 degrees. The results also demonstrate that all differential compaction mechanisms (fault throw, differential depletion for (partly) sealing faults and boundary faults) result in a stress rotation causing an increase in the critical fault dip towards vertical. It seems plausible that the abundant presence of these fault geometries has facilitated the extensively observed seismicity at relatively high fault dips. The presented results apply to depleting reservoirs but the Coulomb stability

function has been extended to incorporate thermal effects in order to determine the seismic hazard for cold water injection during geothermal operations.

References

Geertsma, J. 1973. A basic history of subsidence due to reservoir compaction: the homogeneous case. Verh. Kon. Ned. Geol. Mijnbouwk. Gen., 28. 43-62.

Hettema, M.H.H. 2019. Mechanics of initiation of fault reactivation in depleting reservoirs. Submitted to Rock Mechanics and Rock Engineering.

Kortekaas, M. and Jaarsma, B. 2017. Improved definition of faults in the Groningen field using seismic attributes. Netherlands J. of Geosc.– Special Issue on the Groningen Gasfield., 96 – 5, 71-85.

Wees, J-D. van, L. Buijze, K. van Thienen-Visser, M. Nepveu, B.B.T. Wassing, B. Orlic and P.A. Fokker, 2014. Geomechanics response and induced seismicity during gas field depletion in the Netherlands. Geothermics 52, 206-219.

GeoProc2019: Earthquake and Faulting mechanics

7th International Conference on Coupled THMC Processes in Geosystems
3-5 July 2019 Utrecht (Netherlands)

Cross-Diffusion Triggered Hydro-Mechanical Wave Instabilities

M. Hu[1], *K. Regenauer-Lieb*[2]

Keywords: Transient Waves, Complex Systems, Coupled Processes, Diffusional Length Scales, Poromechanics, HT-HP Systems

Coupled Hydro-Mechanical (HM) patterns are ubiquitous in nature yet their origin is not fully understood. We propose a new approach of wave instabilities triggered by HM-feedbacks in a two-phase porous medium. Fig. 1 shows an example of an HM-instability of melt extraction. We identify the important aspect of cross-diffusion between the two phases and present a linear stability analysis of the governing PDEs. Multiple transient wave instabilities are found as solutions of the coupled HM PDEs, which in the standing wave limit (infinite time scale) form solitary wave patterns that are frozen into the geosystems at characteristic diffusional scales. The findings also shed light on linking slow earthquakes with geological processes in terms of time-scale.

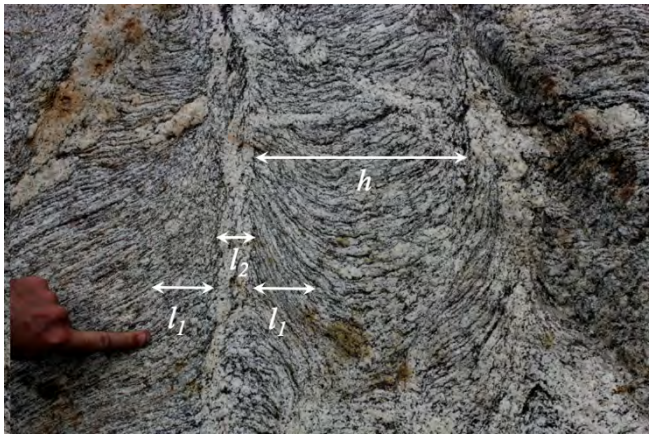

Figure 1 Melt extraction channels in a partially molten metamorphic rock (gneiss) from the Sikkim Higher Himalaya Migmatite gneisses with two parallel vertical melt bands (leucosomes) forming in the hinges of two cuspate folds. The fold has been formed as a consequence of horizontal shortening implying that the direction of the maximum principal stress σ_1 is in the horizontal plane. The melt bands are perpendicular to the direction of σ_1 and have been interpreted as standing cnoidal wave instabilities [1]. Three diffusional length scales have been identified in the figure.

Thermodynamic forces and fluxes of an HM coupled system are defined in Table 1. First we revisit the case of two consolidation processes in classical poromechanics [2]. The primary consolidation process features the diffusion of pore fluid pressure (melt in Fig. 1) and this process (H) is described by Darcy's law, where κ is the matrix permeability and μ_f is the melt viscosity. The secondary consolidation is the compaction of the viscous solid matrix after yielding at p_Y and the mechanical flux (M) represents the incremental change in solid-phase overstress $\bar{p}_s = \langle (p - p_f) - p_Y \rangle$ where p is the total pressure and p_f the fluid pressure. The capital $D./Dt$ denotes the material derivative.

[1] UNSW Sydney, manman.hu@unsw.edu.au
[2] UNSW Sydney, klaus@unsw.edu.au

Table 1. Generalised Thermodynamic Fluxes and Forces in an HM coupled system (1-D)

	Thermodynamic Force	Thermodynamic Flux	Conservation Laws (without cross-diffusion)
H	$F_H = \frac{\partial p_f}{\partial x}$	$q_H = -\frac{\kappa}{\mu_f}\frac{Dp_f}{Dt}$	$\frac{1}{M}\frac{Dp_f}{Dt} = -\frac{\partial F_H}{\partial x} + r^f$ (1)
M	$F_M = \frac{\partial \overline{p}_s}{\partial x}$	$q_M = -\frac{D\overline{p}_s}{Dt}$	$\frac{1}{K}\frac{Dx}{Dt}F_M = -D_M\frac{\partial^2 \overline{p}_s}{\partial x^2} + r^M$ (2)

The conservation laws Eq. 1 and Eq. 2 are derived from the thermodynamic principle that a thermodynamic flux is induced by the gradient of a thermodynamic force. M and K correspond to the effective bulk modulus of the primary and the secondary consolidation, respectively. Based on [3], the mechanical (M) momentum conservation in the creeping flow regime is described as a diffusion wave equation (no inertia) traveling at a wave velocity $\boldsymbol{v} = Dx/Dt$ (see Eq. 2). r^f and r^M denote possible reactive source terms. In classical poromechanics, the two diffusional time-scales of consolidation processes are considered to be sufficiently far apart. In the case of the partially molten rock (Fig. 1) this is not likely to be the case. Then, we refer to the concept of cross diffusion which in a complex system is defined by the phenomenon that a gradient of one generalised thermodynamic force can drive another generalised thermodynamic flux. Now the off-diagonal elements in the diffusion matrix are non-zero. Assuming linear superposition of cross-diffusion terms, we rewrite Eq. 1 and Eq. 2 as:

$$\begin{aligned}\frac{\partial p_f}{\partial t} &= D_H\frac{\partial^2 p_f}{\partial z^2} + h_1\frac{\partial^2 \overline{p}_S}{\partial z^2} + r^f \\ \frac{\partial \overline{p}_S}{\partial t} &= D_M\frac{\partial^2 \overline{p}_S}{\partial z^2} - h_2\frac{\partial^2 p_f}{\partial z^2} + r^M\end{aligned} \quad (3)$$

where $h_1 \geq 0, h_2 \geq 0, h_1 + h_2 > 0$ are the cross-diffusion coefficients [4] triggering wave instabilities from e.g. internal mass transfer or phase transition. We identify at least three diffusional length scales (see Fig. 1): h, l_1 and l_2, corresponding to the large-scale HM instability forming the compaction band and two cross-diffusional length scales adjacent to the band itself, respectively. These length-scales define the wavenumbers of the coupled HM cross-diffusional waves (stationary or transient).

References

1. Weinberg, R., M. Veveakis, and K. Regenauer-Lieb, *Compaction bands and melt segregation from migmatites.* Geology, 2015. **43**(6): p. 471-474.
2. Coussy, O., *Poromechanics*. 2004, Chichester: Wiley.
3. Veveakis, E. and Regenauer-Lieb, *Cnoidal Waves in Solids.* Journal of Mechanics and Physics of Solids, 2015. **78**: p. 231-248.
4. Vanag, V.K. and I.R. Epstein, *Cross-diffusion and pattern formation in reaction–diffusion systems.* Physical Chemistry Chemical Physics, 2009. **11**(6): p. 897-912.

GeoProc2019: Earthquake and Faulting mechanics

7th International Conference on Coupled THMC Processes in Geosystems
3-5 July 2019 Utrecht (Netherlands)

Role of long-term healing in the frictional sliding behavior of simulated Groningen fault material

L. Hunfeld[1], *S. Hol*[2], *C. Spiers*[3]

Keywords: Slide-Hold-Slide experiments, induced seismicity, Groningen gas field

Recent cases of induced seismicity in the Groningen gas field have raised major public concern in The Netherlands. The events are believed to be associated with reactivation of pre-existing faults cross-cutting the reservoir and over- and underburden. As detailed understanding of the controls and evolution of frictional behavior is lacking at present, a quantification of the static- and dynamic fault strength is urgently required to assist risk assessment studies.

In this contribution, we specifically focus on post-slip re-strengthening, as well as reactivation and associated slip weakening behavior, of simulated fault gouge material derived from the main stratigraphic members in the Groningen subsurface, viz. Basal Zechstein caprock, Ten Boer claystone, Slochteren sandstone, and Carboniferous shale/silts. Using a triaxial vessel equipped with a 1-inch diameter direct shear assembly, we performed Slide-Hold-Slide (SHS) experiments at a temperature of 100 °C and an effective normal stress of 40 MPa. In these experiments, initial shearing of the gouge material was followed by healing for periods up to 3 months while exposed to synthetic formation brine. Reactivation of slip was then performed (Figure 1a).

The initial coefficient of sliding friction μ was the highest in the Basal Zechstein (μ=0.65±0.02) and Slochteren (μ=0.61±0.02) gouge materials, and the lowest in the Ten Boer (μ=0.38±0.01) and Carboniferous (μ=~0.45) materials. After long-term healing at 40 MPa effective normal stress, the SHS experiments yield a marked increase in (static) friction coefficient $\Delta\mu$ of up to ~0.16 for the Basal Zechstein and ~0.07 for the Slochteren materials (Figure 1b), followed by considerable strength drop and slip weakening upon reactivation. By contrast, the Ten Boer and Carboniferous materials show negligible change. Furthermore, the healing rate in the Basal Zechstein and Slochteren sandstone gouge materials depends on the effective stiffness of the fault surroundings, which is consistent with existing rate-and-state-friction models.

These new results point to a) strong stratigraphic variation in frictional strength in the Groningen field and healing-induced alteration thereof, and b) significant potential for seismogenesis in faults cutting the Slochteren sandstone reservoir and Basal Zechstein caprock units due to slip weakening.

[1] High Pressure and Temperature Laboratory, Utrecht University, l.b.hunfeld@uu.nl
[2] Geomechanics Experimentation, Shell Global Solutions International B.V., sander.hol@shell.com
[3] High Pressure and Temperature Laboratory, Utrecht University, c.j.spiers@uu.nl

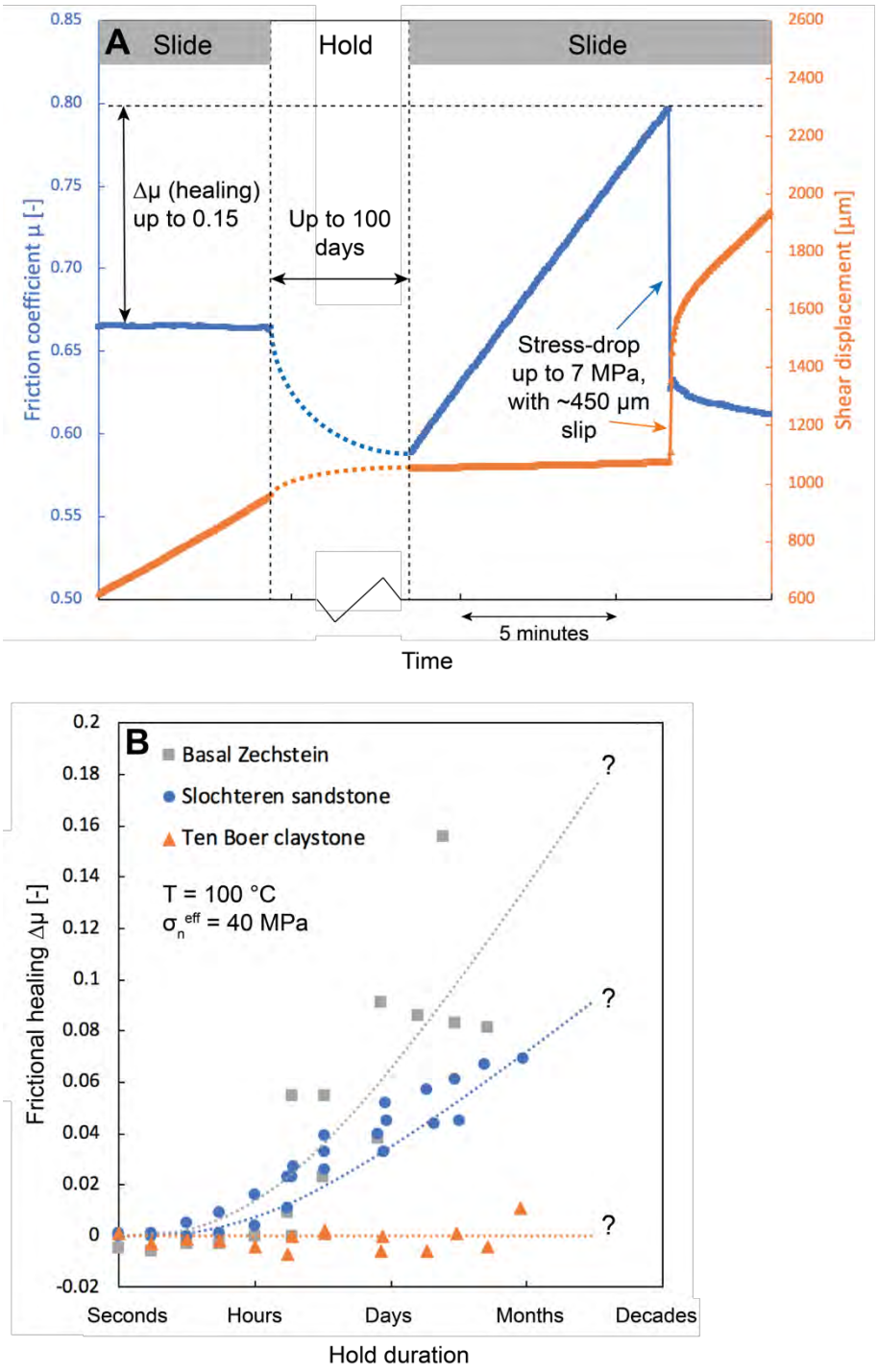

Figure 1. a) Typical example of a Slide-Hold-Slide (SHS) experiment performed on Basal Zechstein gouge, showing the evolution of friction coefficient and shear displacement with time. During the reactivation stage, stress-drops as large as 4-7 MPa were measured for Slochteren sandstone and Basal Zechstein gouges, which are of similar magnitude as those estimated from induced events in the Groningen reservoir. b) Frictional healing versus hold duration for simulated Basal Zechstein, Slochteren sandstone and Ten Boer claystone gouges, obtained in SHS experiments with hold times up to 100 days ($8.6 \cdot 10^6$ s). Basal Zechstein and Slochteren sandstone gouges show marked frictional healing, whereas no healing could be detected in Ten Boer claystone gouge.

GeoProc2019: Earthquake and Faulting mechanics

7th International Conference on Coupled THMC Processes in Geosystems
3-5 July 2019 Utrecht (Netherlands)

Microstructure and Frictional Behavior of Chlorite-Epidote-Amphibole Assemblages

Matt J. Ikari [1], *Åke Fagereng* [2]

Keywords: 3 to 5 keywords separated by commas

On exhumed faults with a significant dip-slip component, greenschist to amphibolite facies mineral assemblages formed near the base of the seismogenic zone may also host active shearing at shallower depths. If the fault rock composition is sufficiently ferromagnesian, these faults could accommodate deformation within a pre-existing amphibole-chlorite-epidote assemblage, or experience changes in frictional properties with increasing retrograde chlorite-epidote growth. These minerals can therefore govern fault behavior; however, little is known of their frictional properties. Here, we present the results of laboratory shearing experiments on chlorite, epidote, hornblende, and mixtures of these minerals, and evaluate their frictional properties and microstructure. All experiments were conducted on powdered rock samples with a grain size of < 125 μm, at room temperature, under fluid-saturated conditions and an applied normal stress of 10 MPa.

The experiments show that chlorite is relatively weak, with a frictional coefficient of about 0.4, whereas epidote and hornblende have friction coefficients of 0.54 and 0.57 respectively. The chlorite-epidote and chlorite-hornblende mixing trends are mostly linear. Chlorite is velocity strengthening, epidote is velocity weakening, and the hornblende end member shows both velocity-strengthening and velocity-weakening friction. Mixtures show intermediate strength velocity-dependent friction.

There is a distinct striation development on the slip surface in samples with chlorite, but such striations are absent or poorly developed in samples without chlorite. The epidote slip surface exhibits a large grain size variation, with a mixture of very fine particles in addition to the coarser crystals. Hornblende, on the other hand, shows a more uniform grain size, likely caused by strongly-developed cleavage. We infer wear at contact asperities rather than pervasive fracturing to be the likely cause of velocity-weakening in our epidote gouges. The addition of chlorite reduces the amount of very fine epidote particles and produces a striated slip surface, which favors strength reduction and velocity-strengthening friction when chlorite is mixed with either epidote or hornblende.

[1] University of Bremen, Germany
[2] Cardiff University, UK

GeoProc2019: Earthquake and Faulting mechanics

7th International Conference on Coupled THMC Processes in Geosystems
3-5 July 2019 Utrecht (Netherlands)

What keeps slow earthquakes slow?

Kyungjae Im[1], *Demian Saffer*[2], *Chris Marone*[3]

Keywords: Fault slip mode, Slow earthquake, Frictional stability

We analyze modes of fault slip using numerical simulations of a single degree of freedom system that incorporates rate and state friction (RSF) with full consideration of inertia. The simulations are conducted for normal stresses ranging over two orders of magnitude and spanning five orders of magnitude in loading velocities. We investigate the effects of both constant and velocity-dependent frictional parameters. The simulation results produce transitions in fault slip modes between stable sliding, stick-slip, slow stick-slip, and quasi-harmonic vibration. These stability transitions, with both constant and non-constant RSF parameters, are predicted with a high degree of accuracy by dimensionless parameters derived from existing formulations of critical stiffness (K_c). Here, K_c should be driven by the velocity-derivative of RSF with full consideration of velocity dependencies of the parameters and also by the full consideration of inertial destabilization effects. As observed in laboratory experiments, slow stick-slip (peak velocity < 1 mm/s) appears at the transition between stable sliding to regular stick-slip. However, when constant friction parameters are assumed, the stable to stick-slip transition occurs abruptly over a very narrow range of K_c, which is inconsistent with both laboratory observations of slow slip that exhibit notably gradual transitions from stable-sliding to slow stick-slip and finally to regular stick-slip, and with the observation of slow slip phenomena on natural faults that span a broad range on inferred in situ conditions. In contrast, the incorporation of rate dependence of the RSF parameters (b-a and/or D_c) as is observed in laboratory experiments, leads to a significant expansion of the conditions that produce slow stick-slip. Our result offers an explanation for widespread observations of a spectrum of fault slip behaviors, with low peak V and small stress drops, in natural geological systems.

[1] Department of Energy and Mineral Engineering and G3 Center, The Pennsylvania State University, University Park, PA 16802, kxi123@psu.edu
[2] Department of Geoscience and G3 Center, The Pennsylvania State University, University Park, PA 16802, demian@psu.edu
[3] Department of Geoscience and G3 Center, The Pennsylvania State University, University Park, PA 16802, marone@psu.edu

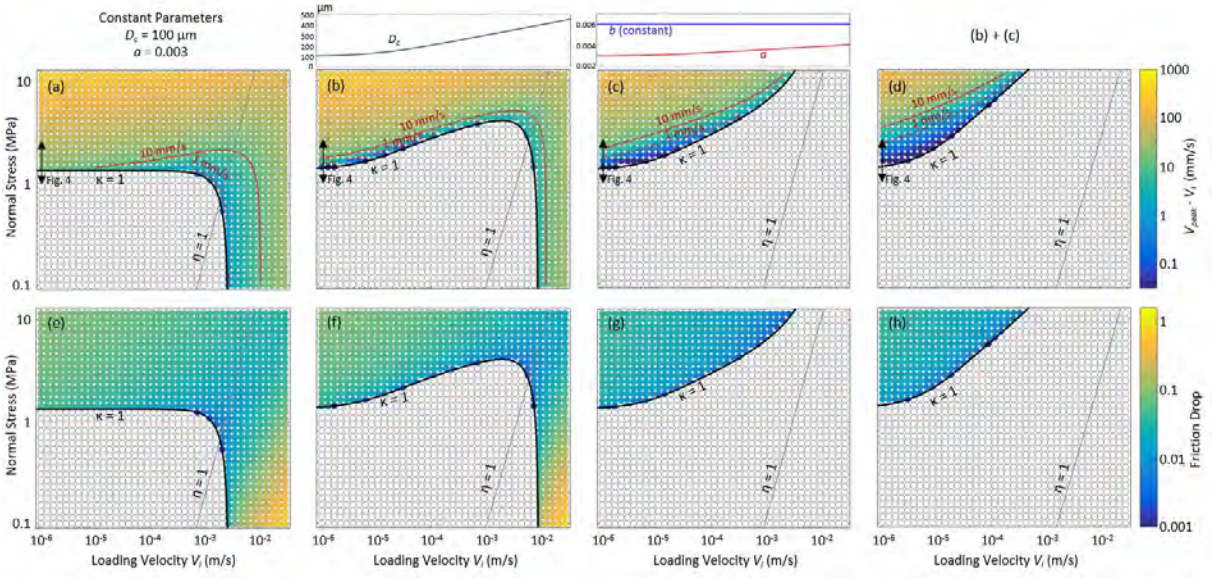

Figure 1. Map of peak velocity (a ~ d) and friction drop (e ~ h) over five orders of loading velocity and two orders of normal stress. Each colored circles represent the peak velocity and friction drop at their limit cycles. Grey empty circles represents that the sliding become stable. Four simulation sets are conducted. (a, d): constant RSF parameters. (b, f): D_c increases with velocity. (c, g): '*a*' increases with velocity. (e, h): both D_c and *a* increases with velocity. Bold solid line (κ = 1) denotes stability criteria calculated by Rice-Ruina stability criteria and gray line (η = 1) denotes where the inertial instability equals to quasi-static instability. Note that the slow stick-slip zone (V_{peak} < 1 mm/s) is trivial at constant friction parameters (a). Conversely, the slow stick-slip zone is significantly expanded when D_c and '*a*' are dependent on velocity (d).

References

Im, K., C. Marone and D. Elsworth (2019) The transition from steady frictional sliding to inertia-dominated instability with rate and state friction, Journal of the mechanics and physics of solids, 10.1016/j.jmps.2018.08.026

Marone, C. and E. Richardson, (2010) Learning to read fault-slip behavior from fault-zone structure, Geology, 38, 767–768; 10.1130/focus082010.1

Saffer, D. and L. Wallace, (2015) The frictional, hydrologic, metamorphic and thermal habitat of shallow slow earthquakes, Nature geoscience, 10.1038/NGEO2490

GeoProc2019: Earthquake and Faulting mechanics

7th International Conference on Coupled THMC Processes in Geosystems
3-5 July 2019 Utrecht (Netherlands)

Multiphysics of faulting: influence of porosity and damage evolutions on the deformation modes within the lithosphere

A. B. Jacquey[1], *M. Cacace*[1]

Keywords: Localised deformation, damage weakening, porosity, numerical modelling

Two main deformation modes are thought to control the long-term strength of the lithosphere: frictional – pressure-dependent – brittle deformation, and Arrhenius-type thermally activated creep. Dynamic changes in terms of forcing conditions (from natural, tectonic driven to anthropogenic ones) can also exert changes in the strength profile. The shape of a strength profile determines at which depth differential stresses could be accumulated and therefore impose self-consistent bounds to the amount of energy which could be released in a seismic or aseismic way. To estimate this amount of energy, some attention has been given in the community to quantify the value of the friction coefficient in fault zones. Several studies have reported lower values of the friction coefficient in existing fault zones as the ones predicted by Byerlee's law [Numelin et al. 2007, Faulkner et al. 2010, Boulton et al. 2017]. In addition, describing the evolution of the friction coefficient after onset of faulting or reactivation of existing faults requires to account for microstructural effects but also for the presence of fluid.

Understanding the evolution of localised deformation in a semi-brittle semi-ductile regime has therefore become of relevance in the geodynamic community to (i) understand the behaviour of fault zones in the vicinity of the brittle-ductile transition and also in the geo-engineering community to (ii) mitigate risk of induced seismicity when targeting high-enthalpy unconventional geothermal resources as found in volcanic settings, where the thermal conditions may activate ductile deformation at shallower depths than expected. This contribution aims at describing the multiphysics coupling characterising the evolution and stability of localised deformation and therefore in a broader sense of faulting mechanics, by means of a damage poro-elasto-visco-plastic rheology.

We make use of the numerical simulator LYNX (Lithosphere dYnamic Numerical toolboX), which relies on an implicit multiphysics coupling of the physics describing the deformation multiphysics as occurring in the rigid portion of the lithosphere including thermal, mechanical and hydraulic feedbacks. In particular, we include effects that control the microstructure evolution and its feedbacks on the macroscopic deformation and frictional behaviour (see Fig. 1), formulated in terms of damage evolution, modified after [Lyakhovsky et al. 2015]. We also account for the presence of fluid (via porosity

[1] GFZ Potsdam, German Research Centre for Geosciences, Germany, ajacquey@gfz-potsdam.de

evolution) and how it impacts the strength of lithospheric rocks and can exert a control on the dominant deformation mode.

In this contribution, we present a thermodynamically-consistent physical framework to describe the physical processes controlling deformation dynamics in a semi-brittle semi-ductile regime. We will focus in particular on (i) the role of damage weakening and its impact on the evolution of localised deformation and (ii) the role of porosity evolution as a driving mechanism to dilatant brittle deformation. These two aspects allow us to gain insights into the influence of localised deformation onto the strength of lithospheric rocks and on their hydraulic behaviours, and therefore on the evolution fault zones. We will present numerical examples describing the dynamics of these two aspects ranging from laboratory to lithosphere scales.

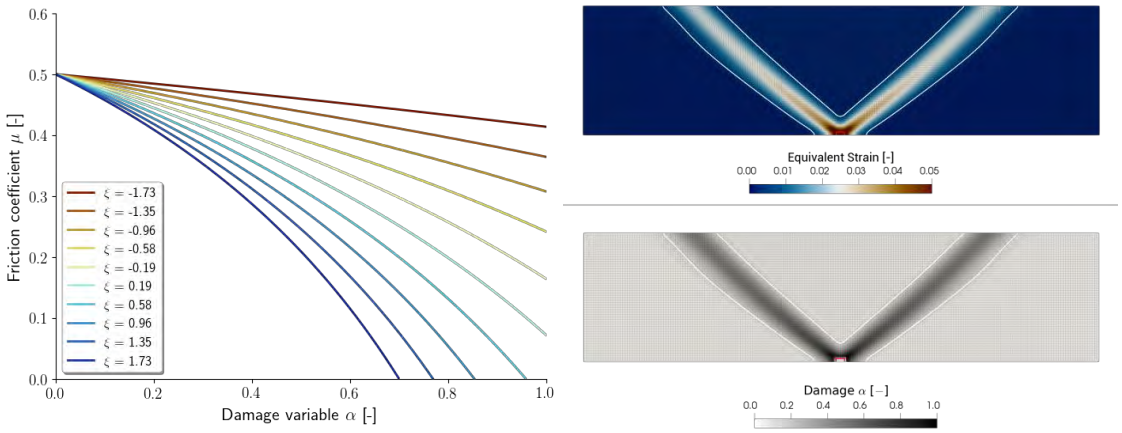

Figure 1. (left) Evolution of the friction coefficient as a function of the damage variable and the elastic strain ratio. (right) Effect of damage weakening on the evolution of localised deformation.

References

Numelin, T., Marone, C., Kirby, E. (2007). Frictional properties of natural fault gouge from a low-angle normal fault, Panamint Valley, California. *Tectonics*, 26, TC2004, doi: 10.1029/2005TC001916.

Faulkner, D. R., Jackson, C.A.L., Lunn, R.J., Schlische, R.W., Shipton, Z.K. Wibberley, C.A.J. Withjack, M.O., (2010). A review of recent developments concerning the structure, mechanics and fluid flow properties of fault zones. *Journal of Structural Geology*. Volume 32, 11, 1557-1575.

Boulton, C. Yao, L., Faulkner, D.R., Townend, J., Toy, V.G., Sutherland, R., Ma, S., Shimamoto, T., (2017), *Journal of Structural Geology*, Volume 97, 71-92.

Lyakhovsky, V., Zhu, W., Shalev, E. (2015). Visco-poroelastic damage model for brittle-ductile failure of porous rocks. *J. Geophys. Res. Solid Earth*. Volume 120, doi:10.1002/2014JB011805.

GeoProc2019: Earthquake and Faulting mechanics

7th International Conference on Coupled THMC Processes in Geosystems
3-5 July 2019 Utrecht (Netherlands)

Meter-Scale Friction Experiment with Gouge: Heterogeneities and Friction Properties

Yuntao Ji[1], Dawin D.H. Baden[1], Luuk B. Hunfeld[1], Ronald P. J. Pijnenburg[1], André R. Niemeijer[1], Christopher J. Spiers[1]

Keywords: Meter-scale experiment, rock friction, fault heterogeneity

In order to simulate rupture and sliding of induced seismic events or natural earthquakes, it is necessary to describe the constitutive law of fault strength evolution as a function of slip or velocity. However, the existing laws (such as rate and state friction and slip weakening models) are based on the results of experiments on samples with a fault length limited to a few centimetres, while an earthquake rupture in nature occurred in a few hundred meters of fault area or more. This raises the question of whether the friction law derived from the small-scale experiments can be directly applied to such a large fault area, or whether larger scale heterogeneities affect the frictional strength and the constitutive parameters. In order to validate this, fault friction must be tested at least at the mesh scale of finite element models, i.e. at the scale of at least 0.5 to 2 meters.

In 2018, a series of experiments has been conducted using the large-scale friction apparatus driven by a shaking table at NIED, Tsukuba, Japan to explore the possibility of scale-dependent frictional properties of simulated fault gouges. We completed a total of 34 experiments with 3 different gouge lengths (0.5m, 1m, 1.5m), 5 different gouge thicknesses and 5 different normal pressures. Most experiments were done with dry gouge derived from Slochteren sandstone. Preliminary results show that 1) the

[1] HPT Laboratory, Department of Earth Science, Utrecht University. Y.Ji@uu.nl, D.H.Baden@uu.nl, l.b.hunfeld@uu.nlR, P.J.Pijnenburg@uu.nl, A.R.Niemeijer@uu.nl, C.J.Spiers@uu.nl

coefficient of friction of dry sandstone gouge is about 0.65~0.7; and the frictional behavior is velocity weakening. 2) Heterogeneities were observed in the initial contact area and normal stress distribution, as well as in the evolution of stress distribution and distribution of dilation and slip both before and during sliding. However, 3) the rate and state friction properties of large, gouge filled, planar fault are comparable to those derived from cm scale samples. In other words, size does not seem to matter too much for the constitutive friction law up to 1-2 m, the minimum FEM mesh scale in the models of induced seismicity.

GeoProc2019: Earthquake and Faulting mechanics

7th International Conference on Coupled THMC Processes in Geosystems
3-5 July 2019 Utrecht (Netherlands)

Discrete element modeling of a subduction zone with a seafloor irregularity and its impact on the seismic cycle

L. Jiao[1], *C. Chan*[2], *L. Scholtès*[3], *F. V. Donzé*[4], *A. Hubert-Ferrari*[5], *P. Tapponnier*[6],

Keywords: seafloor irregularity, seamount, megathrust and splay fault rupture, DEM modeling, super cycle.

Seafloor irregularities influence rupture behavior along the subducting slab and in the overriding plate, thus affecting earthquake cycles. Whether seafloor irregularities increase the likelihood of large earthquakes in a subduction zone remains contested, partially due to a narrow focus either on fault development or on rupture pattern. Here, we simulate a subducting slab with a seafloor irregularity and the resulting deformation pattern of the overriding plate using the discrete element method. Our models illustrate the rupture along three major fault systems: megathrust, splay and backtrust faults (Fig. 1). Our results show different rupture dimensions of earthquake events varying from tens to ca. 140 km. Our results suggest that the recurrence interval of big events with rupture length of 100 km is ca. 140 years and that the length of the rupture could reach ca. 100 km, which is overall comparable to the paleoseismic records. We further propose the coseismic slip amounts decrease and interseismic slip amounts increase from the surface downwards gradually. We conclude that the presence of seafloor irregularities significantly affects rupture events along the slab and fault patterns in the overriding plate. Thus, our models

[1] Earth Observatory of Singapore/Asian School of the Environment, Nanyang Technological University, Singapore, jiao0019@e.ntu.edu.sg
[2] Earth Observatory of Singapore/Asian School of the Environment, Nanyang Technological University, Singapore, hantijun@googlemail.com
[3] Université de Lorraine, Lab. GeoRessources, Nancy, France, luc.scholtes@univ-lorraine.fr
[4] Université Grenoble Alpes, Institut des Sciences de la Terre, Grenoble, France, frederic.donze@3sr-grenoble.fr
[5] Université de Liège, Département de Géographie, Liège, Belgium, aurelia.ferrari@uliege.be
[6]The Institute of Crustal Dynamics, China Earthquake Administration, Beijing, China, tappon@ntu.edu.sg

could contribute to seismic and tsunami hazard assessments in subduction zone systems.

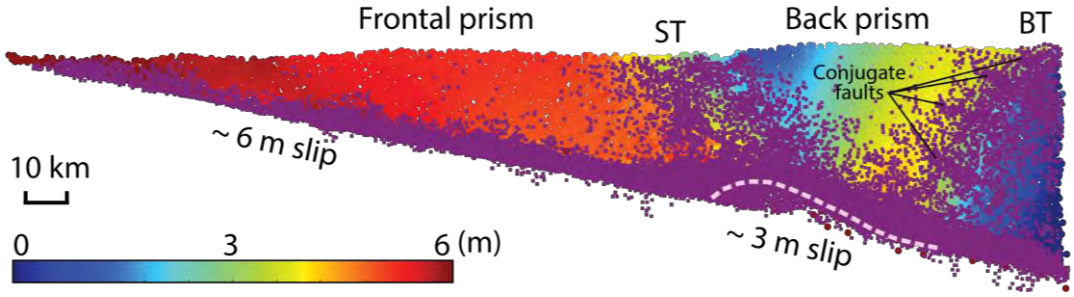

Figure 1. Displacement values of the overriding plate after 400 years (the seamount is represented as a pink dash line): Cracks (purple dots) align along megathrust faults, splay thrust fault (ST), and back thrust fault (BT), respectively. The color fields reveal that the displacement distribution is conspicuously separated by the splay fault, which originates from the landward flank of the seamount.

GeoProc2019: Earthquake and Faulting mechanics

7th International Conference on Coupled THMC Processes in Geosystems
3-5 July 2019 Utrecht (Netherlands)

Fault Stabilization by Dilatant Hardening in Granular Rocks

T. Kanaya[1], *W. Zhu*[2]

Keywords: Fluid-Rock Interaction, Effective Pressure, Slow Earthquakes

Dilatant hardening is thought to be an important coupled hydro-mechano process for governing fault stability. Along a propagating fault, if dilatancy occurs faster than fluid diffusion into newly created pore spaces (e.g., microcracks), the pore pressure decreases, resulting in an increase in the effective pressure that impedes further fault slip. However, laboratory studies of the roles of dilatant hardening on fault stability remain scarce [Martin, 1980; French and Zhu, 2017].

Our recent experiments on quartz sandstones show that fault stability depends on the drainage condition of bulk samples. Under a constant differential pressure (i.e., confining pressure minus pore pressure) of 70 MPa, samples with a lower bulk diffusivity exhibit more stable failure (Figure 1). Samples with an initial porosity of ~4% deformed at *P*c = 130 to 200 MPa show a diffusivity of 10^{-7} to 10^{-6} m^2/s (Figure 2), resulting in an undrained condition in which the time scale of pore pressure equilibration upon a pulse transient is greater than that of axial deformation; these samples fail over $>10^2$ seconds, with limited acoustic emission energy. In contrast, under the same differential pressure, samples with an initial porosity of ~6% deformed at *P*c = 80 to 130 MPa show a diffusivity of 10^{-6} to 10^{-5} m^2/s, in which a drained condition is indicated by equilibration times much shorter than deformation times; failure in these samples is instantaneous (<1 second) with significant acoustic emission energy. Our inference - that the former samples undergo undrained, dilatant hardening relative to the latter - is also supported by the observed higher peak strengths, negligible compressible deformation during axial loading (owing to the incompressible fluid), and time lags between changes in porosity (involving fluid diffusion) and volumetric strain.

Our study provides the first experimental support for the key assumption made in theoretical models of dilatant hardening - that fluid diffusion over the *entire* sample length (as opposed to the length scale of gouge layers or individual grains) governs the effective pressure and stability of the fault [Rudnicki and Chen, 1988; Segall and Rice, 1995]. However, we suggest that the macroscopic effective pressure is the

[1] University of Maryland, kanaya@umd.edu
[2] University of Maryland, wzhu@umd.edu

primary factor governing the diffusivity and thus dilatant hardening, in contrast to factors previously thought to be critical, e.g., pore pressure ratio or absolute pore pressure [Martin, 1980; Rudnicki and Chen, 1988; French and Zhu, 2017]. Our experiments demonstrate that the effective pressure law for the diffusivity of a deforming rock deviates significantly from that with a pore pressure coefficient of unity.

Our study has important implications for the mechanics of earthquake faulting. Experimental determination of relevant parameters (e.g., slip weakening rate, dilatancy rate, diffusivity) as done here is essential for testing theoretical models of dilatant hardening [Rudnicki and Chen, 1988]. Importantly, as a fundamental hydro-mechano mechanism, our study of dilatant hardening sheds light on a range of thermo-hydro-mechano-chemo processes, e.g., dynamic weakening via hydrothermal pressurization, slow earthquakes, dehydration embrittlement involving volume-changing reactions. Furthermore, laboratory quantification of dilatant hardening is required to constrain whether induced seismicity is distinct from tectonic seismicity, and to interpret geophysical observations, e.g., using microseismicity to infer the seismic-aseismic transition depth [Rolandone et al., 2004] and interseismic geodetic transients triggering earthquakes [Khoshmnesh & Shirzaei, 2018], in the context of evolving effective pressure during faulting.

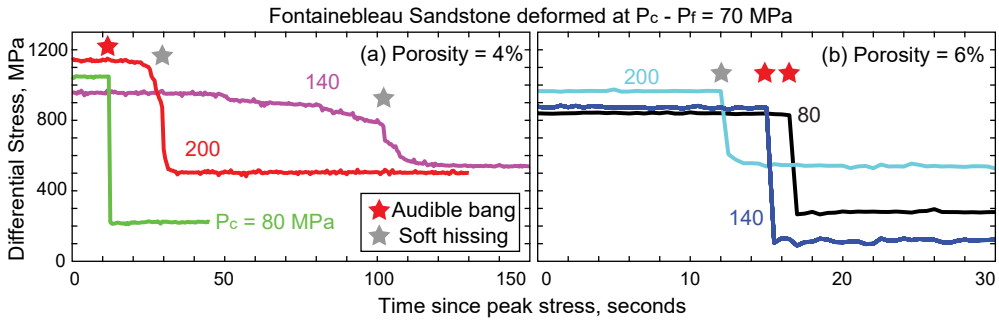

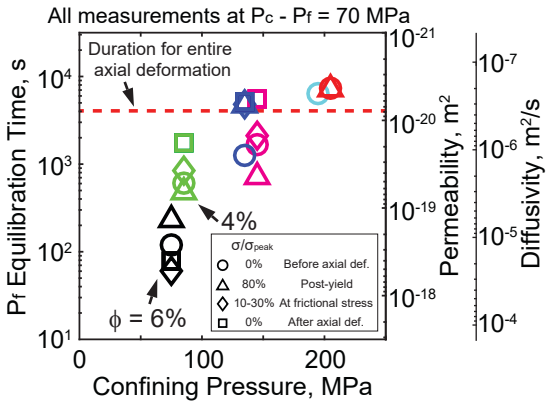

Figure 1 (above). Differential stress versus time for samples deformed at a constant differential pressure of 70 MPa and the confining pressures indicated. Initial porosity of (a) 4% and (b) 6%.

Figure 2 (left). Pore pressure equilibration time upon a pulse transient as a function of confining pressure and differential stress normalized by peak stress, all at a constant differential pressure of 70 MPa. Permeability and fluid diffusivity calculated from the equilibration time are shown by y-axes on the right.

References

French, M. E., and W. Zhu (2017), *Earth Planet. Sci. Lett.*, *473*, 131–140.

Khoshmanesh, M., and M. Shirzaei (2018), *Nat. Geosci.*, *11*(8), 610–614.

Martin, R. J. (2018), *Geophys. Res. Lett.*, *7*(5), 404–406.

Rolandone, F., R. Bürgmann, and R. M. Nadeau (2004), *Geophys. Res. Lett.*, *31*(23).

Rudnicki, J. W., and C.-H. Chen (2018), *J. Geophys. Res. Solid Earth*, *93*(B5), 4745–4757.

Segall, P., and J. R. Rice (1995), *100*(B11), 22155–22171.

GeoProc2019: Earthquake and Faulting mechanics

7th International Conference on Coupled THMC Processes in Geosystems
3-5 July 2019 Utrecht (Netherlands)

Dynamic rupture simulations of the 2016 Kaikoura (New Zealand) Earthquake

Y. Kaneko[1], R. Ando[2], J. Kearse[3]

Keywords: Earthquake Dynamics, Kaikoura Earthquake, Dynamic Rupture Simulations, Complex Fault Geometry, Fault Striation

The 2016 Kaikoura (New Zealand) earthquake is characterized as one of the most complex, multi-fault rupture events ever observed. Here we perform dynamic rupture simulations to address two fundamental questions: (1) to what extent relatively simple forward models accounting for realistic fault geometry can explain the characteristics of the complex multifault rupture and (2) what caused curved fault striations systematically reported along the Kekerengu fault that produced up to 12 m of fault displacement. Without fine parameter tuning, our forward model reproduces many observed features including the multi-fault rupture, overall slip distribution as well as the locations of the maximum slip and rupture arrest. In particular, our model shows spontaneous arrest of dynamic rupture at the both ends of the ruptured fault system due to smaller pre-stress levels expected from a regional tectonic stress field. This modeling results illuminate the importance of the 3D fault geometry in understanding the dynamics of complex, multi-fault rupture. Using another dynamic rupture simulation, we are able to reproduce the observed, curved morphology of near-surface striae on the Kekerengu Fault with remarkable accuracy. Our dynamic model with purely horizontal pre-stress reveals that vertical stress changes induced by fault slip within the so-called cohesive zone result in vertical slip and temporal changes in fault slip direction. The degree of changes in fault slip direction is enhanced at shallow depths (<3 km) where there is low confining stress, and is amplified by a free surface effect. The models show that the geometry and sense of striae curvature is sensitive to the direction of rupture propagation. To match the geometry of the striations observed on the Kekerengu fault, our simulations require the rupture propagating from the south-west to north-east, which is in agreement with the rupture propagation direction of the Kaikoura earthquake. Our study highlights the potential for fault striations to record aspects of earthquake rupture dynamics, including the rupture direction of paleo earthquakes.

[1] GNS Science, y.kaneko@gns.cri.nz
[2] University of Tokyo, ando@eps.s.u-tokyo.ac.jp
[3] GNS Science, jesse@kearse.co.nz

GeoProc2019: Earthquake and Faulting mechanics

7th International Conference on Coupled THMC Processes in Geosystems
3-5 July 2019 Utrecht (Netherlands)

Time-dependent analyses of first motion derived focal mechanism solutions and machine learning algoritms in rock deformation laboratory experiments

T. King[1], S. Vinciguerra[1], P. Benson[2], L. De Siena[3]

Keywords: Acoustic Emissions (AE), Triaxial deformation tests, time-dependent deformation, focal mechanism solutions, failure mode forecasting

Acoustic Emissions (AE), the laboratory analogue to tectonic seismic events, recorded during conventional triaxial deformation tests allow for an unprecedented amount of information on the evolution of fractured media within a controlled environment. This study presents the results of a new, robust, derivation of first motions calculated from AE-derived focal mechanism solutions (FMS) to analyse the induced deformation of samples of Westerly Granite, Stromboli Basalt and Darley Dale Sandstone. For each AE 12 traces were recorded. For the event location, arrival times and the polarity of the first motion were automatically picked using a combined Signal Duration and Root Mean Square (RMS) Envelope procedure. AE were organised into localised groups by minimising the RMS error between polarity signatures of each AE and these were then fitted to idealised FMS models of mode 2 shear, mode 1 shear, mixed-mode, isotropic and CLVD. Selection was dependent on the RMS error of normalised amplitudes between observed and modelled data. Results highlight time-dependent trends in the dominance of compressive, tensile and shearing events that correlate with specific deformation sequences (i.e. dynamic failure) of the samples (Figure 1).

To complement the analysis machine learning algorithms (bootstrapped forest walks) are trained on these results to identify frequency dependent variations between the different mechanisms and improve confidence. Results for the basalt identify a shearing dominance with a strong dependence on a pre-existing fracture network for the eventual distribution, and mechanisms, of the developing failure plane. The granite, which lacks initial microfractures, has a largely isotropic distribution of tensile damage which is then dependent on the clustering of deformation-induced damage. Whilst the sandstone indicates a stronger dominance of compressive events associated with pore collapse. These data provides new insight into the potential forecasting of deformation and failure mode for different lithologies at the laboratory scale and provide support to the search of links between seismic signals and field scale fracturing processes.

[1]Department of Earth Sciences, University of Turin, Turin, Italy, sergiocarmelo.vinciguerra@unito.it
[2] School of Earth and Environmental Sciences, University of Portsmouth, UK, philip.benson@port.ac.uk
[3] Geology and Petroleum Geology, University of Aberdeen, UK, lucadesiena@abdn.ac.uk

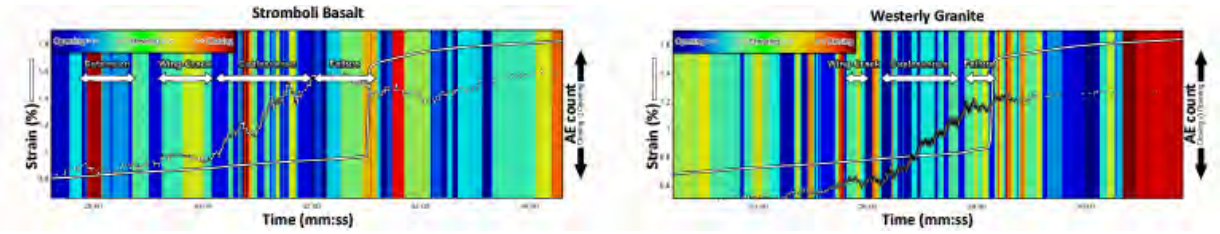

Figure 1. Focal mechanism solutions in the lead up dynamic failure for the Strmboli basalt (Vinciguerra et al., 2005) and Westerly granite (Wong et al., 1982). Both rock types follow a similar series of events of fracture extension, wing crack development (or pore-emanant failure which has a comparable mechanism (Zhu et al., 2016)), shear coalescence and dynamic failure. However, the length of time for each sequence differs significantly. The wing-crack phase takes several minutes in the basalt, whilst it is over within 30 seconds for the granite. Shear zone coalescence also follows a different character for both rocks, where the granite has a significant tensile shear phase that makes up 90% of the data. Many of the differences between the two samples can be readily associated to a pre-existing crack damage network within the basalt which accomodates the majority of the applied strain. The granite which lacks initial crack damage, instead demonstrates rapid and destructive damage propagation as the sample approaches failure.

References

Vavrycuk, V. (2014), Iterative joint inversion for stress and fault orientations from focal mechanisms, *Geophysical Journal International*, 199 (1), 69-77.

Vinciguerra S., Trovato C., Meredith P.G., Benson P.M., (2005) Relating seismic velocities, thermal cracking and permeability in Mt.Etna and Iceland basalts, *International Journal of Rock Mechanics*, 42/7-8, 900-910, doi: 10.1016/j.ijrmms.2005.05.022

Wong, T., (1982) Shear fracture energy of Westerly granite from post-failure behavior. *Journal of Geophysical Research: Solid Earth*, 87 (B2)

Zhu W., Baud P., Vinciguerra S., Wong T.-f., (2016) Micromechanics of brittle faulting and cataclastic flow in Mount Etna basalt, *J. Geophys. Res. Solid Earth*, 121, doi:10.1002/2016JB012826.

GeoProc2019: Earthquake and Faulting mechanics

7th International Conference on Coupled THMC Processes in Geosystems
3-5 July 2019 Utrecht (Netherlands)

Mechanical property of granite under supercritical fluid conditions

M. Kitamura[1], *M. Takahashi*[2]

Keywords: Geothermal energy, granite, supercritical fluid, induced earthquake

To extract geothermal energy effectively and safely from magma and/or adjacent hot rock, we need to tackle many issues which require new technology development. One of them we are targeting on is to develop a technology to mitigate induced-earthquakes. It is required to understand roles of factors on occurrences of the induced-earthquake (e.g., strength, crack density, and fluid-rock reaction) and their intercorrelations (e.g., Asanuma et al., 2012).

Our purpose of this series of experiments is to clarify a relationship between the rock strength and the fracture density under hydrothermally supercritical conditions. We conducted triaxial deformation test on intact granite rock strength under high-temperature (250 – 750°C), high-pressure (104 MPa) condition at a constant load velocity (0.1 μm/sec) using a gas-rig at GSJ, AIST. We used Oshima granite, which has initially ~0.55% of the porosity, 4.95±1.01 km/s in Vp at dry condition (dry). All experimental products showed brittle feature having several oblique fracture surfaces, but both value of peak stress and amount of stress drop became smaller at higher temperature. Additionally, Young's modulus decreases with increasing the temperature from 57.4 GPa at 250°C to 32.3 GPa at 750°C. At 400°C, the stress drop accelerated the deformation with ~98 times faster velocity than that at load-point. In contrast, at 650°C and 750°C, the velocity during stress drop kept the same order of the load-point velocity. Therefore, the deformation feature may start to be of ductile when the temperature exceeds 650°C. The microstructures of samples deformed at 400°C and 550°C showed the shear zone with the grain reduction. In contrast, for the samples deformed at 650°C and 750°C, we partly observed the sintered structure at grain boundaries among feldspar gouge. The sintered structure at >650°C might be the cause of the slow stress drop.

[1] Geological Survey of Japan, National Institute of Advanced Industrial Science and Technology (AIST), 1-1-1 Higashi, Tsukuba 305-8567, Japan, kitamura.m@aist.go.jp
[2] Geological Survey of Japan, National Institute of Advanced Industrial Science and Technology (AIST), 1-1-1 Higashi, Tsukuba 305-8567, Japan, miki.takahashi@aist.go.jp

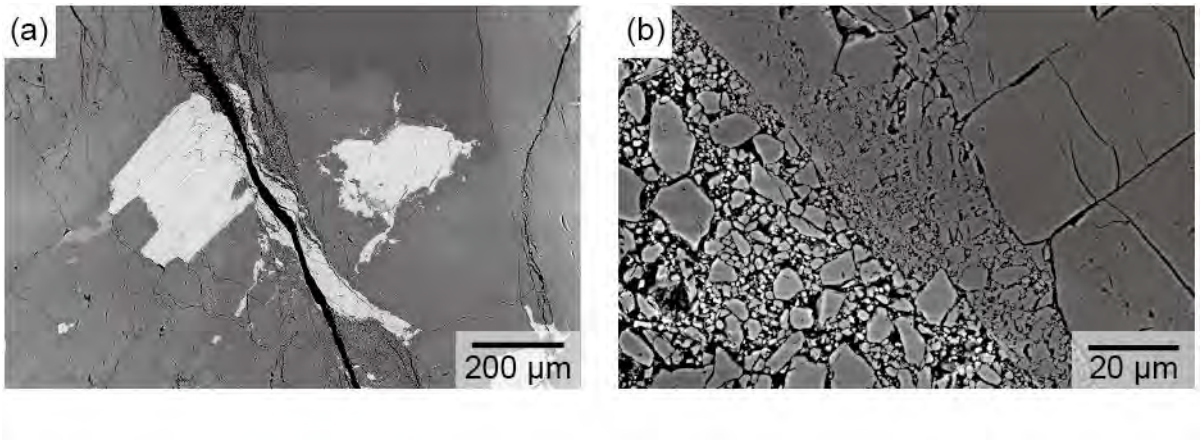

Figure 1. Fracture surfaces after experiments. (a) 550ºC, (b) 650ºC.

References

Asanuma, H., Muraoka, H., Tsuchiya, N., and H. Ito (2012), The concept of the Japan Beyond-Brittle Project (JBBP) to Develop EGS Reservoirs in Ductile Zones, *GRC Transactions*, 36, 359 – 364.

GeoProc2019: Earthquake and Faulting mechanics

7th International Conference on Coupled THMC Processes in Geosystems
3-5 July 2019 Utrecht (Netherlands)

On the seismo-hydromechanical response of a shear zone during hydraulic stimulation

H. Krietsch[1], L. Villiger[2], J. Doetsch[3], V.Gischig[4], M.R. Jalali[5] & F. Amann[6]

Keywords: Hydraulic stimulation experiment, Pressure front propagation, Heterogeneous shear zone reactivation

In spring 2017, six decameter-scale hydraulic shearing experiments were carried out in the framework of the In-situ Stimulation and Circulation (ISC) project at the Grimsel Test Site, Switzerland (Amann et al., 2018). The experiments were conducted with an overburden of approximately 480 m. The maximum principal stress within the test volume is dipping 40° towards East with a magnitude of ~13 MPa. In this contribution, we present the complex seismo-hydromechanical (SHM) response of a shear zone, observed during one of these shearing experiments. A total of 1211 liters of water was injected from a one-meter long borehole interval into the EW-striking, sub-vertical brittle-ductile target shear zone. The fluid volume was distributed over four partly flow and partly pressure controlled injection cycles (Figure 1).

To monitor the SHM responses, ten boreholes were drilled, characterized and completed. Three of them were dedicated to pressure monitoring in seven intervals, from which two intervals covered the target shear zone. The intervals are labeled with the borehole name and an index counted from borehole bottom to top. In three further boreholes, a total of sixty longitudinal Fiber-Bragg Grating strain sensors were installed. These sensors have a base length of one meter and were installed across intact rock, fractures or shear zones. A total of 26 uncalibrated acoustic emission sensors were installed along the tunnel walls and within four boreholes. Five of those sensors at tunnel walls were collocated with accelerometers for calibration purposes.

The recorded seismic cloud reveals a propagation of the seismic activity towards the lower East along the target shear zone with ongoing stimulation. Based on the hydraulic monitoring data, the propagation of pressure fronts within the target shear zone was identified (Figure 1b). Their peak pressures reached ~70 % of the injection pressure. Two different propagation directions of the pressure fronts were observed that occurred at subsequent stages. The earlier direction (i.e., towards the monitoring interval PRP2-2) was sub-normal to this orientation and appeared to be mostly

[1] Department of Earth Sciences, ETH Zurich, Switzerland, hannes.krietsch@erdw.ethz.ch
[2] Swiss Seismological Service, ETH Zurich, Switzerland, linus.villiger@sed.ethz.ch
[3] Department of Earth Sciences, ETH Zurich, Switzerland, joseph.doetsch@erdw.ethz.com
[4] CSD Engineers, Bern, Switzerland, gischig@erdw.ethz.ch
[5] Engineering Geology, RWTH Aachen, Germany, jalali@lih.rwth-aachen.de
[6] Engineering Geology, RWTH Aachen, Germany, amann@lih.rwth-aachen.de

aseismic. The subsequently dominant direction (i.e., towards the pressure monitoring interval PRP1-2) coincided with the stimulation direction, as indicated by the seismicity. Thus, the later pressure front seems to correlate with more seismic deformation. The captured mechanical responses indicate extensional signals and stress transfer induced compressions (Figure 1c). These measurements indicate a combination of shear and normal opening.

Calculation of the slip tendency and opening pressure of the target shear zone at the different monitoring locations indicates local variations in the likelihoods for local shear and normal opening dominated deformation during the stimulation. Thus, a combination of shear and normal is not only measured, but also predicted from the stress state.

Our observations illustrate the heterogeneity of seismo-hydromechanical shear zone response during hydraulic stimulation experiments at the decameter scale.

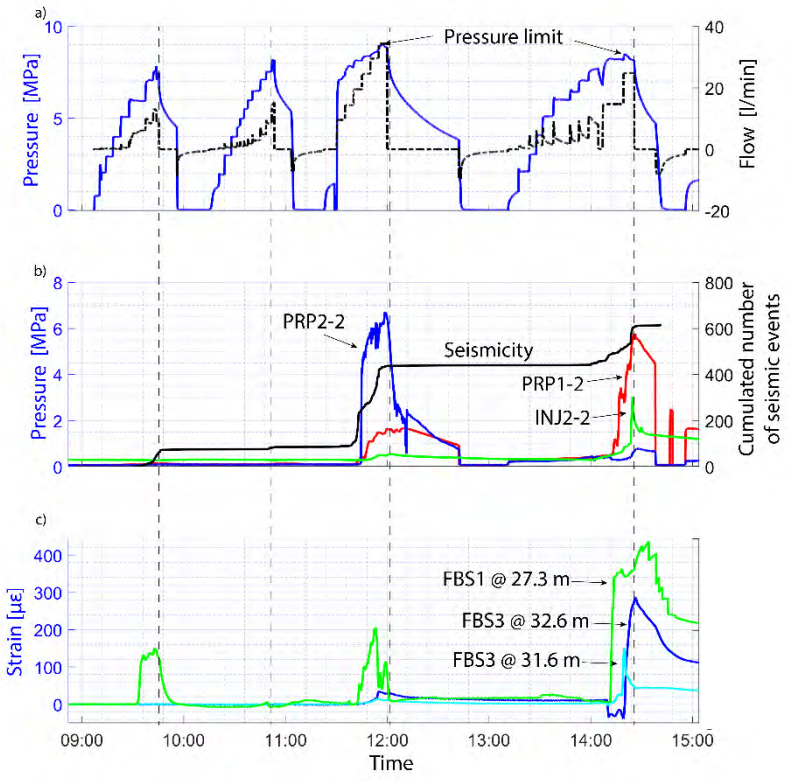

Figure 1. Seismo-hydromechanical observations: a) Injection protocol, b) Pressure monitoring data and cumulated seismicity, and c) Strain data

References

Amann, F., *et al.*, (2018), The seismo-hydromechanical behavior during deep geothermal reservoir stimulations: open questions tackled in a decameter-scale in situ stimulation experiment, *Solid Earth*, *9*(1), 115-137, doi:10.5194/se-9-115-2018.

GeoProc2019: Earthquake and Faulting mechanics

7th International Conference on Coupled THMC Processes in Geosystems
3-5 July 2019 Utrecht (Netherlands)

A-seismic fracture growth driven by fluid injection and remote nucleation of dynamic rupture in a weaker part of the fault

B. Lecampion[1], *A. Mori*[1], *F. Ciardo*[1]

Keywords: fluid induced seismicity, modeling, hydro-mechanical couplings

We investigate the propagation of a shear fracture driven by a continuous fluid injection at constant over-pressure in a pre-existing fault. We focus on the case of injection in a zone of constant friction leading to a-seismic growth and study how such a-seismic growth can trigger a dynamic rupture on a remotely located weaker (and/or frictionally weakening) part of the fault via stress transfer.

In the case of constant fault permeability, such a fluid-driven, a-seismic fracture propagates paced by fluid diffusion in a self-similar manner, i.e. thus proportional to square root of time. However, depending on the initial stress conditions and magnitude of over-pressure, two end-regimes can be encountered. In the limit of a critically stressed fault, the a-seismic crack propagates significantly ahead of the pore pressure perturbation front (up to 100 times) whereas on the contrary in the limit of marginally pressurized fault, the pore pressure perturbation is way ahead of the fracture tip (see Fig. 1). It is interesting to point out that the micro-seismicity that would be observed in conjunction with such an a-seismic growth, cannot be reliably used to invert for fault diffusivity without knowledge of both in-situ stress conditions and fault frictional properties. After benchmarking our numerical model with an analytical solution for that case (Fig. 1), we investigate the case of a weaker (and/or frictionally unstable) part of the fault located away from the injection point. We determine when (and at what distance from the injection point) such a weaker part gets activated (producing a secondary / “daughter” fracture), and how a dynamic rupture nucleates from this daughter fracture. The limit of a critically stressed fault is particularly interesting as we show that a dynamic rupture can nucleate significantly away from the pore-pressure disturbance due to the stress perturbation associated with the a-seismic growth of the mother fracture surrounding the injection location. We also investigate how a-seismic growth continues after shut-in of the injection and how it modifies the observed remote nucleation of a dynamic rupture in the critically stressed case.

[1] Geo-Energy Lab - EPFL, brice.lecampion@epfl.ch

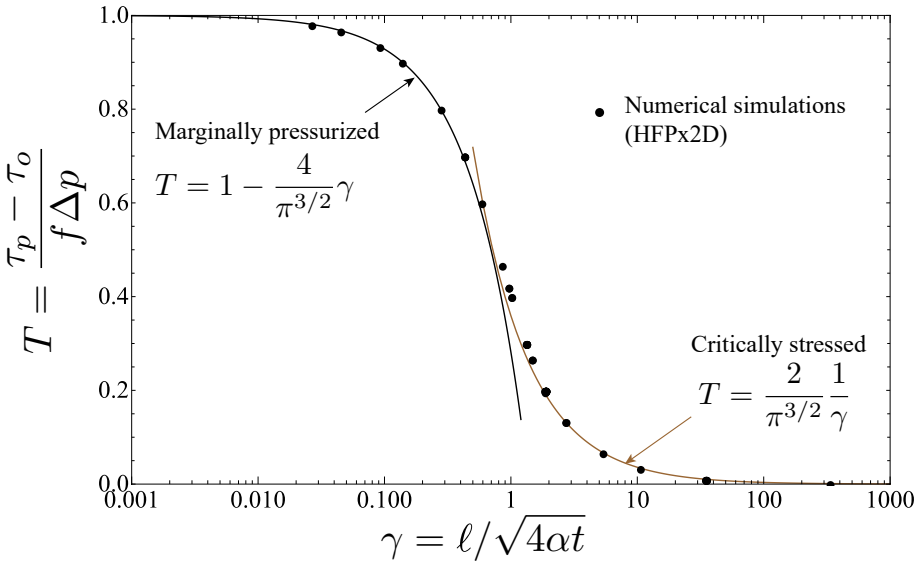

Fig. 1 Evolution of dimensionless a-seismic fracture length γ as function of stress criticality T. The aseismic fracture length scales as $L=\gamma\ (4\ \alpha\ t)^{1/2}$, with α the fault diffusivity. Numerical results displayed as dots, analytical asymptotes for the marginally pressurized and critically stressed cases as continuous lines (asymptotes obtained by R. Viesca – personal communication).

References

D. I. Garagash and L. N. Germanovich. Nucleation and arrest of dynamic slip on a pressurized fault. *Journal of Geophysical Research: Solid Earth (1978–2012)*, 117(B10), 2012.

R. Viesca (2018). Constant friction fluid induced shear crack. *Personal Communication*.

Ciardo F. and Lecampion B. (2019), Effect of dilatancy on the transition from aseismic to seismic slip due to fluid injection in a fault, Under revision *J. Geophys. Res. Solid Earth*.

GeoProc2019: Earthquake and Faulting mechanics

7th International Conference on Coupled THMC Processes in Geosystems
3-5 July 2019 Utrecht (Netherlands)

Frictional properties of simulated fault gouges prepared from the Groningen Carboniferous: Effects of any coal present

J. Liu[1,2], L.B. Hunfeld[2], A.R. Niemeijer[2], C.J. Spiers[2]

Keywords: slip-weakening, rate-dependent, direct shear, healing effects

Induced seismicity in the Groningen gas field upon gas production is believed to be in relation to (re)activation of pre-existing faults in the reservoir and immediate under- and overburden formations. Data on the frictional properties of the constituent fault rocks is required, in attempt to better understand induced seismicity in the Groningen gas field and to better model the response of faults present in the field to changes in stress-state upon gas depletion. Recently, geophone data reported by Spetzler and Dost (2017) shows ~5% of earthquake events in the Groningen gas field occurred in the Carboniferous formation, which cannot be explained by the frictional properties of the Carboniferous shale (Hunfeld et al. 2017). One of the hypotheses for these events may be any presence of coal that also exists in the Carboniferous formation of the Groningen gas field. However, this remains unclear, as no available data on frictional properties of coal or Carboniferous shale with any presence of coal under reservoir conditions can be found in the literature.

Here, we document 21 dynamic friction experiments performed on simulated fault gouges prepared from the mixtures of coal and the Carboniferous shale, with the aim of investigating the effects of any coal present (0-100% in volume fraction) on the frictional properties of the Carboniferous shale substrate material collected from the Groningen gas field. The coal samples used in this study are bituminous coal collected from the Upper Silesian Basin in Poland, which is of similar age (Upper Carboniferous) and broad origin to the Groningen gas field source rocks. We performed velocity stepping, constant velocity, slide-hold-slide (SHS), load-unload-load (LUL) friction experiments, under near in-situ conditions of 100℃ and 40 MPa effective normal stress, employing sliding velocities of 0.1-100 μm/s. The experiments demonstrated that the presence of coal in volume fractions ≥ 50% caused strong slip-weakening behaviour of the Carboniferous shale, and significantly lowered frictional strength from ~0.47 to ~0.3, regardless of the experimental conditions employed (see Fig.1). This slip-

[1] Guangdong Provincial Key Lab of Geodynamics and Geohazards, School of Earth Sciences and Engineering, Sun Yat-Sen University, China, liujinf5@mail.sysu.edu.cn
[2] Department of Earth Sciences, Utrecht University, The Netherlands

weakening behaviour likely reflects strain localization in coal-rich shear bands, perhaps accompanied by a change in the coal molecular structure. However, reloading experiments (LUL) show that slip-weakening is limited to small initial displacements (2-3 mm), and does not occur during reactivation. From a rate and state friction point of view, almost all experiments exhibited stable, velocity strengthening behaviour of the carboniferous shale at in-situ stress, pore water pressure (15 MPa) and temperature conditions, regardless of coal content. By contrast, under dry and gas saturated (CH_4, Argon) conditions, and when saturated with water at 1 atm, 50:50 shale-coal mixtures show unstable, velocity-weakening, and even stick-slip behaviour. On the basis of our results, we conclude that reactivated fault rock material derived from the Groningen Carboniferous shale formation will behave stably at in-situ conditions even when coal-bearing, though the mechanisms controlling frictional behaviour remain unclear. At the same time, possible effects of macroscopic compositional heterogeneity on fault stability, such as coal smearing, cannot be completely eliminated.

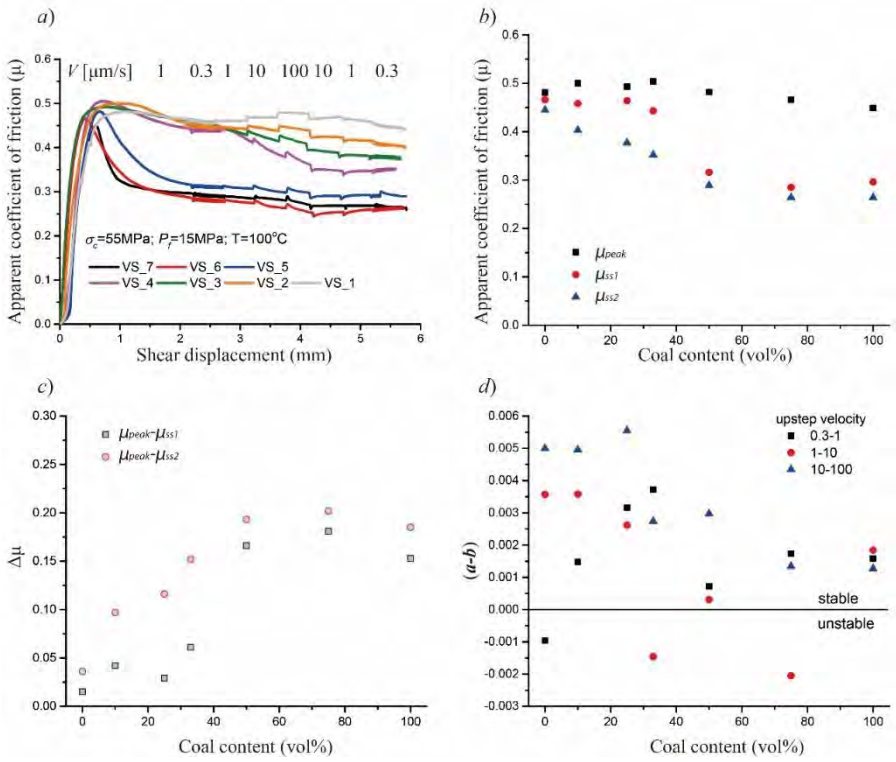

Figure 1. a) Apparent coefficient of friction (μ) against shear displacement. b) Apparent coefficient of friction (μ) against coal content. c) Difference between peak friction (μ) and steady-state friction as a function of coal content. d) (a-b) obtained from upstep velocity steps using a full RSF law upon coal content.

References

Hunfeld, L. B., Niemeijer, A. R., & Spiers, C. J., 2017. Frictional properties of simulated fault gouges from the seismogenic Groningen gas field under in situ P–T chemical conditions. Journal of Geophysical Research: Solid Earth, 122. https://doi.org/10.1002/2017JB014876

Spetzler, J., and B. Dost, 2017. Hypocenter Estimation of Induced Earthquakes in Groningen, Geophys. J. Int., 209(1), 453–465.

GeoProc2019: Earthquake and Faulting mechanics

7th International Conference on Coupled THMC Processes in Geosystems
3-5 July 2019 Utrecht (Netherlands)

Slow Slip on a High-Strength Velocity-Weakening Patch in a Subduction Fault Model

Yue Liu[1], *and Hongfeng Yang*[2]*

Abstract: Since the discovery of slow slip events (SSEs), they have been believed to hold significant implications in understanding fault slip modes and thus seismic hazard evaluations. Numerical simulations in the framework of rate- and state-dependent friction law and seismic evidences both suggest that SSEs often occur in the transition zone from velocity weakening to strengthening, with an extremely low effective normal stress that is caused by near-lithostatic pore pressure. However, we report here that SSE may also occur on a velocity-weakening (VW) patch with higher normal stress than the ambient fault. A two dimensional subducted fault model with a uniform background stress level is constructed, and a patch with elevated effective normal stress is preset in the VW zone. We investigate the conditions to generate SSES in the VW region, including the effects of the location and width of high normal stress zone and the amount of increasements in the effective normal stress. The results show that SSE can be observed in a variety of conditions, before a large earthquake and during the interseismic period. The values of the above three factors satisfied to generate SSEs are distributed in a wide range. Contrary to the traditional view, our results indicate that SSE may occur in a high-strength patch in seismogenic zone, which may change our original interpretation of SSEs in term of seismic hazard assessment.

Keywords: Slow slip events, High effective normal stress, Velocity-weakening region

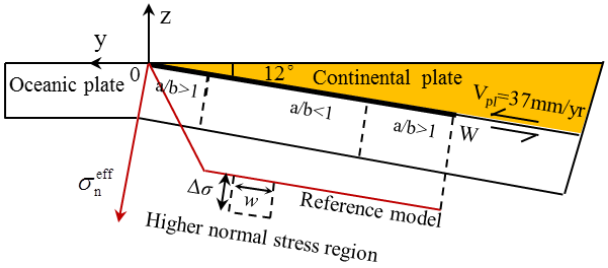

Figure 1. A two dimensional subduction model with a velocity weakening region (0<x<W). a and b are friction parameters. A uniform motion with convergence rate V_{pl} is imposed at W<x <+∞. σ_n^{eff} is the effective normal stress. *w* is the width of higher normal stress region, and Δσ is the perturbation relative to the background effective normal stress.

1Institute of Earthquake Forecasting, China Earthquake Administration, Beijing, China, liuyue126liuyue@126.com

2 Earth System Science Programme, Faculty of Science, The Chinese University of Hong Kong, Sha Tin, Hong Kong, China, hyang@cuhk.edu.hk. Corresponding author

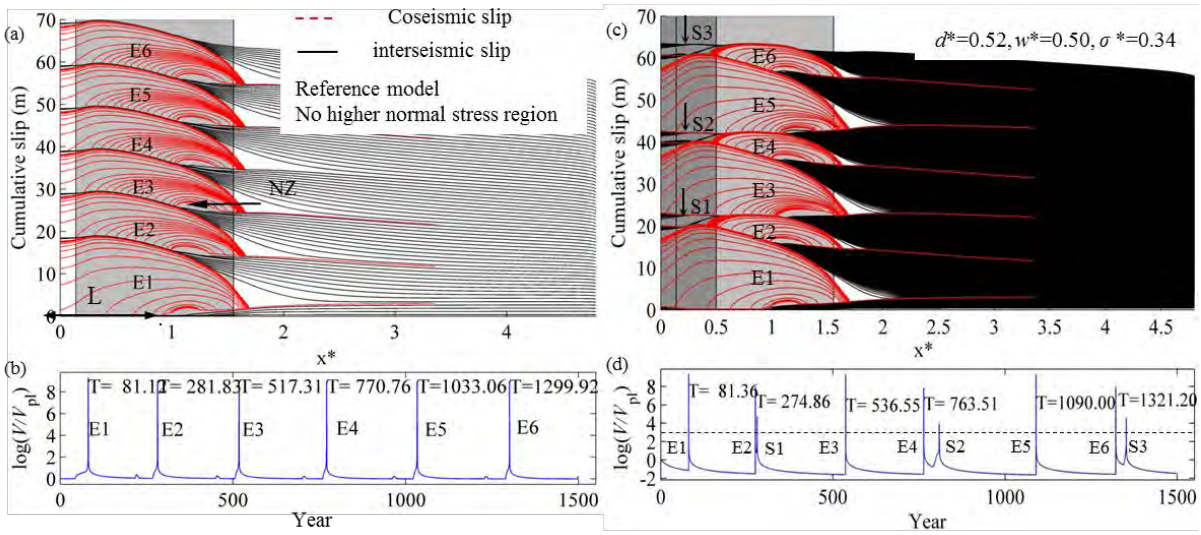

Figure 2. SSEs in VW region. Cumulative coseismic slip (red lines) for every 10 s and interseismic slip (black lines) for every 20 years (a) and 1 year (c) respectively. Light grey area shows VW zone. d^* is the normalized distance of trench to the lower edge of higher strength region. NZ: nucleation zone. L is the distance from the trench to the up-dip edge of the nucleation zone (L=50km). Dark vertical grey bar denotes the higher normal stress region of normalized width w^*=0.50. $\Delta\sigma=\sigma^*\cdot\sigma$ is perturbed on the background stress level of σ=50MPa. E1-E6 denote earthquakes, and S1-S3 are SSEs. (a) Reference model. (b) Maximum log(V/V_{pl}) of reference model during the simulated 1500 years (c) d^*=0.52 and w^*=0.50, SSEs in the VW region. (d) Maximum log(V/V_{pl}) of the high strength region of figure 2c.

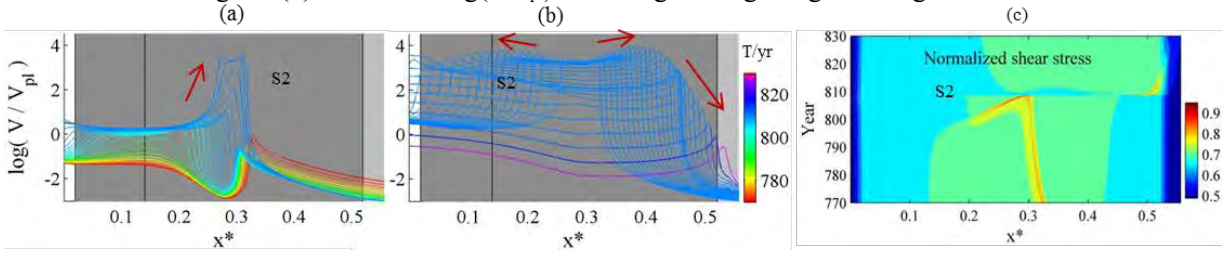

Figure 3. Snapshots of SSEs S2. log(V/Vpl) and normalized shear stress along x*=0~0.55 befor and after S2. Red arrows indicate the front propagation. The color indicates the years from 770 to 830. (a)-(b) Variations of slip rate are divided into two parts, and the results in figure (b) is followed that in figure (a). (c) Evolution of normalized shear stress from 770 yr to 830 yr.

References

Liu, Y., and J. R. Rice (2007), Spontaneous and triggered aseismic deformation transients in a subduction fault model, J. Geophys. Res., 112, B09404, doi:10.1029/2007JB004930.

Matsuzawa, T., H. Hirose, B. Shibazaki, and K. Obara (2010), Modeling short - and long - term slow slip events in the seismic cycles of large subduction earthquakes, *J. Geophys. Res*., 115, B12301, doi:10.1029/2010JB007566.

Obara, K., and A. Kato (2016), Connecting slow earthquakes to huge earthquakes. Science, 353(6296), 253-257, doi: 10.1126/science.aaf1512

Rubin, A. M. (2008), Episodic slow slip events and rate-and-state friction, *J. Geophys. Res*., 113, B11414, doi:10.1029/2008JB005642.

Saffer, Demian M., and Laura M. Wallace (2015), The frictional, hydrologic, metamorphic and thermal habitat of shallow slow earthquakes, *Nature Geoscience*,8(8), 594, doi: 10.1038/NGEO2490.

Yang, H., Y. Liu, and J. Lin (2012), Effects of subducted seamounts on megathrust earthquake nucleation and rupture propagation, *Geophys. Res. Lett*., 39, L24302, doi:10.1029/2012GL053892.

GeoProc2019: Earthquake and Faulting mechanics

7th International Conference on Coupled THMC Processes in Geosystems
3-5 July 2019 Utrecht (Netherlands)

Featuring temporal fault zone behavior and its evolution from crossing-fault vertical borehole seismic array

K.F. Ma[1,3], Y. Y. Lin[2], R. J. Hung[3]

Keywords: fault zone, borehole seismometers, temporal variation, anisotropy

Pervious studies from Taiwan Chelungpu-Fault Drilling Project borehole seismometers (TCDPBHS) observed occurrence of isotropic events below the primary slip zone, which were explained as events with explosive/implosive mechanism driven by the fluid within a complete stress drop regime capped by a low permeability primary slip zone. It suggests the significant role of fluid in the fault zone, and behaved as a natural hydroulic fracturing. TCDPBHS is a 7-level three-component vertical borehole seismic array installed in Hole-A of the Taiwan Chelungpu-Fault Drilling Project (TCDP) in July 2006. This array covers a depth range from 946 to 1274 m at intervals of 50–60 m, that crosses the main fault of the 1999 M_W 7.6 Chi-Chi earthquake at a depth of 1111 m. Through almost a decade of observation of TCDPBHS, significant and intriguing features had been discovered. We investigated the relationship between seismic moment M_0 and source duration t_W of microearthquakes recorded by TCDPBHS, and applied a waveform cross-correlation method to the three-component records and identified several event clusters with high waveform similarity, with event magnitudes ranging from 0.3 to 2.0. These events were mainly from decollment at the depths of about 10-15 km. To determine how M_0 scales with t_W for these event clusters, we remove path effects by using a path-averaged Q. The results indicate a nearly constant t_W for events within each cluster, regardless of M_0. This constant duration may arise either because all events in a cluster are hosted on the same isolated seismogenic patch, or because the events are driven by external factors of constant duration, such as fluid injections into the decollment. It may also be related to the earthquake nucleation size. However, although with constant t_W, we observed also some difference in frequency content for various M_0, suggesting dynamic rupture pattern rather than simple circular fault model might take place during slipping. This observation from TCDPBHS might give good comparison to other observations of LFE that observed similar feature as having similar duration but different magnitudes. Through yearly observation of TCDPBHS, we also reveal the fault zone with temporlal

[1] Earthquake- Disaster & Risk Evaluation and Management (E-DREaM) Center, National Central University, fong@ncu.edu.tw

[2] Seismological Labortary, California Instiute of Technology, yylinm22@gmail.com

[3] Department of Earth Sciences, National Central University, hungrj@gmail.com

variation in fast shear direction (FSD) as resulted in the observation from anisotropy. We observed an epitemic changes in FSD with rotation of 105-75 degree temporally, and with the stable anistropy within 8-10% with the disturbance from local or distant eartqhuakes with large dynamic stress change as observed in peak ground velocity. This observation gives the hint that the fault zone could be influenced by distant earthquakes, and thus, brought the possible remote conversation among fault zones in the world after a large earthquake although the fault zone would intend to come back to the background level in stress direction and anisotropy. Through the years observation from fault zone in-situ borehole seismometers, we could give a first hand close-in observation of fault zone behavior and its temporal evolution

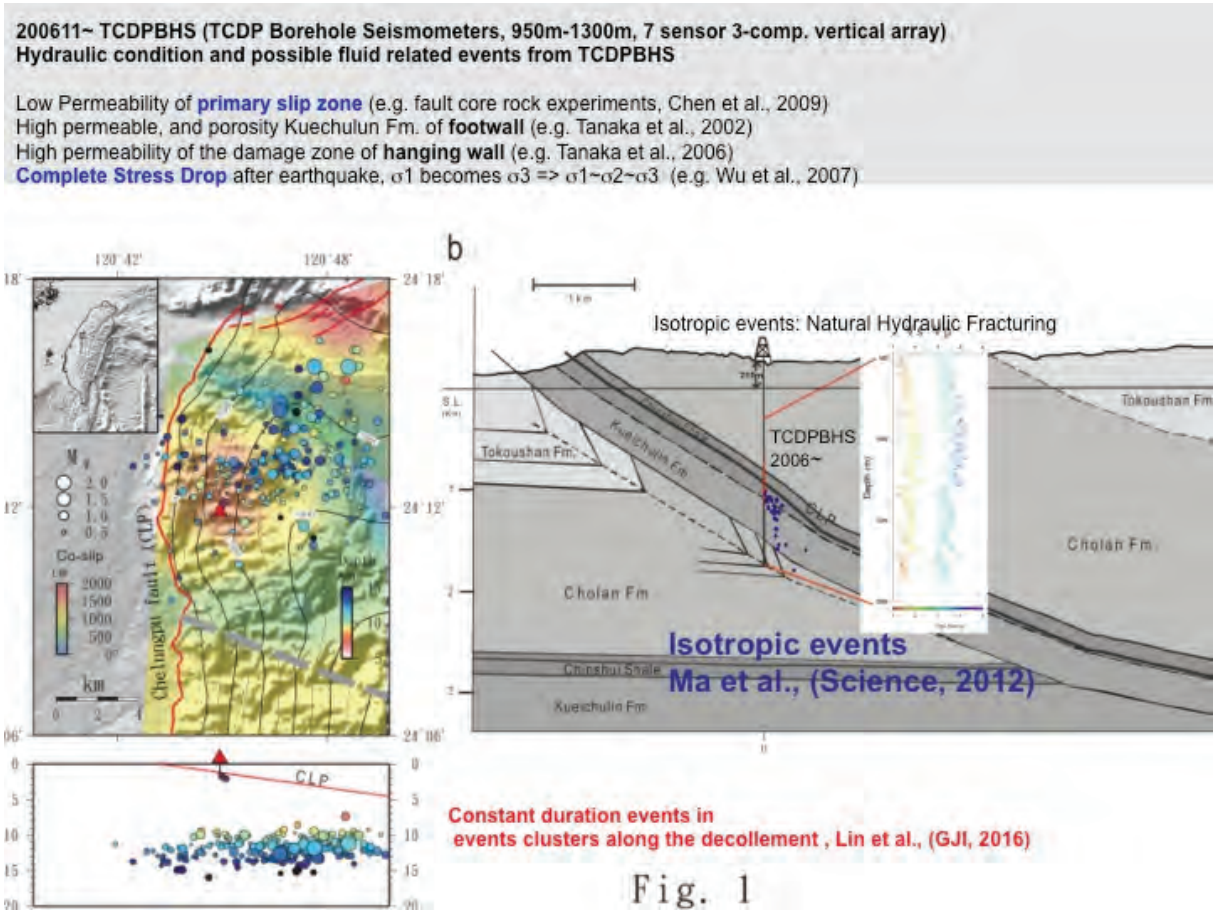

Fig. 1. Taiwan Chelungpu fault zone status after a large earthquake from previous studies, and the lay out of the TCDPBHS, the isotropic events, and the event clusters from decollment

GeoProc2019: Earthquake and Faulting mechanics

7th International Conference on Coupled THMC Processes in Geosystems
3-5 July 2019 Utrecht (Netherlands)

Chemo-Mechanical Processes of Cemented Volcanic Ashes

J. MacFarlane[1], T. Vanorio[2], A.C. Clark[3], G. Ledingham[4]

Keywords: Ash cementation, calcite precipitation, seal stability

The development and stability of seals play a critical role in the long-term containment of pressurized fluids and gases. Chemically altered ash beds are known to act as seals that can effectively arrest crack propagation in a range of environments, from hydrocarbon to hydrothermal reservoirs (Rodrigues et al., 2009; Vanorio & Kanitpanyacharoen, 2015). The diagenesis of volcanic ash in CaO-rich systems can result in hydrated calcium-alumino-silicate minerals forming seals of variable permeability and strength. Calcite precipitation can also occur through excess CaO-rich fluids or exposure to CO_2 both of which are products of decarbonation reactions in limestone and shale maturation. This study investigates how the permeability and mechanical properties (strength and brittleness) change through the factors that control the development of these seals in order to understand the long-term stability of the reservoirs they contain.

We carried out our investigations using laboratory cemented volcanic ash-CaO samples. Increased cementation through the ash-CaO reaction results in a decrease in permeability and increase in compressive strength. Once the ash is fully altered, the addition of CaO results in the precipitation of calcite, resulting in similar permeabilities to the fully cemented ash samples with lower compressive strengths (Figure 1). The precipitation of calcite was also induced through carbonation by exposure to high pressure CO_2 in an aqueous environment, which showed a decrease in permeability over time (Figure 2). The precipitation of calcite in similar cemented ashes through carbonation has been noted to increase the strength and mode of failure of the cement (Chang & Chen, 2005). The permeability of the CO_2 exposed cemented ash samples increased during rapid depressurization at low effective stresses, relevant to regions of extreme overpressure, due to cracking.

The changing relationship between permeability and strength over the life cycle of cemented ash beds is considered in the context of caprock stability. Assessing the controls of the mechanical properties of a sealing ash bed is important as it dictates whether strain energy due to reservoir overpressure will be released through slow-slip events or catastrophic brittle fracture. Our results show that while the permeability is lowered in all of the chemical processes, the changes in the mechanical properties

[1] Stanford Rock Physics Laboratory, Stanford, CA, jmacfarl@stanford.edu
[2] Stanford Rock Physics Laboratory, Stanford, CA, tvanorio@stanford.edu
[3] Stanford Rock Physics Laboratory, Stanford, CA, clarkac@stanford.edu
[4] Washington University in St. Louis, MO, greg.ledingham@wustl.edu

(strength and brittleness) are very different. These results highlight the importance of incorporating chemo-mechanical interactions in long-term seal stability modeling.

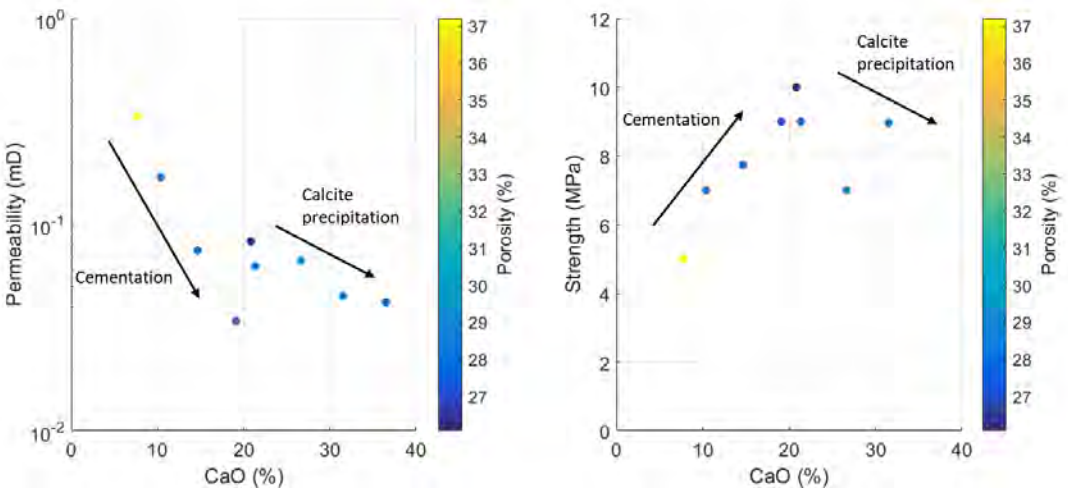

Figure 1. Permeability (left) and strength (differential stress at failure) (right) as a function of CaO content, color coded by porosity. Full cementation occurs at ~20% CaO content with calcite precipitation at higher CaO contents. Cementation affects both strength and permeability while calcite precipitation predominantly affects strength.

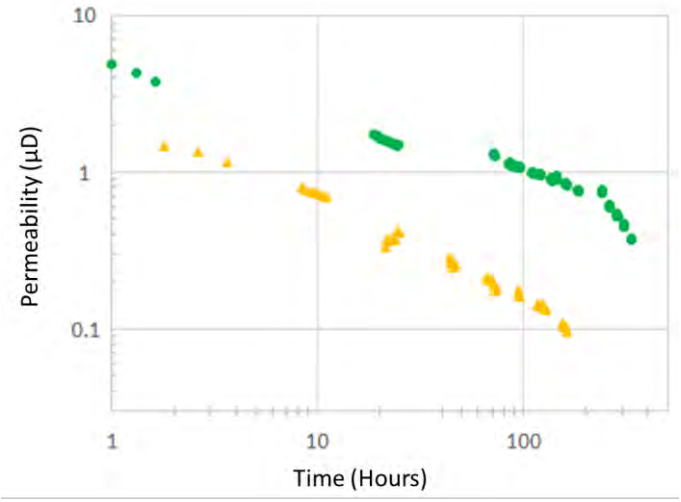

Figure 2. Permeability of cemented ash samples with exposure to CO_2. Samples represented by the yellow triangles and green circles have an initial water saturation of 68% and 49%, respectively.

References

Chang, C. F., & Chen, J. W. (2005). Strength and elastic modulus of carbonated concrete. *ACI Materials Journal*, *102*(5), 315–321. https://doi.org/10.14359/14710

Rodrigues, N., Cobbold, P. R., Loseth, H., & Ruffet, G. (2009). Widespread bedding-parallel veins of fibrous calcite ('beef') in a mature source rock (Vaca Muerta Fm, Neuquen Basin, Argentina): evidence for overpressure and horizontal compression. *Journal of the Geological Society*, *166*(4), 695–709. https://doi.org/10.1144/0016-76492008-111

Vanorio, T., & Kanitpanyacharoen, W. (2015). Rock physics of fibrous rocks akin to Roman concrete explains uplifts at Campi Flegrei Caldera. *Science*, *349*(6248), 617–621. https://doi.org/10.1126/science.aab1292

GeoProc2019: Earthquake and Faulting mechanics

7th International Conference on Coupled THMC Processes in Geosystems
3-5 July 2019 Utrecht (Netherlands)

Foreshocks occurrence and their links to nucleation during experimental earthquakes.

S. Marty[1], A. Schubnel[1], B. Gardonio[1], H. S. Bhat[1], J. Aubry[1], E. Fukuyama[2] and Raul Madariaga [1]

Keywords: experimental earthquakes, aseismic slip, nucleation, foreshock

Over the past decades, the increasing number of seismological observations and the improvement of data quality have allowed to better detect foreshock sequences prior to large earthquakes. However, due to strong spatial and temporal variations of foreshock occurrence, their underlying physical processes and their links to earthquake nucleation are still under debate. Here we address these issues by using precursory acoustic activity recorded during laboratory earthquakes (stick-slip instabilities) as a proxy to foreshock activity preceding natural earthquakes.

Laboratory earthquake experiments were performed in saw-cut Indian metagabbro under upper crustal stress conditions ranging from 30 to 90 MPa confining pressure. Using a high-frequency monitoring system and calibrated piezoelectric acoustic sensors we continuously record particle velocity field at 10 MHz sampling rate during the experiments. Based on a trigger logic we identify acoustic emissions (AE) within continuous data. From P-wave arrival-time data and from spectral analysis we are able to estimate the following seismological parameters for each AE: location, absolute magnitude, stress-drop and size. Our preliminary observations show that: (i) Regardless of the confining pressure, we always observe a sharp acceleration of the number of AE before failure. The higher the confining pressure, the shorter the time-scale of this acceleration phase, which follows an inverse Omori law; (ii) The locations of the recorded AE draw patterns that reveal seismic and aseismic patches over the fault surface. Zones of precursory acoustic activity shrink with confining pressure; (iii) AE preceding failure migrate toward the nucleation zone and (iv) Even though our observations show that AE precursory activity can arise by both cascading failure and preslip mechanisms, AE source parameters and locations suggest that aseismic preslip is the prevalent mechanism. Finally, we find a simple empirical scaling law for foreshock time series in all our experiments, which involves applied stress and time to failure only.

[1] Laboratoire de Géologie, École Normale Supérieure/CNRS UMR 8538, PSL Research University, 24 rue Lhomond, F-75005 Paris, France, marty@geologie.ens.fr, gardonio@geologie.ens.fr, alexandre.schubnel@ens.fr, harshasbhat@gmail.com, jerome.aubry@ens.fr
[2] National Research Institute for Earth Science and Disaster Resilience, Tsukuba, Japan, fuku@bosai.go.jp

GeoProc2019: Earthquake and Faulting mechanics

7th International Conference on Coupled THMC Processes in Geosystems
3-5 July 2019 Utrecht (Netherlands)

Seismic cycle recorded in cockade-bearing faults (Col de Teghime, Alpine Corsica)

S. Masoch[1], M. Fondriest[2], G. Di Toro[3]

Keywords: Cockade breccia, fault rock, fluidization, inverse grading, pressure growth.

The study of exhumed fault zones allows us to unravel the deformation processes active at depth in the Earth's crust during the seismic cycle. Here we investigated the mechanism of formation of cockade breccias found in Miocene in age extensional faults from the Col de Teghime area (Alpine Corsica, France) (Fig. 1a). Cockade breccia are relatively common fault rocks consisting of clast cores from the wall rocks bounded by concentric mineral rims from vein precipitation. Structural geology surveys and microstructural (optical and scanning electron microcopy, micro computed tomography, image analysis) and mineralogical/geochemical (optical cathodoluminescence, X-ray powder diffraction, Micro-Raman and Energy-dispersive X-ray spectroscopy) investigations of the fault veins from the Col de Teghime area indicated that: (i) the core clasts of the cockades are composed of quartz fragments larger >300 μm in size which are suspended in the fault veins and disposed in inverse grading (Fig. 1a); (ii) the concentric rims are zoned and made of saddle dolomite, Mg-calcite, goethite and anatase (Fig. 1b); (iii) the cockade-bearing fault veins are associated with minor fault veins made of fine quartz fragments (< 300 μm in size) cemented by the same minerals of the rims.

We propose that cockade-bearing faults formed at shallow crustal depths (< 2 km) and recorded all the phases of the seismic cycle: (1) co-seismic fragmentation of the wall rocks in presence of CO_2- and Fe-rich fluids (Fig. 1c1); (2) co-seismic fluidization of the rock fragments resulting in elutriation of the fine particles, which might be deposited in distal veins, and formation of a residual porous and well-sorted clast assemblage which will make the cores of the cockades (Fig. 1c2). Inverse grading resulted by co-seismic shaking (Brazil-Nut Effect) and shearing; (3) post-seismic to interseismic cementation by deposition of carbonate-rich rims due to slow (years to centuries) mineral pressure growth, resulting in the progressing lift of the clasts in the slipping zones (Fig. 1c3).

Given the scarcity in the current literature of fault zone rock assemblages associated to seismic faulting, the results of this study may allow us a better comprehension of earthquake-related processes at shallow crustal depths and find application in seismic hazard studies.

[1] Dipartimento di Geoscienze, Università degli Studi di Padova (Italy), simone.masoch@gmail.com
[2] Dipartimento di Geoscienze, Università degli Studi di Padova (Italy), michelefondriest@yahoo.it
[3] Istituto Nazionale di Geofisica e Vulcanologia, (Roma, Italy)
Dipartimento di Geoscienze, Università degli Studi di Padova (Italy), giulio.ditoro@unipd.it

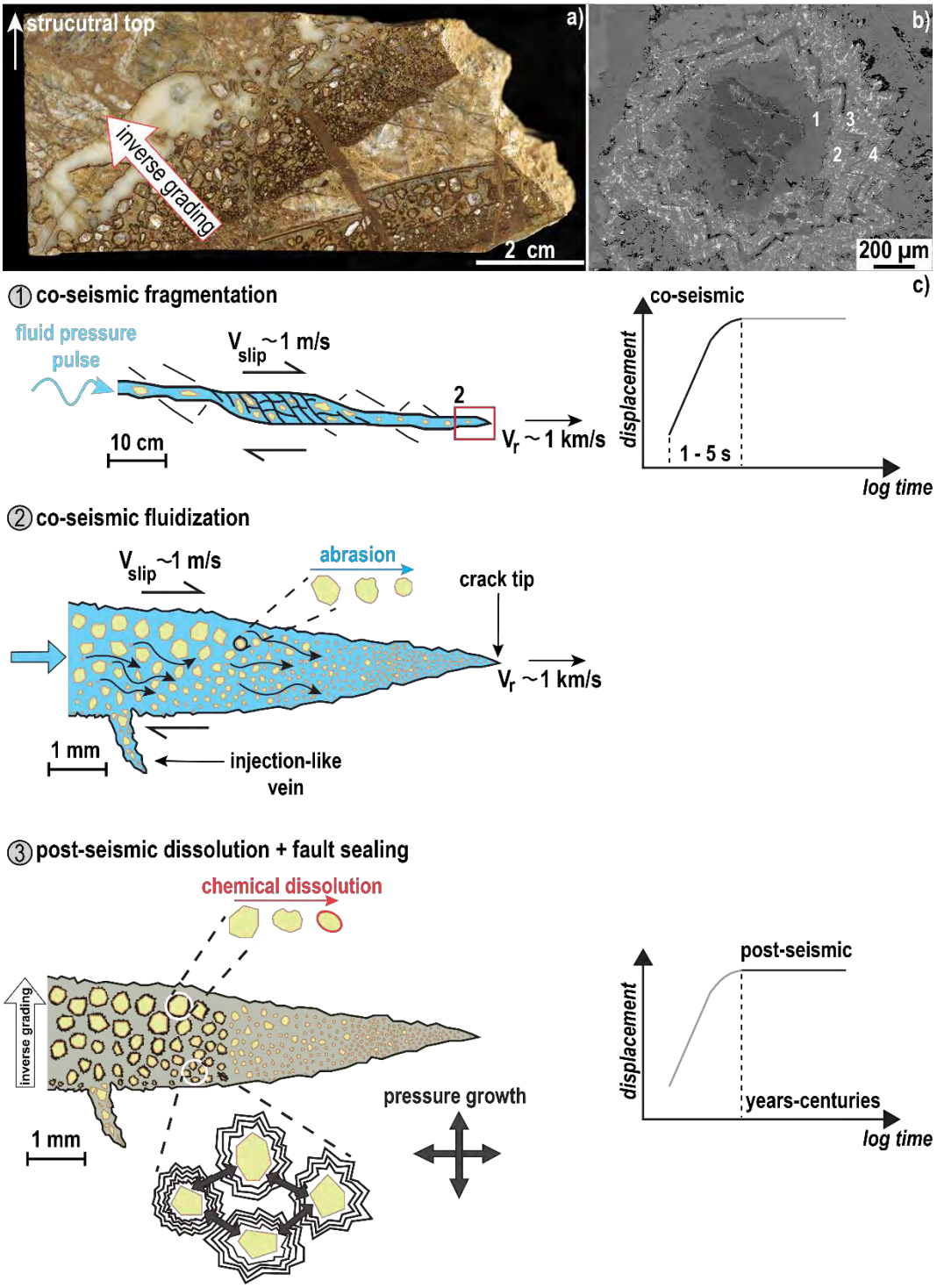

Figure 1. Cockade breccia and model for their formation. (a) Key-type polished sample with multiple cockade-bearing faults with inverse grading. (b) BSE image of a cockade: the quartzite-built core clast is surrounded by four concentric rims of (from the core clast outwards): (1) saddle dolomite enriched in Ca and Fe; (2) Mg-calcite with goethite and anatase microcrystals; (3) zoned saddle dolomite; (4) Mg-calcite with goethite and anatase microcrystals. (c) Conceptual model of the formation of cockade-bearing faults with relationship to displacement and time during the seismic cycle.

GeoProc2019: Earthquake and Faulting mechanics

7th International Conference on Coupled THMC Processes in Geosystems
3-5 July 2019 Utrecht (Netherlands)

Connections between stress rotation, interseismic coupling, and fault-zone property evolution across the brittle-ductile transition of the subducted Gorda plate.

J. J. McGuire[1,3], H. Guo[2], D. Li[3], J. Gong[4], X. Chen[5], Y. Liu[6], and J. L. Hardebeck[11]

Keywords: subduction zones, stress rotation, brittle-ductile transition

One of the most interesting targets for understanding the interactions between various Therm-Hydro-Mechanical-Chemical (THMC) processes within fault-zones is the transition from the interseismically locked portion of megathrusts at ~20 km depth to the primarily aseismic zone of episodic tremor and slip (ETS) at ~30-35 km depth. Not only does this transition zone span an interesting temperature range for frictional stability but both observational and modelling studies imply that there are considerable variations in fault-zone hydrology between the ETS and locked zones. Geophysical imaging of the details of these mechanical and hydrological transitions in subduction zones is often difficult with onshore networks due to the depth of the fault and the typical location of the locked zone occurring just offshore. The subduction of the Gorda Plate beneath Northern California provides a great environment for studying the spatial variations in material properties and stress state of a subduction megathrust. We combine a number of studies using the onshore-offshore seismic networks near the Mendocino Triple Junction (MTJ) of the Cascadia subduction zone to study the evolution of stress orientations, earthquake stress drops, and seismic velocity structure from the deformation front through to the ETS zone.

The stress field in the vicinity of the MTJ is complicated by the collision of the Pacific and Gorda plates resulting in an unusual along-strike orientation of the maximum compressive stress within the mantle of the subducting slab. We observe a rotation of the principle stress axes across the plate boundary coincident with a change in the magnitude of earthquake stress drops. This change in stress orientation and magnitude coincides with a region of elevated fluid content inferred from Vp/Vs anomalies (Figure 1). We utilize this stress rotation to constrain the maximum differential stress on the thrust interface as being at most 50 MPa with an effective friction coefficient of less than 0.2 (Li. et. al. 2018). The relatively low levels of shear-stress within the vicinity of the plate boundary are also evident in earthquake stress drop values that are roughly an order of magnitude lower than those in the adjacent subducted mantle (Chen and McGuire 2016). The moderately high fluid pressures

[1] US Geological Survey, jmcguire@usgs.gov
[2] University of Science and Technology, hguo@mail.ustc.edu.cn
[3] Munich University, dli@geophysik.uni-muenchen.de
[4] MIT-WHOI Joint Program, jgong@whoi.edu
[5] University of Oklahoma, xiaowei.chen@ou.edu
[6] McGill University, yajing.liu@mcgill.ca

inferred within the locked zone (5-20 km depth) do not extend continuously to the ETS zone (30 km depth). In between them lies a region of ordinary Vp/Vs and hence presumably low fluid content (Guo et al., 2019). The transition zone likely represents a low porosity region governed by a ductile rheology. Collectively our observations are similar to the recent rheological models of Beeler et al. (2016) where the brittle-to-ductile transition corresponds to an order of magnitude decrease in porosity and a ductile transition zone separates the higher porosity and brittle ETS and locked regions.

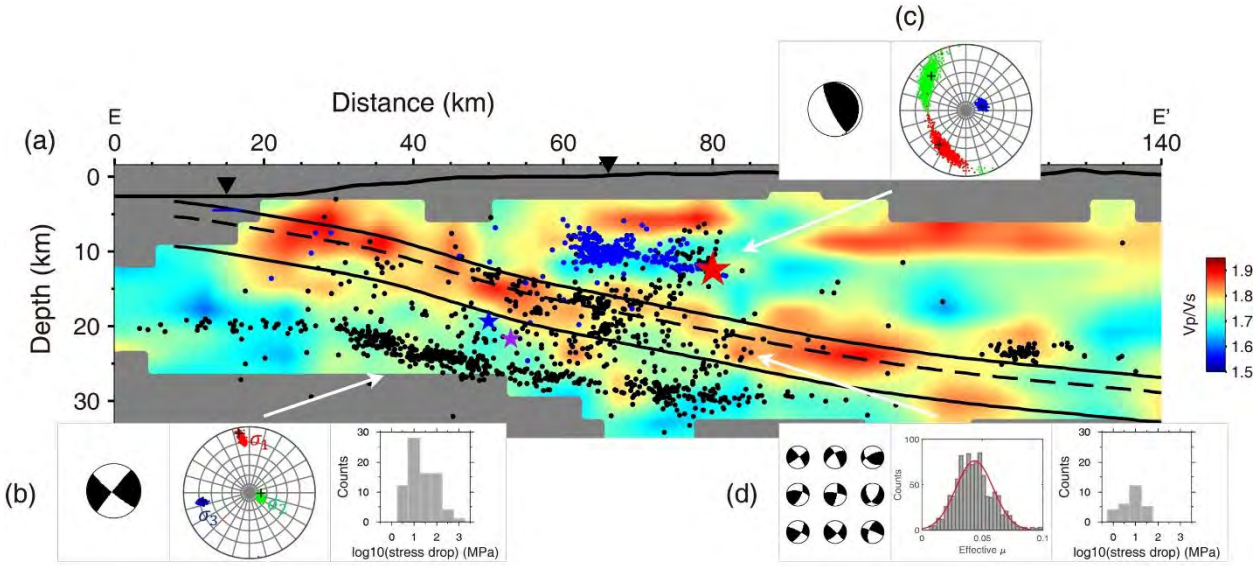

Figure 1. East-West cross section of seismicity, stress, and material properties of the subducted Gorda Plate. (**a**) Vertical cross-section of Vp/Vs model near the MTJ. Black dots represent earthquakes and stars represent the 1992 Petrolia M_w7.1 earthquake (red) and its two largest aftershocks (purple and blue). Blue dots represent the one-month aftershocks in the Cascadia subduction zone following this M_w7.1 earthquake. (**b**) (**left**) A typical focal mechanism of earthquakes in the slab mantle. (**middle**) The stress inversion result for the slab mantle region from Li et al. (2018) (red, σ_1; green, σ_2, blue, σ_3). (**right**) The distribution of earthquake stress drops in the slab mantle from Chen and McGuire (2016). (**c**) (**left**) The focal mechanism of the 1992 M_w7.1 earthquake. (**right**) The stress inversion result for the overriding continental crust region. (**d**) (**left**) The focal mechanisms of nine earthquakes within the plate boundary zone outlined by two solid lines, which are 2 km above and 4 km below the plate interface model (dashed line) of McCrory et al. (2012). (**middle**) Results from 1000 bootstrap stress inversions for the effective frictional coefficient μ of the megathrust interface from Li et al. (2018) assuming the slab mantle has a strength of 150 MPa. (**right**) The distribution of stress drops of earthquakes in the plate boundary zone.

References

Beeler, N.M., Hirth, G., Thomas, A. and Bürgmann, R., 2016. Effective stress, friction, and deep crustal faulting. *Journal of Geophysical Research: Solid Earth*, *121*(2), pp.1040-1059.

Chen, X. and McGuire, J.J., 2016. Measuring earthquake source parameters in the Mendocino triple junction region using a dense OBS array: Implications for fault strength variations. *Earth and Planetary Science Letters*, *453*, pp.276-287.

Guo, H., J. Zhu, J. J. McGuire, H. Zhang, and R. Evans, Variations in fluid content correlate with rheological transitions along the megathrust in the southern Cascadia subduction zone, manuscript in preperation, 2019.

Li, D., McGuire, J.J., Liu, Y. and Hardebeck, J.L., 2018. Stress rotation across the Cascadia megathrust requires a weak subduction plate boundary at seismogenic depths. *Earth and Planetary Science Letters*, *485*, pp.55-64.

GeoProc2019: Earthquake and Faulting mechanics

7th International Conference on Coupled THMC Processes in Geosystems
3-5 July 2019 Utrecht (Netherlands)

Towards a link between local friction and interface kinematics

G. Mollon[1]

Keywords: Tribology, Simulation, Texture, Friction, Soft granular matter

In fault mechanics as well as in tribology, predicting and understanding the value of the friction coefficient within a given interface submitted to certain sliding conditions remains very challenging. One of the reasons is that, most of the time, friction is not related to some properties of contacting *surfaces* (in the mathematical sense), but involves the shearing of a bulk material trapped in the interface, with a certain thickness and various mechanical properties. In a geophysical context this material would be the fault gouge, while the tribological community more generally uses the terminology “third body” for this layer (Berthier 1990).

Since this layer controls the friction (because the two surfaces get completely separated after a sufficient sliding distance), it is essential to understand and predict its rheology and its physics. However, such a task is very challenging in an experimental framework because this layer is strongly confined and is submitted to extreme loading conditions (both in terms of stresses and shear rates), meaning that any local sensor might disturb its behavior.

To overcome this difficulty, this communication proposes an innovative numerical approach based on the Multibody Meshfree Framewok (Mollon 2018a-b). This numerical technique is similar to the more classical Discrete Element Method (DEM), in the sense that it is based on the description of the interfacial material as a discontinuous medium composed by a large number of independent bodies. However, in addition to the DEM framework, these bodies (or grains) are allowed to deform according to the contact loads they are submitted to. This additional feature (which requires the discretization of each body in order to compute its inner fields of strain and stress in a finite deformation framework) gives this approach a much more general ability to represent the wide variety of flow regimes (Couette shearing, strain localization, agglomeration, wall-slip, rolling, viscoplastic flow, etc.) that are experimentally observed in sliding interfaces.

In this communication, we present a comprehensive numerical campaign where such a material was sheared under various sliding conditions, and we investigate in more details the role of three essential mechanical properties of the material composing each grain in the interface: deformability, adhesion, and viscosity. A first striking result is that, despite the large size of the parametric space and the variety of the observed flow regimes that emerge during these simulations, all the resulting friction coefficients remain in a reasonable range for dry friction (i.e. between 0.1 and 1.1, see Fig. 1).

[1] Université de Lyon, LaMCoS, INSA-Lyon, CNRS UMR5259, guilhem.mollon@insa-lyon.fr

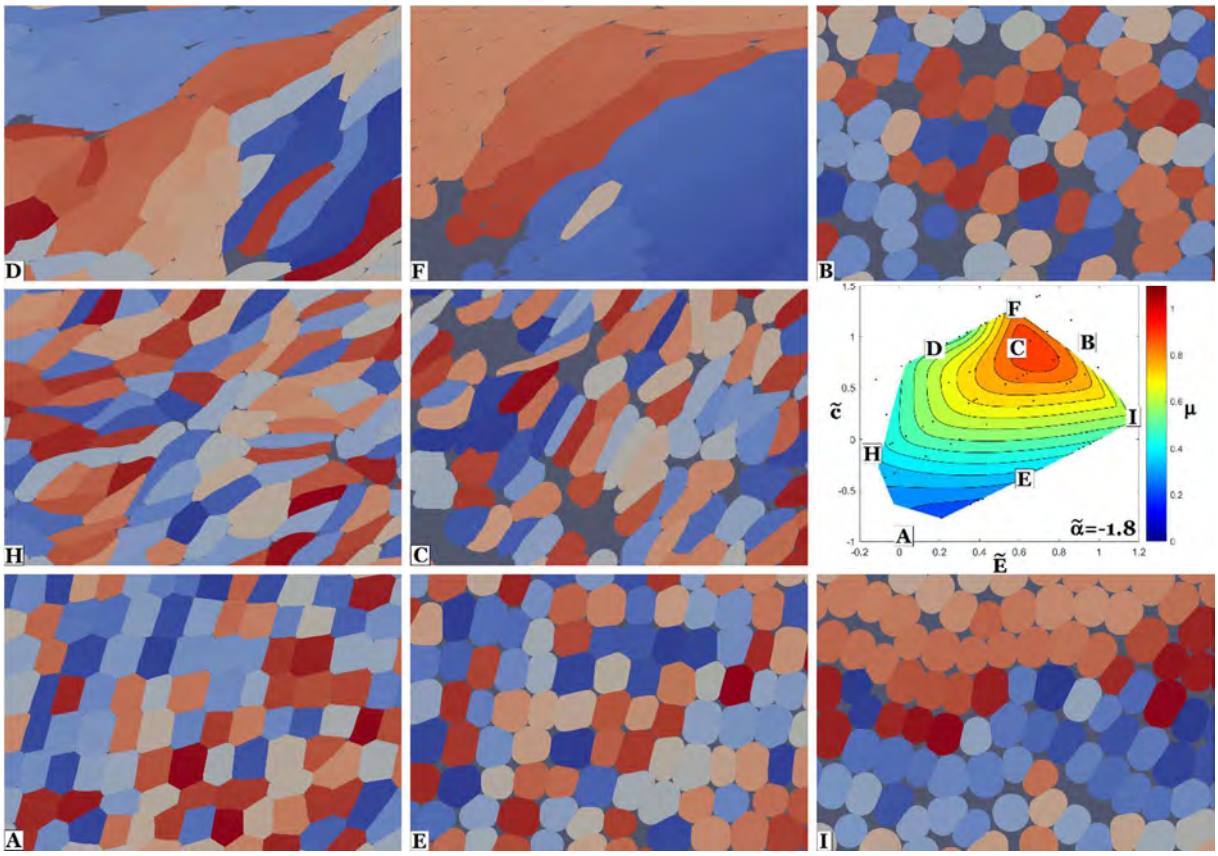

Figure 1. Local textures of the sheared material and corresponding friction coefficients.

A deeper analysis of the energetic phenomena within the interface reveals that there is a competition between energy dissipation related to surface phenomena (i.e. fragmentation and reformation of agglomerates, creation of new surface, localized sliding, etc.) and related to bulk phenomena (viscous dissipation in agglomerates, plasticity, etc.). Large values of the stiffness of the interface material promote surface dissipation, while large values of the adhesion between grains promote bulk dissipation.

Based on these observation, a more quantitative analysis shows that, within the range of the parametric space investigated in this study, it is possible to relate in a rather repeatable way the emerging friction coefficient to the flow regime within the interface, i.e. to such parameters as the specific area and the velocity fluctuations of the sheared material. This work opens avenues to the enrichment of such simulations by multiphysical ingredients such as heat production and flow, and temperature feedback on the mechanical behavior of the interfacial material, in order to investigate rate-dependency in sliding faults.

References

Berthier, Y. (1990), Experimental evidence for friction andwear modelling, *Wear*, *1990*(139), 77–92

Mollon, G. (2018), A unified numerical framework for rigid and compliant granular materials, *Comp. Part. Mech.*, *5*(4), 517–527

Mollon, G. (2018), Solid flow regimes within sliding interfaces: some insights from numerical tribology, *AGU Fall Meeting 2018*, Washington DC, 10-14 December 2018

GeoProc2019: Earthquake and Faulting mechanics

7th International Conference on Coupled THMC Processes in Geosystems
3-5 July 2019 Utrecht (Netherlands)

Determining Mode I fracture toughness in anisotropic rocks

M. Nejati[1], *A. Aminzadeh*[2], *M. O. Saar*[3], *T. Driesner*[4]

Keywords: Fracture toughness, anisotropy, granite, Mode I

Many rock types behave anisotropic in their elastic and inelastic properties due to their complex micro-structure that often caused by two main formation processes: foliation in metamorphic rocks and bedding in sedimentary rocks. Foliation causes the flattening of grains and the alignment of platy minerals along the foliation plane, while bedding and lamination yields a layered structure. Gischig et al. (2018) and Doetsch et al. (2018) have recently demonstrated that rock anisotropy plays a critical role in the in-situ stimulation and circulation experiments in the deep underground laboratory at the Grimsel test site in Switzerland. It was concluded that the anisotropy of the mechanical properties such as elasticity, strength and fracture toughness must be taken into account to accurately predict the rock mass deformation and failure in those experiments (Dutler et al., 2018, Dambly et al., 2019).

When deriving the theory of fracture growth in anisotropic rocks, an assumption is often made on how the Mode I fracture toughness varies between the principal material directions. The most well-known assumption is based on the stress transformation, which suggests that there exists principal values of the fracture toughness in principal directions, and the fracture toughness at any other direction can be obtained based on a sinusoidal fit to the principal values. However, no experiment has been conducted to check the validity of this assumption. The assumed variation of the fracture toughness is of significant importance when predicting the direction of fracture growth. In order to validate the theory of the fracture toughness variation, fracture toughness must be measured at different orientations of crack growth with respect to the principal directions.

We recently modified the semi-circular bend (SCB) test to incorporate the elasticity anisotropy in the determination of the fracture toughness (Nejati at al., 2019). The schematics of this test is shown in Figure 1a. This new test scheme allows to determine the fracture toughness at any orientation with respect to the principal directions. In this paper, we present the results of about thirty Mode I fracture toughness experiments on the metamorphic Grimsel Granite that has a clear foliation plane. Figure 1b shows the variation of the fracture toughness against the angle of the crack extension with respect to the foliation plane. These results show that the fracture toughness in fact varies based

[1] Department of Earth Sciences, ETH Zurich, Switzerland, mnejati@ethz.ch
[2] Department of Earth Sciences, ETH Zurich, Switzerland, ali.aminzadeh@erdw.ethz.ch
[3] Geothermal Energy and Geofluids, Department, Department of Earth Sciences, ETH Zurich, Switzerland, saarm@ethz.ch
[4] Institute of Geochemistry and Petrology, Department of Earth Sciences, ETH Zurich, Switzerland, thomas.driesner@erdw.ethz.ch

on a sinusoidal function. Moreover, theoretical relations for the variation of the critical strain energy density as well as the critical energy release rate are also derived. The results show that these two energy-based parameters also vary based on a sinusoidal fit.

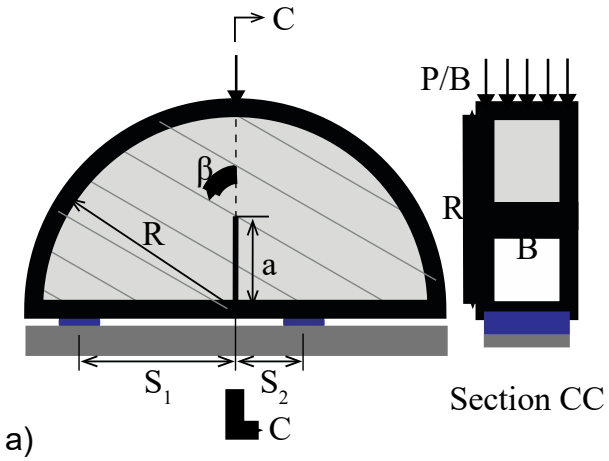

Figure 1. The configuration of the modified SCB test for conducting fracture toughness tests.

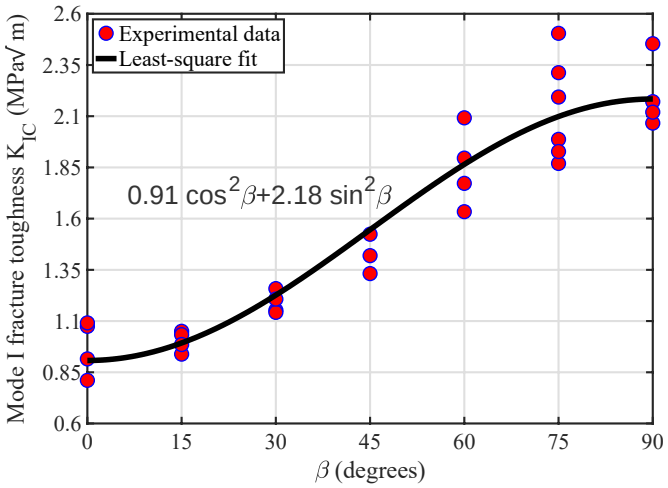

Figure 2. The variation of the fracture toughness against the angle between the crack extension and the foliation plane.

References

Gischig, V., Doetsch, J., Maurer, H., et al., (2018). On the link between stress field and small-scale hydraulic fracture growth in anisotropic rock derived from microseismicity. *Solid Earth* 9 (1), 39–61.

Doetsch, J., Gischig, V., Villiger, L., et al., (2018), Subsurface fluid pressure and rock deformation monitoring using seismic velocity observations. *Geophysical Research Letters* 45, 10389–10397.

Dutler, N., Nejati, M., Valley, B., Amann, F., Molinari, G., (2018). On the link between fracture toughness, tensile strength, and fracture process zone in anisotropic rocks. *Engineering Fracture Mechanics* 201, 56–79.

Dambly, M., Nejati, M., Vogler, D., Saar, M. O., (2019). On the direct measurement of the shear moduli in transversely isotropic rocks using the uniaxial compression test. *International Journal of Rock Mechanics and Mining Sciences* 113, 220–240.

Nejati, M., Aminzadeh, A., Driesner, T., Saar, M. O., (2019). Semi-circular bend test designed for mode I fracture toughness experiments in anisotropic rocks. *Engineering Fracture Mechanics*, Under Review.

GeoProc2019: Earthquake and Faulting mechanics

7th International Conference on Coupled THMC Processes in Geosystems
3-5 July 2019 Utrecht (Netherlands)

Identifying active tectonic structures by Ag oxides' recording, obtained by upward migration hydrochemical fluids on their surfaces

D. Ntokos[1,2]

Keywords: active faults, rock varnish, mineralization, Portable X-Ray Fluorescence, Northwestern Greece

During the last 200 years, many scientists from different disciplines have tried to understand the Geochemistry-Tectonics relationship, mainly conducting chemical analyzes and observing chemical elements, which do not come from those that form the bedrock. In order to identify these elements, processes such as deposition, migration, and replacement were studied to register all the possible causes of the existence of these new chemical elements. An important fact in the progress of these studies was the exploitation of precious metals as there was funding for both the identification of the positions and the conditions for their creation (Stiros, 1988; Jones, 1991; Benson and Jones, 1996; Nur and Burgess, 2008). In several cases, like that of San Luis deposit (Sangre de Cristo Mountains, Colorado, Western United States of America; Jones, 1991; Benson and Jones, 1996), the existence of ephemeral deposits was associated with the circulation of hot transfer metallurgical fluids along extensional tectonic structures (mostly deep normal faults) that transported gold-silver deposits to smaller depths.

Although these studies focused on the advance of exploitable areas and hydrothermal fields, they have given answers and have succeeded in creating a series of axioms that can construct a qualitative method of identifying open active tectonic structures. More specifically, the elements that can be criteria are the following:

1. The detection of chemical elements (not belonging to/ other than the bedrock) in rock varnishes of tectonic structures surfaces through chemical analyzes: The analyzing of the chemical elements is done by using either Scanning Electron Microscope or Portable X-Ray Fluorescence.
2. The detection of elevated temperatures which are recorded either within or outside the tectonic plates' boundaries: These expected temperatures are common within the boundaries of the plates as magma finds a way out to smaller depths. Outside

[1] Department of Civil Engineering, School of Engineering, University of Thessaly, Volos, Greece, ntokos@uth.gr.
[2] School of Mining and Metallurgical Engineering, National Technical University of Athens, Athens, Greece.

of the boundaries, such temperatures may be a result of the following geological factors:

- In areas where there are granite bodies in deeper horizons that warm the surrounding rock, thereby presenting an abnormality in the geothermal gradient.
- In sedimentary basins where the diapiric movement of the evaporites (gypsum, anhydrite and mineral salt, which are good heat conductors) transfers heat from large to smaller depths.
- Also, the water during its descent to deeper horizons through deep faults acquires high temperatures due to the geothermal gradient.

The chosen area for the application of methodology is northwestern Greece, since it features active as well as potentially active tectonic structures, which have been studied in various ways. The study area extends across a region of ~8,000 km2, which are identified by the formations of the Ionian geotectonic zone (evaporites and carbonate and flysch formations), as well as post-Alpine formations (Neogene sediments and Quaternary deposits; Ntokos, 2018a,b; Fig. 1).

According to the methodology of the present study, chemical analyzing was carried out with Portable X-Ray Fluorescence at more than 500 positions along 88 tectonic structures in which high concentrations of Silver (Argentum - Ag; up to 300 ppm) were detected, although silver does not belong to the Ionian zone formations' chemical composition. Obviously this is an element that comes from the rise of hydrochemical fluids along these tectonic structures, which are either developed at great depths and intersect a magmatic source, or intersect diapirisms or neo-diapirisms, which in many cases also occur at low depths.

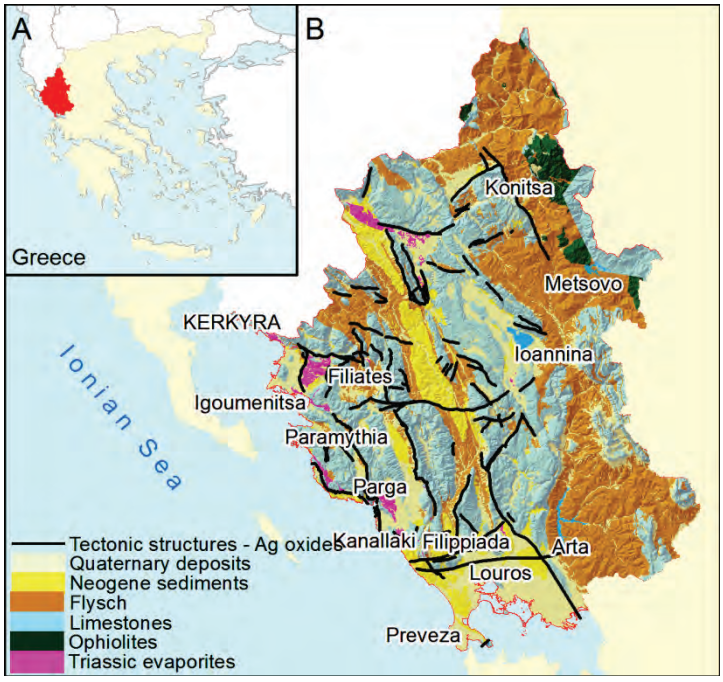

Figure 1. (A) Study area and (B) geological map of Northwestern Greece with marked tectonic structures where Ag oxides were detected.

The identification of oxides such as those of Silver in the rock varnishes of tectonic structures can be an initial stage for identifying deposits of economic interest - mineral resources, which originate from larger depths, and also for identifying geothermal fields, which find the tectonic structure's surface as an outlet to the earth surface through which fluid circulation is facilitated and the permissive hydraulic permeability develops.

References

Benson R.G., and D.M. Jones (1996), Geology of the San Luis gold deposit, Costilla County, Colorado; an example of low-angle normal fault and rift-related mineralization in the Sangre De Cristo Range of Colorado, Special Publication - Colorado Geological Survey.

Jones D.M. (1991), Low-angle normal faulting and gold mineralization in the Sangre de Cristo Range of southern Colorado, Abstracts with Programs - Geological Society of America, 23(5), 246.

Ntokos, D. (2018a), Formulation of the conceptual model for the tectonic geomorphological evolution of an area: five main rivers of Greece as a case study, CATENA, 167, 60-77.

Ntokos, D. (2018b), Neotectonic study of Northwestern Greece, Journal of Maps, 14, 2, 178-188.

Nur, A., and D. Burgess (2008), Apocalypse: Earthquakes, Archaeology and the Wrath of God, Princeton University Press, Princeton and Oxford, 309.

Stiros, S. (1988), Archaeology, a tool to study active tectonics – The Aegean as a case study, Eos, Transactions, American Geophysical Union, 13, 1636-1639.

GeoProc2019: Earthquake and Faulting mechanics

7th International Conference on Coupled THMC Processes in Geosystems
3-5 July 2019 Utrecht (Netherlands)

Dating the varnishes of active Kamena Vourla - Arkitsa fault zone (Northwestern Evoikos Gulf, Central Greece) using Portable XRF

D. Ntokos [1,2], *P. Ntokou* [3]

Keywords: Geochemistry, Chemical analyzing, Cation-ratio, Rock varnishes, tectonic structures

In this paper, the dating of Kamena Vourla - Arkitsa fault zone (KVAF) is being studied through a chemical analysis of the rock varnishes which identified in the outer fault surface. Several attempts have been made to identify the ages of geological and tectonic phenomena that develop on the surface of the earth. Other times using absolute dating methods, such as Radiocarbon dating (^{14}C) and Luminescence dating, and others through the use of more qualitative analyzes which, although they lag behind in accuracy, outweigh the speed at which the result is obtained. Such a method is the dating from the observations, the chemical analysis of rock varnishes, the calculation of the ratio of calcium, potassium and titanium cations (Dorn, 1983; Eq. 2), and the calibration of Nobbs and Dorn (1988; Eq. 1):

$$T = e^{\frac{16.218 - R_C}{1.137}} \quad (1)$$

where, T: is time and R_C: is the cation-ratio, resulting from equation (2):

$$R_C = {(Ca^{2+} + K^{+})}/{Ti^{4+}} \quad (2)$$

where, Ca^{2+}: is the percentage concentration of Calcium (%), K^{+}: is the percentage concentration of Potassium, and Ti^{4+}: is the percentage concentration of Titanium (%).

It is a method that has been applied in many areas of the world and especially in petroglyphs, using either a Scanning Electron Microscope or Portable X-Ray Fluorescence. More specifically, in this study the chemical analysis was applied using the EDX POCKET III P730 - QUALITEST XRF mobile spectrometer.

As the study area determined the KVAF located on the western border of the North Evoikos Gulf (Fig. 1A). This fault zone represents a series of normal fault segments, with a E-W to NW-SE mean strike and a N dip, and is classified as active

[1] Department of Civil Engineering, School of Engineering, University of Thessaly, Volos, Greece, ntokos@uth.gr, dimitriosntokos@yahoo.gr
[2] School of Mining and Metallurgical Engineering, National Technical University of Athens, Athens, Greece
[3] Department of Mathematics, School of Science, University of Ioannina, University Campus, Ioannina, Greece

because of its intense morphology and the impressive surface trace consisting of well-preserved fault surfaces which has deep and well-marked striations and canellures (Fig. 1B). A further element of its characterization as active is the stress axes, which produced of microtectonic analysis of the KVAF (Fig. 1C) and are in conformity with the current elongation axes of Aegean area (Papazachos and Kiratzi, 1996). The surface of the fault in the area of Arkitsa and Kamena Vourla, up to 70 m high, is a curved rocky surface, which is not identical to the flat geometry and is the most extensive and clear fracture face that is observed in Greece. According to paleoseismological data, the KVAF seems to have given the last 20,000 years at least four major earthquakes, with the latter occurred between 1300 and 1110 BC. The archaeological finds of the destruction of the nearby ancient settlement of Kunos (today's settlement of Livanates) as well as the radioactive dating of the tsunami deposits in the excavation area and the underwater coastline during the same period (1200-1100 BC) are probably linked to the last activation of the KVAF.

Due to its well-preserved fault surfaces and the limited erosion effect (since a part of this surface was discovered in 1996 by the quarry operation in the area), this tectonic structure is indicated to apply the R_C method. Specifically, by fieldwork, rock varnishes were found both in the Arkitsa segment and in Kamena Vourla ones. According to the methodology, calcium, titanium, and potassium cations were analyzed, and their concentration was determined in percentages at 16 sites. From these measurements using the Dorn's equation (2; 1983), the R_C ratio takes values between 1.53 and 15.22 corresponding to ages from 730 to 410,000 years ago (Eq. 1). More specifically, the rock varnishes that were identified correspond to the following ages: four ~1,000 year-old rock varnishes, one of 3,000, 7,700, 70,000, and 110,000 years old, and two of 400,000 years old. It observed that all rock varnishes correspond to Upper Pleistocene - Holocene ages, which are confirmed by the literature and correspond to the overall configuration of tectonic trench of this Gulf (Rondoyanni-Tsiambaou, 1984; Roberts and Jackson, 1991).

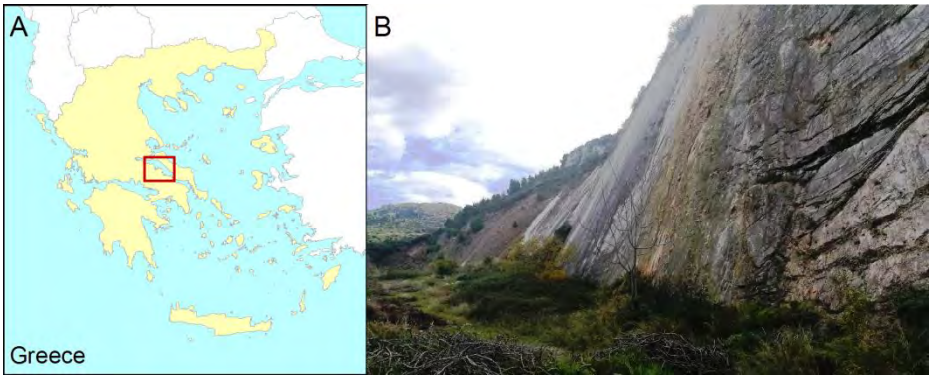

Figure 1. (A) Study area and (B) field photograph of the KVAF surfaces in the area of Arkitsa.

It is worth mentioning that in the Arkitsa fault segment the dating of the rock varnishes gave better results compared to other areas, e.g. Epirus, Greece (Ntokos, 2018), where the same method was applied to faults due to the well-preserved fault surface, verifying the application of the method to tectonic structures.

References

Dorn, R.I. (1983), Cation-ratio dating: A new rock varnish age determination technique, *Quaternary Research*, 20, 49-73.

Nobbs, M.F., and R.I. Dorn (1988), Age determinations for rock varnish formation within petroglyphs: cation-ratio dating of 24 motifs from the Olary region, South Australia, *Rock Art Res.*, 5, 108-146.

Ntokos, D. (2018), Can cation-ratio dating of rock varnishes be applied in faults?, *Proceedings of the 9th International Symposium on Eastern Mediterranean Geology*, Abstract Volume, Akdeniz University, Antalya, Turkey, 07-11 May 2018, 221.

Papazachos, C.B. and A.A. Kiratzi (1996), A detailed study of the active crustal deformation in the Aegean and surrounding area, *Tectonophysics*, 253, 129-153.

Roberts, S., and J. Jackson (1991), Active normal faults in central Greece: An overview, in Holdsworth, R.E., and Turner, J.P., compilers, Extensional tectonics: Faulting and related processes: Key Issues in Earth Sciences, Volume 2: London, Geological Society of London, 151-168.

Rondoyanni-Tsiambaou, T. (1984), Etude néotectonique des rivages occidentaux de Canal D' Atalanti (Grèce - Central), Thèse, Université de Paris-Sub, Orsay.

GeoProc2019: Earthquake and Faulting mechanics

7th International Conference on Coupled THMC Processes in Geosystems
3-5 July 2019 Utrecht (Netherlands)

Material and Stress Rotations: The Key to Reconciling Crustal Faulting Complexity with Rock Mechanics

Amos Nur[1]

Key Words: Faults, faulting, material and stress rotations

"Rotations ... make nonsense of the two-dimensional reconstructions that are still so popular among structural geologists". (McKenzie, 1990, p. 109–110)

A perennial problem in fault mechanics is that the fault geometries *in situ*—especially of strike- slip faults—often contradict theoretical predictions. According to experimental and theoretical rock mechanics as captured by Coulomb's law, fault directions and motions should correspond simply to stresses in the crust. However, the complex geometrical distribution and regional trends of observable faults in the crust often seem at odds with the regional state of stress. Fortunately, these discrepancies can be neatly reconciled with Coulomb's law if we recognize that many faults did not form in their current orientations, but have rotated over time, and/or the stress field has rotated as well.

We describe a comprehensive tectonic model for the strike-slip fault geometry, seismicity, material rotation, and stress rotation, in which new, optimally oriented faults can form when older ones have rotated about a vertical axis out of favorable orientations. The model was successfully tested in the Mojave region using stress rotation and three independent data sets: the alignment of epicenters and fault plane solutions from the six largest central Mojave earthquakes since 1947, material rotations inferred from paleomagnetic declination anomalies, and rotated dike strands of the Independence dike swarm.

The success of the rotation model in the Mojave has applications well beyond this special region alone. The implication for crustal deformation in general is that rotations—of material (faults and the blocks between them) and of stress—provide the key link between the geology of faults and the mechanical theory of faulting. Excluding rotations from the kinematic and mechanical analysis of crustal deformation makes it impossible to explain the complexity of what geologists see in faults, or what seismicity shows us about active faults. However, when we allow for rotation of material and stress, Coulomb's law becomes consistent with the actual complexity of faults and faulting observed *insitu.*

[1] *Dept of Geophysics, Stanford University, Stanford CA 94305, amos.nur@stanford.edu*

Table 1. History and trends of thought about material and stress rotations in crustal deformation.

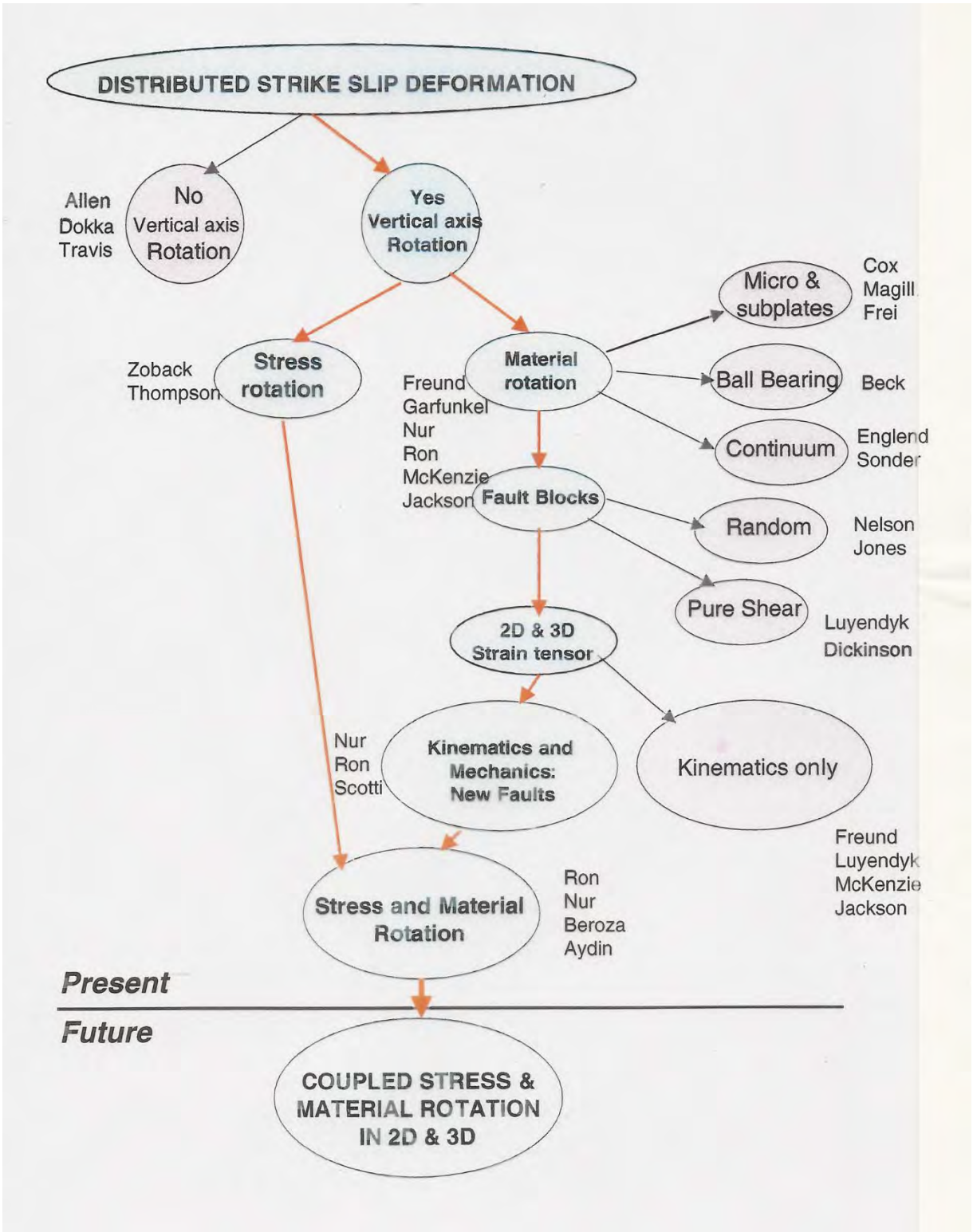

References

Beck, M. E., Jr., 1976, Discordant paleomagnetic pole position as evidence of regional shear in the Western Cordillera of North America: American Journal of Science, v. 276, p. 694–712.

Dickenson, W. R., 1996, Kinematics of trans-rotational tectonism in the California Transverse Ranges and it's contribution to cumulative slip along the San Andreas transform system: Geological Society of America Special Paper 305, p. 46.

Dokka, R. K., and Travis, C. J., 1990, Late Cenozoic strike-slip faulting in the Mojave Desert, California: Tectonics, v. 9, p. 311–340.

Frei, L. S., Magill, J. R., and Cox, A., 1984, Paleomagnetic results from the central Sierra Nevada: Constraints on reconstruction of the Western United States: Tectonics, v. 2, p. 157–177.

Freund, R., 1970, Rotation of strike-slip faults in Sistan, southeastern Iran: Journal of Geology, v, 78, p. 188– 200.

Garfunkel, Z., 1974, Model for the late Cenozoic tectonic history of the Mojave Desert, California, and its relation to adjacent regions: Geological Society of America Bulletin, v. 5, p. 141–188.

Luyendyk, B. P., Kamerling, M. J., and Terres, R., 1980, Geometric model for Neogene crustal rotations in southern California: Geological Society of America Bulletin, v. 91, p. 211–217.

McKenzie, D., 1990, The spinning continents: Nature, v. 344, p. 109–110.

McKenzie, D., and Jackson, J., 1983, The relationship between strain rates, crustal thickening, paleomagnetism, finite strain, and fault movements within a deforming zone: Earth and Planetary Science Letters, v. 65, p. 182–202.

Nelson, M. R., and Jones, C. H., 1987, Paleomagnetism and crustal rotations along the shear zone, Las Vegas Range, southern Nevada: Tectonics, v. 6, p. 13–33.

Nur, A., Ron, H., and Beroza, G., 1993a, The nature of the Landers-Mojave earthquake line: Science, v. 261, p. 201–203.

Nur, A., Ron, H., and Scotti, O., 1989, Kinematics and mechanics of tectonic block rotations, *in* Cohen, S. C. and Vanicek, P., eds., Slow deformation and transmission stress in the earth: American Geophysical Union Geophysical Monograph 49 (IUGG series 4), p. 31–46.

Nur, A. & Hagai Ron (2003) Material and Stress Rotations: The Key to Reconciling Crustal Faulting Complexity with Rock Mechanics, International Geology Review, 45:8, 671-690

Ron, H., Freund, R., Garfunkel, Z., and Nur, A., 1984, Block rotation by strike-slip faulting: Structural and paleomagnetic evidence: Journal of Geophysical Research, v. 89, p. 6256–6270.

Terres, R. R., and Luyendyke, P. B., 1985, Neogene tec- tonic rotation of the San Gabriel region, California, suggested by paleomagnetic vectors: Journal of Geophysical Research, v. 90, no. B7, p. 12,467–12,484.

Zoback, M. L., Anderson, R., and Thompson, G. A., 1981, Cenozoic evolution of the state of stress and style of tectonism in the western United States: Philosophical Transactions of the Royal Society, London, ser. A., v. 300, p. 407–434.

GeoProc2019: Earthquake and Faulting mechanics

7th International Conference on Coupled THMC Processes in Geosystems
3-5 July 2019 Utrecht (Netherlands)

Slip- and Velocity-Weakening Behaviors of Brucite Nanoparticle

H. Okuda[1], I. Katayama[2], H. Sakuma[3], K. Kawai[4]

Keywords: Sheet-structure nanoparticle, Fault instability, Friction experiment

The dynamics of the fault is mainly controlled by the frictional characteristics of the materials in a fault gouge, which is the highly communicated area of the fault. In natural fault gouges, sheet-structure minerals are common materials and their frictional characteristics are important for the fault behaviors due to their low friction coefficients (Saffer & Marone, 2003). The previous studies suggest that the materials with low friction coefficients like sheet-structure minerals show velocity-strengthening behaviors, which indicates that the fault with sheet-structure minerals is aseismic (Ikari et al., 2011). On the other hand, a fault gouge is known to contain nanometer size particles (nanoparticles) (Chester et al., 2005) and moreover recent experimental studies found that the nanoparticles show both slip- and velocity-weakening behaviors and make the fault unstable (Han et al., 2011). Therefore, it is essential to study the frictional stability of sheet-structure nanoparticles for the understanding of the fault dynamics.

In this study, friction experiments with chemically synthesized nanoparticles of brucite ($Mg(OH)_2$) (grain size: 70 nm; purchased from WAKO) as an analog of sheet-structure minerals were conducted using a biaxial testing machine at Hiroshima University. The amount of the gouge was 1 g and the thickness of the gouge was 0.5 mm for each gouge at the initial conditions. The applied normal stresses were 10, 20, 40, and 60 MPa, and the loading rate was 3 μm/sec. The maximum displacement was 20 mm and velocity step tests (3-33 μm/sec) were conducted several times after the shear displacement of 10 mm. The thin sections of the experimental species showed that the internal structures and the crystal orientations within the gouge were observed by a scanning electron microscope and a polarized microscope.

Both slip- and velocity-weakening behaviors for all experiments and stick-slip behaviors were observed with the normal stress higher than 40 MPa (Fig. 1). These results show that the sheet-structure nanoparticles could make the fault unstable. The observations of the internal structures and the crystal orientation within the gouge (Fig. 2) indicate that this instability was due to: (1) the evolution of a smooth boundary shear, (2) the alignment of the crystal basal plane parallel to the shear direction, and (3) the shear localization at the boundary shear. (1) and (2) contribute to a slip-weakening behavior (Anthony &

[1] Department of Earth and Planetary Science, University of Tokyo, Japan, okuda@eps.s.u-tokyo.ac.jp
[2] Department of Earth and Planetary Systems Science, Hiroshima University, Japan, katayama@hiroshima-u.ac.jp
[3] Research Center for Functional Materials, National Institute for Materials Science, Japan, SAKUMA.Hiroshi@nims.go.jp
[4] Department of Earth and Planetary Science, University of Tokyo, Japan, kenji@eps.s.u-tokyo.ac.jp

Marone, 2005; Kawai et al., 2015), and (3) contributes to a velocity-weakening behavior (Scruggs & Tullis, 1998). These results imply that the existence of the sheet-structure nanoparticles could induce seismic behaviors in mature faults containing finer particles. For the precise understanding of the fault dynamics, the spatial distribution of the nanoparticle in the fault should be investigated in the future.

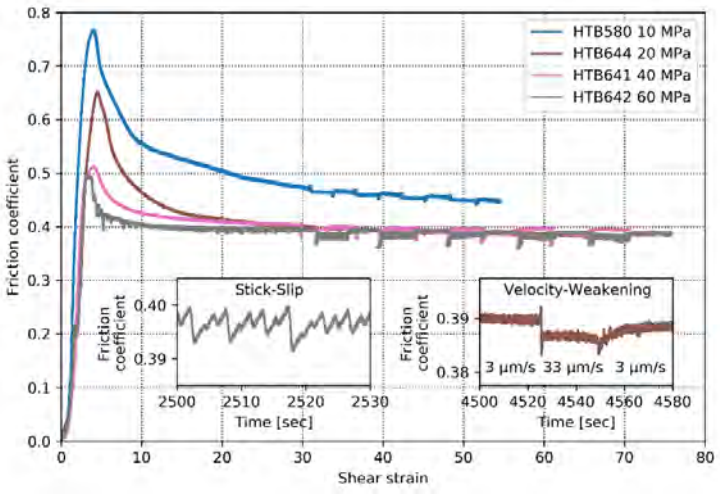

Figure 1. Results of the friction experiments.

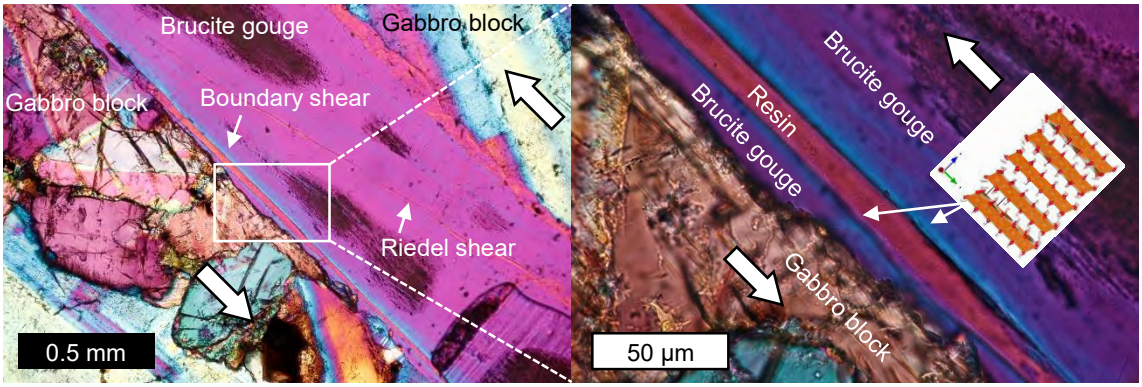

Figure 2. Internal structure and crystal orientation within the gouge. Brucite crystal aligns its basal plane parallel to the shear direction at boundary shear.

References

Anthony, J., and C. Marone (2005), Influence of particle characteristics on granular friction, *J. Geophys. Res.*, 110(B8), B08409, doi: 10.1029/2004JB003399.

Chester, J., F. Chester, and A. Kronenberg (2005), Fracture surface energy of the Punchbowl fault, San Andreas system, *Nature*, 437(7055), 133-136, doi: 10.1038/nature03942

Han, R., T. Hirose, T. Shimamoto, Y. Lee, and J. Ando (2011), Granular nanoparticles lubricate faults during seismic slip, *Geology*, 39(6), 599-602, doi: 10.1130/G31842.1.

Ikari, M., C. Marone, and D. Saffer (2011), On the relation between fault strength and frictional stability, *Geology*, 39(1), 83-86, doi: 10.1130/G31416.1.

Kawai, K., H. Sakuma, I. Katayama, and K. Tamura (2015), Frictional characteristics of single and polycrystalline muscovite and influence of fluid chemistry, *J. Geophys. Res. Solid Earth*, 120(9), 6209-6218, doi: 10.1002/2015JB012286.

Saffer, D., and C. Marone (2003), Comparison of smectite- and illite-rich gouge frictional properties: application to the updip limit of the seismogenic zone along subduction megathrusts, *Earth Planet. Sci. Lett.*, 215 (1-2), 219-235, doi: 10.1016/S0012-821X(03)00424-2.

Scruggs, V., and T. Tullis (1998), Correlation between velocity dependence of friction and strain localization in large displacement experiments on feldspar, muscovite and biotite gouge, *Tectonophysics*, 295(1-2), 15-40, doi: 10.1016/S0040-1951(98)00113-9.

GeoProc2019: Earthquake and Faulting mechanics

7th International Conference on Coupled THMC Processes in Geosystems
3-5 July 2019 Utrecht (Netherlands)

Mechanics of fluid-saturated granular gauges under seismic oscillations

S. Parez[1], *M. Svoboda*[1], *T. Travnickova*[1], *S. Ben Zeev*[2], *E. Aharonov*[3]

Keywords: dynamic triggering, fluid-saturated granular matter, fault weakening, effective stress

Slip on geological faults can be triggered by remote earthquakes up to a thousand kilometers away. This phenomenon, known as dynamic triggering, has been found susceptible to pore fluid pressure in preexisting faults. We numerically study the pore pressure evolution in fluid-saturated granular layers under oscillatory shear (Fig. 1). This setup mimics arrival of seismic waves at the fault and their interaction with the fluid-filled granular gauge. The coupled dynamics of pressure and granular deformation (Fig. 2) is solved using Discrete-Element- and Finite-Element methods within a two-scale model [1]. The model has been applied to shallow-soil conditions (low normal stress, high drainage), where it successfully predicted pressure gradients in response to compaction rate due to oscillations, and explained why liquefaction can occur in drained granular aggregates [2]. Here, the setup is changed from a thick granular layer bounded by a free upper surface (representing shallow conditions) to a thin layer confined between two surfaces, experiencing high normal stress (simulating a fault). We systematically study the fault slip for a range of boundary conditions differing in the frequency and the amplitude of the oscillations, stress across the fault, permeability of the fault zone and degree of water drainage. We identify conditions that lead to weakening of the fault and draw relations for fluid pressure/pressure gradients as function of amplitude and frequency of the driving oscillations.

[1] Institute of Chemical Process Fundamentals of the CAS, Prague, Czech Republic, parez@icpf.cas.cz
[2] Université de Strasbourg, CNRS, Institut de Physique du Globe de Strasbourg, France, shahar.benzeev@mail.huji.ac.il
[3] Institute of Earth Sciences, Hebrew University of Jerusalem, Israel, einatah@mail.huji.ac.il

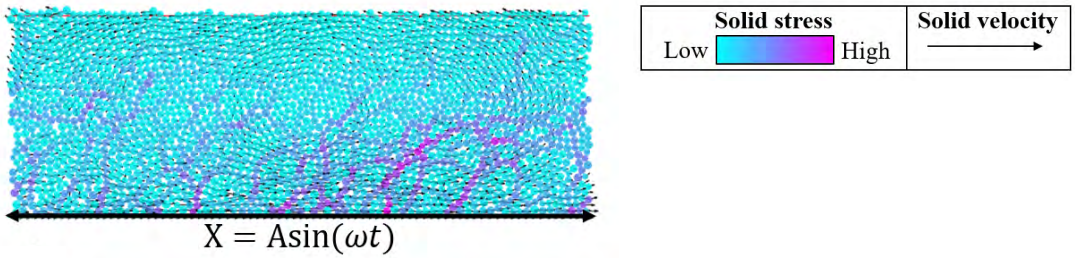

Figure 1. Dynamics of grains (a snapshot from a simulation) on shaking of the bottom wall. The color indicates magnitude of normal stress on a grain and the black arrows are proportional to grain velocities.

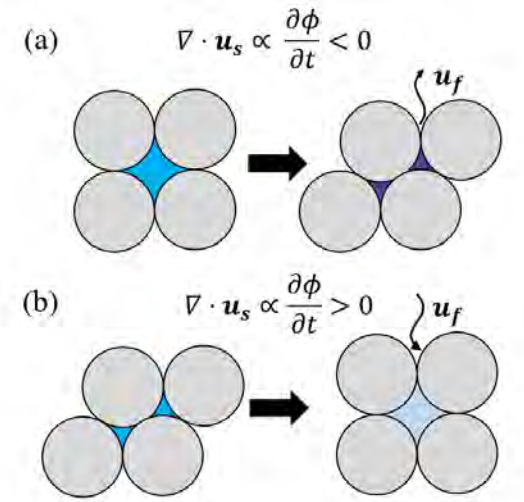

Figure 2. Schematic representation of the concept of the model. (a) Negative divergence of solid velocity $\nabla \cdot \boldsymbol{u}_s$, proportional to compaction rate $\partial \phi / \partial t$, acts as a positive source for pore pressure (purple) and the fluid tends to escape the pore (curly black arrow). (b) Positive divergence of solid velocity acts as a sink for pore pressure (light blue) and the fluid tends to flow into the pore (curly black arrow).

References

Goren, L., Aharonov, E., Sparks, D., and R. Toussaint (2011), The Mechanical Coupling of Fluid-Filled Granular Material Under Shear, *Pure Appl. Geophys.*, *168*, 2289–2323, doi:10.1007/s00024-011-0320-4.

Ben Zeev, S., Goren, L., Parez, S., Toussaint, R., and E. Aharonov (2018), The coupling between compaction and pressurization in cyclically sheared drained granular layers: implications for soil liquefaction, 20th EGU General Assembly, Proceedings from the conference, 9371.

GeoProc2019: Earthquake and Faulting mechanics

7th International Conference on Coupled THMC Processes in Geosystems
3-5 July 2019 Utrecht (Netherlands)

Modelling earthquake cycles using a continuum based poro-visco-elasto-plastic two-phase flow formulation

C. Petrini[1], T. Gerya[1], Y. v. Dinther[1,2], J.A.D. Connolly[3], C. Madonna[4], V. Yarushina[5]

Keywords: Earthquake cycle simulation, poro-visco-elasto-plastic flow

Fault slip along subduction zones, from slow slip events to large destructive megathrust events, is believed to be strongly influenced by fluids and their interaction with the surrounding host rock. To better understand fault slip or strain, it is crucial to understand the role fluids play in their mechanics. Observational data, such as e.g. GPS or earthquake catalogues, are limited in space and time. Therefore a numerical model overcoming such limitations is needed. The development of a numerical model coupling deformation of both fluids and solids in the same framework is an indicated approach. The goal of this study is the development of a fully coupled seismo-hydro-mechanical model and subsequently the identification of different parameters controlling the slip mode.

A newly developed finite difference poro-visco-elasto-plastic numerical code with marker-in-cell technique, coupling inertial mechanical deformation and fluid flow, is presented. Localised brittle/plastic deformation is treated accurately through global iterations. To simulate deformation on both long- and short-time scale, an adaptive

[1] Institute of Geophysics, ETH Zurich, Switzerland (claudio.petrini@erdw.ethz.ch)

[2]Institute of Geochemistry and Petrology, ETH Zurich, Switzerland

[3]Department of Earth Sciences. Utrecht University, Netherlands

[4]Geological Institute, ETH Zurich, Switzerland

[5]Institute for Energy Technology, NO-2007 Kjeller, Norway

time step is introduced allowing the resolution of large seismic events with time steps on the order of milliseconds.

This new numerical tool allows to explore how the presence of fluids in the pore space of a visco-elasto-plastic (de)compacting rock matrix affects elastic stress accumulation and release along a fluid-bearing subduction interface. The model is capable of simulating spontaneous quasi-periodic seismic events without requiring a reduction in friction. These events nucleate near the brittle-ductile transition and propagate along self-consistently forming highly localized ruptures. The spontaneous elastic rebound events show slip velocities ranging from μm/s to m/s, thereby covering the range from slow to seismic slip. These different forms of slip occur on the same interface and are no tuned through explicit formulations or parameters. The governing strength decrease along the propagating fracture is related to a small drop in total pressure, due to shear localization, in combination with an increase of fluid pressure generated by deformation induced fluid flux. The reduction of the differential pressure decreases the brittle/plastic strength of fluid-bearing rocks along the rupture, thus providing a dynamic feedback mechanism for the accumulated elastic stress release at the megathrust interface.

GeoProc2019: Earthquake and Faulting mechanics

7th International Conference on Coupled THMC Processes in Geosystems
3-5 July 2019 Utrecht (Netherlands)

The effect of ion-species on limestone failure dynamics

A. Pluymakers[1], A. Ougier-Simonin[2], A. Barnhoorn[3]

Keywords: fluid-rock interaction, mechanical strength, triaxial testing

At the relatively low pressure and temperatures of the upper crust, the two main water-assisted deformation mechanisms are pressure solution (Rutter, 1976) and subcritical crack growth (Atkinson, 1984). Due to their high solubility, carbonates are especially prone to such fluid-assisted deformation processes. These rocks are also of high interest regarding geo-energy applications: hydrocarbon reservoirs can be found in porous carbonates or topped by low porosity carbonate rocks, and saline carbonate aquifers are potential CO_2 storage formation and targeted geothermal energy site. To date, laboratory research has mainly focused on the effects of different acids and plain NaCl on carbonate deformation behavior (for a review, see Rohmer et al., 2016) whilst the effect of salinity and ion species is yet to be more fully addressed. Indeed, changing the chemistry of the fluid affect the chemistry of the fluid-solid interface (e.g. Bergsaker et al., 2016), for example, by changing the surface energy, or changing the dissolution/precipitation kinetics. Such microstructural chemo-mechanical effects are very likely affecting how the solid fails and fractures propagate, in an aseismic or seismic fashion.

We performed rock failure experiments on carbonate samples subjected to 2 saline solution, namely $MgSO_4$ and Na_2SO_4, reducing the complexity of all mechano-chemical effects. We ran 18 room temperature, conventional triaxial experiments on limestone samples from the Ragusa Formation, Italy (also tested by Bakker et al., 2015; Castagna et al., 2018). Confining pressures were 7, 30 and 70 MPa. All the samples were pre-saturated under vacuum with 0.4 M Na_2SO_4 or 0.4 M $MgSO_4$, and further saturated with respect to $CaCO_3$; a reference set saturated with a $CaCO_3$ solution only was tested too. The results indicate that short-term exposure (S; <24 h) to the $MgSO_4$ solution changes the failure dynamics of the limestone, from type I to type II failure, without significantly altering the strength (see Figure 1). Samples exposed to Na_2SO_4 or $CaCO_3$ solution did not exhibit these effects. A longer exposure of 200 day exposure – so short on geological timescales, but comparable to engineering timescales – significantly affected failure strength: samples exposed to $MgSO_4$ are up to 50 MPa stronger, and samples exposed to Na_2SO_4 are up to 50 MPa weaker than the reference sets. Note that a 200 day exposure to Mg-ions at

[1] Civil Engineering & Geosciences, TU Delft, the Netherlands, anne.pluymakers@tudelft.nl
[2] Rock Mechanics and Physics Laboratory, British Geological Survey, Nottingham, UK, audreyo@bgs.ac.uk
[3] Civil Engineering & Geosciences, TU Delft, the Netherlands, auke.barnhoorn@tudelft.nl

room temperature is too short for a chemical reaction to Mg-calcite or dolomite to take place (Usdowski, 2009). These results highlight that Coupled Hydro-Mechanical-Chemical processes governing the dynamics of carbonate failure behavior are yet to be fully understood. In particular, under conditions in which time-dependent sub-critical crack growth is active the exact chemical composition of the brine in the pores of limestone rocks is a paramount factor.

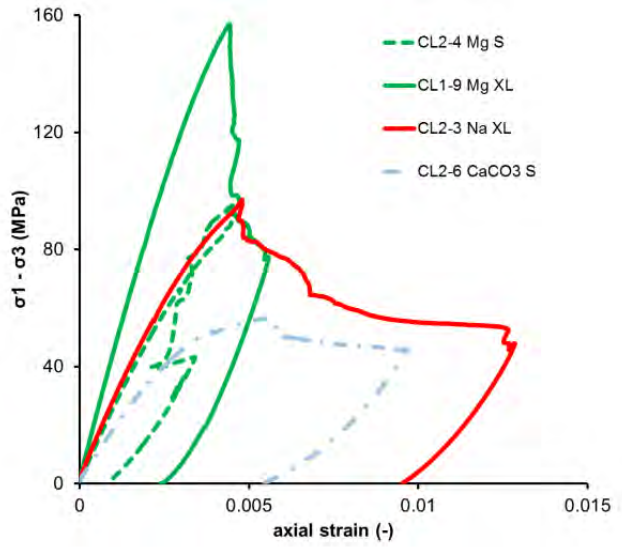

Figure 1. Stress-strain curves from selected experiments at 7 MPa. Green lines indicated expoure to $MgSO_4$, red indicates exposure to Na_2SO_4, and blue is the reference case. <24 hour exposure is indicated with S, 200 day exposure is indicated with XL. The curves indicate class II failure for short exposure to $MgSO_4$, and class I failure for the other experiments.

References

Atkinson, B. (1984). Subcritical crack growth in geological materials. *J. Geophys. Res.*, *89*(B6), 4077–4114. https://doi.org/10.1029/JB089iB06p04077

Bakker, R. R., Violay, M. E. S., Benson, P. M., & Vinciguerra, S. C. (2015). Ductile flow in sub-volcanic carbonate basement as the main control for edifice stability: New experimental insights. *Earth and Planetary Science Letters*, *430*, 533–541. https://doi.org/10.1016/J.EPSL.2015.08.017

Bergsaker, A. S., Røyne, A., Ougier-Simonin, A., Aubry, J., & Renard, F. (2016). The effect of fluid composition, salinity and acidity on subcritical crack growth in calcite crystals. *Journal of Geophysical Research: Solid Earth*, *121*(3), 1631–1651. https://doi.org/10.1002/2015JB012723

Castagna, A., Ougier-Simonin, A., Benson, P. M., Browning, J., Walker, R. J., Fazio, M., & Vinciguerra, S. (2018). Thermal Damage and Pore Pressure Effects on Brittle-Ductile Transition of Comiso Limestone. *Journal of Geophysical Research: Solid Earth*, *123*(9), 7644–7660. https://doi.org/10.1029/2017JB015105

Rohmer, J., Pluymakers, A., & Renard, F. (2016). Mechano-chemical interactions in sedimentary rocks in the context of CO2 storage: Weak acid, weak effects? *Earth-Science Reviews*, *157*. https://doi.org/10.1016/j.earscirev.2016.03.009

Rutter, E. (1976). The Kinetics of Rock Deformation by Pressure Solution. *Philosophical Transactions of the Royal Society of London. Series A, Mathematical and Physical Sciences*, *283*(1312), 203–219. https://doi.org/10.1098/rsta.1976.0079

Usdowski, E. (2009). Dolomites: A Volume in Honour of Dolomieu. In B. H. Purser, M. E. Tucker, & D. H. Zenger (Eds.), *Dolomites: A Volume in Honour of Dolomieu* (p. 464).

GeoProc2019: Earthquake and Faulting mechanics

7th International Conference on Coupled THMC Processes in Geosystems
3-5 July 2019 Utrecht (Netherlands)

GARNET: A new library for modeling tightly coupled, nonlinear, transient phenomena in arbitrary spatial dimensions

C. Pranger[1], D. May[2], A. Gokhberg[3]

Key Words: multi-physics library, nonlinear processes, automatic discretization

Experimental and geological observations, as well as theoretical considerations, increasingly reinforce our understanding that deformation of rocks at various scales of space and time is governed by a multitude of coupled nonlinear processes. An example of particular interest is the 'earthquake cycle' both at lesser and at greater depth. Numerical modeling is an essential tool to improve our understanding of these phenomena and can tell us a lot about the domain over which they can be active without having to perform a large number of experiments. It also gives access to data that are simply not available in the laboratory or in the field. However, numerical modeling on the forefront of material science is often done by domain scientists in lower-dimensional space in e.g. Matlab or Python. The increased computational complexity that comes with solving coupled, non-linear, and transient problems in higher-dimensional space is usually so severe that it requires specialist knowledge of numerical and computational techniques. So-called multi-physics packages (e.g. ABAQUS, COMSOL, OpenFOAM (Weller et al., 1998), MOOSE (Gaston et al., 2009), or FEniCS (Logg, 2012) aim to provide a way for non-specialists to still harness significant computational power. Each of these has its own advantages and disadvantages for a particular purpose. Flexible finite element discretizations that are well suited for engineering problems may be unwieldy and degrade performance when modeling geo-materials in continua. Also, multi-physics packages are frequently built on a system of pre-existing physics modules that might suit ones needs very well, but again require specialist knowledge when they don't.

Here we present GARNET: a new, freely available multi-physics library that facilitates easy experimental set-up and that enables its users to enter the model equations in a very intuitive way. Any partial or ordinary differentials in space or time are discretized automatically by second-order accurate central differences (in space) or higher-order linear multistep methods (in time) in a user-defined number of spatial dimensions. Discretized nonlinear equations are solved by either: an explicit scheme, Newton-Raphson, or pseudo-transient continuation. GARNET interfaces to scientific computing libraries PETSc (Balay et al., 1997) for parallel (nonlinear) solvers and preconditioners, and to Kokkos (Edwards et al., 2014) for optimized low-level grid computations and

[1] Institute of Geophysics, ETH Zurich, casper.pranger@erdw.ethz.ch
[2] Department of Earth Sciences, Oxford University, david.may@earth.ox.ac.uk
[3] Institute of Geophysics, ETH Zurich, alexey.gokhberg@erdw.ethz.ch

fine-grained parallelism/concurrency. The GARNET interface hides nearly all of the complexity of these libraries, including much of the complexity of its programming language C++ itself. Different levels of parallelism -- including intra-node (MPI), inter-node (MPI-3 shared memory), and thread-level parallelism on CPU and GPU -- make GARNET suitable for laptops as well as supercomputers. A drawback of GARNET is the restrictions placed upon the mesh geometry and mesh topology, making it most suited for simulating processes operating in a (more or less) rectangular continuum. However, one could argue that most geological processes are (at least on some scale) continuum processes.

We will demonstrate GARNET's capabilities with simulations of sequences of aseismic slip and dynamic rupture propagation in realistic geological media.

Figure 1. GARNET logo.

References

Weller, H. G., G. Tabor, H. Jasak, and C. Fureby (1998). A tensorial approach to computational continuum mechanics using object-oriented techniques. *Computers in Physics, 12(6), 620–631*. http://doi.org/10.1063/1.168744

Gaston D., C. Newman, G. Hansen, D. Lebrun-Grandi (2009) Moose: a parallel computational framework for coupled systems of nonlinear equations. *Nuclear Eng Design 239(10):1768–1778.* doi:10.1016/j.nucengdes.2009.05.021

Logg, A., K.-A. Mardal, G. N. Wells et al. (2012) Automated Solution of Differential Equations by the Finite Element Method. Springer, 2012.

Balay, S., W. D. Gropp, L. Curfman McInnes, B. F. Smith (1997) Efficient Management of Parallelism in Object Oriented Numerical Software Libraries. In: Modern Software Tools in Scientific Computing (pp. 163--202), E. Arge and A. M. Bruaset and H. P. Langtangen (eds.), Birkhäuser Press.

Edwards, H. C., C. R. Trott, d. Sunderland (2014) Kokkos: Enabling manycore performance portability through polymorphic memory access patterns, *Journal of Parallel and Distributed Computing, Volume 74, Issue 12, 3202-3216*, https://doi.org/10.1016/j.jpdc.2014.07.003.

GeoProc2019: Earthquake and Faulting mechanics

7th International Conference on Coupled THMC Processes in Geosystems
3-5 July 2019 Utrecht (Netherlands)

Analysis of hydromechanical process effect on water-induced landslides

J.F. Shao[1], M. Wang[2], Y.L. Zhang[3], Q.Z. Zhu[4]

Keywords: Landslides, hydromechanical process, numerical modeling, multi-scale modeling

Landslides are frequently countered in many countries and can cause heavy economic and human lost. A large number of landslides are generated by water content change in soils and rocks due to rain or reservoir water level change. Although many studies have been devoted to understanding and modeling of water-induced landslides, a number of issues are still open and need further investigations.

In this study, we shall first present a review analysis of some typical cases of landslides in China during recent years. The effect of pore water pressure and saturation degree on mechanical properties of soils and rocks will be outlined and discussed. Some typical laboratory tests in drained and undrained conditions of soils and rocks will also be presented to show the evolution of pore water pressure during deformation.

Based that background, we shall develop a micro-mechanics based constitutive model for soil-like granular materials under different levels of confining pressure. The model is formulated within the general framework of homogenization for granular materials and with the consideration of irreversible thermodynamics. Further, new rigorous stress localization laws are proposed. Macroscopic plastic deformation is related to local plastic sliding along inter-granular contact surfaces. Material softening is also described by involving damage process of contact surfaces fabrics. The plastic sliding at each contact surface is described by a non-associated plastic flow rule, taking into account normal dilatancy. The creep deformation is also included by using a unified formulation and considering time-dependent sliding along contact surfaces.

The model is further extended to saturated and partially saturated media. The effect of water pressure or capillary pressure on the local elastic and strength properties of

[1] Hohai University (China) and University of Lille (France), jian-fu.shao@polytech-lille.fr
[2] University of Lille, France, w.meng1993@gmail.com
[3] Hohai University, China, zyhohai@163.com
[4] Hohai University, China, qizhi_zhu@163.com

contact surface is taken into account. The concept of generalized effective stress tensor is revisited.

The proposed model is first assessed through comparisons with laboratory tests on typical soil-like materials. It is implemented in a computer code and applied to studying basic failure mechanisms of some typical landslides under various raining conditions.

GeoProc2019: Earthquake and Faulting mechanics

7th International Conference on Coupled THMC Processes in Geosystems
3-5 July 2019 Utrecht (Netherlands)

Brittle-plastic fault zone architecture along the Median Tectonic Line, SW Japan

Norio Shigematsu[1], Takuma Katori[2], Jun Kameda[3], Ayumu Miyakawa[1]

Keywords: fault zone architecture, exhumed fault zone, mylonite, cataclasite, brittle-plastic transition

The heterogeneous fault deformation around the brittle-plastic transition possibly affects the fault behavior significantly including the generation of earthquakes (e.g., Scholtz, 2001). To understand the effect, a detailed fault zone architecture is essential. In this study we constructed a 700 m scale 3D fault zone architecture model based on the geological study of an exhumed fault zone, the Median Tectonic Line (MTL) in the western Kii peninsula SW Japan. In the studied area, the Ryoke granitoids widely exposed on the northern side of the MTL, while the Sanbagawa metamorphic rocks are exposed on the southern side.

To reveal the 3D structures, accurate positions were determiend by applying SfM (structure from motion) and MVS (multi-view stereo) calculation (e.g., Furukawa and Hernández, 2013) to photos taken by an UAV (Unmanned Aerial Vehicles), and GNSS (Global Navigation Satellite system) surveying (e.g., Bemis et al., 2014). The microstructural observations, chemical analyses of minerals and crystallographic analyses of quartz using an electron back-scatter diffraction (EBSD) (Prior, et al., 1998) were performed to characterize the defomation of fault rocks. Based on these deformation features, the 3D fault zone architcture were constructed using a 3D-CAD software.

Figure 1 shows the constructed 3D fault zone architecture. The fault plane of the MTL (lithological boundary) is an almost perfect plane with dip and dip azimuth of 61°/357°. The structures can be divided into two main structures. One includes mylonite and cataclasite showing sinistral sense of shear. The other structures consist of scaly cataclasite showing dextral sense of shear and further younger structures including the lithological bonadry. The later structures cut the former structures indicating the sequence of deformation within the fault zone.

Scaly cataclasite only apper in the vicinity of the MTL, and is characterized by the strong foliation defined by the alignment of chlorite. Moldal fraction chlorite is much larger than that in the surrounding Ryoke drived rocks, and pressure-solution seam is well developed.

[1] Geological Survey of Japan, AIST, n.shigematsu@aist.go.jp
[2] Geological Survey of Japan, AIST, t.katori@aist.go.jp
[3] Hokkaido University, kameda@sci.hokudai.ac.jp
[4] Geological Survey of Japan, AIST, miyakawa-a@aist.go.jp

The estimated temperature based on the chlorite geothermometry is about 300 ºC (Bourdelle et al., 2013).

The deformation of the structures showing sinistral sense of shear varies from mylonite deformed at temperature of about 450 ºC (Higher-T mylonite), that deformed at about 300 ºC (Lower-T mylonite) to cataclasite deformed at about 300 ºC, suggesnting these structures record the brittle-plastic transition. One conspicuous feature in these structures is a altanation zone of black cataclasite and ultramylonite. This zone is a narrow and planar zone with width of 10 m. The cataclasite in this zone is black colored and strongly foliated. The ultramylonite in this zone show almost ramdom CPO (crstallographic preffered orientation) of quartz. We consider that this zone was the fault core when the present exhumed level experienced the brittle-plastic transiton.

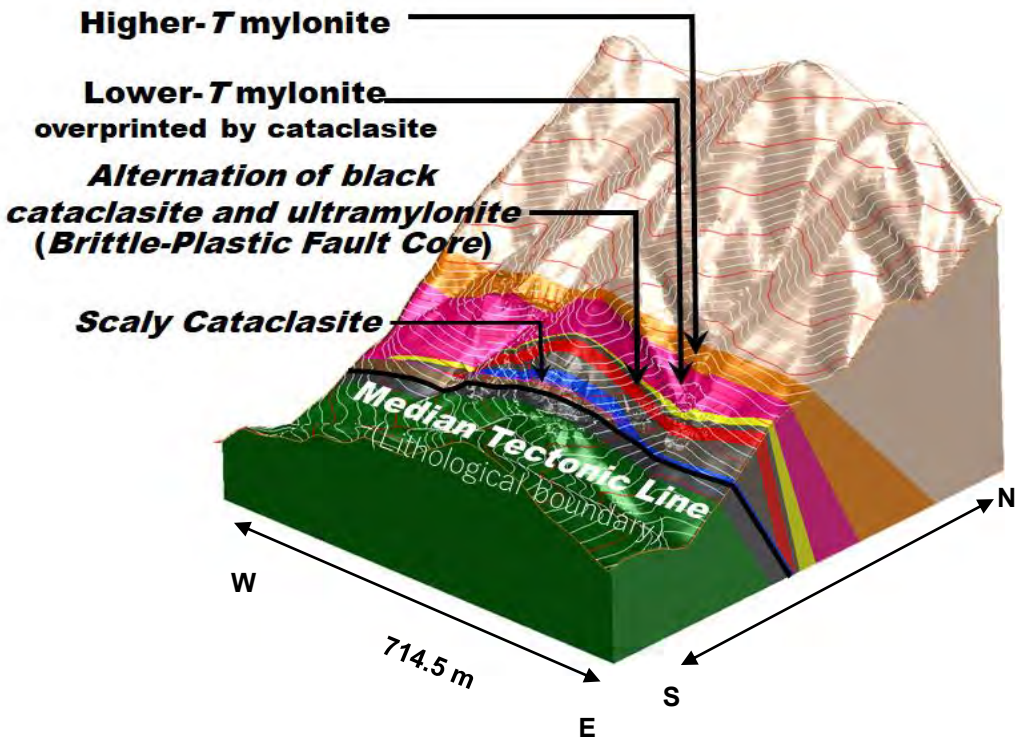

Figure 1. 3D fault zone architecture looking from the southeast.

References

Bemis, S.P., Micklethwaite, S., Turner, D., James, M.R., and Akciz, S., (2014), Ground-based and UAV-Based photogrammetry: A multi-scale, high highresolution mapping tool for structural geology and paleoseismology, *J. Struct. Geol.*, 69, 163-178.

Bourdelle, F., Parra, T., Chopin, C., and Beysacc, O., (2013), A new chlorite geothermometer for diagenetic to low-grade metamorhpic conditon, *Contrib. Mineral. Petrol.*, 165, 723-735.

Furukawa, Y., and Hernández, C., (2013), Multi-View Stereo: A Tutorial. Foundations and Trends, *Comp. Graph. Vis.*, 9, 1-148.

Prior, D. J., et al. (1999), The application of electron backscatter diffraction and orientation contrast imaging in the SEM to textural problems in rocks, Am. Mineral., 84(11–12), 1741–1759, doi:10.2138/am-1999-11-1204.

Scholtz, C.H. (2001), The Mechanics of Earthquakes and Faulting, Cambridge Univ. Press, Cambridge, 2001, 471 pp.

GeoProc2019: Earthquake and Faulting mechanics

7th International Conference on Coupled THMC Processes in Geosystems
3-5 July 2019 Utrecht (Netherlands)

Precursory changes in on- and off-fault elastic wave properties linked to accelerated fault creep during laboratory slip instabilities

S. Shreedharan[1], J. Rivière[2], P. Shokouhi[2], C. Marone[1]

Keywords: Earthquake precursors, stick-slip, slow earthquake, seismic velocity

Precursory temporal changes in seismic velocities have been observed prior to earthquakes in nature (*Niu et al., 2008*) as well as in controlled laboratory experiments on stick-slip and slow slip instabilities on fault gouge (*Scuderi et al., 2016*). However, the microphysical mechanisms responsible for these observed precursors are not well understood. Here, we report on double-direct shear friction experiments conducted on rough Westerly Granite surfaces at normal stresses up to 15 MPa. We study the evolution of elastic wave properties during the lab seismic cycle for a range of stick-slip modes from slow to fast, representing the spectrum of fault slip behaviors observed in nature. The range of slip modes is understood in terms of the ratio of elastic loading stiffness k to the critical frictional weakening rate k_c and its evolution with fault surface roughness, gouge accumulation, comminution due to accumulated shear strain, and fault normal stress. An increase and subsequent decrease in ultrasonic amplitudes and velocities for both the p- (compressional) and s- (shear) waves are observed during the inter-seismic period. We document that the precursory decrease in amplitude temporally occurs prior to the decrease in seismic velocities. More specifically, when accounting for elastic deformation of the faults, we observe that the precursory decrease in amplitude is perhaps due to fault 'unlocking' or slow creep and the decrease in velocities is due to accelerated slip at the fault interface. This indicates that seismic amplitudes are sensitive to small changes in the fault state and grain-scale processes. Moreover, we observe that elastic wave speed and amplitude precursors exist in the direction perpendicular to shear, away from the fault interface as well as at the interface. The amplitude of these precursors decreases with distance from the fault. Recasting amplitude as a proxy for the real contact area (RCA) or number of contact junctions indicates that the precursory changes in amplitudes and seismic velocities could be due to an increase in RCA due to frictional healing during the preparatory, quasi-locked stage and subsequent rejuvenation of the contact junctions due to accelerated slip. Our results indicate that the use of active seismic experiments could be a viable form of real-time monitoring of active fault zones to detect seismic precursors.

[1] Rock and Sediment Mechanics Laboratory, Pennsylvania State University, srisharan@psu.edu
[2] Dept. Of Engineering Science and Mechanics, Pennsylvania State University

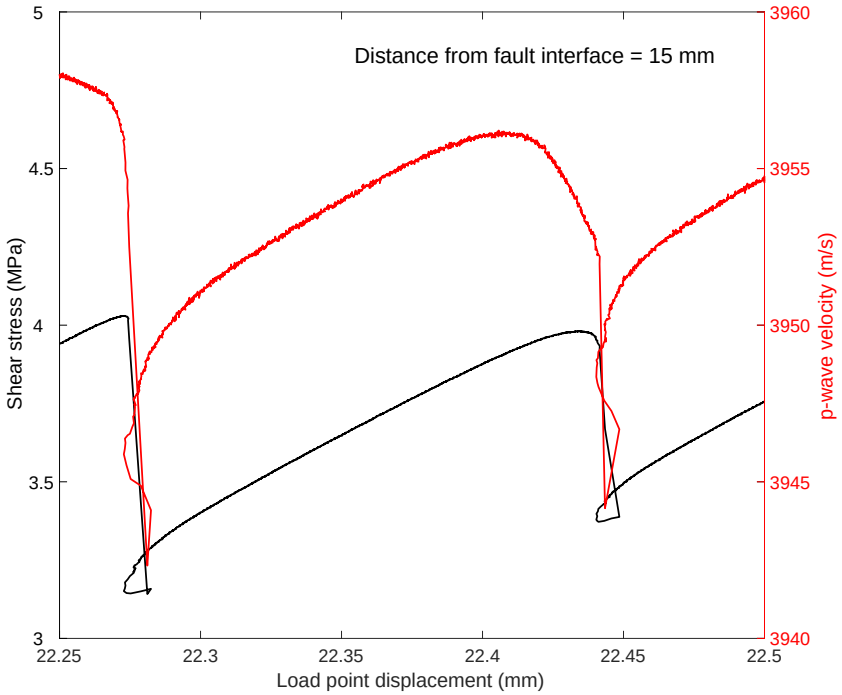

Fig. 1: Evolution of p-wave velocity in the fault-parallel direction 15 mm away from the fault interface for a stick-slip cycle. The p-wave velocity increases with elastic loading, and decreases prior to failure even as shear stress continues to increase.

References

Niu, F., Silver, P. G., Daley, T. M., Cheng, X., & Majer, E. L. (2008). Preseismic velocity changes observed from active source monitoring at the Parkfield SAFOD drill site. Nature, 454(7201), 204.

Scuderi, M. M., Marone, C., Tinti, E., Di Stefano, G., & Collettini, C. (2016). Precursory changes in seismic velocity for the spectrum of earthquake failure modes. Nature geoscience, 9(9), 695.

GeoProc2019: Earthquake and Faulting mechanics

7th International Conference on Coupled THMC Processes in Geosystems
3-5 July 2019 Utrecht (Netherlands)

Carbonaceous Materials in the Longmenshan Fault Belt Zone: Records of Seismic Slip from the Trench and Implications for Faulting Mechanisms

J.L. Si[1], , H.B. Li [1], L-W Kuo [2] , J-R Huang [3], S-R Song [4], J.L. Pei [5], H. Wang [1], L. Song[6], J-N Fang [7] and H-S Sheu [8]*

Keywords: Carbonaceous materials; Trench; Longmenshan fault zone; Faulting mechanism

In recent studies on the recognition of graphitized gouges within the principal slip zone (PSZ) of the Longmenshan fault in China, we proposed that the presence of graphite might be evidence of fault slip. Here, we characterized the clay- and carbonaceous-rich gouges of the active fault zone of the Longmenshan fault belt using samples collected from the trench at Jiulong, which was deformed during the 2008 MW-7.9 Wenchuan earthquake, to determine if graphite is present and study both the processes influencing fault behavior and the associated faulting mechanism. Mineralogical and geochemical analyses of the Jiulong trench sample show the presence of a hydrothermal mineral (i.e., dickite) integrated with dramatic relative chemical enrichment (Ti) and relative depletion (K) within a yellowish zone (Fig.1), suggesting the presence of vigorous high-temperature fluid–rock interactions, which are likely the fingerprint of thermal pressurization. This is further supported by the absence of carbonaceous materials (CMs) given the spectrometric data obtained. Interestingly, the Raman parameters measured near the carbonaceous-rich gouge fall within the recognized range of graphitization in the mature fault zone, implying the origin of a mature fault, as shown in the companion paper. According to both the sharp boundary within the very recent

[1] *Key Laboratory of Deep-Earth Dynamics of Ministry of Natural Resources, Institute of Geology, Chinese Academy of Geological Sciences, Beijing 100037, China; lihaibing06@163.com (H.L.); wanghuan4585@126.com (H.W.)*

[2] *Department of Earth Sciences, National Central University, Taoyuan 320, Taiwan; liweikuo@ncu.edu.tw*

[3] *Department of Earth Sciences, National Taiwan Normal University, Taipei 106, Taiwan; hjrou0906@hotmail.com*

[4] *Department of Geosciences, National Taiwan University, Taipei 106, Taiwan; srsong@ntu.edu.tw*

[5] *Institute of Geomechanics, Chinese Academy of Geological Sciences, Beijing 100081, China; peijl@aliyun.com*

[6] *Boyue Instruments (Shanghai) Co., Ltd., Shanghai 201612, China; m.song@boyuesh.com*

[7] *National Taiwan Museum, Taipei 100, Taiwan; jnfang@ntm.gov.tw*

[8] *National Synchrotron Radiation Research Center, Hsinchu 30076, Taiwan; hsheu@nsrrc.org.tw*

coseismic rupture zone of the 2008 MW-7.9 Wenchuan earthquake and the presence of kinetically unstable dickite, it is strongly implied that the yellow/altered gouge likely formed from a recent coseismic event as aconsequence of hydrothermal fluid penetration. We further surmise that the CM characteristics varied according to several driving reactions, e.g., transient hydrothermal heating versus long-term geological metamorphism and sedimentation.

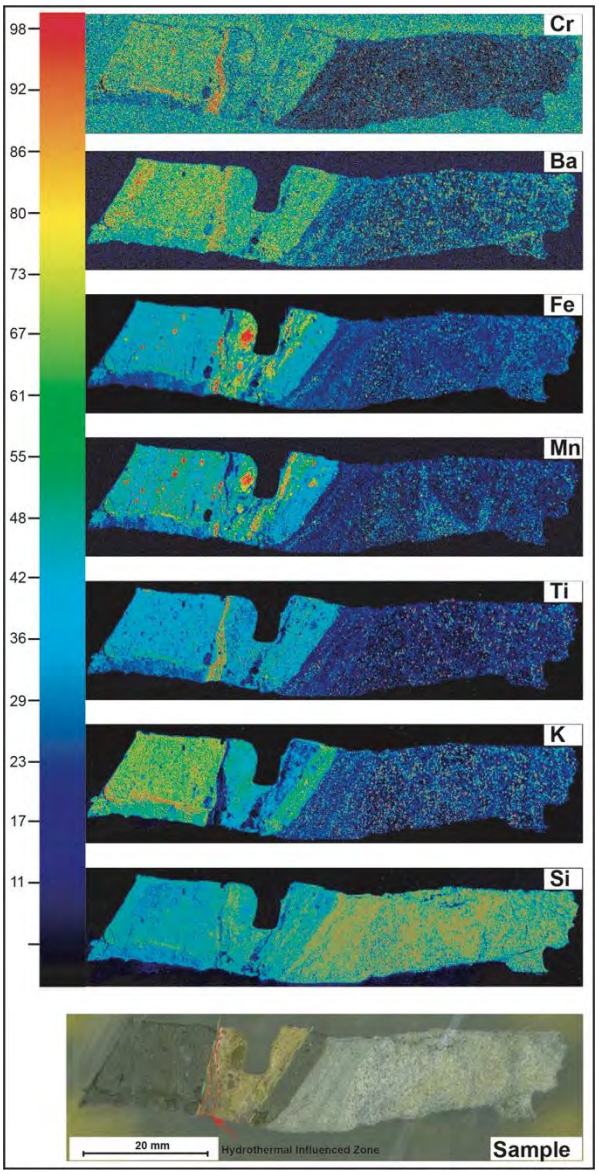

Figure 1. X-ray fluorescence (XRF) map of the Jiulong trench samples. The 2008 slip zone lies at the top of the middle yellowish gouge layer. The chromatographic column numbers indicate the element abundances. The red lines show the location of the hydrothermal influenced zone (HIZ).

GeoProc2019: Earthquake and Faulting mechanics

7th International Conference on Coupled THMC Processes in Geosystems
3-5 July 2019 Utrecht (Netherlands)

Simplified Elastodynamic Modeling of Potential Dynamic Rupture Through Creeping Fault Sections

O.Stephenson[1], *N. Lapusta*[2]

Keywords: Thermal pressurization, dynamic weakening, dynamic rupture modeling

Recent evidence from modeling, experiments and observations indicate that faults can dramatically weaken during seismic slip (e.g., Rice, 2006; Di Toro et al. 2011, Viesca and Garagash, 2015). Such dynamic weakening can potentially allow creeping sections of faults, often assumed to be barriers to earthquake rupture, to rupture coseismically. Dynamic weakening of velocity-strengthening fault areas has been used to explain a range of observations about the region that hosted the 2011 Mw 9 Tohoku earthquake (Noda and Lapusta 2013, Cubas et al. 2015) as well as the lack of microseismicity on several segments of the southern San Andreas fault (Jiang and Lapusta 2016, 2017). These lines of evidence suggest the need for further investigation into the circumstances where creeping sections can rupture dynamically.

In this work, we use a highly simplified 2D model of a single 1D shear zone embedded into an elastic bulk to investigate the possibility of a rupture propagating through creeping sections of faults due to dynamic weakening via thermal pressurization (TP) of pore fluids. We apply this model to the Parkfield section of the San Andreas fault, a richly instrumented area which lies at the transition between the locked and creeping sections of the San Andreas and hosts relatively large, quasi-periodic Mw 6 events.

In the model, a velocity-weakening (VW) patch on a rate-and-state fault produces ruptures that propagate towards a steadily creeping section governed by velocity-strengthening (VS) friction at low slip rates. The properties of the VW patch are chosen to produce a series of events similar to the Mw 6 Parkfield events. The modeled creeping section has properties that can lead to TP for suitably high slip rates and slips and hence weaken the section dynamically. We impose a limit on the slip velocity as a proxy for off-fault damage (following Andrews, 2005) and vary several parameters affecting the efficiency of TP. In particular, we investigate the effect of varying the hydraulic diffusivity and the width of the dynamically shearing zone, which are the most uncertain parameters that can potentially vary by orders of magnitude. One observational constraint is that the 2004 Mw 6.0 Parkfield earthquake did not penetrate far into the creeping section, and that puts constraints onto how efficient the thermal pressurization can be in the creeping section.

[1] California Institute of Technology, Pasadena, USA, olstephe@caltech.edu
[2] California Institute of Technology, Pasadena, USA, lapusta@caltech.edu

In our simulations, the 2004-style rupture events propagate over the creeping section for a range of dynamic-weakening cases that we considered, allowing us to rule these out. The 2004-style rupture events arrest in the creeping region for a range of parameters that can potentially lead to TP in larger events. For example, with an interseismic shear stress of 15 MPa, hydraulic diffusivity of 10^{-4} m^2/s, and width of the dynamically shearing zone of 1 mm, we find that Mw 6 style events arrest in the creeping section, whereas Mw 7.2 style events coming from the south can rupture the entirety of the creeping section. Future work will extend this modeling to 3D and examine the effects of changing fault strength and proxies for multiple fault strands.

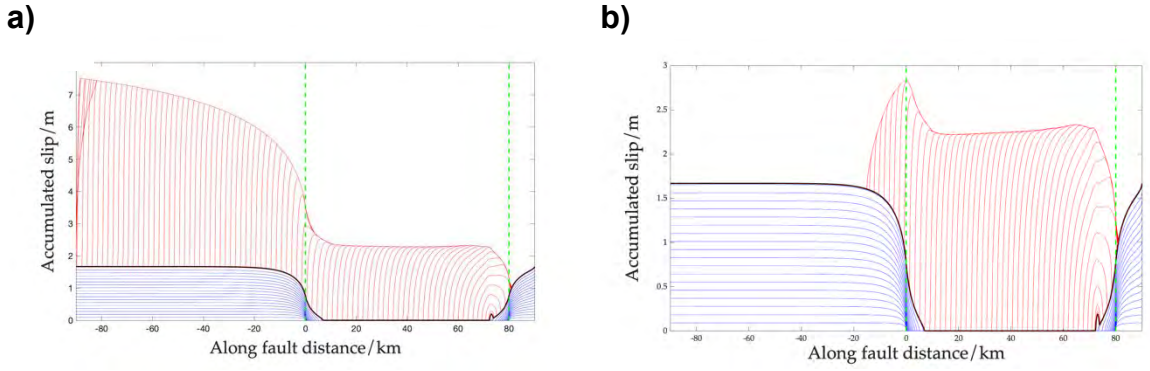

Figure 1. Output from our simulations showing the effects of dynamic weakening on the penetration of Mw 7.2 style events into the creeping section. Blue lines indicate aseismic slip at two-year intervals. Red lines show seismic slip every 0.5 seconds. The 90km long creeping section is on the left-hand side of both figures The green dashed lines indicate the extent of the velocity weakening zone, with velocity strengthening properties outside of this. **a)** With strong dynamic weakening, left going events rupture through the entire 90km creeping section in this model. **b)** Weak dynamic weakening causes the left going event to rapidly die out after hitting the creeping section (note the difference in scale).

References

Andrews, D. J. (2005). Rupture dynamics with energy loss outside the slip zone. *Journal of Geophysical Research: Solid Earth*, *110*(1), 1–14. https://doi.org/10.1029/2004JB003191

Cubas, N., Lapusta, N., Avouac, J. P., & Perfettini, H. (2015). Numerical modeling of long-term earthquake sequences on the NE Japan megathrust: Comparison with observations and implications for fault friction. *Earth and Planetary Science Letters*, *419*, 187–198. https://doi.org/10.1016/j.epsl.2015.03.002

Di Toro, G., Han, R., Hirose, T., De Paola, N., Nielsen, S., Mizoguchi, K., … Shimamoto, T. (2011). Fault lubrication during earthquakes. *Nature*, *471*(7339), 494–498. https://doi.org/10.1038/nature09838

Jiang, J., & Lapusta, N. (2016). Deeper penetration of large earthquakes on seismically quiescent faults. *Science*, *352*(6291), 1293–1297. https://doi.org/10.1126/science.aaf1496

Jiang, J., & Lapusta, N. (2017). Connecting depth limits of interseismic locking, microseismicity, and large earthquakes in models of long-term fault slip. *Journal of Geophysical Research: Solid Earth*. https://doi.org/10.1002/2017JB014030

Noda, H., & Lapusta, N. (2013). Stable creeping fault segments can become destructive as a result of dynamic weakening. *Nature*, *493*(7433), 518–521. https://doi.org/10.1038/nature11703

Rice, J. R. (2006). Heating and weakening of faults during earthquake slip. *Journal of Geophysical Research: Solid Earth*, *111*(5), 1–29. https://doi.org/10.1029/2005JB004006

Viesca, R. C., & Garagash, D. I. (2015). Ubiquitous weakening of faults due to thermal pressurization. *Nature Geoscience*, *8*(11), 875–879. https://doi.org/10.1038/ngeo2554

GeoProc2019: Earthquake and Faulting mechanics

7th International Conference on Coupled THMC Processes in Geosystems
3-5 July 2019 Utrecht (Netherlands)

Spontaneous fault slip acceleration relating to a switch of the deformation mechanism

M. Takahashi[1]

Keywords: pressure solution creep, halite-muscovite mixture gouge, rotary shear experiment, shear stress step change test, spontaneous slip acceleration/deceleration, critical velocity for a runaway slip

Earthquake nucleation and propagation involves the acceleration of slip on a fault from a background, quasi-static, low-velocity state towards meter-per-second values. From shear experiments using brine-saturated simulated gouge composed of 80:20 wt.% mixtures of halite and muscovite (following e.g. Niemeijer & Spiers, 2007), Takahashi et al., [2017] recently reported a switch in the dominant deformation process, from distributed viscous flow (pressure solution creep) to localized brittle deformation, at a critical velocity V_c (~20 μm/sec). The direct effect which is normally observed upon perturbations in sliding rate disappears for $V > V_c$, suggesting that runaway fault-slip may be achieved when the sliding velocity exceeds V_c.

At relatively low shear stress, pressure solution creep will be fast enough to effectively suppress slip acceleration. However, with increasing the shear stress, there may be a velocity range in which pressure solution creep still works but not as effective. I hypothesize that, under constant shear stress boundary conditions, this may lead to spontaneous acceleration followed by deceleration, analogous to a slow slip event. Moreover, imposing the constant shear stress with equal or larger value of the maximum strength of the simulated gouge, I also hypothesize that slip acceleration may proceed as $V > V_c$, inducing a dynamic weakening.

To address these hypotheses, I conducted torque-controlled rotary shear experiments, using brine-saturated, 80:20 wt % mixtures of halite (grain size < 75 μm) and muscovite (grain size < 33 μm) powders. Approximately 1.65 g of the gouge mixture was sandwiched between two teethed steel piston rings, forming an initially 1 mm thick layer. The piston rings had an inner diameter of 38 mm, and an outer diameter of 50 mm. I used a high-velocity rotary shear apparatus designed by T. Shimamoto [e.g., Togo and Shimamoto, 2012], and now installed at the Geological Survey of Japan (GSJ). The apparatus was modified to enable torque control with an accuracy of ±0.002 in the friction coefficient (μ), at a normal stress of 5 MPa. Rotation displacement is measured using a potentiometer installed close to the piston ring at the rotating side. I obtained a well-reproducible relationship between steady-state friction coefficient and

[1] Geological Survey of Japan, National Institute of Advanced Industrial Science and Technology (AIST), 1-1-1 Higashi, Tsukuba 305-8567, Japan, miki.takahashil@aist.go.jp

steady-state sliding velocity, comparable with the results from Takahashi et al. [2017] and Niemeijer and Spiers [2007].

Figure 1 shows a preliminary result of the velocity evolution after stepwise changes in the shear stress. At low shear stresses, corresponding to the pressure solution creep-controlled regime, transient increasing velocity towards a steady-state values suggests stable sliding (blue line in Fig. 1). At $\mu \approx 0.6$, the simulated gouge shows spontaneous acceleration to $V \approx 1$ μm/sec, followed by deceleration (green and purple lines in Fig.1). Lastly, under a constant shear stress condition equivalent to $\mu = 0.67$, spontaneous slip acceleration occurred followed by dynamic weakening at $V \approx V_c = 20$ μm/sec (red line in Fig. 1). More experiments and microstructural observations will help to elucidate the relationship between the critical velocity and the switch among dominant deformation mechanisms.

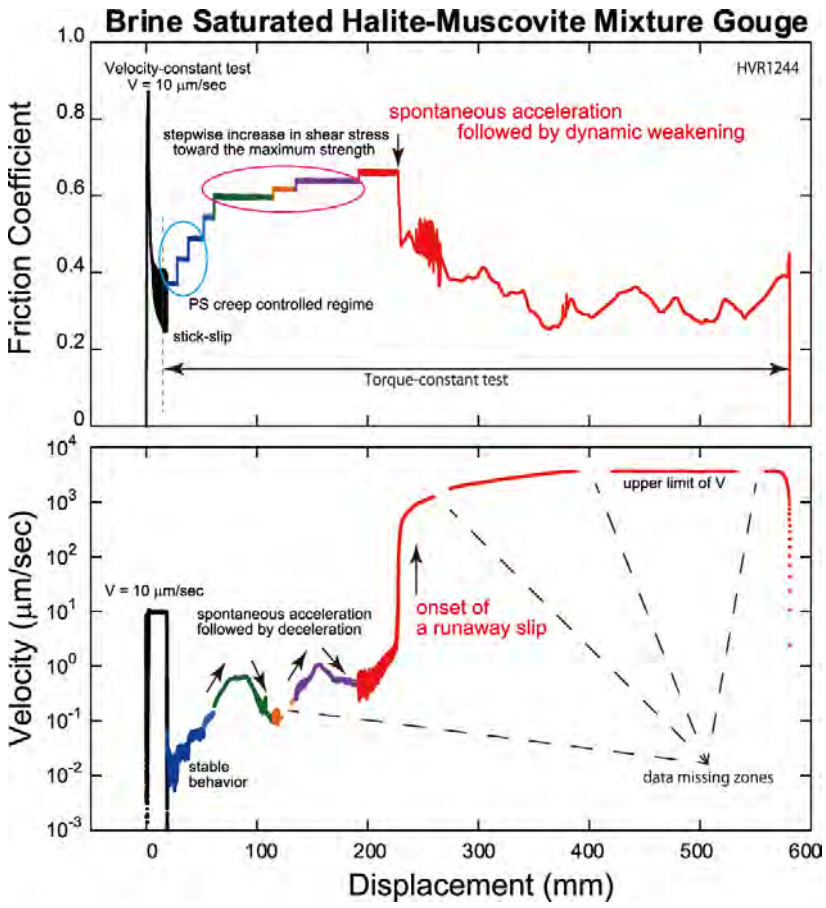

Figure 1. A typical run of shear stress step change tests.

References

Takahashi, M., M. P. A. van den Ende, A. R. Niemeijer, and C. J. Spiers (2017), Shear localization in a mature mylonitic rock analog during fast slip, Geochem. Geophys. Geosyst., 18, doi:10.1002/2016GC006687.

Niemeijer, A. R., and C. J. Spiers (2007), A microphysical model for strong velocity weakening in phyllosilicate-bearing fault gouges, J. Geophys. Res., 112, B10405, doi:10.1029/2007JB005008.

Togo, T. and T. Shimamoto, (2014), Energy partition for grain crushing in quartz gouge during subseismic to seismic fault motion: An experimental study, Journal of Structural Geology 38, 139-155, doi:10.1016/j.jsg.2011.12.014

GeoProc2019: Earthquake and Faulting mechanics

7th International Conference on Coupled THMC Processes in Geosystems
3-5 July 2019 Utrecht (Netherlands)

Relationship research on anthropogenic seismicity using satellite radar interferometry and IS-EPOS data

A. Tama[1], A. Guzy[2], A. Malinowska[3], R. Hejmanowski[4], W. Witkowski[5]

Keywords: human-induced earthquake, mining impacts, DInSAR analysis, IS-EPOS data

Nowadays, human-induced seismicity has become one of the important topic among the general community. Increased interest in this subject is associated with regions that are constantly exposed to this type of dynamic phenomena. In many cases, the occurrence of these phenomena has its foundation in underground mining. In combination with natural geological, physical and geomechanical conditions of the rock mass, they constitute an ideal place for the formation of mining-induced earthquakes.

Authors of the article focused on the study of two mining-induced earthquakes in the regions of Legnica-Glogow Copper District (LGCD) and Upper Silesia Coal Basin (USCB) in Poland (Figure 1). The main purposes of the research were examination of mutual relationships between these phenomena using data from IS-EPOS platform and satellite radar interferometry technique (DInSAR). Data analysis was performed for the induced earthquakes with the magnitude M=3.7 on 8 April, 2017 (LGCD region) and 23 April, 2018 (USCB region).

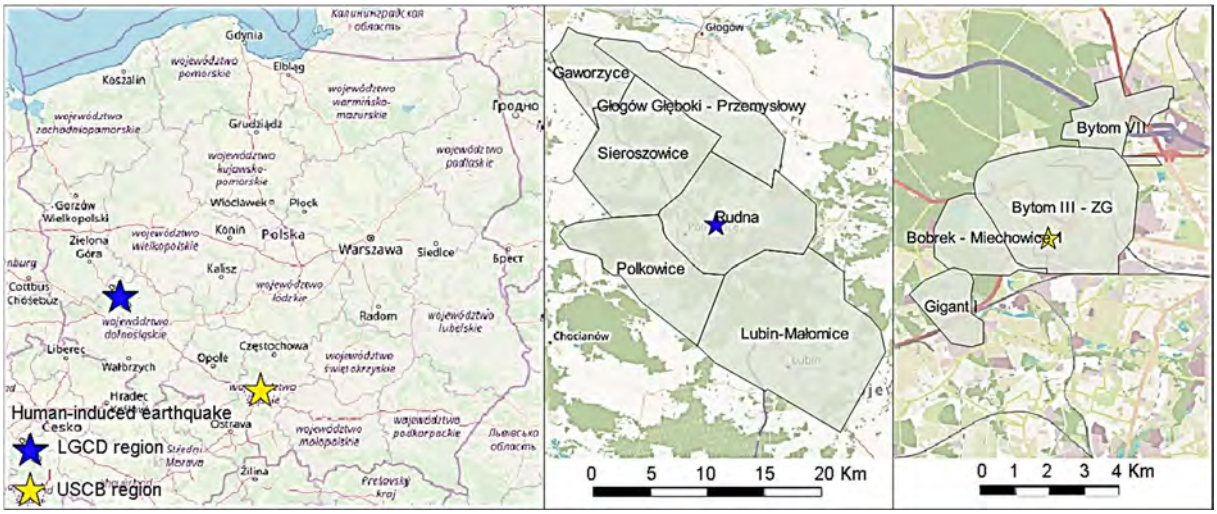

[1] AGH University of Science and Technology, atama@agh.edu.pl
[2] AGH University of Science and Technology, aguzy@agh.edu.pl
[3] AGH University of Science and Technology, amalin@agh.edu.pl
[4] AGH University of Science and Technology, hejman@agh.edu.pl
[5] AGH University of Science and Technology, wwitkow@agh.edu.pl

Figure 1. Research area (OSM map foundation).

In case of interferometric data analysis, the research was mainly carried out towards vertical ground movements. The data included a period of about two weeks before and after the earthquakes to investigate the actual changes in the surface area that were caused by these earthquakes. The research included satellite images from the ascending and descending orbits (Table 1).

Table 1. Interferometric data included induced earthquakes in both research areas.

Amount of interferograms	Pass	First master image	Last slave image	Time interval [days]	Orbit track
4	ascending	28.03.2017	21.04.2017	6	73
4	descending	31.03.2017	24.04.2017	6	22
4	ascending	12.04.2018	06.05.2018	6	102
3	descending	14.04.2018	02.05.2018	6	124

References

Jian-po, L., X. Shi-da and L. Yuan-hui (2018), Relationship between microseismic activities and mining parameters during deep mining process, *J. of Applied Geophysics*, *159*, 814–823, doi: 10.1016/j.jappgeo.2018.10.018

Konicek, P., and P. Waclawik (2018), Stress changes and seismicity monitoring of hard coal longwall mining in high rockburst risk areas, *Tunnelling and Underground Space Technology*, *81*, 237–251, doi: 10.1016/j.tust.2018.07.019

Kozłowska, M., B. Orlecka-Sikora, Ł. Rudziński, S. Cielesta and G. Mutke (2016), *International J. of Rock Mechanics and Mining Sciences, 86*, 5-15, doi: 10.1016/j.ijrmms.2016.03.024

Kurzeja, J. (2017), Seismometric monitoring in the area of the Piekary Śląskie junction of the A1 motorway in terms of recording the vibrations resulting from mining tremors, *J. of Sustainable Mining, 16(1),* 14-23, doi: 10.1016/j.jsm.2017.06.002

Li Y., T. Yang, H. Liu, H. Wang, X. Hou, P. Zhang and P. Wang (2016), Real-time microseismic monitoring and its characteristic analysis in working face with high-intensity mining, *J. of Applied Geophysics, 132,* 152-163, doi: 10.1016/j.jappgeo.2016.07.010

Wu J., X. He, Y. Li, P. Shi, T. Ye and N. Li (2019), How earthquake-induced direct economic losses change with earthquake magnitude, asset value, residential building structural type and physical environment: An elasticity perspective, *J. of Environmental Management, 231,* 321-328, doi: 10.1016/j.jenvman.2018.10.050

GeoProc2019: Earthquake and Faulting mechanics

7th International Conference on Coupled THMC Processes in Geosystems
3-5 July 2019 Utrecht (Netherlands)

Microphysical modelling of laboratory and field injection tests

M. van den Ende[1], *M. Scuderi*[2], *F. Cappa*[1,3], *J.-P. Ampuero*[1,4]

Keywords: fault friction, fluid injection, microphysical modelling, laboratory experiments

Induced seismicity is of primary concern in human subsurface activities, including geothermal energy production, wastewater and CO_2 injection, and hydrocarbon extraction. Seismicity triggered around injection sites is generally attributed to elevated pore fluid pressures, which lower the clamping stress that keeps the fault locked (*Elsworth et al., 2016*). Additionally, recent field injection tests at decametric scale reveal the importance of aseismic creep in driving seismicity (*Duboeuf et al., 2017*), and long-range poroelastic effects have been inferred to trigger seismicity well beyond the extent of the stimulated region (*Goebel & Brodsky, 2018*). To better assess the earthquake hazard associated with the injection and extraction of geofluids, potential mechanisms underlying the nucleation of induced seismic events need to be identified.

Laboratory experiments provide the means to investigate the mechanisms for (unstable) fault slip at high resolution under well-controlled conditions, but lack the complexity typical of real-world injection systems. Field-scale injection tests strike a suitable compromise between observational resolution and inherent system complexity, and so the combined analysis of laboratory and field injection tests advances the understanding of induced seismicity at the reservoir scale (*Cappa et al., subm.*).

In the present study, the laboratory results of *Scuderi et al. (2017)* are re-interpreted using a numerical simulator based on the Chen-Niemeijer-Spiers microphysical model (*Chen & Spiers, 2016; Niemeijer & Spiers, 2007*). Some of the main advantages of the CNS model over empirical methods are that it explicitly prescribes the volumetric deformation of the gouge, and that many model parameters can be constrained by microstructural observations and independent laboratory tests. Following the procedure detailed by *Scuderi et al.*, we have modelled the injection of fluids in a thin fault gouge layer, and tested different pore fluid injection rates and micromechanical properties. Preliminary results show that the microphysical model reproduces the main trends of the evolution in fault slip velocity and volumetric deformation in response to step-wise pressure stimulation (see Fig. 1). The adopted modelling framework is suitable to incorporate into numerical codes for field-scale modelling of fluid injection tests and production-related induced seismicity, and so the nucleation of injection-induced seismicity can be investigated, incorporating observations from the laboratory and the coupling between fluid pressure diffusion and gouge frictional behaviour.

1) Université Côte d'Azur, IRD, CNRS, Observatoire de la Côte d'Azur, Géoazur, France
2) Dipartimento di Scienze della Terra, La Sapienza Università di Roma, Rome, Italy
3) Institut Universitaire de France, Paris, France
4) California Institute of Technology, Seismological Laboratory, USA

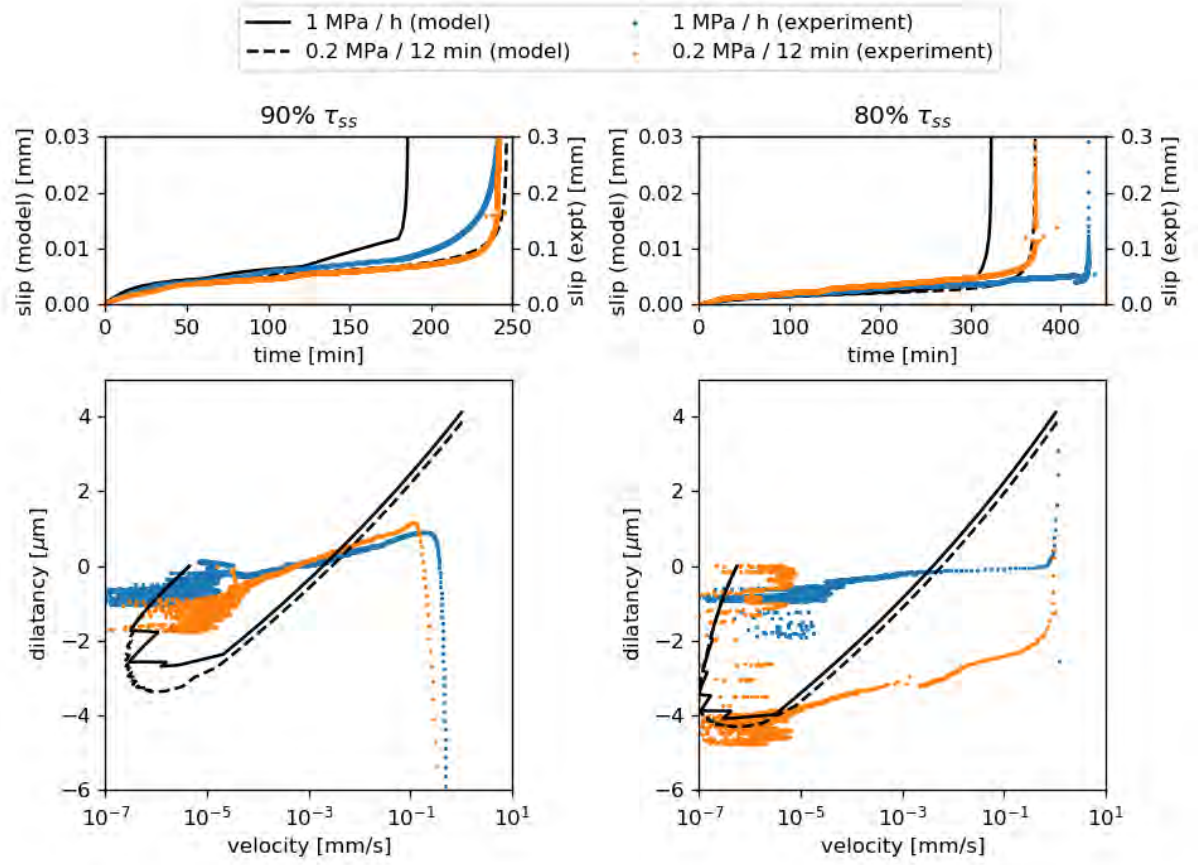

Figure 1: CNS model predictions (black solid and dashed lines) of shear and volumetric deformation of a gouge in response to stepwise fluid pressure stimulation compared with the laboratory data of *Scuderi et al. (2017*; blue and orange dots*)*. The main experimental trends are captured qualitatively. To achieve quantitative agreement, further refinement of the model is needed.

References

Cappa, F., M. M. Scuderi, C. Collettini, Guglielmi Y. and J.-P. Avouac (submitted), Stabilization of fault slip by fluid injection in the laboratory and in-situ, *Sci. Adv.*

Chen, J., and C. J. Spiers (2016), Rate and state frictional and healing behavior of carbonate fault gouge explained using microphysical model, *J. Geophys. Res. Solid Earth.*, *121*, doi:10.1002/2016JB013470

Duboeuf, L., L. de Barros, F. Cappa, Y. Guglielmi, A. Deschamps, and S. Seguy (2017), Aseismic motions drive a sparse seismicity during fluid injections into a fractured zone in a carbonate reservoir, *J. Geophys. Res. Solid Earth*, 122, doi:0.1002/2017JB014535

Elsworth, D., A. R. Niemeijer, and C. J. Spiers (2016), Understanding induced seismicity, Science, 354(6318), 1380-1381, doi:10.1126/science.aal2584

Goebel, T. H. W., E. E. Brodsky (2018), The spatial footprint of injection wells in a global compilation of induced earthquake sequences, Science, 361(6405), 899-904, doi:10.1126/science.aat5449

Niemeijer, A. R., and C. J. Spiers (2007), A microphysical model for strong velocity weakening in phyllosilicate-bearing fault gouges, *J. Geophys. Res.*, 112, doi:10.1029/2007JB005008,

Scuderi, M. M., C. Collettini, and C. Marone (2017), Frictional stability and earthquake triggering during fluid pressure stimulation of an experimental fault. *EPSL*, 477, 84-96, doi:10.1016/j.epsl.2017.08.009

GeoProc2019: Earthquake and Faulting mechanics

7th International Conference on Coupled THMC Processes in Geosystems
3-5 July 2019 Utrecht (Netherlands)

Panoramic View of Fault failure modes from laboratory and numerical experiments

Deepa Mele Veedu[1], Carolina Giorgetti[2], Marco Scuderi[3], Sylvain Barbot[4], Chris Marone[5], and Cristiano Collettini[3,6]

Keywords: slow slip, dynamic events, short-term forecasting

Certain phenomena in nature occur in Goldilocks zones that provide just the right conditions. One such phenomenon in earthquake science seems to be the occurrence of slow slip preceding dynamic slip. For example, the slow slip before the 2011 Mw 9.0 Tohoku-Oki, Japan (Ito et al., 2013; Kato et al., 2012), 2014 Mw 8.2 Iquique, Chile (Meng et al., 2015; Ruiz et al., 2014) and 2015 Mw 8.4 Illapel, Chile (Huang and Meng, 2018) add to the growing number of such observations. Our quest is to understand the physics behind such phenomena.

One way to find the reasons for the slow-fast phenomena is to test the fault in a controlled setting. Several studies report the occurrence of transient deformation in rock frictional studies (Gu and Wong, 1994; Leeman et al., 2015, 2016; McLaskey and Yamashita, 2017). However, a comprehensive understanding of the possible parameters that can influence the slow transients is yet to be known. The primary goal of this work is to investigate the effect of material properties on the slow-fast transitional boundary. Here, we report the results of alternating slow and fast events from the Brittle Rock DeformAtion Versatile Apparatus (BRAVA) at the National Institute of Geophysics and Volcanology (INGV) (Figure 1).

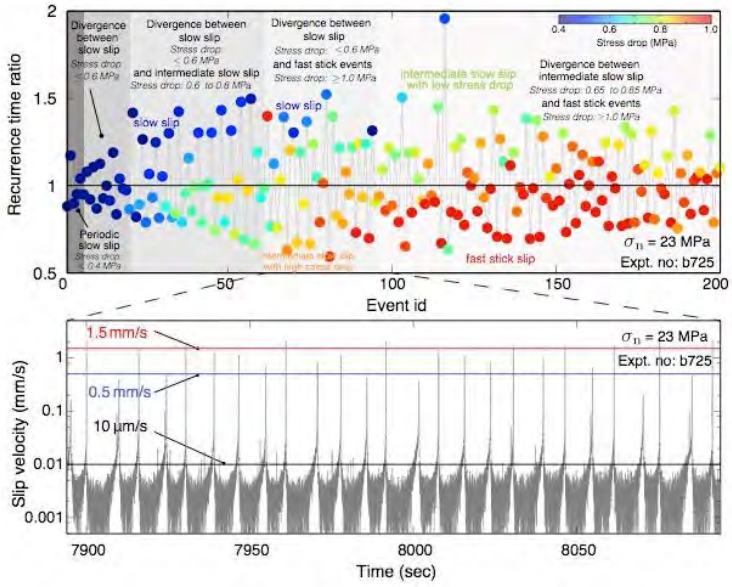

Figure 1: Slip events from the BRAVA apparatus at normal load 23 MPa. (a) Alternating slow and fast slip events emerge at constant loading conditions. (b) Average slip velocities from the fault gouge sample. Events show slow and fast slip velocities crossing 0.5 mm/s and 1.5 mm/s at 23 MPa.

[1]Earth Observatory of Singapore (deepa004@e.ntu.edu.sg) [2]Ecole Polytechnique Federale de Lausanne, Switzerland (carolina.giorgetti@epfl.ch), [3]Universit degli Studi La Sapienza, Italy, (marco.scuderi@uniroma1.it), [4]University of Southern California, United States, (sbarbot@usc.edu), [5]Penn State University, United States (cjm38@psu.edu), [6]Istituto Nazionale di Geofisica e Vulcanologia, Italy (cristiano.collettini@uniroma1.it).

We show that a mixed slow-fast rupture sequences occur under a set of physical conditions (friction, ambient pressure, fault geometry) in between those that produce distinct slow-slip events and fast earthquakes (Leeman et al., 2015, Leeman et al., 2016, Scuderi et al., 2016). The laboratory results from the Biax machine at the Penn State University confirms that the same material can exhibit the dual mode deformation at a constant normal load (Figure 2). To depict a broad view of possible failure modes, we integrate the results from double direct shear biaxial experiments (Leeman et al., 2015, 2016, Scuderi et al., 2016} and dynamic fault modeling (Lapusta and Liu, 2009).

In the laboratory, we vary the stiffness of the system to demarcate the boundaries of failure modes, identifying those with period-doubling and chaotic recurrence intervals. The bifurcation from slow-slip to period-two slow and fast ruptures is reproduced in numerical simulations, but only in models that adequately capture the fault dynamics in three dimensions. Our findings highlight a range of possible slip behaviors emerging from the fundamental nature of the fault and provide clues into a potential long preparatory phase that precedes earthquake nucleation.

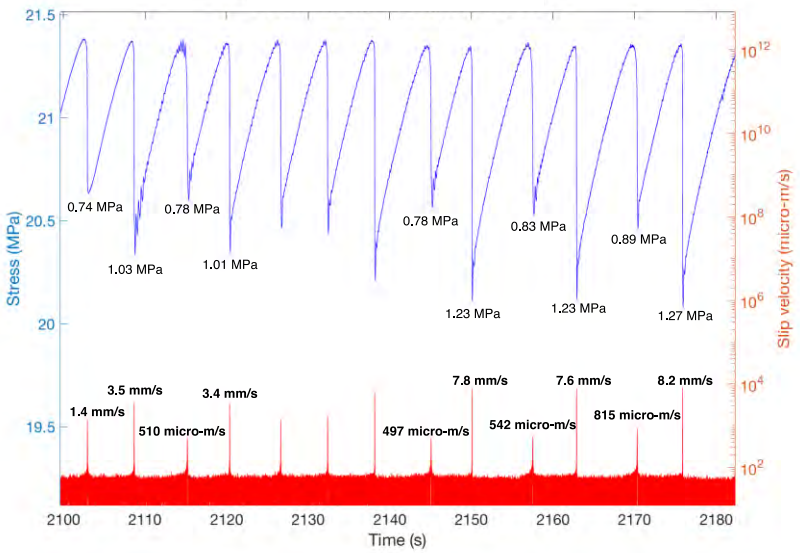

Figure 2: Consecutive slow and fast slip events are reproduced at constant load 33 MPa using the Biax machine at the Penn State laboratory. The audible stick-slip events are 6 to 16 times faster than the preceding inaudible slow events.

References

Ito, Y., et al., Episodic slow slip events in the japan subduction zone before the 2011 Tohoku-oki earthquake, Tectonophysics, 600, 14 - 26, 2013.

Kato, A., et al., Propagation of slow slip leading up to the 2011 Mw 9.0 Tohoku-oki earthquake, Science, 335 (6069), 705-708, 2012.

Meng, L., H. Huang, R. Burgmann, J. P. Ampuero, and A. Strader, Dual megathrust slip behaviors of the 2014 Iquique earthquake sequence, Earth Planet. Sci. Lett., 411, 177-187, 2015.

Ruiz, S., M. Metois, A. Fuenzalida, J. Ruiz, F. Leyton, R. Grandin, C. Vigny, R. Madariaga, and J. Campos, Intense foreshocks and a slow slip event preceded the 2014 Iquique mw 8.1 earthquake, Science, 345 (6201), 1165-1169, 2014.

Huang, H., and L. Meng, Slow unlocking processes preceding the 2015 mw 8.4 Illapel, Chile, earthquake, Geophys. Res. Lett., 45, 2018.

Leeman, J. R., M. M. Scuderi, C. Marone, and D. M. Saffer, Stiffness evolution of granular layers and the origin of repetitive, slow, stick-slip frictional sliding, Granular Matter, 17, 447-457, 2015.

Leeman, J. R., , D. M. Saffer, M. M. S. Saffer, and C. Marone, Laboratory observations of slow earthquakes and the spectrum of tectonic fault slip modes, Nat. Commun., 7 (7:11104), 2016.

Scuderi, M. M., C. Marone, E. Tinti, D. D. Stefano, and C. Colletini, Precursory changes in seismic velocity for the spectrum of earthquake failure modes, Nat. Geosci., 9, 695{700, 2016.

Lapusta, N. & Liu, Y. Three-dimensional boundary integral modeling of spontaneous earthquake sequences and aseismic slip. J. Geophys. Res. 114, 25 PP. (2009).

Gu, Y., and T.-F. Wong, Nonlinear dynamics of the transition from stable sliding to cyclic stick-slip in rock, in Nonlinear Dynamics and Predictability of Geophysical Phenomena, Geophysical Monograph Series, pp. 15{35, AGU, 1994.

McLaskey, G. C., and F. Yamashita, Slow and fast ruptures on a laboratory fault controlled by loading characteristics, J. Geophys. Res., 122 (5), 3719-3738, 2017.

GeoProc2019: Earthquake and Faulting mechanics

7th International Conference on Coupled THMC Processes in Geosystems
3-5 July 2019 Utrecht (Netherlands)

Simulated quartz-feldspar faults sheared under conditions spanning the brittle-plastic transition

B. A. Verberne[1], S. Arai[2], M. Takahashi[3], J. Muto[4]

Keywords: quartz, feldspar, friction, faults, seismogenesis

The material-physical processes controlling earthquake rupture are lacking observations of fault-slip under real, in-situ conditions of the seismogenic zone, even for the most abundant minerals in the continental crust - quartz and feldspar. With the aim to unravel the deformation processes controlling fault strength and stability in the quartzofeldspathic upper-crust, we conduct shear experiments on ~1 mm thick simulated faults composed of 50/50 wt.% quartz-feldspar mixtures (Fig. 1a).

Experiments are conducted under room-dry conditions using the Argon-medium high-pressure high-temperature deformation apparatus ("Argo") installed at the Geological Survey of Japan (GSJ) (Masuda et al., 2002) (Fig. 1b), and using the Griggs solid medium deformation apparatus installed at Tohoku University (Kido et al., 2016) (Fig. 1c). Imposing realistic geothermal (30°C/km) and lithostatic pressure gradients (~27 MPa/ km) for the continental crust, we explore intrinsic fault stability transitions with increasing pressure and temperature, i.e. at strain rates of ~10^{-3} s^{-1}. To assess the importance of increasing confining pressure for simulating transitions in fault stability pertaining to the base of the seismogenic zone, we repeat this series, however while maintaining a constant confining pressure of ~185 MPa. Sheared samples are investigated using light and electron microscopes installed at GSJ, as well as through the open research platform of Tsukuba Innovation Arena (TIA). The results will be used to construct the first, fully experimentally-based fault strength and stability profile for the quartzofeldspathic continental crust, which provides input for existing numerical codes for crustal fault rupture while serving as a starting-point for microphysically-based fault-slip models.

[1] Geological Survey of Japan, National Institute of Industrial Science and Technology, Tsukuba, Japan, ba.verberne@aist.go.jp
[2] Department of Earth Science, Tohoku University, Sendai, Japan, shun.arai.t4@dc.tohoku.ac.jp
[3] Geological Survey of Japan, National Institute of Industrial Science and Technology, Tsukuba, Japan, miki.takahashi@aist.go.jp
[4] Department of Earth Science, Tohoku University, Sendai, Japan, jun.muto.a3@tohoku.ac.jp

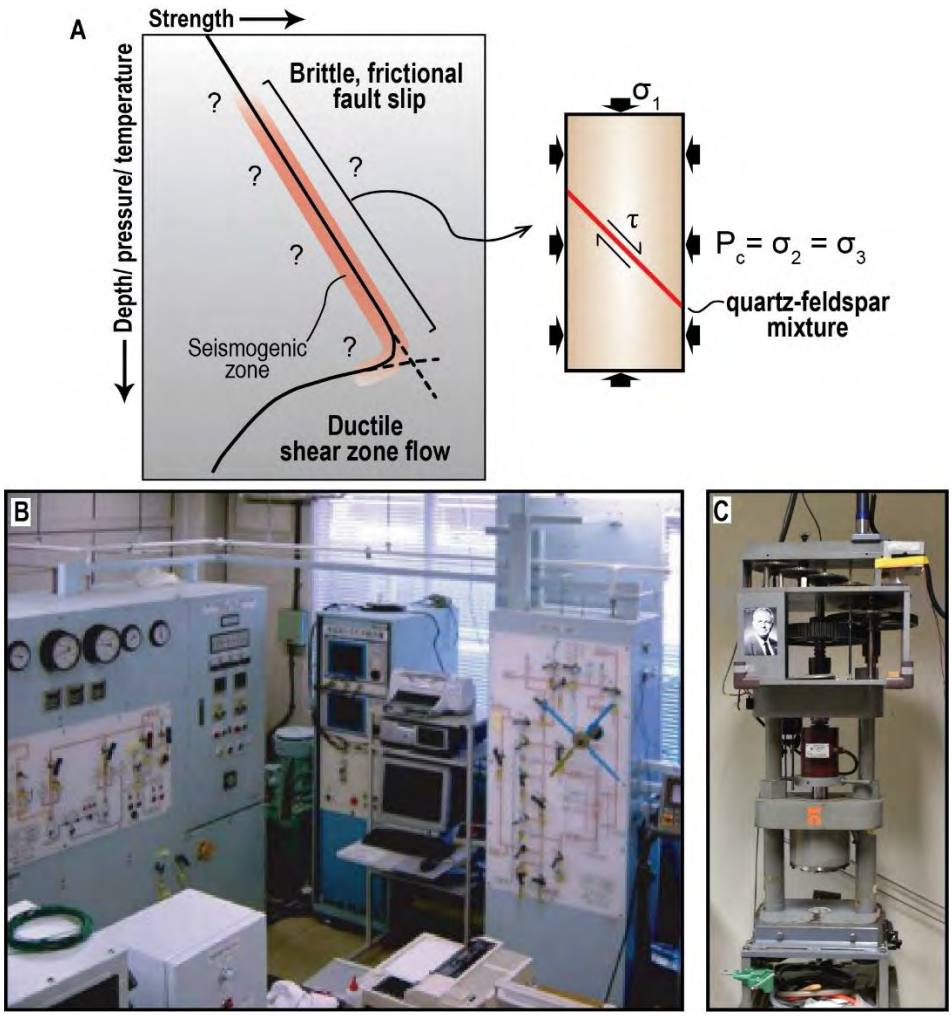

Figure 1. A. Saw-cut shear experiments on simulated gouge layers composed of quartz-feldspar mixtures are used to unravel fault strength and -stability under conditions pertaining to the upper continental crust. B. The Argon-medium HPHT deformation apparatus ("Argo") at the Geological Survey of Japan. C. The Griggs-type deformation apparatus at Tohoku University.

References

Kido, M., J. Muto, and H. Nagahama (2016), Method for correction of differential stress calculations from experiments using the solid salt assembly in a Griggs-type deformation apparatus, *Tectonophysics*, *672-673*, 170-176, doi: 10.1016/j.tecto.2016.02.011.

Masuda, K., K. Fujimoto, and T. Arai (2002), A new gas-medium, high-pressure and high-temperature deformation apparatus at AIST, Japan. *Earth Planets Space*, *54*, 1091-1094, https://doi.org/10.1186/BF03353307.

GeoProc2019: Earthquake and Faulting mechanics

7th International Conference on Coupled THMC Processes in Geosystems
3-5 July 2019 Utrecht (Netherlands)

Geochemistry of pseudotachylyte formed at shallow depths during large in magnitude earthquakes

H. Wang[1], H.B. Li[2], J.L. Si[3], G. Di Toro[4]

Keywords: Pseudotachylyte, Geochemistry, Earthquake, WFSD, Longmen Shan

Pseudotachylytes, produced by frictional heating during seismic slip, convey information about earthquake source process (e.g., coseismic fault strength) that are extremely difficult to retrieve by means of seismological observations. Pseudotachylytes are commonly reported to be generated at > 5 km depth and exposed at the surface by tectonic exhumation and uplift. Because of the fluid-rock interaction concomitant to the exhumation of the fault zone, the chemical composition of the pseudotachylytes at the Earth's surface may not correspond to their pristine composition when produced at depth (Wang et al., 2019). As consequence, pseudotachylyte alteration during exhumation may render very speculative the reconstruction of the ambient conditions in which they formed or the estimation of the viscosity of the friction melt.

The Wenchuan earthquake Fault Scientific Drilling (WFSD) project was conducted along the Yingxiu-Beichuan and Guanxian-Anxian faults to improve our understanding of the mechanics of the 2008 Mw7.9 Wenchuan earthquake. The first borehole (WFSD-1), with a final depth of 1201.15 m, was drilled in the hanging wall of the southern Yingxiu-Beichuan fault (Li et al., 2013). The drilling cores are composed of the Pengguan Complex rocks above 585.75 m-depth and of the Xujiahe Formation sedimentary rocks below 598 m-depth.

A ~2 mm-thick pseudotachylyte was recognized at the depth of ~732.6 m in the non-cohesive fault gouges of the WFSD-1. Under the Scanning Electron Microscope, the glassy matrix of the pseudotachylyte is cut by a dense network of microcracks, probably produced during melt quenching. Most of the microcracks are open with few filled by barite (see below). These microstructural features imply that during or just after seismic slip, the fault core materials were permeated by a vigorous fluid influx, likely dissipating the frictional heat and resulting in a rapid temperature drop, which further facilitated the solidification of the melt, thus welded fault (Mitchell et al., 2016) and hampered the post-seismic fault afterslip.

Geochemical analysis with micro X-ray fluorescence scanner (μXRF) show that the pseudotachylytes are highly enriched in Ba, Ti and S, and depleted in Si, Fe, Ca, Mn,

[1] Institute of Geology, Chinese Academy of Geological Sciences, China, wanghuan4585@126.com
[2] Institute of Geology, Chinese Academy of Geological Sciences, China, lihaibing06@163.com
[3] Institute of Geology, Chinese Academy of Geological Sciences, China, gongrenbaqin@126.com
[4] University of Padova, Italy, giulio.ditoro@unipd.it

Mg with respect to the fault gouge (Fig. 1). Focused Ion Beam-Transmission Electron Microscope investigations show that some microcracks cutting the glassy matrix of the pseudotachylyte are filled by newly formed nano barites (high abundance of Ba and S), a low temperature hydrothermal mineral. However, Ti, a highly immobile element, is enriched in the glass with respect to the fault gouge. We infer that the high temperature fluid-rock interaction may play an important role in the diffusion and migration of chemical elements in fault zones. The specific mechanisms responsible for the enrichment of Ti and depletion of Fe, Mn in the slipping zone need further investigations. A promising result of this preliminary study is that the recovering of less altered pseudotachylytes, possibly associated to the Wenchuan Mw7.9 2008 earthquake, will allow us to reconstruct frictional melting processes during seismic slip at shallow depths.

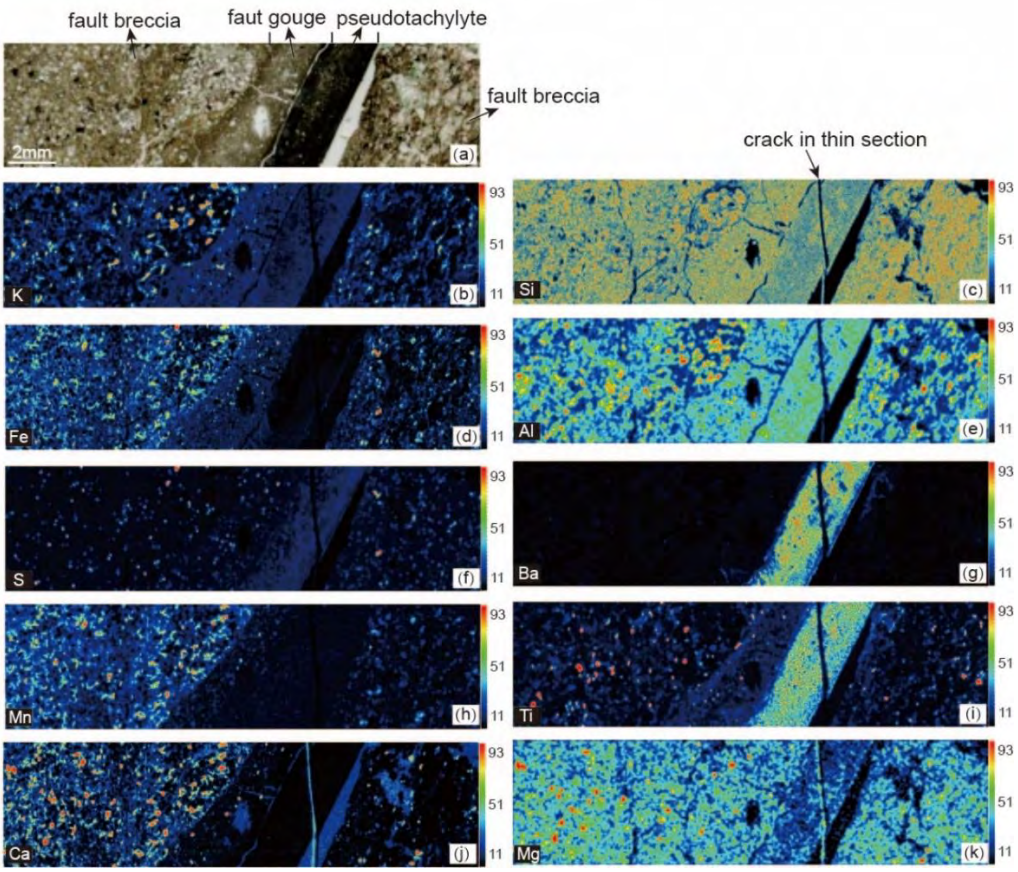

Figure 1. Single element maps measured with μXRF scanner on a thin section of the pseudotachylyte recovered from the WFSD1 core. (a) Microstructure of pseudotachylyte. (b-k) Single elemental maps of K, Si, Fe, Al, S, Ba, Mn, Ti, Ca and Mg. Color bars represent XRF intensity (cps/mA), the red areas correspond to high abundance.

References

Li, H.B., H. Wang, Z.Q. Xu, J.L. Si, J.L. Pei, and T.F. Li, et al. (2013). Characteristics of the fault-related rocks, fault zones and the principal slip zone in the wenchuan earthquake fault scientific drilling project hole-1 (WFSD-1). Tectonophysics, 584, 23-42.

Mitchell, T. M., Toy, V., Toro, G.D., Jörg Renner, and Sibson, R. (2016). Fault welding by pseudotachylyte formation. Geology, 44(12), G38373.1.

Wang, H., H.B. Li, J.L. Si, L. Zhang, and Z.M. Sun. (2019). Geochemical features of the pseudotachylytes in the Longmen Shan thrust belt, eastern Tibet, Quaternary International, doi:10.1016/j.quaint.2018.12.030.

GeoProc2019: Earthquake and Faulting mechanics

7th International Conference on Coupled THMC Processes in Geosystems
3-5 July 2019 Utrecht (Netherlands)

Along strike variation of fault friction constrained by GPS observations

Lifeng Wang[1]

Keywords: seismic cycle, GPS, friction

Determination of the constitutive frictional parameters is crucial for describing the dynamic behaviors of natural faults. In this study, we explore the along-strike variation in fault friction along the San Andreas Fault in Parkfield, where characteristic M6 earthquakes occur nearly every 25 years. Using displacement data measured over decades encompassing the inter-, co- and post-seismic phase of the 2004 M6 event, which involve inherent fault rheological responses to tectonic loading, we construct a physical model based on the rate-dependent friction law to describe the fault slip and stress evolution. Our modeled friction rate parameter is consistent with available laboratory measurements using fault cores collected from the San Andreas Fault Observatory at Depth (SAFOD). Based on the physical model linking inter-, co- and post-seismic phase, we predict that the 25-year slip deficit following the 2004 M6 earthquake will predominantly accumulate in the area to the south of the 2004 event hypocenter, with an energy equivalent to a M6.0 event. Together with the slip deficit accumulated over the 25 years prior to the 2004 event that was unreleased by this event, the total slip deficit amounts to a moment magnitude of M6.35±0.11, suggesting the upper limit of the seismic release level until 2029. The proposed model (1) involves only two free quantities (the friction rate parameter and velocity coefficient used to determine the effective normal stress), (2) is well constrained by available inter-, co- and post-seismic displacement data, and (3) highlights along-strike variations in the fault friction.

[1] Affiliation, wanglf@ies.ac.cn; State Key Laboratory of Earthquake Dynamics, Institute of Geology, China Earthquake Administration

GeoProc2019: Earthquake and Faulting mechanics

7th International Conference on Coupled THMC Processes in Geosystems
3-5 July 2019 Utrecht (Netherlands)

The Role of Fault Slippage and Permeability Evolution of Faults in Supercritical CO_2 Fracturing

Xiaochen We[1,3], *Jingxuan Zhang*[1], *Qi Li*[2*], *Xiangjun Liu*[3], *Lixi Liang*[3]

Keywords: Supercritical CO_2 fracturing, Fracture propagation, Undetected Fault, Fault slippage, Permeability evolution

Understanding the hydromechanical responses of faults during supercritical CO_2 fracturing is important for reservoir management and the design of energy extraction systems. Reservoirs of thin sand and mudstone interbedding were developed in Chang 7 member of the Yanchang Formation, Ordos Basin, China, the supercritical CO_2 fracturing operation have the potential to reactive the undetected faults and leads to unfavorable fracking fluid migrate (Birdsell et al., 2015).

In this work, we examined the role of fault slippage and permeability evolution along a small fault connecting the pay zone and the confining formation during the whole process of fracturing and production (Fig. 1). A coupled hydromechanical model conceptualized from actual engineering results was introduced to address the main concerns of this work, including (1) the mechanical response of fault to CO_2 fracturing and (2) whether the permeability change would affect the vertical conductivity of the confining formation and thus increase the risk for the fracturing fluid to leak.

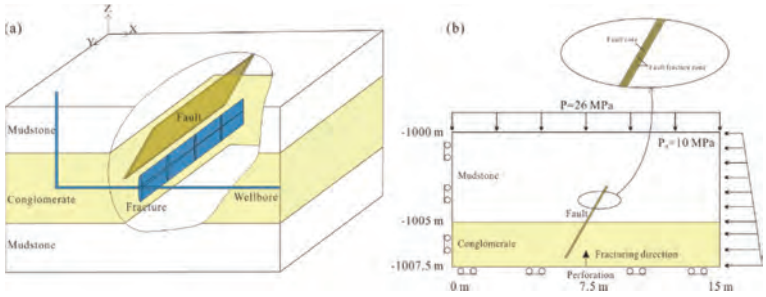

Fig. 1. The generalized geologic structural features (a) and the initial/boundary conditions (b).

Early in the evolution, hydrofractures only form at the perforation, and later, they may fully develop and merge with the fault surface (Davies et al., 2013). Once merged, fault slippage is concentrated there due to the presence of elevated pore pressures generated by the hydrofracturing operation. Further slippage spreads from the zone of high permeability to shallower levels; consequently, the slippages concentrate in the

[1] Southwest Petroleum University, China.
[2] Institute of Rock and Soil Mechanics, Chinese Academy of Sciences. qli@whrsm.ac.cn
[3] State Key Laboratory of Oil and Gas Reservoir Geology and Exploitation, Chengdu, China.

high-permeability fault portion in the conglomerate rather than in the mudstone. The fault experiences the strongest pore pressure migration and induced fault slippage at the end of the “Pump” stage, and afterward, the slip velocity decreases to negative values, and the fault slippage finally reaches stabilization at the end of extraction (Fig. 2).

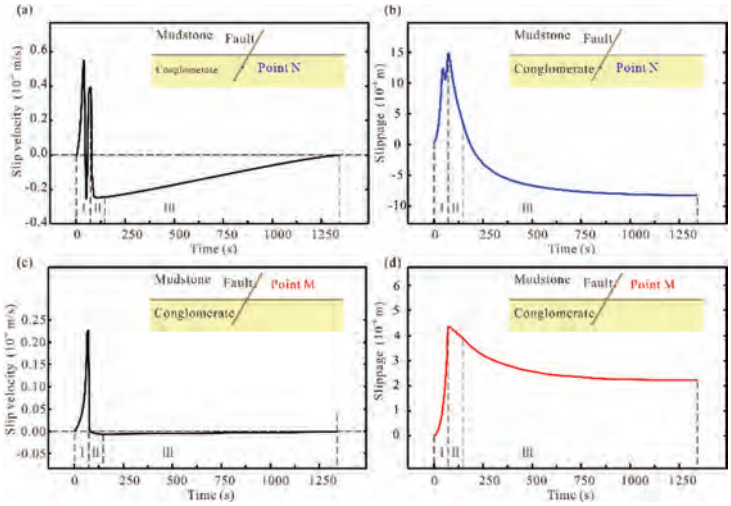

Fig. 2. Evolution of the fault slip velocity and slip displacement at monitoring points M and N through the whole Pump-Hold-Extraction process.

The upward migration of the permeability-enhanced zone enables the capped pore water within the high-permeability fault portion in the conglomerate to diffuse into the surrounding formation and even promotes upward migration of the fracturing fluid into the low-permeability fault portion in the mudstone, which increases the risk of fracturing fluid leakage. As a mechanism for the escape of high pore pressures that cannot be accommodated, the permeability evolution is formed naturally as a result of both fault slippage generated by excess pore pressures within the fault and stress disturbance caused by hydraulic fracturing. The permeability-enhanced zone is concentrated at the fracture-fault intersection and mainly localized in the high-permeability fault portion in the conglomerate, and the extent of this zone depends on the magnitude of the fault slippage. However, due to the limited fault slippage and lower initial permeability, the change in conductivity within the upper portion of the fault in the mudstone is relatively insignificant (Fig. 3).

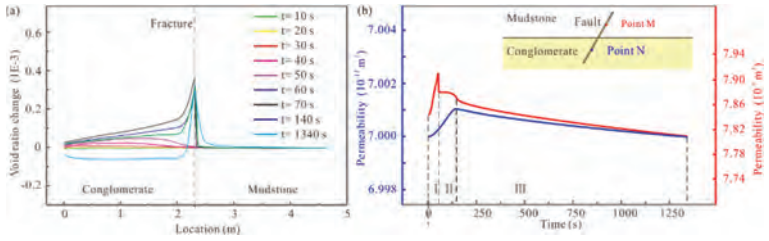

Fig. 3. The void ratio change along the fault surface at different times (a) and the permeability evolution at monitoring points N and M continuously throughout the whole process (b).

References

Birdsell, D.T., Rajaram, H., Dempsey, D., Viswanathan H.S. (2015), Hydraulic fracturing fluid migration in the subsurface: A review and expanded modeling results. *Water Resources Research*, 51, 7159-7188, doi: 10.1002/2015wr017810

Davies, R., Foulger, G., Bindley, A., Styles, P. (2013). Induced seismicity and hydraulic fracturing for the recovery of hydrocarbons. *Marine and Petroleum Geology*, 45, 171-185, doi: 10.1016/j.marpetgeo.2013.03.016

GeoProc2019: Earthquake and Faulting mechanics

7th International Conference on Coupled THMC Processes in Geosystems
3-5 July 2019 Utrecht (Netherlands)

Rupture modelling of a recent substantial tremor in the Groningen field using constraints from ground motion recordings and field data

H.M. Wentinck[1] and K.K.Hindriks[2]

Keywords: induced seismicity, gas production, dynamic rupture modelling, heterogeneous reservoir compaction

This work is part of an ongoing effort to understand small earthquakes or tremors in the giant Groningen gas field, their ground motions and effects on buildings. The tremors follow from reservoir compaction due to gas production over almost 60 years. The tremor hypocentre locations and focal mechanisms have been accurately determined by KNMI, SGS-I and ExxonMobil from ground displacements recordings using the extensive seismometer network in the Groningen field. Now the task is to combine this data with geomechanical data to improve the understanding of fault failure conditions in the Groningen gas reservoir.

This work is about the source mechanism of the recent M 3.4 Zeerijp tremor in January 2018, which is one of three largest tremors in the Groningen field. The hypocentre is in the reservoir at about 3 km depth, like the vast majority of the tremors. The slip direction of the hanging wall is primarily downwards along fault dip indicating that stresses on the fault follow from differential vertical and horizontal field stresses and from compaction due to gas production.

The ground motion spectra of this tremor indicate that the seismic energy has been released quite rapidly for a tremor of this magnitude. The rapid energy release, and herewith the moderate size of the slip plane, imply that the required breakdown stress drop over the slip plane during the rupture is considerable, i.e. several MPa.

The mFS7-Fault-54 fault, which slipped, has a relatively little throw of 40 m when compared to the reservoir thickness of 270 m and has a dip angle of about 80 degrees. The fault has been well characterised by EBN, NAM and SGS-I. The rock properties of the reservoir near the fault are well characterised from well logs, core samples and a distributed strain sensor in one of three wells within 2 km distance of the Zeerijp tremor epicentre. The measured strain in the reservoir reasonably agrees with reservoir compaction data derived from subsidence measurements.

[1] Independent consultant, rickwentinck@kpnmail.nl
[2] Shell Global Solutions International, Kees.K.Hindriks@shell.com

Combining all data and using reasonable estimates for the in-situ field stresses, we could constrain many parameters of a dynamic rupture model for this fault. In particular, we have incorporated the heterogeneous compaction in the reservoir around the fault and the effect of pressure depletion in the upper part of the Carboniferous underburden over the production time of the gas field.

Geomechanical calculations indicate that the shear stress on the fault considerably increases with several MPa due to gas production. This increase is comparable with the shear stress before gas production from differential vertical and horizontal field stresses. Other possible tectonic forces, we are not aware of, have been disregarded.

Dynamic rupture modelling indicates that the observed short release time of seismic energy requires a substantial stress drop during rupture. If the stress in the reservoir only follows from expected field stresses and stresses induced by compaction, this implies that the dynamic friction coefficient should be substantially lower than the static one.

Pressure diffusion into the Carboniferous underburden and dynamic friction of the Carboniferous rock determine whether and how far the rupture could penetrate into the underburden. So far, there is no observational evidence that the rupture substantially penetrated into the Carboniferous. This may indicate that the reduction in friction from static to dynamic in the Carboniferous rock is less than in the reservoir.

GeoProc2019: Earthquake and Faulting mechanics

7th International Conference on Coupled THMC Processes in Geosystems
3-5 July 2019 Utrecht (Netherlands)

Frictional properties and microstructures of the active creeping Chihshang fault from experimental slip and its implications

W.-J. Wu[1], L.-W. Kuo[2], J.-C. Lee[3], W.-J. Huang[4], J.-J. Dong[5]

Keywords: Rate-and-state friction, microstructure, creep, Chihshang fault

The active Chishang thrust fault in eastern Taiwan is the southern segment of Longitudinal Valley Fault, documented as the most rapid creeping rate at shallow crust and seismic sliding at deeper part (Angelier et al. 1997; Lee et al., 2006). The creeping behavior on the Chihshang fault may play important role for stress accumulation during earthquake period, as deformation mechanism controls fault slip zone with its breadth, slip rate, temperature, tectonic stress, and rock friction during faulting (Sibson, 1977). Based on our previous study (Wu et al., under review), the Chishang fault gouge was partially amorphized by fault creeping at shallow crustal depths. However, the frictional characteristics of the fault gouge and the presence of amorphous materials would affect fault strength and stability are still unclear. Here we conduct a series of mechanical experiments and microstructural observations to determine the slip behavior of the Chihshang fault and possible deformation mechanisms. At sub-seismic slip rate (from 1E10-6 to 1E10-3 m/s), steady state friction and frictional properties (a-b) of the Chihshang fault gouge show that frictional behaviors is significantly different due to the presence of water (Fig. 1a and 1b). To date, the mineralogical and microstructural characterization of the experimental products, e.g. XRD, FESEM, and FIB-TEM, were not completed, but our preliminary results imply that different frictional strengths of the Chishang fault gouge (dry: $0.45 < \mu < 0.55$; wet: $\mu < 0.2$) could be responsible for the seasonally variation of creeping rates, as observed from the geodetic data and creep meter record at shallow crust depths (Lee et al., 2003, 2006).

[1] Department of Earth Sciences, National Central University, Taiwan, wuwenjay1012@msn.com
[2] Department of Earth Sciences, National Central University, Taiwan, liweikuo@gmail.com
[3] Institute of Earth Sciences, Academica Sinica, Taiwan, jclee@earth.sinica.edu.tw
[4] Graduate Institute of Applied Geology, National Central University, Taiwan, huang22@ncu.edu.tw
[5] Graduate Institute of Applied Geology, National Central University, Taiwan, JJDong@geo.ncu.edu.tw

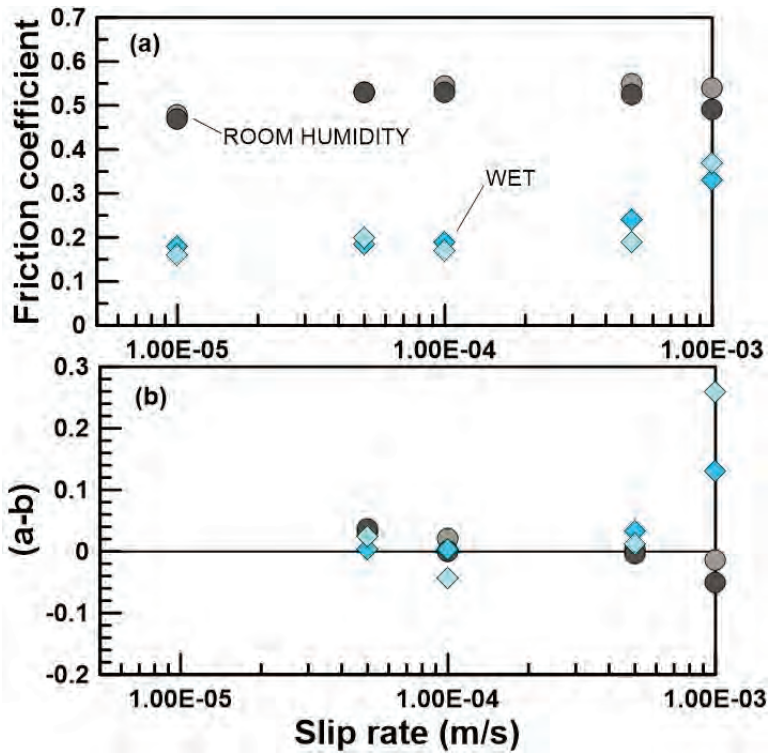

Figure 1. (a) steady state friction; (b) frictional properties of experimental gouge.

References

Angelier, J., H.-T. Chu, J.-C., Lee (1997), Shear concentration in a collision zone: kinematics of the Chihshang Fault as revealed by outcrop-scale quantification of active faulting, Longitudinal Valley, eastern Taiwan, *Tectonophysics*, 274, 117-143, doi:10.1016/S0040-1951(96)00301-0.

Lee, J.-C., J. Angelier, H.-T. Chu, J.-C. Hu, F.-S. Jeng, and R.-J. Rau (2003), Active fault creep variations at Chihshang, Taiwan, revealed by creep meter monitoring, 1998-2001, *Journal of Geophysical Research*, 108(B11), 2528, doi:10.1029/2003JB002394.

Lee, J.-C., H.T. Chu, J. Angelier, J.-C. Hu, H.-Y. Chen, S.-B. Yu (2006), Quantitative analysis of surface coseismic faulting and postseismic creep accompanying the 2003, M_w=6.5, Chengkung earthquake in eastern Taiwan, *Journal of Geophysical Research*, 111, B02405, doi:10.1029/2005JB003612.

Sibson, R.H. (1997), Fault rocks and fault mechanisms, *Journal of the Geological Society*, 133, 191-213, doi:10.1144/gsjgs.133.3.0191.

Wu, W.-J., L.-W. Kuo, C.-S. Ku, J.-C. Lee, C.-Y. Chiang, W.-J. Huang, J.-J. Dong, H.-S. Sheu, (under review), Gouge amorphization led by fault creeping at shallow crustal depths, *Geology*.

GeoProc2019: Earthquake and Faulting mechanics

7th International Conference on Coupled THMC Processes in Geosystems
3-5 July 2019 Utrecht (Netherlands)

Foreshock activities controlled by slip rate on a 4-meter-long laboratory fault

F. Yamashita[1], E. Fukuyama[2], S. Xu[3]

Keywords: laboratory experiment, foreshock, slow slip, slip rate

We report foreshock activities associated with evolving local slow slip events preceding the main rupture on a laboratory fault. To investigate the preparation process of laboratory earthquake with enough spatial resolution, we used a large-scale friction apparatus newly developed and installed at National Research Institute for Earth Science and Disaster Resilience (NIED) as shown in Figure 1. We used two rectangular metagabbro blocks as experimental specimens, whose nominal contacting area was 4.0 m long and 0.1 m wide. Height of each specimen was 0.2 m. Normal load was applied by eight flat jacks on the top surface of the upper specimen, and the associated pressures were kept at around 6 MPa during the experiments. After applying normal load, we applied shear load to the side surface of the lower specimen by manually pumping up a hydraulic jack, which was fixed at the western end of the apparatus. To monitor local phenomena on the fault, we installed 16 AE sensors, 40 triaxial rosette strain gauges, and 10 eddy current displacement sensors along the fault.

We conducted experiments with relatively high shear loading rate (67-185 kPa/s) and low shear loading rate (2-7 kPa/s). In each experiment, displacement data showed that both the eastern and western edges of the fault kept slipping during the shear loading, though the slip rate was very low (< ~20 μm/s). It is consistent with FEM calculation that fault should start to slip at both edges in this configuration. This steady slip was significant during the experiments with low loading rate, in both quantity and area. However, such steady slip did not immediately trigger seismic events. Most of seismic events occurred just before the main rupture, and therefore should better be termed foreshocks.

To understand what controls the occurrence of foreshocks, we first investigated the amount of stable slow slip accumulated after the previous main rupture. We found that foreshocks were not activated at around both fault edges even after the accumulated slip attained around 10 μm there (Figure 2a). On the other hand, foreshocks occurred around the central locked area with only a small amount of slip. We next compared the spatiotemporal distribution of foreshocks with that of slip rate. Displacement and strain data indicated that precursory slow slip began at the central locked area and then propagated outward over the fault area preceding the main rupture. We found that this slow slip had caused high slip rate (several hundreds of μm/s), which coincided with the

[1] National Research Institute for Earth Science and Disaster Resilience, Japan, yamafuto@bosai.go.jp
[2] National Research Institute for Earth Science and Disaster Resilience, Japan, fuku@bosai.go.jp
[3] National Research Institute for Earth Science and Disaster Resilience, Japan, shiqing@bosai.go.jp

occurrence of foreshocks (Figure 2b). These observations suggest that the key factor controlling the occurrence of foreshocks in this experiment is not the amount of accumulated slip but that of slip rate. The mechanism may be associated with the unstable fault slip triggered by fast loading in the laboratory (McLaskey and Yamashita, 2017; Xu et al., 2018), and the seismicity episodically activated in nature such as emergence of repeating earthquakes due to increased loading rate by afterslip of the 2011 *M*9.0 Tohoku-oki earthquake (Hatakeyama et al., 2017).

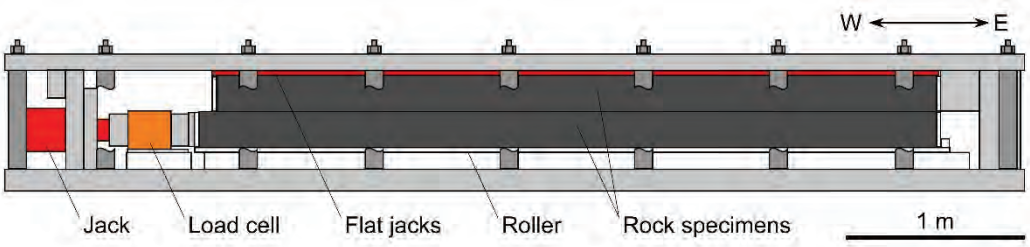

Figure 1. Schematic diagram of newly developed apparatus at NIED

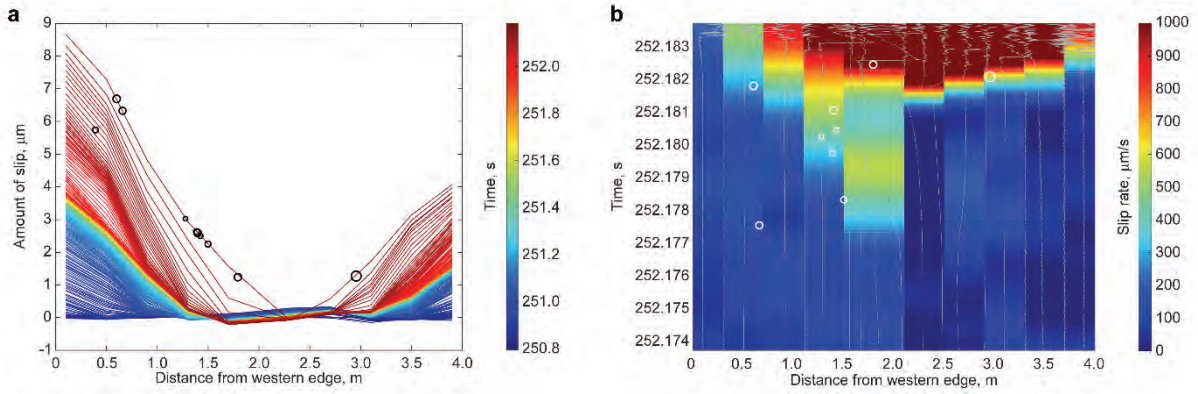

Figure 2. Spatiotempral distribution of foreshocks on (a) amount of accumulated slip, and on (b) that of slip rate along the laboratory fault for a typical event. Foreshocks are represented with open circles. Gray lines in (b) show local shear stresses estimated with strain measurements.

Acknowledgements: This study was supported by the NIED research project "Large Earthquake Generation Process" and JSPS Kakenhi Grant Numbers JP17H02954, JP16H06477.

References

Hatakeyama, N., N. Uchida, T. Matsuzawa, and W. Nakaumra (2017), Emergence and disappearance of interplate repeating earthquakes following the 2011 *M*9.0 Tohoku-oki earthquake: Slip behavior transition between seismic and aseismic depending on the loading rate, *J. Geophys. Res. Solid Earth*, *122*, 5160–5180, doi:10.1002/2016JB013914.

McLaskey, G. C., and F. Yamashita (2017), Slow and fast ruptures on a laboratory fault controlled by loading characteristics, *J. Geophys. Res. Solid Earth*, *122*(5), 3719–3738, doi:10.1002/2016JB013681.

Xu, S., E. Fukuyama, F. Yamashita,K. Mizoguchi, S. Takizawa, and H. Kawakata (2018), Strain rate effect on fault slip and rupture evolution: Insight from meter-scale rock friction experiments, *Tectonophysics*, *733*, 209–231, doi:10.1016/j.tecto.2017.11.039.

GeoProc2019: Earthquake and Faulting mechanics

7th International Conference on Coupled THMC Processes in Geosystems
3-5 July 2019 Utrecht (Netherlands)

A gas refined theory for cause of tectonic earthquakes, illustrated with 2008 Wenchuan 8.0 Earthquake

Z. Q. Yue[1]

Keywords: Methane gas, Tectonics, Geological Fault, Gas-Rock Interaction

It has been accepted, believed and utilized that tectonic earthquakes are caused by rock ruptures along active geological faults. It is the so-called classical elastic rebound theory and has been an essential component of the modern plate tectonic theory of the Earth. This cause theory was developed 100 years ago from the observation of co-seismic surface ruptures and topographical deformation induced by the 1906 California Earthquake. Since then, this fault cause theory of tectonic earthquakes has been used for the prediction of next damaging earthquakes. Although numerous attempts have been made for such predictions, successful prediction cases are few.

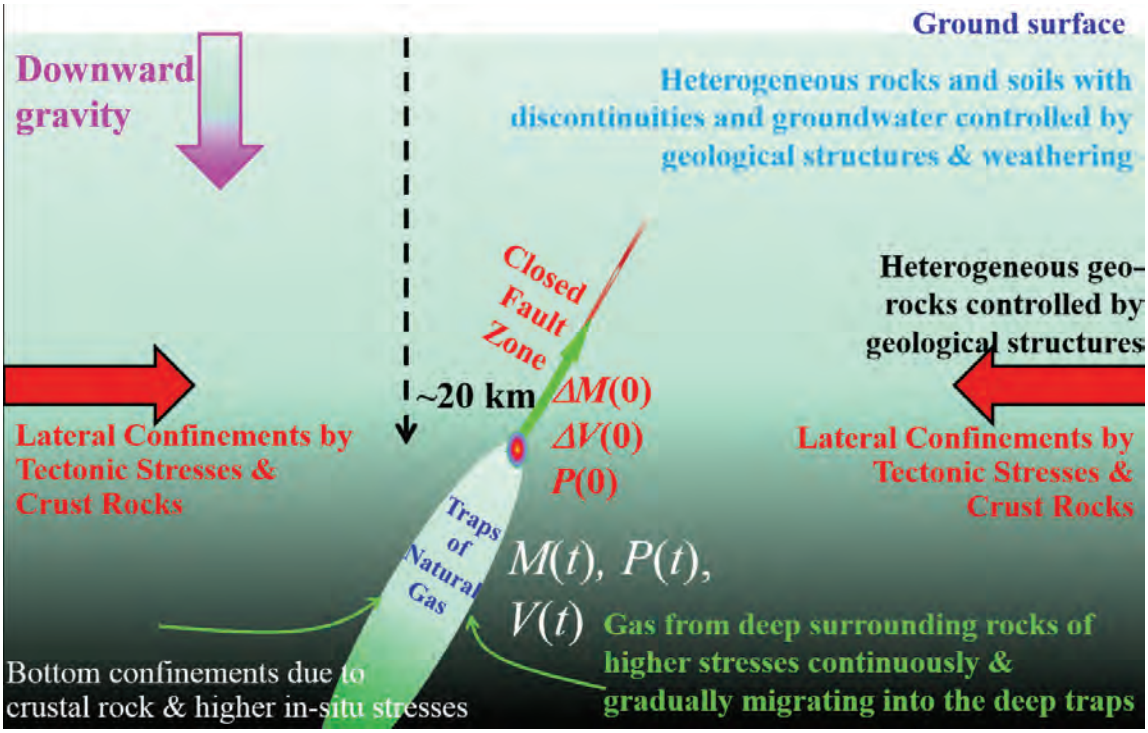

Figure 1. Geological Fault Infilled with Compressed Gas Model for Cause of Tectonic Earthquakes.

[1] Department of Civil Engineering, The University of Hong Kong, Hong Kong, PR China, yueqzq@hku.hk

As shown in Figure 1, the author of this paper has put forward a refined theory for the cause of tectonic earthquakes since 2008 two months after the occurrence of the Wenchuan earthquake of May 12, 2008. He has achieved this refinement by only adding a highly compressed gas mass in the apertures, gaps and/or caverns of geological fault zones. He has used this refined theory of geological faults partially infilled with gas mass of highly pressure to explain many phenomena that observed before, during and after an earthquake. In particular, the author has logically and consistently and quantitatively explained the various phenomena associated with 2008 Wenchuan Ms 8.0 (or 7.9) earthquake with this refined cause theory.

He further demonstrates that this faulting mechanics due infilling of compressed gas mass can make a breakthrough in earthquake prediction, although it may be a simple refinement of the classical elastic rebound theory of tectonic earthquakes. Moreover, the process of a tectonic earthquake can be descried as the following statement. An earthquake is the rapid expansion and flow of a large amount of highly dense and compressed nature gas from deep crust to shallow ground with speed of 1 to 3 km/s along tectonic faults. It is an adiabatic process of the interaction between (a) the rapid migrating and expanding of a huge mass of highly compressed natural methane gas and (b) the surrounding crustal rock mass, under the confinements of downward gravity, in-situ tectonic stresses and rock rigidness & strengths. He assumes that the gas is generated in mantle/core, flows upward, accumulated and stored in deep fault traps. Part of the trapped gas suddenly and rapidly ruptures and escapes the rock (or materials) traps along deep geological fault zones. The process of ground shaking during and after an earthquake is a cooling process.

References

Xiao, H.T., Yue, Z.Q. (2014), *Fracture Mechanics in Layered and Graded Solids: Analysis Using Boundary Element Methods*, De Gruyter & Higher Education Press, Berlin, Germany, ISBN 978-3-11-029787-4, p305.

Yue, Z.Q. (1988), Solutions for the thermoelastic problems in vertically inhomogeneous media, *Acta Mechnica Sinica*, 4(2): 182-189.

Yue, Z.Q., Selvadurai,A.P.S. (1995), On the mechanics of a rigid disc inclusion in a fluid saturated poroelastic medium, *International Journal of Engineering Science*. 33(11): 1633-1662.

Yue, Z.Q. (2010), Features and mechanism of coseismic surface ruptures by Wenchuan Earthquake, in *Rock Stress and Earthquake*, edited by Furen Xie, Taylor & Francis Group, London, ISBN 978-0-415-60165-8, pp.761-768.

Yue, Z.Q. (2013), On nature of earthquakes with cause of compressed methane gas expansion and migration in crustal rocks, in *Proceedings of Fifth Biot Conference on Poromechanics in Memory of Karl von Terzaghi* (1883-1963), July 10-12, 2013, Vienna, Austria, edited by Christian Hellmich, Bernhard Pichler and Dietmar Adam, ASCE, pp. 507-516.

Yue, Z.Q. (2014), On cause hypotheses of earthquakes with external tectonic plate and/or internal dense gas loadings, *Acta Mechnica* 225(4), 1447–1469 (2014), DOI 10.1007/s00707-013-1072-2.

Yue, Z.Q. (2015a), Yue's solution of classical elasticity in n-layered solids: Part 1, mathematical formulation, *Front. Struct. Civ. Eng*., 9(3): 215–249. DOI 10.1007/s11709-015-0298-6.

Yue, Z.Q. (2015b), Yue's solution of classical elasticity in n-layered solids: Part 2, mathematical verification, *Front. Struct. Civ. Eng*., 9(3): 250–285. DOI 10.1007/s11709-015-0299-5.

GeoProc2019: Earthquake and Faulting mechanics

7th International Conference on Coupled THMC Processes in Geosystems
3-5 July 2019 Utrecht (Netherlands)

Compaction front in horizontally shaken granular layers: application to soil liquefaction in drained conditions.

S Ben-Zeev[1], E. Aharonov[2], L. Goren[3], S Parez[4], R Toussaint[5]

Keywords: soil liquefaction, hydro-mechanical coupling in soils, earthquakes

We study compaction of an unconfined, fluid-saturated, granular layer, using theoretical analysis and a coupled two-scale numerical model (DEM granular model coupled with a continuum fluid model). The layer undergoes cyclic horizontal shearing, in a situation that mimics shaking during an earthquake. Fluid is free to flow in and out of the layer, i.e. the system has a drained upper boundary condition.

Results show that when acceleration exceeds a critical level (but still shaking amplitude is very small, less than 1 grain diameter), the layer compacts at a constant rate. A compaction front forms, and progresses from the bottom upwards. Behind the front the granular media is fully compacted and fluid pressure is low, while above it the fluid pressure is high due to the compacting grains. The compaction rate and front advancement depend on the fluid flow parameters, i.e. the permeability and fluid viscosity, but are independent of the shaking parameters (frequency, amplitude and acceleration). In the region where the fluid pressure is high, it supports the granular skeleton and the imposed shear is not transmitted through the layer.

Our results present a different mechanism for pore pressure rise in granular media, contrasting with the known mechanism of undrained liquefaction. In fact, we find that drainage is a crucial component in this new liquefaction initiation mechanism.

[1] Hebrew University of Jerusalem & Universite de Strasbourg shahar.benzeev@mail.huji.ac.il,
[2] Hebrew University of Jerusalem, einatah@mail.huji.ac.il
[3] Ben Gurion University of the Negev, gorenl@bgu.ac.il

[4] Institute of Chemical Process Fundamentals, TheCzech Academy of Sciences in Prague, stanislav.parez@gmail.com

[5] IPGS, CNRS / EOST-University of Strasbourg & PoreLab, The Njord Center, Physics Department, University of Oslo, renaud.toussaint@unistra.fr

GeoProc2019: Earthquake and Faulting mechanics

7th International Conference on Coupled THMC Processes in Geosystems
3-5 July 2019 Utrecht (Netherlands)

Unstable Frictional Slip of Basalt and Slip Weakening Behavior under High Fluid Pressure

Lei Zhang, Changrong He

State Key Laboratory of Earthquake Dynamics, Institute of Geology, China Earthquake Administration

Keywords: Basalt, slip weakening, unstable slip

In order to investigate frictional behavior of basalt under hydrothermal conditions, we apply sliding experiments using basalt gouge under temperature of 100-600°C, effective normal stress of 150MPa and fluid pressure of 30MPa and 100MPa, respectively. Experiment results under 30MPa pore pressure show that basalt exhibits velocity strengthening behavior at 100-200°C and changes to velocity weakening behavior at 400-600°C, meanwhile at 400°C, velocity dependence of basalt evolves with slip from initial velocity weakening to velocity strengthening. Results under 100MPa fluid pressure shows similar transition of velocity dependence at 300°C, however, at higher temperatures of 400-600°C velocity strengthening behavior occurs, accompanied with strong slip weakening behavior at slowest loading rate (0.04μm/s). During velocity step, shear stress only exhibits instantaneous direct response of velocity without transient evolution with slip, which is significantly different from typical frictional slip. Observation of microstructure reveals significant difference between samples sheared under 30MPa and 100MPa fluid pressure. At higher fluid pressure and temperatures of 400-600°C, porosity of basalt gouge layer is intensively reduced and deformation is characterized by pervasive shear with no obvious localization. Such results suggest healing process/plastic deformation is activated at higher fluid pressure and leads to strong slip weakening behavior. A sets of comparative experiment are conducted using nano-grain basalt gouge (grains size ranges from 100s nm to 5μm) with fluid pressure of 100MPa. Results show that basalt exhibits nearly neutral velocity dependence behavior at 100°C and velocity weakening behavior at 200°C. Stick slip behavior is observed at 300-600°C and stress drop increases with temperature. Microstructure observation found that brittle fracture of grains is rare and how such fine grain size controls frictional behavior of basalt will be studied further.

The topics to be addressed by GeoProc 2019 will include:

1. Complexity of frictional properties of basalt under various experimental conditions
2. Effects of pore pressure and grain size on frictional properties of basalt

3. Mechanism of strong slip weakening behavior

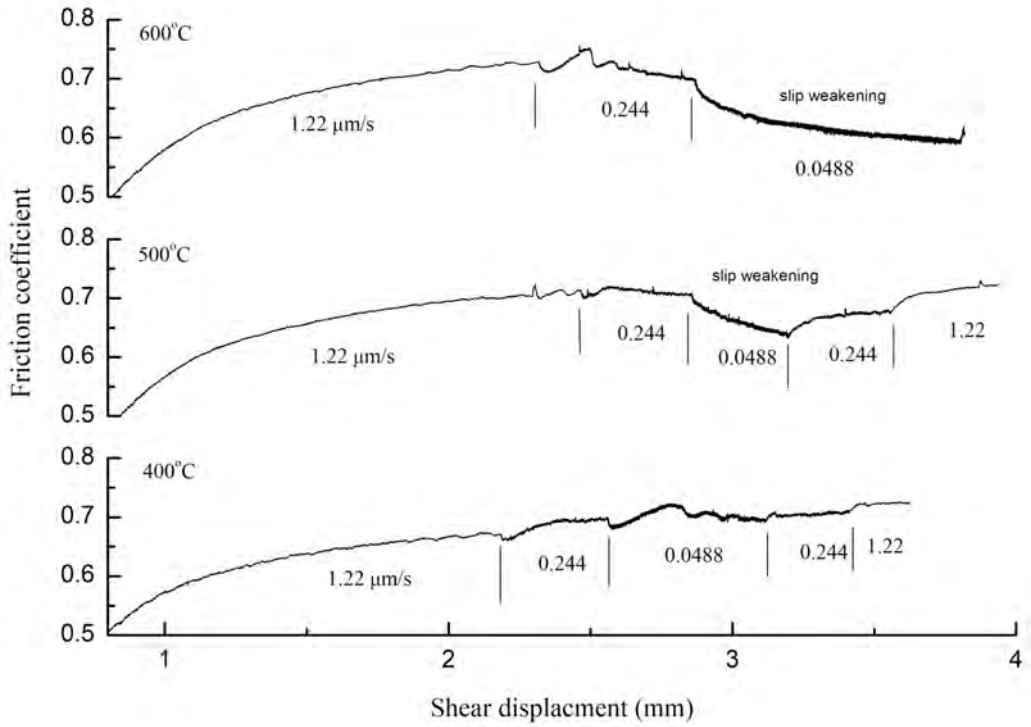

Figure 1. Friction coefficient versus shear displaceme. Strong slip weakening behavior occurs at 500 °C and 600°C.

GeoProc2019: Earthquake and Faulting mechanics

7th International Conference on Coupled THMC Processes in Geosystems
3-5 July 2019 Utrecht (Netherlands)

Effects of Fault Geometrical Complexities on Rupture Process and Earthquake Sequences in Longmenshan Fault Zone

Lei Zhang[1,2], Yajing Liu[2], Duo Li[2], Hongyu Yu[3], Changrong He[1]

[1] State Key Laboratory of Earthquake Dynamics, Institute of Geology, China Earthquake Administration

[2] Department of Earth and Planetary Sciences, McGill University

[3] Ruhr-University Bochum, Institute of Geology, Minerology & Geophysics

Keywords: Longmenshan fault zone, rupture process, earthquake sequence

On 12 May 2008, the devastating Mw 7.9 Wenchuan earthquake occurred on the imbricate, listric-reverse Longmenshan fault zone. Finite fault slip inversion reveals the event initiated on Beichuan fault and ruptures unilaterally northeastward exhibiting complex rupture process with highly inhomogeneous coseismic slip distribution (Zhang et al. 2009). Field observation and geodetic inversion suggest a complex geometry of Beichuan fault characterized by varying dip angle along down-dip and strike and discontinuity in fault strike inferred from surface rupture (Xu et al., 2008; Shen et al., 2009, Wan et al., 2017). Motivated by the complex rupture process and geometry of Beichuan fault, we conducted a 3D numerical modeling of earthquake on Beichuan fault, incorporating the lab-derived rate and state friction law, to investigate the role of fault geometry in controlling coseismic rupture process and earthquake cycles. In our modeling, a nonplanar Beichuan fault model with length of ~310 km and width of 34 km is constructed based on the kinetic inversion from geodetic data (Wan et al., 2017). A continuous nucleation zone appears where the fault is velocity-weakening (a-b<0) from 5 km to 19 km depth, based on the distribution of hypocenter of mainshock and aftershocks (Chen et al., 2009). Moreover, in order to isolate the effects of fault geometry, a simplified parameter setting, e.g. constant (a-b) value along the strike and uniform friction coefficient (μ=0.6), is used. Background tectonic loading rate near the fault trace varies from 0.8 mm/yr to 2.2 mm/yr according to long-term GPS observation. In our model, we firstly apply pure dextral slip and thrust slip on fault plane to simulate dip-slip and strike-slip earthquakes, respectively. Secondly, oblique slip, which is assigned by the realistic direction from long-term geodetic observation, is also applied to model oblique-slip events. Results of the three types of slip mode will help us to understand different responses of slip modes to geometric complexities in numerical model. Preliminary results of purely dip-slip and strike-slip earthquakes indicate that heterogeneity of fault geometry significantly affects the coseismic rupture process. Intense changes of both dip and strike angle appear to serve as a barrier to arrest

coseismic slip. Our ongoing work will include a quantitative study on the effect of geometric barriers on the coseismic slip rupture and earthquake cycles.

The topics to be addressed by GeoProc 2019 will include:

1. Effect of complex fault plane geometry on rupture process and coseismic distribution
2. How to incorporate normal stress evolution into modeling and its effect on modeling results.

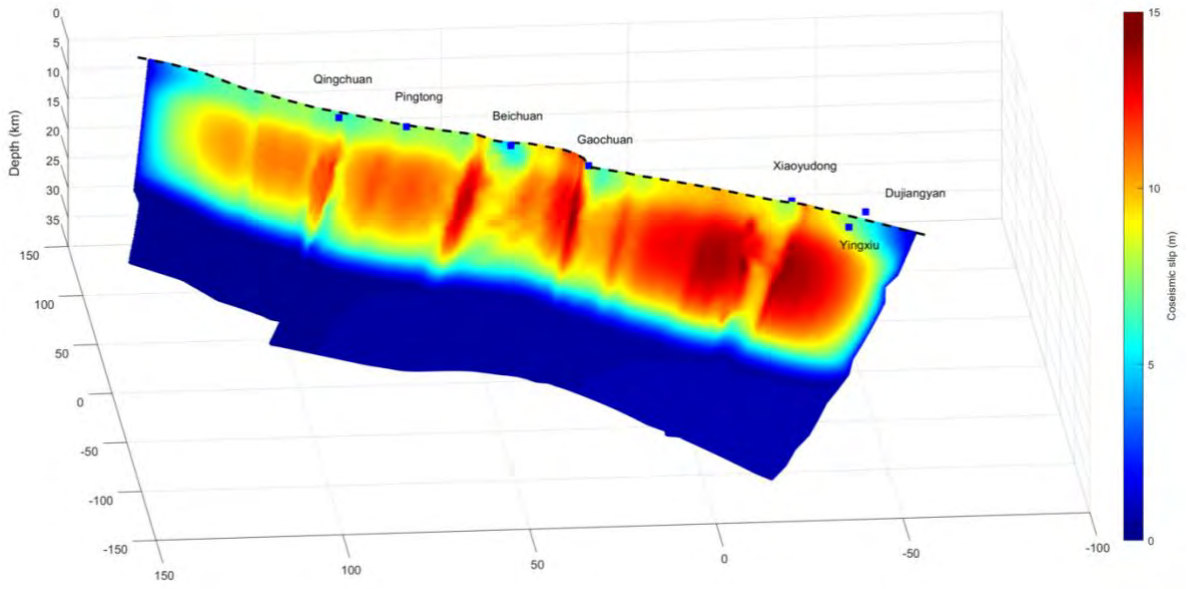

Figure 1. Coseismic slip distribution on fault plane (oblique slip model)

Reference

Chen J. H.， liu Q. Y.， Li S. C., et al., Seismotectonic study by relocation of the Wenchuan Ms8.0 earthquake sequence. Chinese J. Geophys. (in Chinese), 2009, 52(2):390~ 397.

Shen, Z.-K., Sun J. B., Zhang P. Z., et al., 2009. Slip maxima at fault junctions and rupturing of barriers during the 2008Wenchuan earthquake. Nature, 2009, 2.

Wan Y., Shen Z.-K., Bürgmann R., Sun J., et al., 2017. Fault geometry and slip distribution of the 2008 Mw 7.9 Wenchuan, China earthquake, inferred from GPS and InSAR measurements. Geophysical Journal International 208, 748-766.

Zhang Y., Feng W., Xu L., Zhou C., Chen Y., 2009. Spatio-temporal rupture process of the 2008 great Wenchuan earthquake. Science in China Series D: Earth Sciences 52, 145-154.

GeoProc2019: Earthquake and Faulting mechanics

7th International Conference on Coupled THMC Processes in Geosystems
3-5 July 2019 Utrecht (Netherlands)

The deep reducing seismogenic environment in Longmen Shan: evidences from the metallic iron in pseudotachylyte

L. Zhang[1], H.B. Li[2], Z.M. Sun[3] Y.M. Chou[4], Y. Cao[5], H. Wang[6]*

Keywords: Pseudotachylyte, Metallic iron, Seismogenic environment, Heating experiments, Longmen Shan

Based on geochemical analysis, metallic iron was found in the pseudotachylyte from the Wenchuan Earthquake Fault Scientifc Drilling borehole 2 (WFSD-2) cores, Longmen Shan thrust belt, China. The pseudotachylyte veins were formed in 15 km-depth (Zheng et al., 2016). However, the morphological characteristics, forming environment and indication of metallic iron are ambiguous. Here, heating experiments were performed at elevated temperatures on WFSD-2 cores, and the results of the microstructure, geochemistry and rock magnetic properties of samples subjected to different heating temperatures (room temperature, 400, 700, 900, 1100, 1300, 1500 and 1750 °C) were obtained (Zhang et al., 2018). The melting occurred at 1100 °C and the quartz is partially molten at 1300 °C. The high freezing rate and high temperature (≥1500 °C) may impede the formation of microlites during large earthquakes. Many circular spherulites with regular polygonal shape were well‐developed in the samples heated above 1300 °C (figure 1). The spherulites are composed of metallic iron, formed by the reducing action of Fe‐bearing minerals at high temperature in a reducing environment (≥1300 °C). As the temperature increased, metallic iron content and magnetic susceptibility increased, indicating that the newly formed metallic iron was responsible for the high magnetic susceptibility values. The frictional melting temperature reached 1300 °C during ancient earthquakes in the Longmen Shan thrust belt, indicating that metallic iron might be responsible for the strong magnetic highs in pseudotachylyte. The metallic iron in pseudotachylyte from WFSD-2 cores suggest a deep reducing earthquake sliding environment in the Longmen Shan thrust zone.

The topic: 4. Role of THMC processes in controlling natural destructive earthquakes

[1] Key Laboratory of Deep-Earth Dynamics of Ministry of Natural Resources, Institute of Geology, Chinese Academy of Geological Sciences, China, zhanglei881102@126.com
[2] Key Laboratory of Deep-Earth Dynamics of Ministry of Natural Resources, Institute of Geology, Chinese Academy of Geological Sciences, China, lihaibing06@163.com
[3] Institute of Geomechanics, Chinese Academy of Geological Sciences, China, sunzm1209@163.com
[4] South University of Science and Technology, China, chouym@sustc.edu.cn
[5] Institute of Geomechanics, Chinese Academy of Geological Sciences, China, geocao@126.com
[6] Key Laboratory of Deep-Earth Dynamics of Ministry of Natural Resources, Institute of Geology, Chinese Academy of Geological Sciences, China, wanghuan4585@126.com

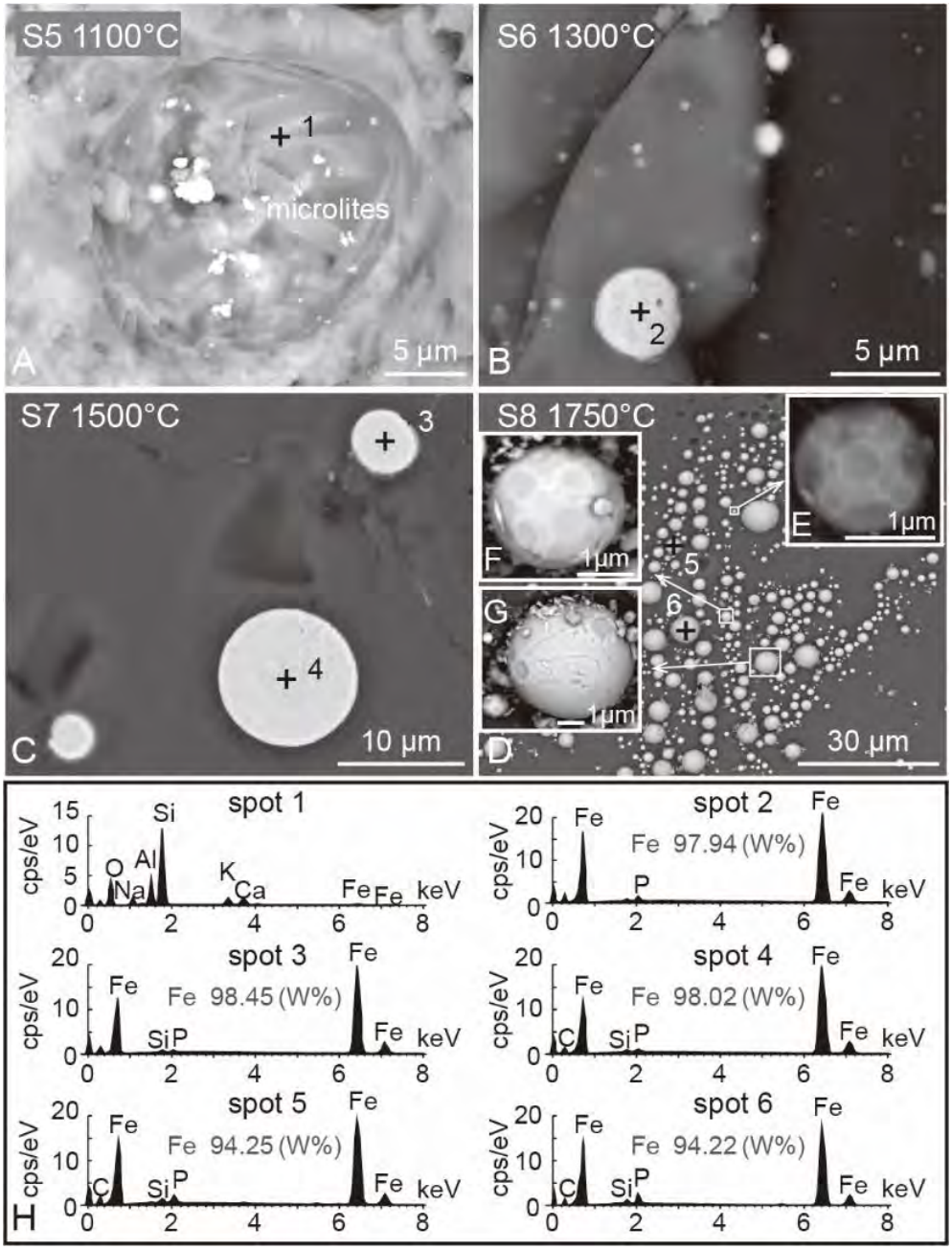

Figure 1. Scanning electron microsopy (SEM) results of the samples from Wenchuan Earthquake Fault Scientific Drilling WFSD-2 cores (Longmen Shan thrust belt, China). A: Image of sample S5 shows a floriform microlite. B-G: Samples S6, S7 and S8 show different spherulites. H: SEM-EDX results for the spots in A, B, C, and D.

References

Zheng, Y., Li, H.B., Sun, Z.M., Wang, H., Zhang, J.J., Li, C.L., and Cao, Y. (2016), New geochronology constraints on timing and depth of the ancient earthquakes along the Longmen Shan fault belt, eastern Tibet, Tectonics, 35, 2781-2806, doi: 10.1002/2016TC004210.

Zhang, L., Li, H.B., Sun, Z.M., Chou, Y.M., Cao, Y., and Wang, H. (2018), Metallic iron formed by melting: A new mechanism for magnetic highs in pseudotachylyte, *Geology*, 46(9), 779–782, doi: 10.1130/G40153.1.

GeoProc2019: Earthquake and Faulting mechanics

7th International Conference on Coupled THMC Processes in Geosystems
3-5 July 2019 Utrecht (Netherlands)

Acoustic emissions associated with slow-slip events in quartz gouge friction experiments

W. Zhou[1], J. Chen[1], A. Niemeijer[1], H. Paulssen[1]

Keywords: slow-slip, fore-shock, acoustic emission, rotary shear, quartz gouge

To investigate how the evolution of the microstructure affects slip characteristics in quartz gouge in the presence of pressurized pore water, we performed experiments to high shear strain with a rotary shear apparatus, equipped with two AE sensors (400 kHz and 4kHz), located ~25 cm below the actively shearing gouge. We sheared a quartz gouge (grain size < 49 μm) at varied shearing velocities and under different temperature and pressure conditions.

The experiment shown in Figure 1 was performed at 6 um/s and room temperature, with 100 MPa pore pressure and effective normal stress of 60 MPa. During initial shearing, we observed a rapid increase in friction to a value of ~0.65, after which friction stabilized. Unstable stick-slip events accompanied by an audible and recordable AE signal start after a displacement of ~6 mm.

We observed fast stick-slip as well as slow-slip events in the friction data. Some periodic slow-slip events occur shortly before the appearance of fast stick-slips, but others occur in the critical friction stage of stick-slips (Figure 1a). Previous work on quartz gouges have shown a transition from slow slip to stick-slips that occurs with ongoing development of localized shear bands (Scuderi et al., 2017) or as a function of decreasing apparatus stiffness. Such an evolution is not clear in our experiment, since slow slip events and stick-slip events occur throughout the experiment.

Throughout the experiment, we continuously recorded AE signals at 5 MHz sampling rate. Fast stick-slip events are usually accompanied with high-frequency initial acoustic emissions (~100 kHz to ~600 kHz), and repetitive lower frequency (~6 kHz) coda, which is inferred to be associated to slip of the entire surface of the gouge layer. Although amplitudes are much smaller, we also detected acoustic emission (high frequency) associated with many slow-slips.

Precursory acoustic emissions (high frequency) were captured that occur up to 10 ms before fast-slip events and some slow-slip events. These high frequency signals should indicate that the gouge was in an unstable state and there must be with small patches sliding, or grains breaking. Additionally, with a the low-frequency (4 kHz) piezoelectric sensor, we have recorded signal that might proportional to strain rate at the vessel

[1] Department of Earth Sciences, Utrecht University, w.zhou@uu.nl, j.chen3@uu.nl, a.niemeijer@uu.nl, h.paulssen@uu.nl

bottom that represents the acceleration and decelerations of slips, which shows that these are asymmetrical.

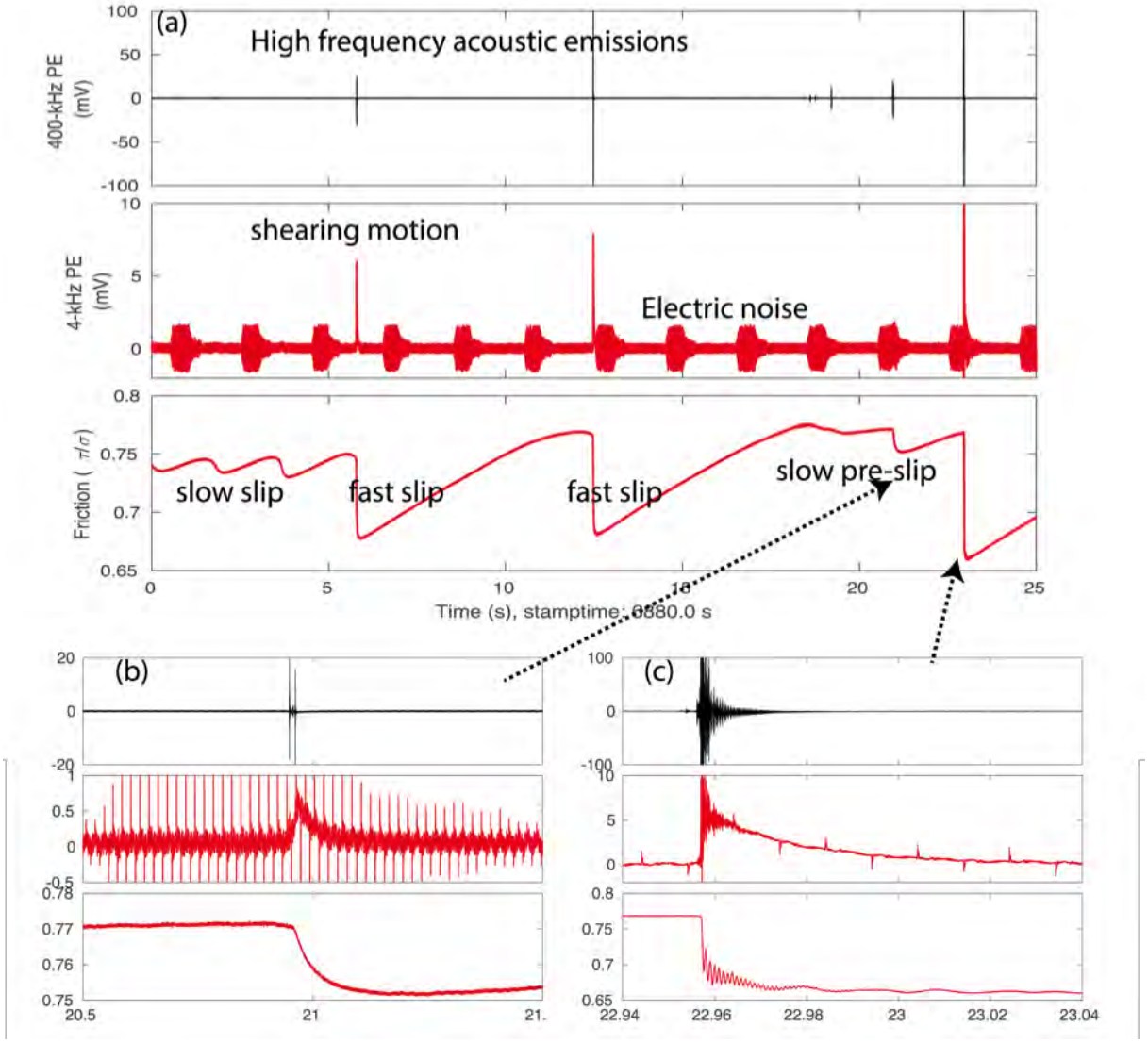

Figure 1. (a) 25 seconds of recording by two piezoelectric sensors and friction. (b) Slow-slip that occurred 2 seconds before a major slip. (c) Main slip corresponding to a stress drop of 14%.

References

Scuderi, M.M., Collettini, C., Viti, C., Tinti, E. and Marone, C., 2017. Evolution of shear fabric in granular fault gouge from stable sliding to stick slip and implications for fault slip mode. Geology, 45(8), pp.731-734.

GeoProc2019: Earthquake and Faulting mechanics

7th International Conference on Coupled THMC Processes in Geosystems
3-5 July 2019 Utrecht (Netherlands)

P wave travel time changes in the Groningen reservoir

W. Zhou[1], H. Paulssen[1], A. Niemeijer[1]

Keywords: P wave velocity, time lapse, reservoir compaction, Groningen

After the M 3.6 Huizinge earthquake of 2012, the Groningen gas field in the Netherlands has become one of the most densely instrumented regions of induced seismicity in the world. In 2013 two former production wells were equipped with geophone strings at the reservoir level at 3 km depth. In a previous study Zhou & Paulssen (2017) showed that anthropogenic noise is the dominant noise source at the reservoir level, and they found that the P and S wave velocity structure along borehole SDM-1 could be accurately retrieved from noise interferometry by cross-correlation.

In this study we show that signals from nearby passing trains can be used to infer time-lapse variations in the reservoir. High-frequency (30-100 Hz) train noise is identified in the spectrograms of the 10 geophones in borehole SDM-1. Deconvolution of 20 s of train signal recorded on the vertical component of the top geophone with that of the other geophones produces a clear downgoing P wave as well as weak bottom and top reflections from the reservoir (Fig. 1). The travel times of the downgoing P wave allowed very accurate estimates of the inter-geophone velocities in the reservoir. In addition, small time-lapse variations were measured in the data of the two geophone deployments that were analyzed: Jan-Jun 2015 and Jul-Dec 2015. The travel times within the reservoir decrease by 0 – 0.1% per half year with a larger decrease in the second half of 2015. This observation correlates with bigger surface subsidence for the second half of 2015. Albeit tiny, the travel time variations cannot be explained by vertical shortening only, so an additional P wave velocity increase related to compaction is required to explain the data.

Furthermore, we found a clear travel time anomaly (up to 0.8 ms) in the time span Jul 17-Sep 2 between the bottom geophone, located just below the gas-water-contact in the reservoir, and the one above (or any of the other geophones). This anomaly is associated with the drilling of a deep borehole at 5 km distance (Jul 9-Aug 28).

[1] Department of Earth Sciences, Utrecht University, w.zhou@uu.nl, h.paulssen@uu.nl, a.niemeijer@uu.nl

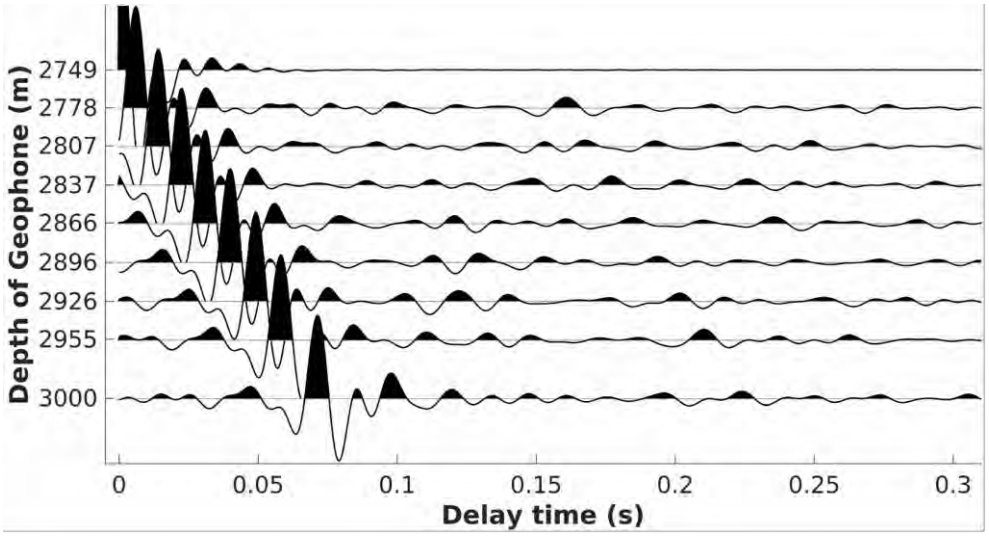

Figure 1. Train noise deconvolutions with virtual source at the top geophone (Vertical components, Jul-Dec 2015).

References

Zhou, W., and Paulssen, H., 2017. P and S velocity structure in the Groningen gas reservoir from noise interferometry. Geophysical Research Letters, 44(23).

GeoProc2019: Earthquake and Faulting mechanics

7th International Conference on Coupled THMC Processes in Geosystems
3-5 July 2019 Utrecht (Netherlands)

Numerical simulation of rupture processes of the 2008 Wenchuan, China earthquake

S. Zhu[1], *J. Yuan*[1]

Keywords: Seismic damage; Supershear rupture; Gaochuan right bend; Beichuan area; Yingxiu-Beichuan fault; Wenchuan earthquake

The Beichuan area suffered the most serious seismic damage in the 2008 Wenchuan, China earthquake although the Beichuan is over 100 km away from the instrumental epicenter of the mainshock. The mechanism for this peculiar phenomenon remains unclear even though 10 years has passed since the Wenchuan event. For this purpose, we construct a spontaneous rupture model in which Gaochuan right bend (GRB) is included in the middle of Yingxiu-Beichuan fault, a major seismogenic fault for the Wenchuan event. The simulated results show that the complex geometry of the GRB played a controlling role in the rupture propagation. Once the rupture was initiated at the epicenter of the Wenchuan mainshock, it propagated spontaneously, and the rupture speed on the first segment of the fault is ~2.79 km/s, slower than the shear wave speed of local medium. When the rupture front spread near the end of the Yingxiu-Gaochuan fault, a new rupture was re-nucleated at the curve section of the Gaochuan bend, and propagated in the northeast direction with the speed of 5.02 km/s, greater than the S wave velocity. In addition, this rupture speed transition from subshear to supershear does not need any time delay, much distinct from the case of fault stepover in which delay is needed in supershear transition. The result also demonstrates that the relation between the high values of peak ground acceleration (PGA) and the supershear rupture is strong. The large area with high values of PGA distributed in the Beichuan directly led to grave seismic catastrophe there. Therefore, this work may give some insight into why the most serious seismic damage occurred in the Beichuan area, and may have important implications for understanding earthquake dynamics and assessing seismic hazards.

[1] Institute of Crustal Dynamics, China Earthquake Administration, Beijing 100085, China, zhusb@pku.edu.cn, zhushoubiao@gmail.com.